Uniwersytet Przyrodniczy w Poznaniu

Wydział Nauk o Żywności i Żywieniu

Katedra Biotechnologii i Mikrobiologii Żywności

Natalia Małgorzata Tomaś

Wpływ wybranych olejków eterycznych na metabolizm zależny od systemu quorum sensing u *Pseudomonas psychrophila* KM02 wyizolowanych z żywności

Impact of selected essential oils on the quorum sensing-related metabolism of *Pseudomonas psychrophila* KM02 isolated from food

Rozprawa doktorska w dziedzinie nauk rolniczych
w dyscyplinie technologia żywności i żywienia

Promotor rozprawy doktorskiej:

prof. UPP dr hab. inż. Kamila Myszka

Katedra Biotechnologii i Mikrobiologii Żywności
Uniwersytet Przyrodniczy w Poznaniu

Poznań, 2023 rok

"The mind will not be cultivated at the expense of the heart"

~ Basil Moreau

Serdeczne podziękowana kieruję:

~ Prof. Kamili Myszce za osobiste zaangażowanie, wszelką pomoc oraz czas poświęcony w przygotowaniu niniejszej pracy;

~ Współautorom publikacji za udostępnienie przestrzeni do badań oraz wsparcie merytoryczne przy ich realizacji;

~ Najdroższym Rodzicom za umożliwienie podjęcia pracy naukowej i wszelkie okazane wsparcie do rozwoju osobistego;

~ Koleżankom Doktorantkom za pomoc, miłe spotkania i rodzinną atmosferę;

~ oraz wszystkim tym, których nie wymieniłam, a którzy dobrym słowem i uśmiechem wspierali codzienne zmagania w pracy Doktoranta.

Niniejszą pracę dedykuję Łukaszowi i Franciszkowi

Spis treści

Publikacje wchodzące w skład rozprawy doktorskiej

P-1 **Tomaś N**., Myszka K.* Current advances in the concept of quorum sensing - based prevention of spoilage of fish products by Pseudomonads. *Applied Sciences* 12, 6719 (2022). https://doi.org/10.3390/app12136719

IF_{2022} = 2,679; punkty wg MEiN = 100

P-2 **Sobieszczańska N.***, Myszka K., Szwengiel A., Majcher M., Grygier A., Wolko Ł. Tarragon essential oil as a source of bioactive compounds with anti-*quorum sensing* and anti-proteolytic activity against *Pseudomonas* spp. isolated from fish – in vitro, *in silico* and *in situ* approaches. *International Journal of Food Microbiology* 331, 108732 (2020). https://doi.org/10.1016/j.ijfoodmicro.2020.108732.

IF_{2020} = 5,277; **punkty wg MEiN = 100**

P-3 **Tomaś N.***, Myszka K., Wolko Ł, Nuc K., Szwengiel A., Grygier A., Majcher M. Effect of black pepper essential oil on quorum sensing and efflux pump systems in the fish-borne spoiler *Pseudomonas psychrophila* KM02 identified by RNA-seq, RT-qPCR and molecular docking analyses. *Food Control* 130, 108284 (2021). https://doi.org/10.1016/j.foodcont.2021.108284.

IF_{2021} = 5,548; punkty wg MEiN = 140

P-4 **Tomaś N.*,** Myszka K. & Wolko Ł. Black pepper and tarragon essential oils suppress the lipolytic potential and the type II secretion system of *P. psychrophila* KM02. *Scientific Reports* 12, 5487 (2022). https://doi.org/10.1038/s41598-022-09311-9

IF_{2022} = 4,379; punkty wg MEiN = 140

Sumaryczny współczynnik Impact Factor publikacji wchodzących w skład rozprawy doktorskiej wynosi **17,883**

Całkowita liczba punktów według listy czasopism punktowanych MEiN za publikacje wchodzące w skład rozprawy doktorskiej wynosi **480**

* Autor korespondencyjny

Źródło finansowania badań

Niniejsza praca powstała w ramach projektu „Molekularna charakterystyka sposobu hamowania procesu quorum sensing przez wybrane olejki eteryczne u *Pseudomonas* spp. wyizolowanych z żywności" nr 2016/23/D/NZ9/00028, finansowanego przez Narodowe Centrum Nauki, którego kierownikiem była Prof. UPP dr hab. Kamila Myszka.

Wykaz skrótów stosowanych w rozprawie

Oznaczenie	Pełna nazwa
TEO	olejek eteryczny z estragonu
ME	metyleugenol
PHE	β-felandren
BPEO	olejek eteryczny z pieprzu czarnego
CAR	β-kariofilen
LIM	limonen
subMIC	stężenie subinhibicyjne
TSB	bulion tryptozowo-sojowy
zTSB	zmodyfikowany bulion tryptozo-sojowy
NA	kwas nalidyksowy
DMSO	dimetylosulfotlenek
GC-MS	chromatografia gazowa sprzężona ze spektrometrią mas
RI	czas retencji
m/z	stosunek masy jonu do jego ładunku
GC-FID	chromatografia gazowa z detektorem płomieniowo-jonizacyjnym
BAME	bakteryjne estry metylowe kwasów tłuszczowych
UHPLC-MS/MS	wysokosprawna chromatografia cieczowa z tandemową spektrometrią mas
LOD	limit detekcji
AI	autoinduktory; cząsteczki sygnałowe
AHL	acylowany lakton homoseryny
HSL	lakton homoseryny
HHQ	2-heptyl-4-chinolon
PQS	2-heptyl-3-hydroksy-4-chinolon
CID	identyfikator związku w bazie PubChem
PDB ID	identyfikator w bazie danych białek
NCBI	Narodowe Centrum Informacji Biotechnologicznej
DNA	kwas deoksyrybonukleinowy
cDNA	komplementarny kwas deoksyrybonukleinowy
RNA	kwas rybonukleinowy
mRNA	matrycowy kwas rybonukleinowy
COG	klastry genów ortologicznych
GO	ontologie genowe
CDS	sekwencja kodująca
G+C	guanina+cytozyna

pz	par zasad
Pfam	baza danych rodzin białek
CARD	kompleksowa baza danych oporności na antybiotyki
RAST	szybkie adnotacje przy użyciu technologii podsystemów
T2SS	system sekrecyjny typu II
RPKM	odczyty na 1000 par zasad, na milion zmapowanych odczytów
PCR	reakcja łańcuchowa polimerazy
RT-qPCR	PCR z odwrotną transkrypcją w czasie rzeczywistym
RND	Oporność-Nodulacja-Podział
FJM	pożywka z ryby (imitująca produkt z ryb)
PI	inhibicja aktywności proteolitycznej
A_t	wartość absorbancji dla próby traktowanej
A_c	wartość absorbancji dla próby kontrolnej
LI	inhibicja aktywności lipolitycznej
EI	inhibicja syntezy egzopolisacharydów
EPS	egzopolisacharydy
EPS_t	stężenie egzopolisacharydów dla próby traktowanej
EPS_c	stężenie egzopolisacharydów dla próby kontrolnej
jtk/g	jednostki tworzące kolonie w gramie produktu
TYR	tyrozyna
TRP	tryptofan
THR	treonina
ASP	kwas asparaginowy
ASN	asparagina
ARG	arginina
ALA	alanina
ILE	izoleucyna
LEU	leucyna
SER	seryna
PRO	prolina
GLU	kwas glutaminowy
GLY	glicyna
PHE	fenyloalanina
VAL	walina
PaβN	inhibitor β-naftyloamidu fenyloalaniny-argininy
QZN	3-amino-7-chloro-2-nonylochinazolin-4-on

Streszczenie w języku polskim

Świeże schłodzone ryby oraz produkty rybne o minimalnym stopniu przetworzenia łatwo ulegają mikrobiologicznemu zepsuciu. Za ten proces odpowiadają głównie psychrotrofowe gatunki *Pseudomonas* spp., w tym *Pseudomonas psychrophila*, których aktywność metaboliczna jest zależna od systemu quorum sensing. W tym systemie cząsteczki autoinduktorów (AI) rozpoznawane są przez białka receptorowe będące regulatorami transkrypcyjnymi określonej grupy genów. Ingerencja w powyższy mechanizm olejkami eterycznymi i ich składnikami, może wpłynąć na syntezę enzymów i egzopolisacharydów (EPS) oraz na proces degradacji tłuszczu przez drobnoustroje. Weryfikacja działania przeciw-quorum sensing w układach: *in vitro, in silico* oraz *in situ* może wspomóc opracowywanie w przyszłości alternatywnych/uzupełniających rozwiązań, zmierzających do eliminacji lub/i wyraźnego ograniczenia aktywności fizjologicznej drobnoustrojów saprofitycznych w matrycy żywności.

Celem głównym niniejszej pracy była ocena wpływu olejku eterycznego z estragonu (TEO) i pieprzu czarnego (BPEO) na system quorum sensing i aktywność metaboliczną bakterii *P. psychrophila* KM02 wyizolowanej z ryb.

W pracy TEO i BPEO otrzymano metodą hydrodestylacji, a ich skład chemiczny oceniono systemem GC-MS. Metodą szeregu seryjnych rozcieńczeń wyznaczono stężenia subinhibicyjne (subMIC) olejków eterycznych względem *Pseudomonas* spp. Systemem GC-FID oceniono zmiany w profilu kwasów tłuszczowych osłon komórkowych. Potencjał przeciw-quorum sensing testowanych czynników charakteryzowano poprzez: (i) ocenę zmian syntezy AI systemem UHPLC-MS/MS oraz (ii) komputerową analizę dokowania molekularnego głównych składników olejków eterycznych do białek receptorowych. Analizę całego genomu oraz transkryptomu przeprowadzono oceniając potencjał *P. psychrophila* KM02 do wzrostu/aktywności metabolicznej w matrycy żywności. Komputerową analizę dokowania molekularnego oraz technikę RT-qPCR wykorzystano w ocenie wpływu badanych czynników na systemy: efflux i T2SS, zależne od quorum sensing. Stopień inhibicji właściwości proteolitycznych i lipolitycznych oraz zmiany syntezy EPS przez TEO, BPEO i główne składniki olejków eterycznych u *P. psychrophila* KM02 oceniono prowadząc analizy spektrofotometryczne oraz RT-qPCR. Metodą płytkową Kocha, scharakteryzowano wzrost *P. psychrophila* KM02 w modelowym produkcie spożywczym, do którego zaaplikowano stężenia subMIC TEO i BPEO.

Na podstawie przeprowadzonych doświadczeń stwierdzono, iż stężenia subMIC TEO (70-75 µL/mL) i BPEO (100-135 µL/mL) ingerują w system *quorum sensing* i zaburzają aktywność metaboliczną badanych drobnoustrojów. Ekspozycja komórek *Pseudomonas* spp. na testowane czynniki skutkowała obniżeniem udziału nienasyconych kwasów tłuszczowych oraz kwasów tłuszczowych o budowie rozgałęzionej w osłonach komórkowych. *Pseudomonas* spp. w warunkach *in vitro* syntezowały autoinduktory (AI) systemu *quorum sensing* należące do grupy AHL (tj. 3-okso-C12-HSL, 3-okso-C14-HSL, 3-okso-C6-HSL, 3-okso-C8-HSL, C12-HSL, C4-HSL, C6-HSL) oraz związek chinolowy PQS. Stężenia subMIC TEO, BPEO oraz składników olejków eterycznych (tj. metyleugenolu (ME) 10-12 µL/mL, β-felandrenu (PHE), 8-10 µL/mL, limonenu (LIM) 60-65 µL/mL i β-kariofilenu (CAR) 20-35 µL/mL) hamowały syntezę cząsteczek AI *Pseudomonas* spp.. ME, PHE, LIM i CAR wiązały się z białkami receptorowymi LasR, RhlR, TraR oraz PqsR systemu *quorum sensing* oraz białkami Mfs, MexB, MuxB systemu efflux *Pseudomonas* spp. W genomie i transkryptomie *P. psychrophila* KM02 odnotowano obecność czynników świadczących o zdolności bakterii do rozkładu białek i tłuszczu oraz sekrecji enzymów. W prezentowanej pracy, w zaproponowanych układach doświadczeń, stężenia subMIC: TEO, BPEO, ME, PHE, LIM i CAR obniżały aktywność proteolityczną, lipolityczną oraz syntezę EPS przez *P. psychrophila* KM02. Badane czynniki wprowadzone do marynaty octowo-olejowej hamowały wzrost komórek *P. psychrophila* KM02 w rybnym produkcie modelowym.

Niniejsza praca wykazała wpływ TEO i BPEO oraz ich głównych składników, tj. ME, PHE, CAR i LIM na system quorum sensing i aktywność metaboliczną *P. psychrophila* KM02. Powyższa zależność może spowolnić proces psucia ryb przechowywanych w warunkach chłodniczych, w który zaangażowany jest *P. psychrophila* KM02. Uzyskane w niniejszej pracy wyniki uzupełniają również wiedzę dotyczącą systemu quorum sensing u bakterii saprofitycznych wyizolowanych z żywności.

Słowa kluczowe: quorum sensing, psucie ryb, system efflux, T2SS, dokowanie molekularne, genom, transkryptom

Abstract

Fresh chilled fish and minimally processed fish-based products are prone to microbiological spoilage. Psychrotrophic *Pseudomonas* spp. including *Pseudomonas psychrophila*, whose metabolic activity is dependent on the quorum sensing system, are mainly responsible for spoilage. In quorum sensing system, autoinducers (AI) are recognized by receptor proteins that are transcriptional regulators of a specific group of genes. Interference in the above mechanism with essential oils and their components may affect the synthesis of enzymes and exopolysaccharides (EPS) or the process of lipids degradation by microorganisms. Anti-quorum sensing verification in *in vitro*, *in silico* and *in situ* systems may support the development of alternative/additional solutions in the future, aimed at eliminating or/and reducing the physiological activities of saprotrophic microorganisms in the food matrix.

The major aim of the current study was the assessment of the impact of tarragon (TEO) and black pepper (BPEO) essential oils on quorum sensing system and metabolic activity of *P, psychrophila* KM02 isolated from fish.

In the work, TEO and BPEO were obtained by hydrodistilation, and their chemical compositions were determined with the GC-MS system. Subinhibitory concentrations (suMIC) of essential oils and their major compounds were estimated with the serial dilutions method. GC-FID system was used for the assessment of the fatty acids profile of cellular envelopes. Anti-quorum sensing potential of analyzed factors were characterized by: (i) the estimation of the changes in AI synthesis with the UHPLC-MS/MS system, and (ii) the molecular docking analysis of major compounds of essential oils with receptor proteins.

The whole genome and transcriptome analyses were conducted in order to assess the *P. psychrophila* KM02 potential to grow/metabolic activity in the food matrix. Molecular docking and RT-qPCR analyses were used to evaluate the impact of the analyzed agents on quorum sensing-related efflux and T2SS systems. The degree of inhibition of proteolytic and lipolytic properties, and the reduction of EPS synthesis were verified with spectrophotometric and RT-qPCR analyses. The Koch plate method was used to characterize the growth of *P. psychrophila* KM02 in a model food product containing subMIC of TEO and BPEO.

In the work, the subMICs of TEO (70-75 μL/mL) and BPEO (100-135 μL/mL) interfered with the quorum sensing system and disturbed the metabolic activity of

examined microorganisms. The exposition of *Pseudomonas* spp. cells on tested agents resulted in the reduction of unsaturated fatty acids and with branched structure in cellular envelopes. *Pseudomonas* spp. synthesized AI belonging to AHL group (i.e. 3-oxo-C12-HSL, 3-oxo-C14-HSL, 3-oxo-C6-HSL, 3-oxo-C8-HSL, C12-HSL, C4-HSL, C6-HSL) and quinolone compound PQS *in vitro*. SubMICs of TEO, BPEO and their components (i.e. methyl eugenol (ME) 10-12 μL/mL, β-phellandrene (PHE), 8-10 μL/mL, limonene (LIM) 60-65 μL/mL and β-caryophyllene (CAR) 20-35 μL/mL) inhibited AI synthesis in *Pseudomonas* spp. ME, PHE, LIM and CAR bonded with the receptor proteins LasR, RhlR, TraR and PqsR of quorum sensing system and with proteins MFS, MexB and MuxB of efflux system of *Pseudomonas* spp. The genome and transcriptome of *P. psychrophila* KM02 showed the presence of factors indicating the the ability of the bacteria to decompose of proteins and lipids and secrete the enzymes. SubMIC of TEO, BPEO, ME, PHE, LIM and CAR reduced the proteolytic and lipolytic activity and EPS synthesis by *P. psychrophila* KM02. Tested agents introduced into vinegar-oil marinade inhibited *P. psychrophila* KM02 growth in fish-based product.

The current work showed impact of TEO and BPEO and major components, i.e. ME, PHE, LIM and CAR on quorum sensing system and metabolic activity of *P. psychrophila* KM02. The above relationship may delay the spoilage process of fish stored under refrigeration, in which *P. psychrophila* KM02 is involved. The results obtained in this work introduce new information about the quorum sensing system in saprotrophic bacteria isolated from foods

Key words: quorum sensing, fish spoilage, efflux system, molecular docking, genome, transcriptome

1. Wstęp

Wysoka wartość odżywcza ryb, a także ich stosunkowo niska cena i dostępność, determinują ciągły wzrost produkcji, która według prognoz ma osiągnąć 200 mln ton w 2029 roku. Rocznie około 44% całkowitej produkcji przemysłu rybnego to ryby świeże schłodzone i produkty o minimalnym stopniu przetworzenia, przechowywane w warunkach chłodniczych (Food and Agriculture Organization of the United Nations, FAO, 2018). Zastosowanie procesu chłodzenia nie gwarantuje zahamowania wzrostu lub/i aktywności metabolicznej specyficznej mikroflory ryb (Comi, 2017). Obecność białek i tłuszczów, pH w zakresie od 6,1 do 6,9 oraz aktywność wody powyżej 0,95 dodatkowo promują wzrost mikroorganizmów w surowcu. Powyższe własności sprawiają, że ryby łatwo ulegają mikrobiologicznemu zepsuciu.(Hassoun i Emir Çoban, 2017).

Za mikrobiologiczne psucie się świeżych schłodzonych ryb i produktów o minimalnym stopniu przetworzenia odpowiedzialne są głównie psychrotrofowe gatunki bakterii z rodzaju *Pseudomonas* (Raposo i in., 2017). Powyższe drobnoustroje są zdolne do rozkładu związków organicznych, co skutkuje zmianą tekstury oraz nieprzyjemnym zapachem produktów (Xie i in., 2018). Pomimo wdrożenia programów kontroli jakości w przemyśle spożywczym, około 30% złowionych ryb ulega utracie wskutek przedwczesnego zepsucia. Zjawisko to jest przyczyną strat ekonomicznych i wizerunku przedsiębiorstw (Ghaly i in., 2010). Dlatego konieczne jest wypracowanie nowych rozwiązań zapobiegających psuciu się produktów na bazie ryb powodowanemu przez *Pseudomonas* spp.

Aktywność metaboliczna *Pseudomonas* spp. jest regulowana przez system quorum sensing (Meliani i Bensoltane, 2015; Venturi, 2006), który szczegółowo został omówiony w publikacji P-1. W tym systemie cząsteczki sygnałowe (autoinduktory; AI) syntezowane przez komórki drobnoustrojów oddziałują z regulatorami transkrypcyjnymi, co kontroluje ekspresję genów w populacji (Papenfort i Bassler, 2016). Zgodnie z doniesieniami literaturowymi, quorum sensing reguluje nawet 10% genów ulegających ekspresji w komórkach *P. aeruginosa* i są to głównie geny, których produkty zaangażowane są w syntezę toksyn i enzymów oraz degradację tłuszczu (Schuster i in., 2003; Smith i in., 2004). System quorum sensing warunkuje również adaptację komórek do zasiedlanego środowiska (Schuster i Greenberg, 2006).

U *P. aeruginosa* AI należą głównie do grupy acylowanych laktonów homoseryny (AHL), które są syntezowane przez białka z rodziny LuxI. Cząsteczki AHL różnią się liczbą atomów węgla wchodzących w skład kwasu tłuszczowego, stopniem utlenienia i liczbą wiązań nienasyconych w nim występujących. W profilach AI u *Pseudomonas* spp. dominują: lakton N-3-okso-dodekanylo-homoseryny (3-okso-C12-HSL) oraz lakton N-butanoylo-L-homoseryny (C4-HSL), syntezowane odpowiednio przez białko LasI oraz RhlI (Skandamis i Nychas, 2012). Cząsteczki 3-okso-C12-HSL i C4-HSL tworzą specyficzne układy z białkami należącymi do rodziny LuxR: odpowiednio z receptorami LasR oraz RhlR (Myszka i Czaczyk, 2010).

Do AI *P. aeruginosa* należą także cząsteczki chinolowe powstające na skutek kondensacji antranilanu i β-ketododekanu. Zidentyfikowano ponad 50 różnych homologów 2-alkilo-4-chinolonu, lecz główne znaczenie w fizjologii drobnoustrojów mają 2-heptylo-3-hydroksy-4-chinolon (PQS) oraz jego prekursor 2-heptylo-4-chinolon (HHQ) (Diggle i in., 2007). Powyższe cząsteczki również oddziałują z białkami receptorowymi. Opisane układy tworzące system quorum sensing są wzajemnie powiązane i funkcjonują według określonej hierarchii (Lee i Zhang, 2015).

Rola quorum sensing w procesach wirulencji została bardzo dobrze opisana w literaturze (Sonbol i in., 2022); niewiele badań wykonano celem określenia wpływu tego systemu na aktywność metaboliczną saprofitycznych gatunków *Pseudomonas* spp. Obecność cząsteczek AI zidentyfikowano w zepsutych rybach przechowywanych na lodzie, produktach wędzonych na zimno oraz burgerach rybnych (Bai i Rai, 2011), a stopień zepsucia skorelowano ze stężeniem AI (Li i in., 2016).

Pseudomonas spp. syntezują metaloproteazy, które uczestniczą w degradacji tkanki ryb. Proces ten prowadzi do wzrostu udziału wolnych aminokwasów i lotnych związków siarkowych oraz do zmiany tekstury produktu (Venugopal, 1990; Sterniša i in., 2020b). Wykazano, że w żywności bogatej w białko występują cząsteczki AHL, a ich obecność jest powiązana z aktywnością proteolityczną mikroflory (Ammor i in., 2008). Przykładowo cząsteczki AHL były obecne w filetach pstrąga tęczowego, z którego wyizolowano *P. fluorescens* i *P. putida* (Bai i Rai, 2011). Dodatek syntetycznych C4-HSL oraz C14-HSL promował aktywność proteolityczną *P. fluorescens* w próbach schłodzonego turbota. Odnotowano również istotne zmiany parametru całkowitego lotnego azotu zasadowego (TVB-N) do wartości przekraczającej dopuszczalny poziom (Li i in., 2018). Podobnie w pracy Liu i in. (2007) zauważono, że cząsteczki C4-HSL oraz 3-okso-C8-HSL powodują nadekspresję genu kodującego

metaloproteazę *aprX* u *P. fluorescens* wyizolowanego z mleka. U mutantów delecyjnych *P. fluorescens*, *ΔluxI* i *ΔluxR*, aktywność proteolityczna była wyraźnie zredukowana w stosunku do komórek niepoddanych mutagenezie (Tang i in., 2019).

Komórki *Pseudomonas* spp. izolowane z ryb charakteryzują się również zdolnością syntezy enzymów lipolitycznych, odpowiadających za hydrolizę tłuszczu do glicerolu i wolnych kwasów tłuszczowych (Ge i in., 2017). Procesy degradacji tłuszczu w rybach skutkują niekorzystną zmianą zapachu (Comi, 2017). Lipazy kodowane są przez geny *lipA* oraz *lipB*, których ekspresja regulowana jest systemem quorum sensing (Christensen i in., 2003). Powyższą zależność potwierdziły badania przeprowadzone przez Myszka i in., (2021) oraz Bai i Rai (2014). Ponadto Riedel i in. (2001) wykazali, że system sekrecyjny Lip, odpowiedzialny za skuteczne wydzielanie lipaz również jest regulowany przez system quorum sensing. U *P. fluorescens* aktywność lipaz generuje zmianę zapachu, „mydlany" posmak i inne wady jakościowe ryb (Beven i in., 2001). Wprowadzenie egzogennych cząsteczek AHL do pożywek skutkowało wzrostem poziomu transkrypcji genów *lipA* oraz *lipB* w komórkach *Brukholderia cenocepacia* (Udine i in., 2013).

System quorum sensing reguluje proces tworzenia biofilmu bakteryjnego, szczególnie etap adhezji pojedynczych komórek do powierzchni stałych i dojrzewanie błon biologicznych (Warrier i in., 2021). Wpływ 3-okso-C12-HSL na dojrzewanie biofilmu *P. aeruginosa* opisali Cherepushkina i in. (2021) oraz Davies i in. (1998). W pracy Davies i in. (1998), szczepy *P. aeruginosa*, które nie produkowały cząsteczek 3-okso-C12-HSL, nie były zdolne do tworzenia trójwymiarowej struktury biofilmu. Biofilm utworzony przez mutanty delecyjne *ΔlasI* łatwo ulegał dyspersji w wyniku działania dodecylosiarczanu sodu (Davies i in., 1998). Cherepushkina i in. (2021) wykazali, że wprowadzenie egzogennej cząsteczki 3-okso-C12-HSL do hodowli *P. aeruginosa* promuje wzrost komórek i tworzenie biofilmu.

W procesie tworzenia biofilmu istotne znaczenie mają: mechanizmy ruchu, warunkujące zbliżanie się komórek do powierzchni docelowej oraz synteza egzopolisacharydów (EPS) i ramnolipidów (Rasamiravaka i in., 2015). Zadaniem EPS jest utrzymywanie komórek w bliskim sąsiedztwie (Vetrivel i in., 2021). Produkcja ramnolipidów wpływa na tworzenie mikrokolonii i utrzymywanie otwartej struktury mikrokolonii (Pamp i Tolker-Nielsen, 2007). Synteza EPS i ramnolipidów u *Pseudomonas* spp. jest również zależna od systemu quorum sensing (Li i in. 2018).

Powiązanie aktywności metabolicznych bakterii z quorum sensing wywołało zainteresowanie poszukiwaniem związków hamujących/zaburzających ten system (Bai i Rai, 2011). Ich zastosowanie w przetwórstwie ryb znacznie pomogłoby w wysiłkach podejmowanych na rzecz ograniczenia aktywności metabolicznej drobnoustrojów psujących żywność i ostatecznie wydłużenie okresu przydatności do spożycia produktów. Te podejścia w przeciwieństwie do zabiegów bakteriobójczych wywierają mniejszą presję selekcyjną wobec drobnoustrojów i zmniejszają prawdopodobieństwo rozwoju zjawiska oporności (Bai i Rai, 2014).

Szczegółowy opis sposobów ingerencji w system quorum sensing przedstawiono w publikacji P-1. Ocena działania przeciw-quorum sensing polega przede wszystkim na wykazaniu zdolności badanego czynnika do zaburzania syntezy AI (Bouyahya i in., 2022). Wśród związków o działaniu przeciw-quorum sensing wyróżnia się enzymy z klasy laktonaz, acylaz i oksydoreduktaz. Ich aktywność może powodować degradację AI, inaktywację syntaz AI i/lub modyfikację AI (Fetzner, 2015). W pracach Rémy i in. (2020) i Wahjudi i in. (2011), laktonazy i acylazy hamowały syntezę C4-HSL i 3-oxo-C12-HSL u *P. aeruginosa*. Natomiast modyfikacje łańcucha acylowego w wyniku aktywności oksydoreduktaz zaburzały wytworzenie kompleksu AI z białkiem LasR (Chen i in., 2013; Bijtenhoorn i in., 2011).

Związki o działaniu przeciw-quorum sensing mogą również oddziaływać z białkami receptorowymi (Zhou i in., 2020). Wraz z rozwojem technik komputerowych możliwa stała się ocena potencjału różnych związków do wiązania się z białkami LasR, RhlR i innymi, kluczowymi w regulacji metabolizmu drobnoustrojów. Wykorzystanie wirtualnego screeningu jest znacznie szybsze i efektywniejsze w stosunku do analiz laboratoryjnych i pozwala na efektywną selekcję potencjalnych inhibitorów quorum sensing (Sadiq i in., 2020). Dokowanie molekularne w ocenie ingerencji w system quorum sensing wykorzystywali m.in. Hong i in. (2021), Yu i in. (2022), Zhou i in. (2020). Doświadczenia te polegały na porównaniu siły powinowactwa oraz sposobu wiązania (konformacji oraz orientacji cząsteczki w miejscu wiązania) badanych związków z białkami receptorowymi. Podobne podejście analityczne można zastosować w przypadku badania inhibicji systemu efflux oraz systemu sekrecyjnego typu II (T2SS), które są ściśle powiązane z systemem quorum sensing (Pena i in., 2019; Seukep i in., 2019). Powyższe systemy są niezbędne w procesach wymiany cząsteczek między komórką o środowiskiem zewnętrznym (Sionov i Steinberg, 2022). Wykazano, że związki będące potencjalnymi inhibitorami systemu efflux są zdolne do blokowania

transportu komórkowego. W ten sposób zaburzona zostaje sekrecja AI oraz sekrecja enzymów produkowanych przez komórki drobnoustrojów (Agreles i in., 2021). Przykładowo, naringenina konkurując z cząsteczką 3-okso-C12-HSL o miejsce wiązania białka LasR, doprowadziła do inhibicji syntezy czynników wirulencji u *Pseudomonas* spp. (Hernando-Amado i in., 2020).

W literaturze szczególną uwagę zwrócono na olejki eteryczne w aspekcie ingerencji w system quorum sensing drobnoustrojów (Deryabin i in., 2019). Ich aplikacja w żywności pochodzenia morskiego wpisuje się w aktualny trend zainteresowania żywnością pozbawioną syntetycznych dodatków (Hassoun i Emir Çoban, 2017). W skład olejków eterycznych wchodzą głównie związki terpenowe, odpowiadające zarówno za intensywny zapach jak i działanie przeciwdrobnoustrojowe (Yu i in., 2020). Aktywność biologiczna olejku eterycznego jest ściśle związana z jego stężeniem (Pandey i in., 2017). Stężenia olejków eterycznych wymagane do całkowitej inaktywacji komórek mikroorganizmów w żywności mogą powodować niekorzystne zmiany organoleptyczne. W związku z tym proponuje się stosowanie stężeń subinhibicyjnych (subMIC), aby zapewnić równowagę między akceptowalnością sensoryczną a skutecznością przeciwdrobnoustrojową (Leite de Souza, 2016). Istotny jest również fakt wykorzystania w żywności olejków eterycznych pozyskanych z surowców stosowanych jako przyprawy, aby zachować naturalny charakter produktu (Kalia, 2013; Macwan i in., 2016).

Działanie przeciw-quorum sensing olejków eterycznych opiera się głównie na ingerencji w syntezę cząsteczek AI oraz inaktywacji białek receptorowych na skutek oddziaływania z miejscem wiązania właściwych AI. Powyższe działanie wykazano dla olejku eterycznego z mirtu, jałowca, oregano, majeranku, tymianku, szałwii czy rozmarynu (Myszka i in., 2020; Myszka i in., 2021; Camele i in., 2019; Kerekes i in., 2013). Natomiast niewiele badań wykonano celem określenia wpływu olejku eterycznego z estragonu i pieprzu czarnego do hamowania aktywności quorum sensing u *Pseudomonas* spp.

Podsumowując, olejki eteryczne stanowią naturalne źródło związków o działaniu przeciwdrobnoustrojowym oraz przeciw-quorum sensing; mogą z powodzeniem zastępować chemiczne środki konserwujące żywność. Ograniczeniem ich wykorzystania w żywności jest silny aromat, który może negatywnie wpływać na cechy organoleptyczne produktu. Dlatego konieczne jest prowadzenie badań nad aktywnością biologiczną olejków eterycznych zastosowanych w stężeniach subMIC wobec komórek drobnoustrojów psujących żywność (Kalia, 2013; Koh i in., 2013).

2. Hipotezy badawcze i cele pracy

Celem głównym niniejszej pracy była ocena wpływu TEO i BPEO na system quorum sensing i aktywność metaboliczną bakterii *P. psychrophila* KM02 wyizolowanej z ryb.

Cele szczegółowe pracy obejmowały:

C1. Ocenę aktywności przeciwdrobnoustrojowej TEO i BPEO oraz ich składników bioaktywnych wobec *Pseudomonas* spp. poprzez wyznaczenie stężeń subMIC oraz ocenę zmian w profilu kwasów tłuszczowych osłon komórkowych;

C2. Ocenę zdolności syntezy AI przez *Pseudomonas* spp.

C3. Określenie potencjału przeciw-quorum sensing TEO i BPEO w oparciu o analizę zmian syntezy AI oraz komputerową ocenę stopnia wiązania głównych składników olejków eterycznych z białkami receptorowymi quorum sensing *Pseudomonas* spp.;

C4. Analizę całego genomu i całego transkryptomu *P. psychrophila* KM02 pod kątem obecności czynników determinujących wzrost/aktywność metaboliczną komórek w matrycy żywności;

C5. Ocenę wpływu TEO, BPEO oraz ich składników bioaktywnych na system efflux i T2SS *P. psychrophila* KM02 w warunkach *in situ*;

C6. Ocenę wpływu TEO, BPEO oraz ich składników bioaktywnych na właściwości proteolityczne, lipolityczne i syntezę EPS przez *P. psychrophila* KM02 w warunkach *in vitro* oraz *in situ*;

C7. Ocenę wzrostu *P. psychrophila* KM02 w modelowym produkcie spożywczym, suplementowanym subMIC TEO i BPEO.

Niniejsza praca podejmuje próbę wyjaśnienia czy poprzez zaburzanie systemu quorum sensing można wpłynąć selekcyjnie na metabolizm komórek *Pseudomonas* spp. i ograniczyć procesy psucia się żywności? Zaplanowane zadania badawcze umożliwiły sformułowanie następujących hipotez badawczych:

H1. Stężenia subMIC TEO i BPEO ingerują w system quorum sensing u *Pseudomonas* spp. wyizolowanych z żywności.

H2. Skutkiem ingerencji w system quorum sensing przez TEO i BPEO jest zaburzanie aktywności metabolicznych komórek *P. psychrophila* KM02, odpowiedzialnych za psucie się żywności.

H3. Zaburzanie aktywności metabolicznych komórek *P. psychrophila* KM02 kształtuje jakość mikrobiologiczną ryb.

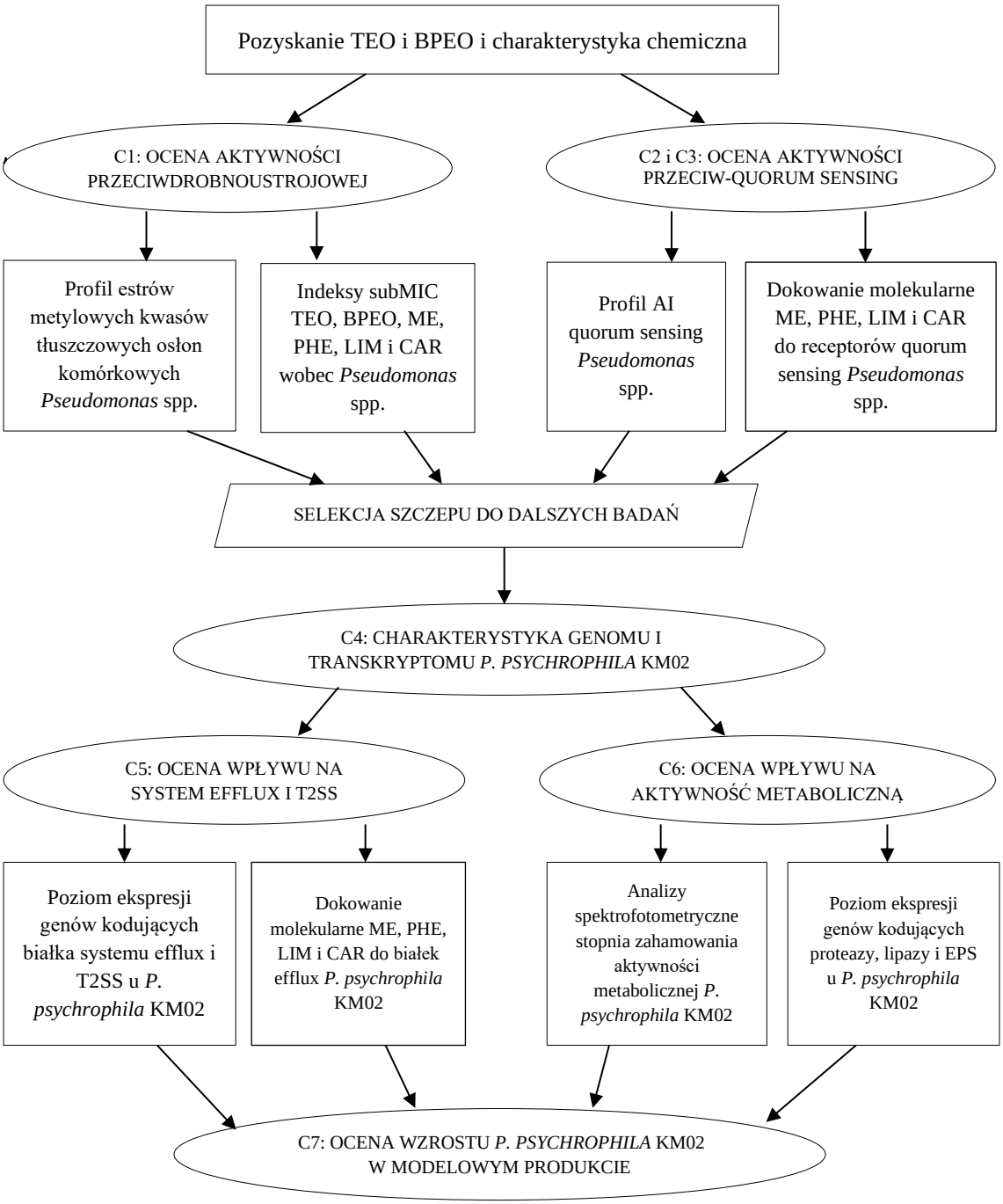

Rycina 1. Schemat badań

3. Część doświadczalna

3.1. Drobnoustroje wykorzystane w badaniach

W początkowych etapach pracy obejmujących badanie aktywności przeciwdrobnoustrojowej i przeciw-quorum sensing olejków eterycznych wykorzystano trzy gatunki bakterii należących do rodzaju *Pseudomonas* spp. – *P. fluorescens* KM148, *P. orientalis* KM249 oraz *P. psychrophila* KM02. Drobnoustroje wyizolowano z prób świeżego łososia atlantyckiego (*Salmo salar*) dostępnego w handlu. W procedurze izolacji wykorzystano pożywkę Pseudomonas CFC Agar zgodnie z Normą PN-EN ISO 13720:2010. Proces inkubacji prowadzono w temperaturze 4 ± 1°C przez 72 h. Uzyskane izolaty zidentyfikowano poprzez sekwencjonowanie i analizę polimorfizmu restrykcyjnych długości amplikonu genu 16S rRNA. Drobnoustroje zdeponowano w Katedrze Biotechnologii i Mikrobiologii Żywności Uniwersytetu Przyrodniczego w Poznaniu. Drobnoustrojem wykorzystanym we wszystkich analizach był szczep *P. psychrophila* KM02.

3.2. Materiał roślinny

W badaniach wykorzystano wysuszone ziarna pieprzu czarnego (*Piper nigrum* L.) oraz wysuszone liście estragonu (*Artemisia dracunculus* L.) pochodzące odpowiednio z upraw konwencjonalnych w Wietnamie i w Hiszpanii. Materiał zakupiono od lokalnego dostawcy gwarantującego jednorodność materiału.

3.3. Pożywki

W celu ożywiania szczepów, prowadzenia hodowli kontrolnych, wyznaczenia indeksów subMIC oraz prowadzenia hodowli przeznaczonej do sekwencjonowania genomu wykorzystywano bulion tryptozowo-sojowy (TSB) (BD Bioscences, USA) o składzie: trzustkowy hydrolizat kazeiny 17,0 g/L, enzymatyczny hydrolizat sojowy 3,0 g/L, chlorek sodu 5,0 g/L, wodorofosforan (V) potasu 2,5 g/L oraz glukoza 2,5 g/L. Wartość pH pożywki wynosiła 7,0.

Przy profilowaniu transkryptomu wykorzystano zmodyfikowaną pożywkę TSB (zTSB), w której zastąpiono trzustkowy hydrolizat kazeiny oraz enzymatyczny hydrolizat sojowy peptonem wytworzonym z ryby (HiMedia, Niemcy) w ilości 20.0 g/L. Pozostałe składniki pożywki: chlorek sodu, wodorofosforan (V) potasu oraz

glukozę wprowadzono w ilościach odpowiadających standardowemu składowi podłoża TSB. Odczynniki zakupiono w Sigma-Aldrich (USA). W celu zbadania poziomu mRNA genów kodujących białka systemu efflux oraz T2SS zmodyfikowaną pożywkę TSB suplementowano kwasem nalidyksowym (NA) (Biomaxima, Polska) w stężeniu 30 μg/mL. Wartość pH pożywki wynosiła 7,0.

Do hodowli *Pseudomonas* spp mających na celu odtworzenie ekosystemu produktów z ryb, wykorzystano pożywkę wg. Dalgaard, (1995) (FJM). Porcję ryby o masie 1000g pozbawioną części stałych zawieszano w 500 mL wody wodociągowej i poddano homogenizacji w urządzeniu Pulsifier (Microgen Bioproducts, Wielka Brytania). Próby sączono przez jałową gazę i suplementowano buforem fosforanowym 0,10 M, diwodorofosforanem (V) potasu 0,056 M i wodorofosforanem (V) potasu 0,044 M. Odczynniki zakupiono w POCH (Polska). Po wyjałowieniu (121°C, 15 min) pożywkę wzbogacono tlenkiem trimetyloaminy 1,6 g/L, L-cysteiną 40 mg/L oraz metioniną 40 mg/L. Odczynniki zakupiono w Sigma-Aldrich (USA).

3.4. Warunki hodowli

Pobrane z depozytu zamrożone szczepy bakterii wprowadzano do probówek typu eppendorf i wstępnie namnażano w podłożu TSB. Hodowle prowadzone na podłożu TSB (warunki *in vitro*) oraz w FJM (warunki *in situ*) suplementowano TEO i BPEO oraz składnikami bioaktywnymi: metyleugenolem (ME), β-felandrenem (PHE), limonenem (LIM) oraz β-kariofilenem (CAR). Procedurę otrzymywania olejków eterycznych opisano w podrozdziale 3.5.1. Roztwory olejków eterycznych i ich składników bioaktywnych przygotowywano w dimetylosulfotlenku (DMSO) (POCH, Polska), którego udział w hodowli *Pseudomonas* spp. nie przekraczał 1%. Wszystkie hodowle inkubowano w 4 ± 1°C przez 72 h.

3.5. Metody badań

3.5.1. Hydrodestylacja TEO i BPEO i charakterystyka składu chemicznego techniką GC-MS

Proces hydrodestylacji olejków eterycznych prowadzono w aparacie Clevengera. Masę 100g materiału roślinnego, rozdrobnionego w moździerzu, umieszczano w kolbie okrągłodennej o pojemności 1000 mL i następnie uzupełniano wodą destylowaną do pojemności 500 mL. Zawartość kolby aparatu Clevengera

utrzymywano w stanie wrzenia przez około 2-3 h. Otrzymane olejki eteryczne z odbieralnika pobierano do fiolek z ciemnego szkła i szczelnie zamykano. Skład chemiczny pozyskanych olejków eterycznych oceniano techniką chromatografii gazowej (Hewlett-Packard HP 7890A, USA) sprzężonej ze spektrometrią mas (Agilent Technologies 5975C, USA). W pracy do rozdziału chromatograficznego wykorzystano kolumny kapilarne: Supelcowax-10 (30 m×0,25 mm×0,5 μm) oraz DB-5 (30 m x 0,25 mm x 0,25 um). Gazem nośnym był hel o stałym przepływie wynoszącym 0,8 mL/min. Do rozdziału zastosowano następujący program temperaturowy: temperatura początkowa pieca 40°C (2 min.) podniesiona do 240°C z szybkością 8°C/min i utrzymywana przez 6 min. Nastrzyk wykonano w trybie podziału strumienia 20:1 (split) w temperaturze 220°C. Temperatura źródła jonów wynosiła 220°C a widma masowe rejestrowano w zakresie skanowania m/z 30-350. Związki identyfikowano, porównując indeksy retencji (*retention index*, RI) i widma masowe z RI i widmami masowymi wzorców. Dodatkowo przeprowadzono wstępną identyfikację związków olejków eterycznych poprzez porównanie ich widm masowych z danymi spektralnymi oraz RI dostępnymi w bazie NIST 05. RI dla każdego związku oceniano na podstawie szeregu homologicznego n-alkanów C6-C16. Oznaczenia wykonano we współpracy z Zespołem Pracowni Badania Związków Lotnych i Aktywnych Sensorycznie Uniwersytetu Przyrodniczego w Poznaniu.

3.5.2. Wyznaczenie indeksów subMIC TEO, BPEO, ME, PHE, LIM i CAR względem *Pseudomonas* spp.

Wartości indeksów subMIC olejków eterycznych oraz składników bioaktywnych wyznaczano metodą seryjnych rozcieńczeń zgodnie z rekomendacjami The Clinical and Laboratory Standards Institute (CLSI, 2012). W oznaczeniach wykorzystano zawiesiny *Pseudomonas* spp. o gęstościach odpowiadających 0,5 McFarlanda. Jałowe podłoże TSB oraz jałowe podłoże TSB suplementowane wybranymi stężeniami olejków eterycznych i składnikami bioaktywnymi wykorzystano jako próby kontrolne. Ocenę makroskopową wzrostu drobnoustrojów dokonano po procesie inkubacji prowadzonej w temperaturze 4°C przez 72h.

3.5.3. Ekstrakcja kwasów tłuszczowych i ich identyfikacja techniką GC-FID

Ekstrakcję kwasów tłuszczowych z osłon komórkowych bakterii *Pseudomonas* spp. eksponowanych na działanie subMIC olejków eterycznych prowadzono według metodyki opisanej w pracy Whittaker i in., (2005). Drobnoustroje zawieszano w 3,75 N roztworze NaOH i ogrzewano przez 30 min. we wrzącej łaźni wodnej. Po schłodzeniu, do prób wprowadzano 3,25 N roztwór HCl i ogrzewano w temperaturze 80°C przez 10 min. Kwasy tłuszczowe ekstrahowano mieszaniną heksanu i eteru metylo-*tert*-butylowego. Do uzyskanej warstwy organicznej dodawano 3 mL roztworu NaOH.

Profil chemiczny kwasów tłuszczowych *Pseudomonas* spp. oceniono techniką chromatografii gazowej z detekcją płomieniowo-jonizacyjną ((GC-FID) (Thermo Scientific TRACE 1300, USA)). W badaniach wykorzystano kolumnę kapilarną HP-5MS 30 m x 0.25 mm x 0.25 μm (Agilent Technologies, USA) i autosampler AI/AS 1310 (Thermo Scientific, USA). Próbki wstrzykiwano w trybie splitless, a gazem nośnym był wodór o stałym przepływie 35 mL/min. Czasy retencji porównywano z danymi uzyskanymi dla standardów bakteryjnych estrów metylowych kwasów tłuszczowych (BAME Mix; Sigma Aldrich, USA) w identycznych warunkach rozdziału.

3.5.4. Ekstrakcja AI systemu quorum sensing *Pseudomonas* spp. i ich identyfikacja techniką UHPLC-MS/MS

Cząsteczki AI ekstrahowano z płynów pohodowlanych *Pseudomonas* spp. według procedury opisanej przez Ravn i in., (2001). Po odwirowaniu (3000 g, 10 min) hodowli, supernatant filtrowano przez sterylny filtr Millex-GP (Millipore, USA) o średnicy porów 0,22 μm. Próby traktowano mieszaniną octanu etylu i kwasu mrówkowego w stosunku 99,5:0,5, a następnie odparowywano w wyparce i przechowywano w temperaturze -20°C. Profile AI systemu quorum sensing należące do grupy AHL i związków chinolowych oceniano przy pomocy wysokosprawnej chromatografii cieczowej sprzężonej ze spektrometrią mas (UHPLC-MS/MS) (Dionex UltiMate 3000 (Thermo Fisher Scientific, USA) z systemem qTOF (maXis impact Bruker Daltonic, Niemcy) w układzie odwróconych faz z kolumną Kinetex™ 1,7 μm C18 100 Å 100 x 2,1 mm (Phenomenex Torrance, USA). Ekstrakty zawieszano w 99,9% metanolu i wprowadzano do układu. Fazą ruchomą był 5 mM wodny roztwór

octanu amonu, zawierający 0,1 % kwas octowy (A) oraz 5 mM metanolowy roztwór octanu amonu, zawierający 0,1 % kwas octowy. Związki identyfikowano na podstawie czasów retencji standardów: 3-oxo-C12-HSL, 3-oxo-C14-HSL, 3-oxo-C6-HSL (LOD 0,005 μg/mL), 3-oxo-C8-HSL, C12-HSL, C4-HSL i C6-HSL (LOD 0,004 μg/mL), HHQ (LOD 0.0002 μg/mL) i PQS (LOD 0.0001 μg/mL) oraz mas jonów pseudomolekularnych. Analiza strukturalna widm fragmentacyjnych była wspomagana narzędziami informatycznymi CSI:FingerID (Lehrstuhl Bioinformatik Jena, Niemcy) oraz Met-Frag (Leibniz Institute of Plant Biochemistry, Halle, Niemcy). Analizy ilościowe prowadzono z wykorzystaniem krzywych kalibracyjnych. Oznaczenia wykonano we współpracy z Zespołem Pracowni Fermentacji i Biosyntezy Uniwersytetu Przyrodniczego w Poznaniu.

3.5.5. Modelowanie *in silico* dokowania ME, PHE, LIM i CAR do receptorów systemu quorum sensing u *Pseudomonas* spp. oraz białek efflux

Analizy dokowania molekularnego przeprowadzono według metody opisanej przez Kumar i in., (2015). W pracy zastosowano program komputerowy Schrödinger (wersja 11.7 i 12.6, Schrödinger, USA). Trójwymiarowe cząsteczki ligandów: AI: 3-oxo-C12-HSL (CID: 3246941), C4-HSL (CID: 10130163), 3-oxo-C8-HSL (CID: 4476497) oraz PQS (CID: 2763159); związków bioaktywnych olejków eterycznych: ME (CID: 7127), PHE (CID: 11142), CAR (CID: 5281515) oraz LIM (CID: 22311); inhibitorów quorum sensing i systemu efflux: C30-furanon (CID:10131246), 3-amino-7-chloro-2-nonylochinazolin-4-onu (CID: 71627415) oraz 3,7-dimetyloksantyny (CID: 71627415) pobrano z bazy danych PubChem. Struktury krystalograficzne receptorów LasR (PDB ID: 2UV0), TraR (PDB ID: 1H0M) oraz PqsR (PDB ID: 4JVI) pozyskano bezpośrednio z bazy Protein Data Bank (PDB). Struktury białek RhlR (ID: P54292), Mfs (WP_048352147.1) MexB (WP_048351074.1) oraz MuxB (WP_019828952.1) modelowano przy użyciu programu I-Tasser (Roy i in., 2010; Yang i in., 2015; Zhang, 2008) wykorzystując sekwencje aminokwasowe pozyskane z bazy UniProt oraz NCBI. W zależności od wariantu, do struktur krystalograficznych dodano atomy wodoru, określano stany protonacyjne aminokwasów (LYS, ARG, HIS, ASP, GLU), przypisano ładunki do atomów oraz przypisano brakujące łańcuchy boczne (Madhavi Sastry i in., 2013). Struktury białek minimalizowano do domyślnej wartości pola siłowego OPLS3e

średniego odchylenia kwadratowego (RMSD; Root Mean Square Deviation) wynoszącego 0,30 Å od hydrofobowych miejsc wiążących (Harder i in., 2016). Następnie generowano tzw. siatki dokowania: w przypadku białek LasR, TraR i PqsR były to znane miejsca aktywne, natomiast dla białek RhlR, Mfs, MexB i MuxB wykorzystano analizę optymalnych hydrofobowych miejsc wiążących. Dokowanie prowadzono z wykorzystaniem modu Extra Precision z elastycznym próbkowaniem w wyznaczonych siatkach dokujących (Friesner i in., 2006). Wyboru konformacji danego ligandu względem białka dokonano na podstawie wartości Emodel, natomiast dla porównania siły wiązania ligand-receptor wykorzystano wartości XP GlideScore.

3.5.6. Izolacja genomowego DNA *P. psychrophila* KM02 i sekwencjonowanie WGS

Do izolacji genomowego DNA *P. psychrophila* KM02 wykorzystano zestaw odczynników QIagen DNeasy Blood and Tissue (Qiagen, Niemcy) i postępowano zgodnie z instrukcją dostarczoną przez producenta. Sekwencjonowanie przeprowadzono w komercyjnym laboratorium Genomed S.A. w Warszawie. Sekwencjonowanie przeprowadzono dwoma metodami: MiSeq (Illumina, USA) oraz MinION (Oxford Nanopore Technologies, Wielka Brytania). Przy sekwencjonowaniu na urządzeniu MiSeq (Illumina, USA) wykorzystano zestaw odczynników Nextera XT DNA library 300-bp paired-end preparation kit (Ilumina, USA). Sekwencjonowanie nanoporowe prowadzono na urządzeniu MinION (Oxford Nanopore Technologies, Wielka Brytania) z zastosowaniem odczynników SQK-NSK007 Rapid Sequencing kit. Surowe dane sekwencjonowania analizowano przy użyciu programu CLC Genomics Workbench v. 20.0 i CLC Microbial Genomics Module v. 20.0 (Qiagen, USA). Składanie *de novo* genomu *P. psychrophila* KM02 prowadzono z połączonych odczytów z platformy MiSeq i MinION. Złożoną sekwencję chromosomu bakteryjnego wprowadzono do bazy NCBI GenBank pod numerem NZ_CP049044.1. Porównanie całego genomu z sekwencjami pokrewnych gatunków wykonano przy użyciu Mauve 2.4.023 (Darling i in., 2004), a wizualizację genomu utworzono za pomocą GView Server (Petkau i in., 2010). Analizę pangenomu pod względem rozkładu klastrów ortologicznych grup białek (*Clusters Of Orthologs*, COG) przeprowadzono przy użyciu narzędzia BPGA 1.3 (Chaudhari i in., 2016). Sekwencje kodujące białka (CDS) przypisano do sekwencji całego genomu *P. psychrophila*

KM02 za pomocą narzędzia Find Procaryotic Genes w module CLC Microbial Genomics. Adnotacje funkcjonalne uzyskanych CDS przypisano za pomocą narzędzia SwissPROT z anotacjami ontologii genowych (*gene ontology*; GO) oraz bazą rodzin białkowych Pfam. Rozkład COG genomu obliczono za pomocą serwisu WebMGA (Wu i in., 2011). Dodatkowo przeprowadzano analizę genomu za pomocą narzędzia bioinformatycznego CARD (*The Comprehensive Antibiotic Resistance Database*) (Alcock i in., 2019) i RAST (*Rapid Annotations using Subsystems Technology*) (Aziz i in., 2008) w celu określenia obecności genów systemu efflux i warunkujących oporność *P. psychrophila* KM02 na środki przeciwdrobnoustrojowe. Oznaczenia wykonano we współpracy z Zespołem Katedry Biochemii i Biotechnologii Uniwersytetu Przyrodniczego w Poznaniu.

3.5.7. Izolacja RNA *P. psychrophila* KM02 do profilowania transkryptomu i sekwencjonowanie RNA-seq

Izolację całkowitego komórkowego RNA z hodowli *P. psychrophila* KM02 przeprowadzono zestawem odczynników RNAqueous Kit (Thermo Fisher Scientific, USA) zgodnie z instrukcją dostarczoną przez producenta. RNA rybosomalne usunięto z próby za pomocą Ribominus Transcriptome Isolation Kit (Invitrogen, USA). Biblioteki przygotowano stosując odczynnik Collibri Stranded RNA Library Prep Kit (Invitrogen, USA). Uzyskane biblioteki przed sekwencjonowaniem szacowano ilościowo na podstawie pomiaru fluorymetrycznego na urządzeniu Qubit (Thermo Fisher Scientific, USA) i na elektroforegramie bioanalizatora DNA (Agilent Technologies, USA). Sekwencjonowanie prowadzono w technologii sekwencjonowania przez syntezę na urządzeniu MiSeq (Ilumina, USA) zestawem odczynników MiSeq Reagent kit v3 (Ilumina, USA). Uzyskane dane analizowano przy użyciu programu CLC Genomics Workbench oraz zdeponowano w bazie NCBI SRA (Bioproject: PRJNA509367, Biosample: SRX9799402; SRA: SRR13376050). Po zmapowaniu odczytów do genomu referencyjnego *P. psychrophila* KM02 (NZ_CP049044.1), analizowano poziom transkrypcji genów, normalizując współczynnikiem RPKM (*reads per kilobase per milion mapped reads*). Bazę danych Pfam wykorzystano przy klasyfikacji rodzin i domen białek. Funkcję transkryptów określono za pomocą adnotacji bazy danych GO. Oznaczenia wykonano

we współpracy z Zespołem Katedry Biochemii i Biotechnologii Uniwersytetu Przyrodniczego w Poznaniu.

3.5.8. Charakterystyka genów, izolacja RNA i oznaczenie ich względnej ekspresji techniką RT-qPCR

Zmiany w poziomie mRNA wybranych genów analizowano za pomocą techniki reakcji łańcuchowej polimerazy z odwrotną transkrypcją w czasie rzeczywistym (RT-qPCR). Startery do reakcji PCR zaprojektowano w programie CLC Genomics Workbench (wersja 20.0, Qiagen USA) oraz narzędziem Primer-BLAST (Ye i in., 2012) w serwerze NCBI na podstawie sekwencji genomu *P. psychrophila* KM02. Charakterystykę wszystkich analizowanych genów przedstawiono w Tabeli 1.

Hodowle traktowano odczynnikiem RNAprotect® Bacteria Reagent (Qiagen, Niemcy). W procedurze izolacji mRNA wykorzystano zestaw odczynników PureLink™ RNA Mini Kit (Thermo Fisher Scientific, USA). Uzyskane mRNA oczyszczano zestawem odczynnikowym PureLink™ DNase Set (Invitrogen, USA) zgodnie z protokołem dostarczonym przez producenta. Stężenie oraz jakość wyizolowanego mRNA oznaczono fluorymetrycznie stosując odczynniki Qubit™ XR RNA oraz Qubit™ IQ RNA (Thermo Fisher Scientific) na urządzeniu Qubit 4 (Thermo Fisher Scientific, USA). Odwrotną transkrypcję przeprowadzono zestawem odczynników High Capacity RNA-to-cDNA (Life Technologies, USA) zgodnie z instrukcją załączoną przez producenta. Analizy RT-qPCR prowadzono w systemie CFX96 (BioRad, USA) z wykorzystaniem zestawu odczynników GoTaq® Master Mix (Promega, Niemcy). Wydajność amplifikacji określano w programie komputerowym LinRegPCR (Ruijter i in., 2009). Ekspresję badanych genów normalizowano względem genu referencyjnego kodującego podjednostkę 16S rRNA. W obliczeniach wykorzystano metodą opisaną przez Pfaffl (2001).

Tabela 1. Charakterystyka genów analizowanych w pracy

Nazwa genu	Definicja/przewidywana rola genu	Sekwencja startera przedniego (5'-3')	Sekwencja startera wstecznego (5'-3')	Tm (°C)	Wielkość (pz)
16S rRNA	mała podjednostka rybosomalnego RNA, gen referencyjny	GGAGACTGCCGGTGACAAACT	TGTAGCCCAGGCCGTAAGG	56	75
muxA	błonowe białko infuzyjne należące do system efflux typu RND, część kompleksu MuxABC-OpmB	GTGTACTTCAAGGCGCTG	TTGACCATCTGCCCTTCC	57	110
opmB	białko efflux błony zewnętrznej, współpracujące z systemem MuxABC w wypływie substancji na zewnątrz komórki	GGCAGAGGTGGATCGTAA	CACCTTCAATTGCACCAT	54	112
mexA	błonowe białko infuzyjne należące do system efflux typu RND, część kompleksu MexAB-OprM	CCTTTTACCTTGACCACC	TTTTACATCGCTGCCTTC	53	120
oprM	białko efflux błony zewnętrznej, współpracujące z systemem MexAB w wypływie substancji na zewnątrz komórki	AGAACTACTTTGCAACCGA	GTTTCAGCAGCTCTTTGT	55	108
tetR	lokalny represor transkrypcyjny regulujący funkcjonowanie systemu efflux	TGTGTTTTCGCGCTTTCT	GTAACTCTTCAAGGCTGGG	57	101
marR	globalny represor transkrypcyjny regulujący oporność na antybiotyki	AAGGTGCTGATTATCATGG	AGCTTTTTTTGCTCGAGG	54	119
tadB1	wewnątrzbłonowe białko należące do rodziny F T2SS	CCCAGTACCAAAGCCGTCAT	CAACGTTCAGATGGGGGTGA	60	231
tadC1	wewnątrzbłonowe białko należące do rodziny F T2SS transportuje białka na powierzchnię komórki/przestrzeni pozakomórkowej	TGCTGAAGAATCACGCAGGT	AGAGACGGCAACAGGAAGTG	60	262
gspG	główna pseudopilina T2SS, transportuje toksyny i enzymy	TTGGTGGTACTGGTGGTCCT	CTGCAAGCCTTGTTCGGTTG	60	177
gspH1	białko należące do rodziny GspH, niezbędne do zależnego od energii wydzielania z peryplazmy	CGCTTTTGATGTCTGCCACC	CGCTACTTCAACAGCCTGGA	60	244
gspH2	białko należące do rodziny GspH, niezbędne do zależnego od energii wydzielania z peryplazmy	TCCACCAGCACTTGCAGATT	CCTCGCAACGTGGTTTTACC	60	244
pulG	białko T2SS, pseudopilina PulG	CCACTGACTGGGAAAGTCCG	AAGACCTGTTGCAGGACGAG	60	179

Tabela 1. Charakterystyka genów analizowanych w pracy (c.d.)

pulF	Białko z rodziny F, należące do T2SS, transportuje toksyny i enzymy na powierzchnię komórki/przestrzeni pozakomórkowej	TCAGCCAGGAACTGACAACC	CACAAGTGCAACGTAGAGCG	60	200
Alga	mannoza-1-P-guanylylotransferaza /mannoza-6-P-izomeraza, liaza alginianu	TGGTGACCTTTGGCATTT	CAAACCGCTCGACCTTAAA	55	102
algU	współczynnik sigma σ, aktywator operonu syntezy alginianu	GTTGATCGTGCGTTTTGT	CATGTGTAAAAGGCGCTG	56	117
mucA	Współczynnik anti-sigma σ; negatywny regulator genu a*lgU*	GAAGCGGACGAACTGGAA	GGAATCAACAGGTCCTTG	54	119
M22_1	metalopeptydaza zaangażowana w degradację białek	CGTGCCTACCGAGATTGA	CGGAATACCCCAGGCAAA	56	112
M3_2	metalopeptydaza zaangażowana w degradację białek	GGCGATGGATGAGCTGAA	GAATAGGCGCTCAAGGCA	57	129
S11_3	peptydaza serynowa o szerokim zakresie aktywności peptydazy	AGTCCTACGTTCTGATGG	GTTTTCGCCGATCTGACC	55	146
lipA	lipaza A, zaangażowana w hydrolizę estrów cholesterolu i triacylogliceroli	GTGGGGCAATTGGTTTGA	TGATTGACCATGCGCTGA	57	148
lipB	lipaza B, zaangażowana w produkcję aktywnej lipazy A	CTACCTTTTTGTTACCCGTT	ATCACGTCGTAGCATTTC	53	118

3.5.9. Badanie właściwości proteolitycznych *P. psychrophila* KM02

Zmiany w aktywności proteolitycznej *P. psychrophila* KM02 po inkubacji z olejkami eterycznymi i związkami bioaktywnymi oceniano spektrofotometrycznie według metody opisanej przez Polychroniadou, (1988) z pewnymi modyfikacjami. Hodowle wirowano (3000 g, 10 min.), a do otrzymanego supernatantu wprowadzano 0,5 mL buforu boranowego i 1 mL 1% kwasu 2,4,6-trinitrobenzenosulfonowego (TNBS). Próby inkubowano w temperaturze 37°C przez 1 h, po czym wprowadzano 2 mL 0,1 M diwodorofosforanu sodu zawierającego 1,5 mM siarczanu sodu. Intensywność powstającej żółtopomarańczowej barwy oznaczano spektrofotometrycznie przy długości fali 420 nm. Stopień inhibicji aktywności proteolitycznej badanych drobnoustrojów wyliczano według wzoru:

$$\%PI = 100 - (\frac{A_t}{A_c} \times 100)$$

gdzie:

A_t – wartość absorbancji próby traktowanej

A_c – wartość absorbancji próby kontrolnej

3.5.10. Badanie właściwości lipolitycznych *P. psychrophila* KM02

Zmiany w aktywności lipolitycznej *P. psychrophila* KM02 oceniano metodą spektrofotometryczną zgodnie z procedurą zaproponowaną przez Stuer i in., (1986). W badaniach zastosowano roztwór zawierający 10 mL izopropanolu, 30 mg palmitynianu p-nitrofenylu oraz 90 mL 0,05 M buforu fosforowego Sörensena. Roztwór ogrzewano w temperaturze 37°C. Roztwór w ilości 2,4 mL wprowadzano do 0,1 mL płynu pohodowlanego. Po 15-minutowej inkubacji w temperaturze 37°C mierzono absorbancję przy długości fali 420 nm. Stopień inhibicji aktywności lipolitycznej badanych drobnoustrojów obliczano według wzoru:

$$\%LI = 100 - (\frac{A_t}{A_c} \times 100)$$

gdzie:

A_t – wartość absorbancji próby traktowanej

A_c – wartość absorbancji próby kontrolnej

3.5.11. Badanie zdolności syntezy EPS przez *P. psychrophila* KM02

W pracy wykorzystano procedurę ekstrakcji bakteryjnych EPS opisaną przez Forde i Fitzgerald (1999). Hodowle *P. psychrophila* KM02 wirowano i zawieszano w 1,5 mL 30% roztworu NaOH. Próby ogrzewano we wrzącej łaźni wodnej przez 15 min. Po wirowaniu (10000 rpm/15 min.) do prób dodawano 60% roztworu etanolu, 1 mL sterylnej wody destylowanej oraz 7 mL 77% roztworu kwasu siarkowego. Po zworteksowaniu i schłodzeniu, do prób dodawano 1 mL 1% roztworu tryptofanu. Po inkubacji prób we wrzącej łaźni wodnej prowadzono pomiar absorbancji przy długości fali 500 nm. Stężenie EPS obliczano z krzywej standardowej utworzonej na podstawie znanych stężeń alginianu sodu. Stopień inhibicji syntezy EPS u *P. psychrophila* KM02 obliczano na podstawie wzoru:

$$\%EI = 100 - (\frac{EPS_t}{EPS_c} \times 100)$$

gdzie:

EPS_t – stężenie EPS (μg/10^8 jtk) dla próby traktowanej

EPS_c – stężenie EPS (μg/10^8 jtk) dla próby kontrolnej

3.5.12. Ocena *in situ* wzrostu *P. psychrophila* KM02 w filetach świeżego łososia atlantyckiego

Próby 10 g świeżego łososia atlantyckiego inokulowano 1 mL hodowli *P. psychrophila* KM02 o gęstości 10^4 jtk/g. Marynatę przygotowano z oliwy z oliwek oraz octu winnego w układzie 95:5. TEO i BPEO wprowadzano do marynaty w stężeniach subMIC. Próby łososia pakowano w sterylnej folii z polichlorku winylu; w opakowaniach generowano warunki próżniowe (Multivac T200, Niemcy). Próby przechowywano w 4 ± 1°C przez 5 dni. Wzrost *P. psychrophila* KM02 oceniano 1, 3 i 5 dnia stosując metodę płytkową Kocha. Próby otwierano w sterylnych warunkach i zawieszano w 90 mL 0,1% sterylnej wody peptonowej (Oxoid, Wielka Brytania). Po homogenizacji (Microgen Bioproducts, Wielka Brytania) wykonywano serię rozcieńczeń i posiewano 0,1 mL materiału na agar z cefalorydyną, kwasem fusydowym i cetrymidem (CFC) (Oxoid, Wielka Brytania). Płytki Petriego inkubowano w temperaturze 4 ± 1°C przez 72 h i zliczano wyrosłe kolonie. Wynik przeliczano w jednostce jtk/g produktu.

3.5.13. Analiza statystyczna wyników

Wszystkie doświadczenia wykonano w trzech niezależnych powtórzeniach, a wyniki przedstawiono jako wartość średnią ± odchylenie standardowe. Istotność różnic pomiędzy próbami wyznaczono za pomocą jednokierunkowej analizy wariancji (ANOVA) oraz testów wielokrotnych porównań Tukey'a (dla pozostałych doświadczeń). Analizę rozkładu normalnego oceniono testem Shapiro-Wilka, natomiast jednorodność wariancji testami Levene'a. Analizę statystyczną przeprowadzono w programie komputerowym R Studio (wersja 4.0.5, 2021).

4. Omówienie wyników i dyskusja

4.1. Charakterystyka chemiczna TEO i BPEO

Potencjał aplikacyjny oraz aktywność biologiczna olejków eterycznych zależy od ich składu chemicznego (Yu i in., 2020). Olejki eteryczne zawierające głównie związki terpenowe hamują aktywność metaboliczną drobnoustrojów i ingerują w proliferację komórek bakteryjnych; mogą również charakteryzować się właściwościami przeciwutleniającymi (Rao i in., 2019). Z powyższych względów, olejki eteryczne coraz częściej są rozpatrywane w aspekcie alternatywnego/uzupełniającego składnika hamującego rozwój mikroflory w żywności, szczególnie produktów na bazie ryb o minimalnym stopniu przetworzenia. (Sendra, 2016). Cechy fizykochemiczne ryb jak wartość pH, aktywność wody czy zawartość składników odżywczych sprzyjają rozwojowi mikroflory (Comi, 2017). Liczne doniesienia literaturowe dowodzą, że dodatek olejków eterycznych do produktu zapobiega niekorzystnym zmianom organoleptycznym świeżych ryb, skutecznie wydłużając termin przydatności do spożycia (Farsanipour, 2020; Moosavi-Nasab i in., 2016; Shadman i in., 2017; Socaciu i in., 2021; Vieira i in., 2019; Vital i in., 2018).

W niniejszej pracy do pozyskania olejków eterycznych wykorzystano jednorodny surowiec roślinny, zagwarantowany przez dystrybutora. System GC-MS wykorzystano do analizy jakościowej i ilościowej otrzymanych olejków eterycznych. Wyniki oznaczeń składu chemicznego TEO i BPEO przedstawiono w Tabeli 2 oraz w publikacji P-2 i P-3. W obu ocenianych olejkach eterycznych zidentyfikowano po 19 różnych związków chemicznych. Dominującymi związkami bioaktywnymi w TEO były ME (24,5 %) oraz PHE (19,3%), natomiast w składzie BPEO największy procentowy udział odnotowano dla CAR (19,6 %) oraz LIM (19,1 %). Składy obu badanych olejków eterycznych odpowiadały międzynarodowym normom, które określają minimalne i maksymalne stężenia LIM i CAR dla BPEO oraz ME i PHE dla TEO (ISO 3061:2008, ISO 10115:2013). Jednocześnie warto podkreślić, że dominujące związki danego olejku eterycznego nie występowały bądź ich obecność w drugim badanym olejku eterycznym odnotowana została w śladowych ilościach. Wynika to z różnic botanicznych oraz warunków uprawy.

Względny udział procentowy poszczególnych klas związków chemicznych w TEO był następujący: fenylpropeny (52%), związki monoterpenowe (44,5%) oraz związki seskwiterpenowe (3,5%).

Tabela 2. Skład chemiczny olejków eterycznych BPEO i TEO

Związek chemiczny	Wzór chemiczny	RI (Wax, DB-5)	Udział [%]	
			BPEO	TEO
α-pinen	C10H16	1035, 939	8,7	1,8
Kamfen	C10H16	1000, 953	0,8	-
β-pinen	C10H16	1110, 980	8,4	-
γ-caren	C10H16	1148, -	2,3	-
β-mircen	C10H16	1158, 990	11,4	-
α-felandren	C10H16	1170, 1006	8,2	-
α-terpinen	C10H16	1249, 1072	-	0,-5
Limonen	C10H16	1208, 1030	**19,1**	1,2
1,8-cineol	C10H18O	1222, 1031	-	1,5
β-ocimen E	C10H16	1235, 1042	-	3,5
β-felandren	C10H16	1245, 1042	-	**19,3**
γ-terpinen	C10H16	1249, 1072	0,8	0,9
β-ocimen Z	C10H16	1250, 1051	-	8,8
p-cymen	C10H14	1274, 1026	2,9	-
α-terpinolen	C10H16	1279, 1083	2,5	-
Elemen	C15H24	1456. -	1,9	-
α-cubeben	C15H24	1472, 1348	3,3	-
Linalol	C10H18O	1544, 1100	1,1	-
β-kariofilen	C15H24	1594, 1414	**19,6**	0,9
terpinen-4-ol	C10H18O	1606, 1180	-	3,0
Metylchawikol	C10H12O	1657, 1199	-	1,1
α-humulen	C15H24	1668, 1449	2,7	-
Germacren	C15H24	1705, 1487	-	0,8
β-bisabolen	C15H24	1736, -	1,5	-
β-adamantan	C10H16	1741, -	1,3	-
Δ-kadinen	C1HH24	1748, -	1,7	-
Octan geranylu	C12H20O2	1761, 1384	-	1,2
Elemycyna	C12H16O3	1862, 1514	-	14,4
Izoelemycyna	C12H16O3	1944, 1596	-	11,3
Tlenek kariofilenu	C15H24O	1962, 1573	1,8	-
Metyl eugenol	C11H14O2	2001, 1404	-	**24,5**
Spatulenol	C15H24O	2108, 1578	-	1,8
Tymol	C10H14O	2179, 1283	-	1,7
Izoeugenol metylu	C11H14O2	2188, 1491	-	1,8

Wyniki uzyskane w ramach niniejszej pracy są zbliżone między innymi do rezultatów Szczepanik i in., (2018), w których ME był dominującym związkiem TEO. Jedynie Verma i in., (2010) wykazali udział ME w TEO na poziomie 0,7%.

Większość związków wchodzących w skład BPEO należała do monoterpenów (66,2%), natomiast pozostałą część stanowiły seskwiterpeny (33,8 %), co jest zgodne z pracą Chen i Tawan, (2020), w której wykazano, że niezależnie od pochodzenia surowca, w BPEO dominują związki monoterpenowe i seskwiterpenowe w stosunku około 2:1. Obecność LIM i CAR na poziomie 21 i 15% w BPEO odnotował również Sruthi i in., (2013). Zdaniem Dosoky i in., (2019) powyższe związki są charakterystyczne dla BPEO, niezależnie od regionu geograficznego, z którego pozyskano materiał roślinny.

4.2. Wartości indeksów subMIC TEO, BPEO, ME, PHE, LIM i CAR oraz wpływ subMIC TEO i BPEO na profil kwasów tłuszczowych osłon komórkowych *Pseudomonas* spp.

Aktywność przeciwdrobnoustrojowa olejków eterycznych zależy między innymi od zastosowanego stężenia danego czynnika. Zazwyczaj stężenia olejków eterycznych, które wykazują działanie bójcze wobec komórek drobnoustrojów mogą zmieniać cechy organoleptyczne żywności (Leite de Souza, 2016). Sposobem na ograniczenie negatywnego wpływu olejków eterycznych na jakość produktu jest ich zastosowanie w stężeniach subMIC, wpływających na metabolizm komórki zależny od quorum sensing (Truchado i in., 2015). W niniejszej pracy indeksy subMIC olejków eterycznych TEO i BPEO oraz ich składników bioaktywnych (ME, PHE, CAR i LIM) wobec komórek *P. psychrophila* KM02, *P. orientalis* KM149 oraz *P. fluorescens* KM248 wyznaczano metodą szeregu seryjnych rozcieńczeń.

Wyznaczone wartości indeksów subMIC TEO i BPEO, ME, PHE, LIM i CAR zaprezentowano w Tabeli 3. Część danych przedstawiono w publikacjach P-2 i P-3. W niniejszej pracy odnotowano zbliżoną wrażliwość komórek *Pseudomonas* spp. na testowane czynniki w badanym zakresie stężeń. Wartości indeksów subMIC TEO i BPEO mieściły się w zakresie 70 – 75 µL/mL i 100 – 135 µL/mL odpowiednio. Wartości indeksów subMIC ME, PHE, LIM i CAR wobec komórek *Pseudomonas* spp. wynosiły odpowiednio 10 – 12 µL/mL, 8 – 10 µL/mL, 60 – 65 µL/mL oraz 20 – 35 µL/mL. Istnieje trudność w interpretacji uzyskanych danych i porównania ich

z wartościami dostępnymi w literaturze przedmiotu. Rozbieżności indeksów subMIC mogą wynikać z warunków prowadzenia eksperymentów oraz własności drobnoustrojów wykorzystanych w doświadczeniach (Van de Vel i in., 2019).

Tabela 3. Wartości indeksów subMIC TEO, BPEO, ME, PHE, LIM i CAR wobec *Pseudomonas* spp. inkubowanych na pożywce TSB

Czynnik przeciwdrobnoustrojowy	Wartość indeksów subMIC [µL/mL]		
	P. psychrophila KM02	*P. orientalis* KM249	*P. fluorescens* KM148
TEO	75	70	75
ME	10	12	12
PHE	8	10	8
BPEO	135	120	100
LIM	65	60	60
CAR	35	20	20

Olejki eteryczne i pojedyncze związki wchodzące w ich skład, łatwo przenikają przez błony komórkowe bakterii, zaburzając ich integralność (Calo i in., 2015). Indukują również zmiany w profilu kwasów tłuszczowych błon komórkowych drobnoustrojów (Di Pasqua i in., 2006). Hodowla komórek bakteryjnych na pożywkach suplementowanych olejkami eterycznymi najczęściej determinuje wzrost syntezy nasyconych kwasów tłuszczowych (Mrozik i in., 2004).

W niniejszej pracy oceniano wpływ subMIC olejków eterycznych na profil estrów metylowych kwasów tłuszczowych *Pseudomonas* spp.. Wyniki powyższych oznaczeń przedstawiono w Tabeli 4 i na Rycinie 2 oraz w publikacjach P-2 i P-3. Suplementacja pożywek subMIC TEO i BPEO doprowadziła przede wszystkim do istotnego obniżenia udziału nienasyconych kwasów tłuszczowych (w zakresie od 4 % do 19 %) wraz ze wzrostem udziału nasyconych kwasów tłuszczowych (w zakresie od 9 % do 15 %) u badanych szczepów *Pseudomonas* spp. Wyjątek stanowił *P. fluorescens* KM148, u którego powyższa zmiana nie była istotna statystycznie. Podobnie Di Pasqua i in. (2006), wykazali brak istotnego wpływu związków terpenowych na udział

nasyconych kwasów tłuszczowych w błonach komórek *P. fluorescens*. W niniejszej pracy, zastosowanie TEO i BPEO w hodowli komórek *P. fluorescens* KM148 wpłynęło na istotne obniżenie udziału kwasów tłuszczowych o rozgałęzionej budowie. Zgodnie z pracą Chao i in., (2010), powyższe kwasy tłuszczowe wpływają na właściwości błony komórkowej podobnie jak kwasy tłuszczowe zawierające wiązanie podwójne: determinują odpowiednią płynność i półprzepuszczalność. Natomiast u *P. psychrophila* KM02 oraz *P. orientalis* KM249 odnotowano istotnie zwiększony udział nasyconych kwasów tłuszczowych. Powyższa prawidłowość wpływa na pobór przez komórkę substancji ze środowiska zewnętrznego (Leite de Souza, 2016). Biorąc pod uwagę istotne obniżenie stosunku nienasyconych do nasyconych kwasów tłuszczowych w osłonach komórkowych zakłada się, że subMIC TEO i BPEO wpływają na aktywność enzymu desaturazy (Di Pasqua i in., 2006).

Ekspozycja *Pseudomonas* spp. na stężenia subMIC TEO i BPEO indukowała również syntezę kwasu 2 hydroksydodekanowego (2-OH C12:0). W wariancie hodowli prowadzonej na pożywce z dodatkiem stężenia subMIC TEO udział kwasu 2-OH C12:0 w osłonach *P. psychrophila* KM02 oszacowano na poziomie 8,3%; u *P. orientalis* KM249 i *P. fluorescens* KM148 były to wartości odpowiednio 6,9 i 11,0 %. Po inkubacji komórek w pożywce suplementowanej stężeniem subMIC BPEO stwierdzono obecność kwasu 2-OH C12:0 w osłonach komórkowych *Pseudomonas* spp. na poziomie 13,7% u *P. psychrophila* KM02, 2,3% u *P. orientalis* KM249 i 1,9% u *P. fluorescens* KM148. Narażenie komórek *P. psychrophila* KM02 na stężenia subMIC TEO nie wywołało zmian w ogólnym udziale hydroksylowych kwasów tłuszczowych w stosunku do próby kontrolnej. W powyższym wariancie doświadczenia zaobserwowano spadek procentowego udziału kwasu 3-hydroksytetradekanowego (3-OH C14:0). Obecność hydroksylowych kwasów tłuszczowych w błonach komórkowych zwiększa barierowość błon komórkowych na czynniki hydrofobowe (Sikkema i in., 1995). U *P. psychrophila* KM02 nie zaobserwowano również istotnej zmiany ilości kwasów cyklopropanowych pod wpływem subMIC TEO i BPEO, podczas gdy w błonach komórkowych *P. orientalis* KM249 i *P. fluorescens* KM148 doszło do ich istotnego obniżenia. Powyższe może być wynikiem wpływu stężeń subMIC TEO i BPEO na aktywność enzymu ATPazy, niezbędnej w wytwarzaniu energii wykorzystywanej w syntezie kwasów cyklopropanowych (Nazzaro i in., 2013).

Tabela 4. Profil kwasów tłuszczowych komórek *Pseudomonas* spp. inkubowanych na pożywce TSB suplementowanej subMIC TEO i BPEO

Kwas tłuszczowy	*P. psychrophila* KM02			*P. orientalis* KM249			*P. fluorescens* KM148		
	Pożywka TSB	TSB + subMIC TEO	TSB + subMIC BPEO	Pożywka TSB	TSB + subMIC TEO	TSB + subMIC BPEO	Pożywka TSB	TSB + subMIC TEO	TSB + subMIC BPEO
C12:0	1,8 (± 0,4)	7,7 (± 0,6)	9,0 (± 0,4)	1,8 (± 0,2)	5,5 (± 0,5)	2,2 (± 0,3)	5,7 (± 0,6)	6,4 (± 1,5)	3,1 (± 0,9)
2-OH-C12:0	BD	8,3 (± 1,4)	13,7 (± 1,0)	BD	6,9 (± 0,2)	2,3 (± 0,3)	BD	11,0 (± 1,8)	1,9 (± 0,2)
C14:0	2,3 (± 0,3)	3,3 (± 0,7)	1,8 (± 0,2)	2,0 (± 0,4)	4,7 (± 0,6)	5,6 (± 1,2)	2,1 (± 0,3)	4,6 (± 1,1)	4,3 (± 0,8)
Ante-C15:0	4,0 (± 0,1)	2,0 (± 1,0)	3,5 (± 0,6)	1,0 (± 0,9)	1,3 (± 0,4)	1,9 (± 0,4)	3,7 (± 0,3)	2,1 (± 0,4)	2,6 (± 0,3)
3-OH-C14:0	30,8 (± 21)	21,7 (± 0,7)	24,6 (± 1,0)	15,9 (± 1,8)	22,6 (± 1,2)	26,1 (± 2,1)	6,4 (± 0,8)	16,3 (± 2,4)	25,7 (± 2,7)
C16:1 *cis*-9	7,5 (± 1,2)	13,2 (± 2,2)	6,3 (± 0,4)	14,4 (± 1,2)	15,6 (± 1,0)	18,1 (± 1,7)	21,9 (± 1,3)	19,5 (± 2,6)	14,1 (± 1,6)
C16:0	3,3 (± 0,7)	7,3 (± 0,4)	3,1 (± 0,7)	3,5 (± 0,4)	11,9 (± 0,8)	8,8 (± 1,1)	13,9 (± 0,5)	9,2 (± 2,7)	10,9 (± 2,9)
Iso-C17:0	6,1 (± 0,3)	2,9 (± 0,4)	5,1 (± 0,8)	1,8 (± 0,1)	2,7 (± 0,5)	2,2 (± 0,3)	5,7 (± 0,8)	2,1 (± 0,7)	3,1 (± 0,2)
C17:0 *cyc*	1,4 (± 0,2)	2,2 (± 0,5)	0,3 (±0,3)	1,8 (± 0,2)	2,5 (± 0,2)	5,1 (± 0,6)	6,8 (± 0,4)	2,7 (± 0,7)	4,0 (± 0,3)
C18:2 *cis*-9,12	24,5 (± 1,0)	20,6 (± 1,2)	17,2 (±1,1)	32,9 (± 2,4)	11,7 (± 0,8)	15,5 (± 0,6)	22,8 (± 1,2)	17,9 (± 2,9)	16,6 (± 0,9)
C18:1 *trans*-9	13,8 (± 0,7)	7,2 (± 1,1)	10,6 (±0,9)	8,8 (± 2,2)	10,3 (± 0,7)	8,7 (± 2,1)	5,7 (± 0,9)	6,6 (± 3,2)	10,5 (± 0,7)
C19:0 *cyc*	4,5 (± 0,6)	3,7 (± 0,6)	4,9 (± 0,1)	16,2 (± 2,5)	4,4 (± 0,7)	3,5 (± 1,7)	5,5 (± 0,6)	1,6 (± 0,5)	3,2 (± 0,6)

Udział procentowy obliczono jako średnią wartość z trzech powtórzeń (± odchylenie standardowe) na podstawie powierzchni pików na chromatogramie; BD – brak detekcji

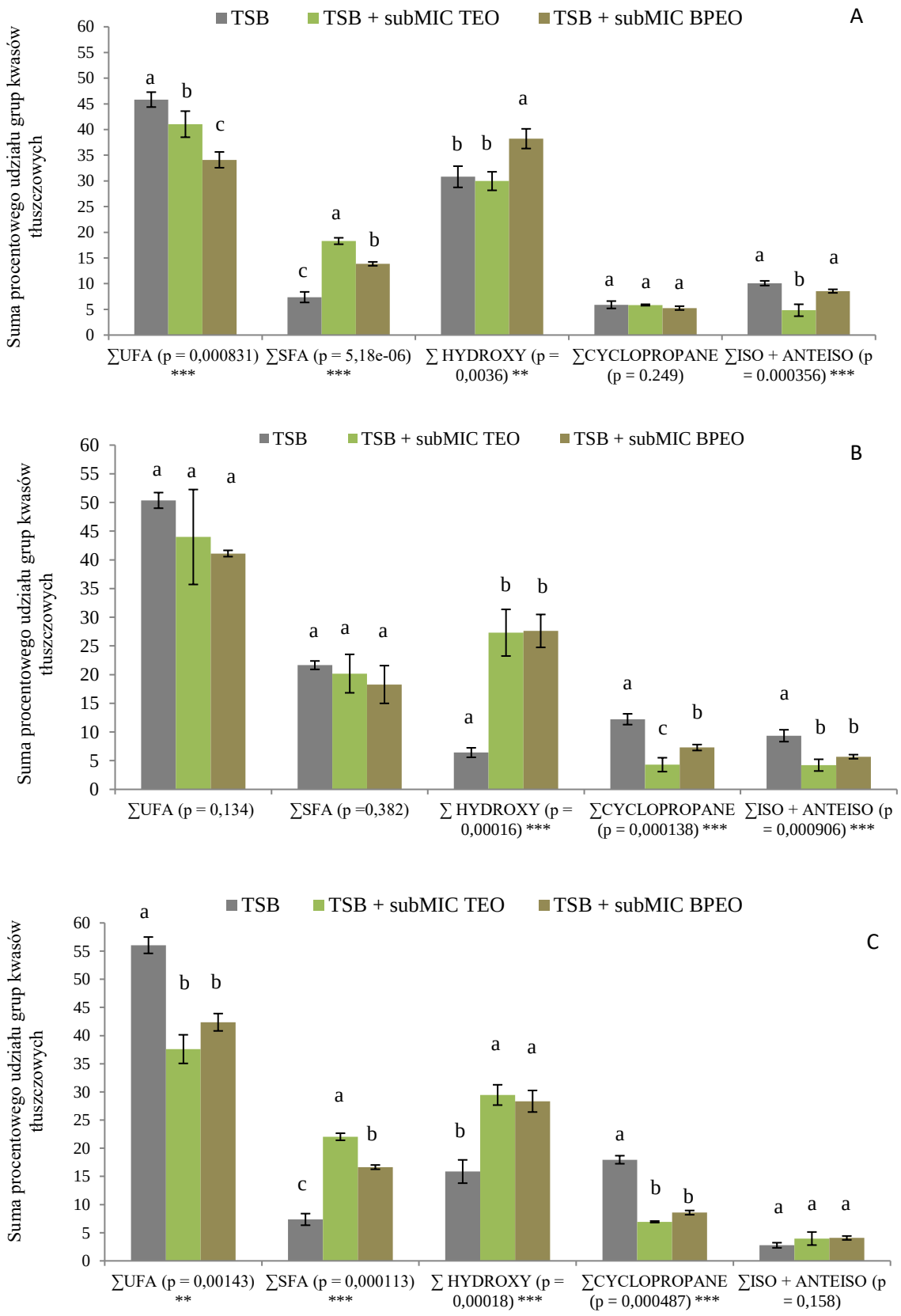

Rycina 2. Suma procentowego udziału poszczególnych grup kwasów tłuszczowych występujących w osłonach komórkowych *Pseudomonas* spp. inkubowanych na pożywce TSB suplementowanej subMIC TEO i BPEO (A – *P. psychrophila* KM02; B – *P. orientalis* KM249, C – *P. fluorescens* KM148)

4.3. Wpływ stężeń subMIC TEO i BPEO, ME, PHE, LIM i CAR na syntezę AI quorum sensing *Pseudomonas* spp.

Cząsteczki sygnałowe są jednym z głównych elementów systemu quorum sensing. Łącząc się z odpowiednim receptorem, AI regulują ekspresję genów kodujących białka enzymatyczne czy białka zaangażowane w wirulencję komórek (Chang i in., 2015; Papenfort i Bassler, 2016). Główne strategie działania przeciw-quorum sensing drobnoustrojów polegają na ingerencji w syntezę cząsteczek AI oraz na oddziaływaniu z białkami receptorowymi (Gopu i in., 2018). Blokowaniu quorum sensing towarzyszy redukcja aktywności metabolicznych, w tym zmiana właściwości chorobotwórczych drobnoustrojów (Venturi, 2006).

Profile AI quorum *sensing* u *Pseudomonas* spp. po inkubacji z subMIC TEO i BPEO oraz ich składnikami bioaktywnymi przedstawiono w Tabeli 5. Wyniki przedstawiono również w publikacjach P-2 oraz P-3.

Na profil AI *Pseudomonas* spp. hodowanych na pożywce TSB składały się następujące cząsteczki AHL: 3-okso-C12-HSL, 3-okso-C14-HSL, 3-okso-C6-HSL, 3-okso-C8-HSL, C12-HSL, C4-HSL oraz C6-HSL. Najwyższe udziały odnotowano dla cząsteczek 3-okso-C12-HSL, 3-okso-C8-HSL oraz C4-HSL. Występowały one w zakresach odpowiednio od 1,908 do 2,028 μg/mL, od 1,119 do 1,953 μg/mL oraz od 1,217 do 1,312 μg/mL. Udział pozostałych AI nie przekroczył wartości 0,03 μg/mL. W płynach pohodowlanych komórek *P. psychrophila* KM2 oraz *P. fluorescens* KM148 oznaczono związek PQS w ilości odpowiednio 0,0076 i 0,0030 μg/mL. Obecność BPEO, TEO i ich składników bioaktywnych w stężeniach subMIC w środowisku wzrostu *Pseudomonas* spp. wpłynęło na wydajność procesu syntezy AI. W tych wariantach doświadczenia, w płynach pohodowlanych drobnoustrojów udział AHL i PQS był poniżej limitu detekcji. Powyższa prawidłowość wskazała na potencjał przeciw-quorum sensing badanych czynników. Uzyskane wyniki są zgodne z analizami prowadzonymi wobec *P. aeruginosa*. Przykładowo w pracy Luciardi i in., (2016) stężenie subMIC olejku eterycznego z mandarynek (4 mg/mL), w składzie którego dominował LIM (około 90%) doprowadziło do obniżenia syntezy cząsteczek AI o 50% i zahamowania aktywność elastazy o 77%. Zastosowanie ME w stężeniu subMIC (10 μg/mL) zredukowało syntezę AI o 86% i wpłynęło na fenotyp *P. aeruginosa* (Sybiya Vasantha Packiavathy i in., 2012). Zdolność innych związków terpenowych oraz fenylpropenów do inhibicji systemu quorum sensing przedstawiono w przeglądzie

literatury dokonanej przez Deryabin i in., (2019). Zastosowanie eugenolu w stężeniu 50 i 200 μM skutkowało inhibicją czynników wirulencji regulowanych przez quorum sensing u *P. aeruginosa* o 32 i 56% (Zhou i in., 2013). Seswkiterpen (salwipizon) pozyskany z szałwii muszkatołowej, zastosowany w stężeniu 37,5 μg/mL redukował tworzenie biofilmu *Staphylococcus aureus* o 85% (Kuźma i in., 2007).

Zaobserwowane w niniejszej pracy zmiany w profilu cząsteczek AI komórek *Pseudomonas* spp. potwierdziły potencjał analizowanych czynników w stężeniach subMIC do ingerencji w system quorum sensing na etapie syntezy AI.

Tabela 5. Profil AI systemu quorum sensing komórek *Pseudomonas* spp. inkubowanych na pożywce TSB suplementowanej subMIC TEO, BPEO, ME, PHE, LIM i CAR

Wariant hodowli		Stężenie AI systemu quorum sensing [µg/mL (±SD)]							
		AHL							związki chinolowe
		3-okso-C12-HSL	3-okso-C14-HSL	3-okso-C6-HSL	3-okso-C8-HSL	C12-HSL	C4-HSL	C6-HSL	PQS
TSB	*P, psychrophila* KM02	1,908 (±0,031)	0,007 (±0,000)	0,015 (±0,000)	1,119 (±0,063)	0,136 (±0,004)	1,217 (±0,010)	0,017 (±0,000)	0,0076 (±0,0000)
	P. orientalis KM249	2,028 (±0,049)	<LOD	0,022 (±0,001)	1,953 (±0,006)	<LOD	1,312 (±0,021)	0,021 (±0,001)	ND
	P. fluorescens KM148	1,976 (±0,099)	<LOD	0,022 (±0,001)	1,853 (±0,006)	0,136 (±0,004)	1,302 (±0,005)	0,021 (±0,001)	0,0030 (±0,0000)
TSB + subMIC TEO	*P. psychrophila* KM02	<LOD	<LOD	0,012 (±0,000)	<LOD	<LOD	<LOD	<LOD	0,0003 (±0,0000)
	P. orientalis KM249	0,001 (±0,000)	<LOD	<LOD	<LOD	<LOD	<LOD	<LOD	ND
	P. fluorescens KM148	<LOD	<LOD	0,011 (±0,001)	<LOD	<LOD	<LOD	<LOD	ND
TSB + subMIC ME	*P, psychrophila* KM02	<LOD	<LOD	0,013 (±0,005)	<LOD	<LOD	<LOD	<LOD	0,0003 (±0,0000)
	P, orientalis KM249	<LOD	<LOD	<LOD	<LOD	<LOD	<LOD	<LOD	ND
	P, fluorescens KM148	<LOD	<LOD	0,011 (±0,001)	0,004 (±0,002)	<LOD	<LOD	<LOD	ND
TSB + subMIC PHE	*P. psychrophila* KM02	<LOD	<LOD	0,016 (±0,001)	<LOD	0,051 (±0,004)	<LOD	<LOD	ND
	P. orientalis KM249	<LOD	<LOD	<LOD	<LOD	<LOD	<LOD	<LOD	ND
	P. fluorescens KM148	<LOD	<LOD	0,007 (±0,000)	0,004 (±0,002)	<LOD	<LOD	<LOD	ND

Tabela 5. Profil AI systemu quorum sensing komórek *Pseudomonas* spp. inkubowanych na pożywce TSB suplementowanej subMIC TEO, BPEO, ME, PHE, LIM i CAR (c.d.)

TSB + subMIC BPEO	*P. psychrophila* KM02	<LOD	<LOD	0,008 (±0,000)	0,003 (±0,000)	<LOD	<LOD	<LOD	0,006713 (±0,000193)
	P. orientalis KM249	0,001 (±0,000)	<LOD	<LOD	<LOD	<LOD	<LOD	<LOD	ND
	P. fluorescens KM148	<LOD	<LOD	0,010 (±0,001)	<LOD	<LOD	<LOD	<LOD	ND
TSB + subMIC LIM	*P. psychrophila* KM02	<LOD	<LOD	0,011 (±0,001)	<LOD	<LOD	<LOD	<LOD	<LOD
	P. orientalis KM249	<LOD	<LOD	<LOD	<LOD	<LOD	<LOD	<LOD	ND
	P. fluorescens KM148	<LOD	<LOD	<LOD	<LOD	<LOD	<LOD	<LOD	ND
TSB + subMIC CAR	*P. psychrophila* KM02	<LOD	<LOD	0,008 (±0,000)	0,002 (±0,000)	<LOD	<LOD	<LOD	<LOD
	P. orientalis KM249	<LOD	<LOD	<LOD	<LOD	<LOD	<LOD	<LOD	ND
	P. fluorescens KM148	<LOD	<LOD	<LOD	<LOD	<LOD	<LOD	<LOD	ND

ND – brak detekcji; <LOD – mniej niż limit detekcji; LOD dla 3-okso-C12-HSL, 3-okso-C14-HSL, 3-okso-C6-HSL: 0,005 μg/mL; dla 3-okso-C8-HSL, C12-HSL, C4-HSL i C6-HSL: 0,004 μg/mL; dla PQS: 0.0001 μg/mL

4.4. Ocena potencjału ME, PHE, LIM i CAR do wiązania się z receptorami systemu quorum sensing *Pseudomonas* spp.

Składniki olejków eterycznych mogą również wiązać się w miejscu aktywnym białek receptorowych systemu quorum sensing (Kalia, 2013). Do weryfikacji powyższego założenia wykorzystano analizy *in silico* dokowania molekularnego głównych związków TEO i PBEO z receptorami quorum sensing *Pseudomonas* spp. Receptory wytypowano na podstawie wyników analiz chromatograficznych. Porównanie sposobu wiązania ME, PHE, LIM i CAR z natywnymi AI i znanymi inhibitorami quorum sensing dało wgląd w potencjalny mechanizm molekularny działania olejków eterycznych na system quorum sensing u *Pseudomonas* spp.

Wyniki dokowania molekularnego składników TEO i BPEO z receptorami systemu quorum sensing (LasR, RhlR, TraR i PqsR) przedstawiono w Tabeli 6 oraz w publikacji P-2 i P-3. Przykładowe wizualizacje kompleksów LasR-ME, RhlR-CAR, TraR-CAR i PqsR-PHE przedstawiono na Rycinie 3. Wartości dokowania molekularnego pozwoliły oszacować wolną energię związania liganda z białkiem receptorowym systemu quorum sensing i służyły do uszeregowania testowanych związków pod względem potencjału wiązania z receptorami LasR, RhlR, TraR, PqsR. Ujemne wartości parametru dokowania świadczą o stabilności kompleksu (Friesner i in., 2004).

Pierwszym w hierarchii quorum sensing u *Pseudomonas* spp. jest białko LasR, które łącząc się z natywnym autoinduktorem, 3-okso-C12-HSL reguluje syntezę enzymów i toksyn, tworzenie biofilmu oraz aktywność pozostałych układów systemu quorum sensing (Lee i Zhang, 2015). W niniejszej pracy dla układu LasR-3-oxo-C12-HSL odnotowano najwyższą wartość dokowania (-9,750 kcal/mol) oraz najniższą energię wiązania (-60,513 kcal/mol). Kompleks LasR-3-oxo-C12-HSL został utworzony głównie przez 4 wiązania wodorowe z resztami TYR56, TRP60, ASP73 i ARG61. Zgodnie z Klebe (2013) wiązania wodorowe zapewniają stabilność układu i odgrywają istotną rolę w rozpoznaniu molekularnym cząsteczek. Te same reszty aminokwasów były zaangażowane w związanie ME z LasR. Dla powyższego układu wartość dokowania wynosiła -6,145 kcal/mol. Oprócz wiązań wodorowych w tym kompleksie występowało wiązanie „π-stacking" pomiędzy pierścieniem ME a pierścieniem aromatycznym TYR56. Ten typ oddziaływania odgrywa istotną rolę w rozpoznaniu biologicznym, organizacji struktury kompleksu oraz stanowi tzw.

kluczowy punkt kontaktu, wpływając na energię wiązania (Brylinski, 2018). Za interakcję PHE z białkiem LasR odpowiadały głównie oddziaływania hydrofobowe dające wartość dokowania -5,750 kcal/mol. Oddziaływania hydrofobowe determinowały również utworzenie kompleksu białka LasR-LIM (wartość dokowania -5,113 kcal/mol) i LasR-CAR (wartość dokowania -5,831 kcal/mol). W powyższych oddziaływaniach uczestniczyły niepolarne reszty aminokwasów: TYR47, ILE52, LEU36, LEU39 i LEU40, obecne w miejscu aktywnym białka LasR. W dostępnej literaturze wykazano istotną rolę reszt ASP73, SER129 i TYR56 w stabilizacji ligandu w białku LasR (Sadiq i in., 2020). Analizowane związki olejków eterycznych miały wyższe wartości dokowania z białkiem LasR (-4,563 kcal/mol) niż udokumentowany syntetyczny inhibitor systemu quorum sensing, C30-Furanon, pomimo utworzenia wiązania wodorowego z TRP60. Uzyskane wyniki są zgodnie z pracą Annapoorani i in. (2012), w której wirtualne badanie przesiewowe 1920 potencjalnych inhibitorów quorum sensing do tego samego miejsca rozpoznania w białku LasR, wykazało wpływ oddziaływań hydrofobowych na stabilność układu ligand-LasR.

Białko receptorowe RhlR tworzy kompleks z C4-HSL. U *P. aeruginosa* utworzenie kompleksu RhlR-C4-HSL warunkuje głównie syntezę EPS i tworzenie biofilmu (Lee i Zhang, 2015). W analizach dokowania z białkiem receptorowym RhlR, najwyższą wartość dokowania (-7,285 kcal/mol) otrzymano dla układu RhlR-CAR. Kompleks ten został utworzony za pomocą oddziaływań hydrofobowych z resztami TRP68, LEU69, TYR72 i TYR42. Wartości dokowania dla pozostałych związków bioaktywnych badanych olejków eterycznych mieściły się w zakresie od -5,589 kcal/mol (RhlR-ME) do -6,566 kcal/mol (RhlR-PHE); zajmowały to samo miejsce aktywne białka RhlR. Obecność wiązania wodorowego odnotowano przy utworzeniu kompleksu C4-HSL-RhlR, ME-RhlR oraz C30-furanonu-RhlR. W tworzeniu wiązań uczestniczyły reszty TRP68 wskazując na istotną rolę tego aminokwasu w miejscu rozpoznania receptora RhlR (Pattnaik i in., 2018). W pracy Kumar i in. (2015) wiązanie wodorowe z cząsteczką C4-HSL było tworzone również z resztą ASP81. Zaobserwowane różnice mogą wynikać z różnej procedury opracowania przestrzennej struktury białka przed przystąpieniem do wizualizacji dokowania potencjalnych inhibitorów quorum sensing do RhlR; w niniejszej pracy zastosowano inny rodzaj pola siłowego OPLS3e. Pole to w porównaniu z zastosowanym przez Kumar i in. (2015) polem OPLS 2005 warunkuje zwiększoną dokładność wpływając na obniżenie względnej swobodnej energii wiązania (Roos i in., 2019).

Białkiem receptorowym dla cząsteczki sygnałowej 3-okso-C8-HSL jest białko TraR, pierwotnie wyznaczone dla *Agrobacterium tumefaciens* (Lang i Faure, 2014). Jednakże obecność cząsteczki 3-okso-C18-HSL odnotowano również jako jeden z głównych AI *Aeromonas veronii*, mikroflory psującej produkty na bazie jesiotra (Gui i in., 2018) czy bakterii *Pseudoalteromonas ulvae* (Mireille Ayé i in., 2015). W pracy Xia i in., (2012) wykazano znaczenie 3-okso-C8-HSL w tworzeniu biofilmu przez *P. aeruginosa*. W niniejszej pracy układ TraR-3-okso-C8-HSL powstał w oparciu o wiązania wodorowe z resztami TRP57, ASP70 i TRP85, dając wynik dokowania -7,272 kcal/mol. Wartości dokowania dla głównych związków TEO i BPEO mieściły się w zakresie od -5,236 kcal/mol (dla TraR-LIM) do -6,811 kcal/mol (dla TraR-CAR). Były to wartości niższe niż dla układu TraR-3-oxo-C8-HSL, ale jednocześnie przewyższały wynik wartości dokowania określony dla układu TraR-C30-furanon (-4,978 kcal/mol). Główne związki olejków eterycznych (LIM, CAR i PHE) oddziaływały hydrofobowo z resztami TYR102, ALA38 i LEU40 białka TraR. Efektywne wiązanie danej cząsteczki skutkuje zmianą konformacji białka receptorowego systemu quorum sensing, co w konsekwencji zaburza jego zdolność do regulacji ekspresji genów zależnych od quorum sensing (Kumar i in., 2015).

Ostatnie analizowane białko receptorowe systemu quorum sensing, PqsR, wymaga do aktywacji AI – PQS (Lee i Zhang, 2015). U *P. aeruginosa* powyższy układ reguluje właściwości chorobotwórcze drobnoustrojów (Lin i in., 2018). W niniejszej pracy najwyższą wartość dokowania (-8,552 kcal/mol) odnotowano dla układu PQS-3-NH2-7Cl–C9-chinazolinon (QZN). Związek ten o strukturze zbliżonej do AI PQS tworzył stabilny kompleks wskutek utworzenia wiązania wodorowego z resztą LEU207 oraz obecności oddziaływań hydrofobowych z resztami TRP234 i ILE23, TYR258 i PRO238. Niższe wartości dokowania (od -4,626 kcal/mol do -5,263 kcal/mol) otrzymane w pozostałych układach z białkiem PqsR, wynikały ze struktury składników bioaktywnych olejków eterycznych oraz liczby potencjalnych reszt aminokwasowych, z którymi związek może wejść w interakcje (Soheili i in., 2019). Zdaniem Soheili i in. (2019) o utworzeniu stabilnego kompleksu ligand-PqsR decyduje obecność akceptorów elektronu, grupy karbonylowej oraz N, O_2 lub NH.

Uzyskane wyniki wskazują na potencjał głównych składników bioaktywnych TEO i BPEO do ingerencji w system quorum sensing zidentyfikowany u badanych szczepów *Pseudomonas* spp. Powyższe związki tworzyły stabilne kompleksy z białkami receptorowymi systemu quorum sensing.

Tabela 6. Wyniki dokowania molekularnego AI, syntetycznych inhibitorów oraz ME, PHE, LIM i CAR z receptorami systemu quorum sensing komórek *Pseudomonas* spp.

Wariant kompleksu	Wartość dokowania [kcal/mol]	Energia kompleksu [kcal/mol]	Reszty aminokwasowe wchodzące w interakcje	Długość wiązań [Å]	Rodzaj wiązania
LasR –ME	-6,145	-31,765	TYR56 SER129 THR75 ARG61 ARG61 TYR56	5,45 1,80 2,74 2,03, 1,91 2,35 3,65	π-stacking wodorowe aromatyczne wodorowe wodorowe z H_2O wodorowe aromatyczne wodorowe
LasR –PHE	-5,750	-22,240	TYR64, TYR47, ILE52, LEU36, LEU39, LEU40, VAL76,ALA127	-	Hydrofobowe
LasR –LIM	-5,113	-19.315	TYR64, TYR47, ILE52, LEU36, LEU39, ALA50,	-	Hydrofobowe
LasR –CAR	-5,831	-0,827	LEU36, LEU39, LEU40, ILE52, ALA70 , TYR47	-	Hydrofobowe
LasR-C30 Furanone	-4,563	-21,048	SER129 TRP60 TRP60	1,88 1,73 3,32	Halogenowe wodorowe aromatyczne wodorowe
LasR–3-oxo-C12-HSL	-9,750	-60,513	ASP73 TRP60 TYR56 TYR56 ARG61 ARG61 TYR56 PHE101	2,30 2,13 1,80 2,73, 2,52 2,03, 1,99 2,35 2,72 2,65	Wodorowe wodorowe wodorowe aromatyczne wodorowe wodorowe z H_2O wodorowe aromatyczne wodorowe aromatyczne wodorowe
RhlR –ME	-5,589	-26,819	TRP68 TRP68	4,82 1,85	π-stacking wodorowe
RhlR –PHE	-6,566	-18,968	VAL60, LEU69, TYR72, TYR77	-	Hydrofobowe
RhlR –LIM	-5,919	-17,917	TRP68, LEU69, TYR72, PRO82	-	Hydrofobowe
RhlR –CAR	-7,285	-23,616	TRP68, LEU69, TYR72, TYR42	-	Hydrofobowe
RhlR-C30 Furanone	-5,518	-18,285	TRP68 TYR42, TYR64	2,04 -	aromatyczne wodorowe hydrofobowe
RhlR –C4HSL	-5,990	-25,471	TRP68 TYR42 ASP81	2,62, 1,99 2,61 -	Wodorowe aromatyczne wodorowe elektrostatyczne

Tabela 6. Wyniki dokowania molekularnego AI, syntetycznych inhibitorów oraz ME, PHE, LIM i CAR z receptorami systemu quorum sensing komórek *Pseudomonas* spp. (c.d)

TraR –ME	-6,101	-28,459	TRP57 TYR53 TYR61	3,52 2,61 3,85	Wodorowe π-stacking π-stacking
TraR –PHE	-5,676	-22,051	TYR102, ALA38, ALA76, LEU40, ALA105	-	Hydrofobowe
TraR – LIM	-5,236	-16,926	TYR102, ALA38, LEU40, ALA105	-	Hydrofobowe
TraR – CAR	-6,811	-10,892	TYR39, ALA38, TYR53, ALA76 THR115	-	Hydrofobowe
TraR – C30 Furanone	-4,978	-21,573	TRP57 TYR61, VAL73	2,12 -	aromatyczne wodorowe hydrofobowe
TraR – 3-oxo-C8-HSL	-7,272	-43,522	TRP57, ASP70 TRP85	2,13, 1,77 3,27	aromatyczne wodorowe wodorowe
PqsR – ME	-4,921	-27,292	LEU208, ILE236, ALA237, PRO238	-	Hydrofobowe
PqsR – PHE	-5,263	-14,894	ILE263, ILE236, TRP234, TYR258	-	Hydrofobowe
PqsR – LIM	-5,138	-13,713	TYR258, TRP234, LEU257, ILE236	-	Hydrofobowe
PqsR – CAR	-4,626	-16,105	TYR258, ILE186, ALA187	-	Hydrofobowe
PqsR – QZN	-8,552	-41,223	LEU207 TYR258, TRP234, PRO238, ILE236	1,70 -	aromatyczne wodorowe hydrofobowe
PqsR – PQS	-7,772	-36,455	LEU207 TRP234, ILE236, LEU208, ALA237	1,73 -	Wodorowe hydrofobowe

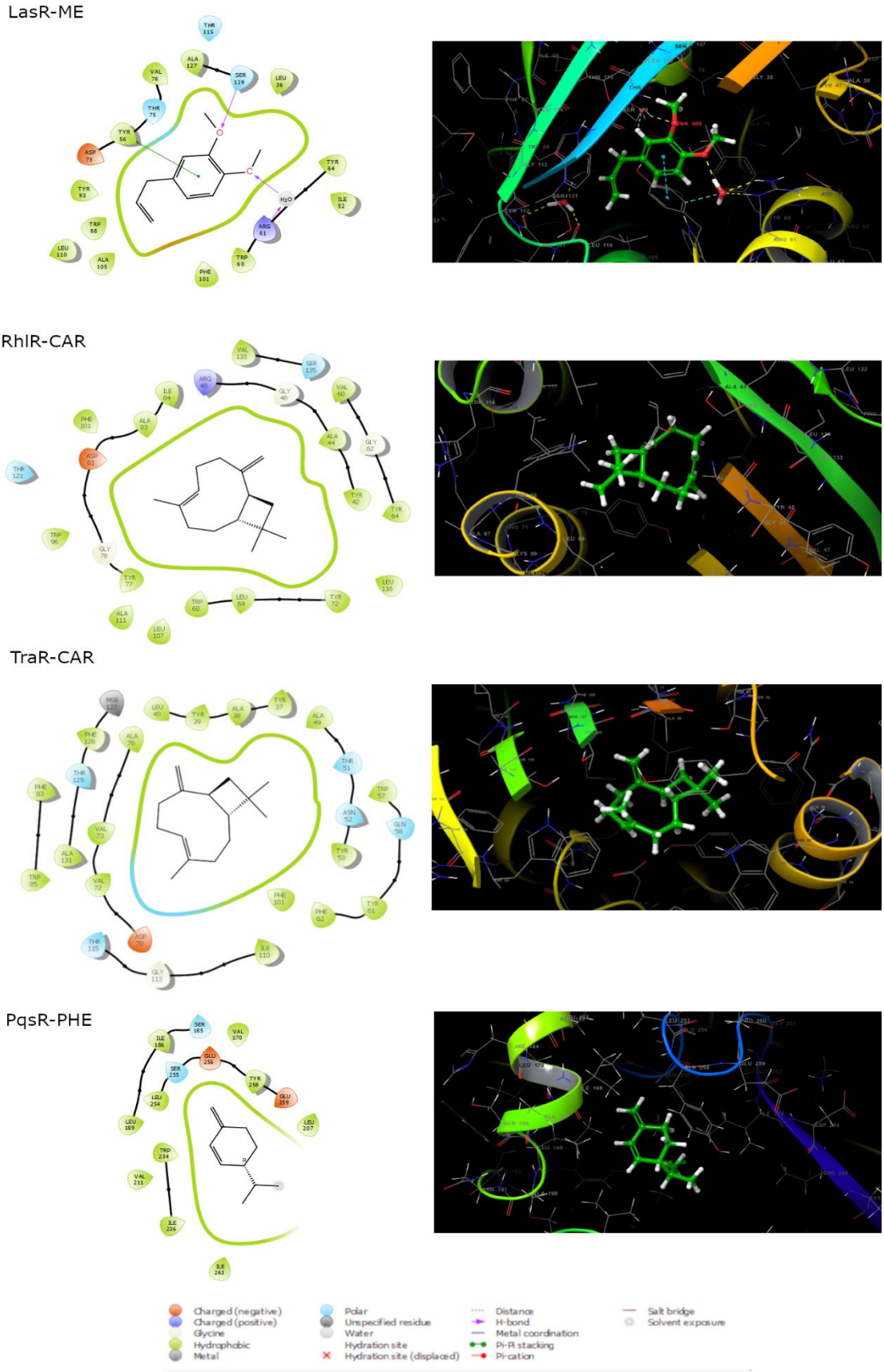

Rycina. 3. Sposób dokowania białek receptorowych *quorum sensing* u *Pseudomonas* spp. z wybranymi związkami bioaktywnymi TEO/BPEO

4.5. Charakterystyka pangenomu i transkryptomu *P. psychrophila* KM02

W związku z brakiem istotnych różnic pomiędzy badanymi gatunkami *Pseudomonas* spp. w odpowiedzi na działanie przeciw-quorum sensing analizowanych czynników, do dalszych doświadczeń wytypowano szczep *P. psychrophila* KM02. Powyższy drobnoustrój jest stosunkowo mało poznany w aspekcie psucia ryb (Jia i in., 2019; Sterniša i in., 2019; Sterniša i in., 2020b). Dzięki odczytaniu i złożeniu *de novo* całego genomu badanego drobnoustroju poznano jego potencjał fizjologiczny oraz przypisano konkretne sekwencje nukleotydowe do wybranych genów związanych z systemem quorum sensing. Analiza całego transkryptomu komórek hodowanych w modelowych warunkach dała wgląd w rzeczywisty udział *P. psychrophila* KM02 w psuciu ryb. Wyniki powyższych analiz przedstawiono odpowiednio w publikacji P-3 i P-4 oraz w Tabeli 7-9 i Rycinie 4-8.

Sekwencjonowanie całego genomu *P. psychrophila* KM02 przeprowadzono z użyciem platform: MiSeq (Illumina, Szwajcaria) oraz MinION (Oxford Nanopore Technologies, Wielka Brytania). U *P. psychrophila* KM02 wyróżniono chromosom zbudowany z 5 313 922 par zasad (pz) z udziałem par G+C na poziomie 57,4%. W obrębie genomu zidentyfikowano 4813 potencjalnych genów, 4713 genów kodujących białka (*protein coding DNA sequences;* CDS) oraz 54 pseudogeny. W porównaniu do wyników uzyskanych dla *P. psychrophila* KM02, genom *P. psychrophila* HA-4 charakteryzował się obecnością 5 235 696 pz, 56,4% udziałem par G+C oraz poziomem 4 721 CDS (Jiang i in., 2012). Genom *P. psychrophila* MTCC 12 324 obejmował 5 269 174 pz z zawartością G+C na poziomie 57,5% (Abraham i Thomas, 2015). Brak istotnej zmienności pomiędzy uzyskanymi danymi a rezultatami innych badaczy może wynikać ze stosunkowo niewielkiej liczby zsekwencjonowanych genomów *P. psychrophila* dostępnych do analizy (Rycina 4) (Land i in., 2015).

Do oceny podstawowych elementów pangenomu *P. psychrophila* wykorzystano 8 złożonych sekwencji dostępnych w bazie danych GenBank NCBI (Tabela 7). Do doświadczeń wytypowano pangenomy *P. psychrophila* wyizolowane z wody oraz żywności. W genomie rdzeniowym *P. psychrophila* odnotowano obecność 3914 genów kodujących białka metabolizmu podstawowego. U *P. psychrophila* KM02 dodatkowo zidentyfikowano 548 geny pomocnicze kształtujące cechy fenotypowe komórek i wspólne dla co najmniej 2 analizowanych szczepów; 2 geny różniły genom szczepu KM02 od innych poddanych ocenie. W ocenianym pangenomie *P. psychrophila* KM02

w obrębie sekwencji unikalnych największy udział wykazywała grupa COG związanych z „replikacją, rekombinacją i naprawą" oraz geny należące do kategorii COG „transport i metabolizm aminokwasów" (udział powyżej 10%) (Rycina 5). Podobne wyniki uzyskano oceniając pangenom patogennych szczepów *Aeromonas hydrophila* wyizolowanych z ryb (Jin i in., 2020). Genom rdzeniowy powyższego gatunku był reprezentowany przez 9,61% genów kategorii COG związanych z funkcją „transportu i metabolizmu aminokwasów". Powyższa grupa genów odnotowana została również w pangenomie *P. fragi,* odpowiedzialnego za psucie się świeżego mięsa i ryb oraz mleka pasteryzowanego wskutek wydzielania lipaz i proteaz (Stanborough i in., 2018). W niniejszej pracy, geny kategorii COG „transport i metabolizm lipidów" odnotowano w pangenomie *P. psychrophila* na poziomie 11%.

Tabela 7. Charakterystyka pangenomu *P. psychrophila*

Szczep	Poziom złożenia	Źródło izolacji	Długość sekwencji	Dostęp w bazie GenBank	Liczba genów rdzenia	Liczba genów pomocni-czych	Liczba genów unikalnych
KM02	Cały Genom	Surowe filety łososia	5,313,922	GCA_011040435.1	3914	548	2
BS3667	Chromosom	Nieznane	5,322,478	GCA_900106105.1	3914	554	42
DSM 17535	126 kontigów	Chłodnia	5,334,010	GCF_001043005.1	3914	489	41
CCUG 53877	36 kontigów	Chłodnia	5,269,270	GCA_008801485.1	3914	537	26
MF6762	77 kontigów	Surowy kurczak	5,804,172	GCF_016405605.1	3914	427	574
CF149	50 kontigów	Hyporeiczna strefa rzeki Clark Fork	5,154,320	GCA_000416155.1	3914	382	219
RGCB 166	150 kontigów	Wody powierzchniowe fiordu arktycznego	5,269,174	GCA_001005765.1	3914	263	144
HA-4	145 kontigów	Próbka osadu czynnego	5,235,696	GCA_000282975.1	-	-	-

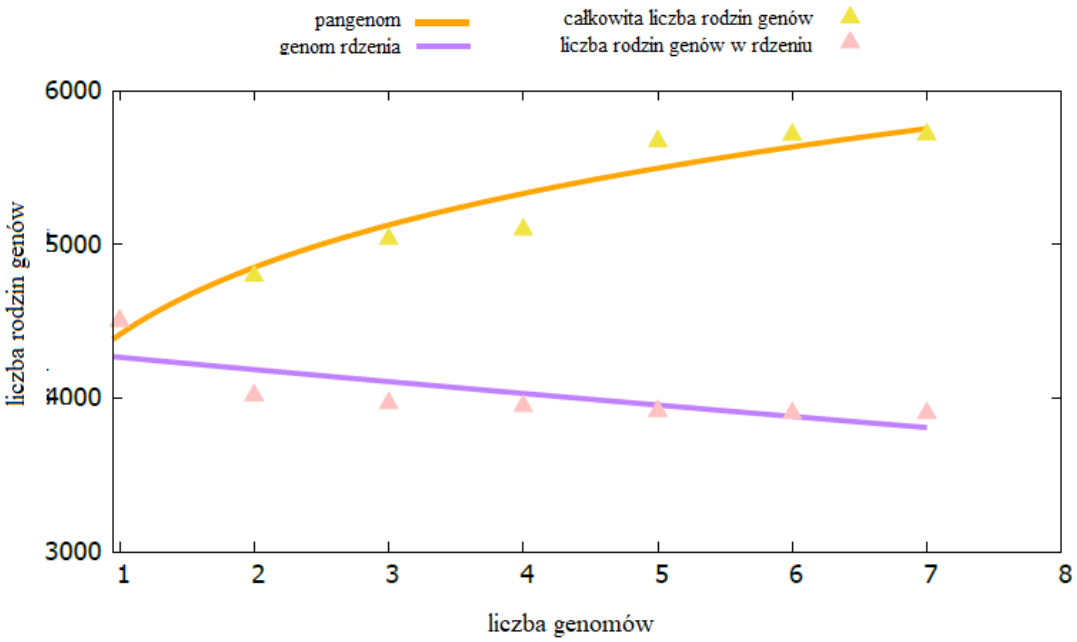

Rycina 4. Wykres rdzeń-pangenom dostępnych sekwencji genomowych *P. psychrophila*

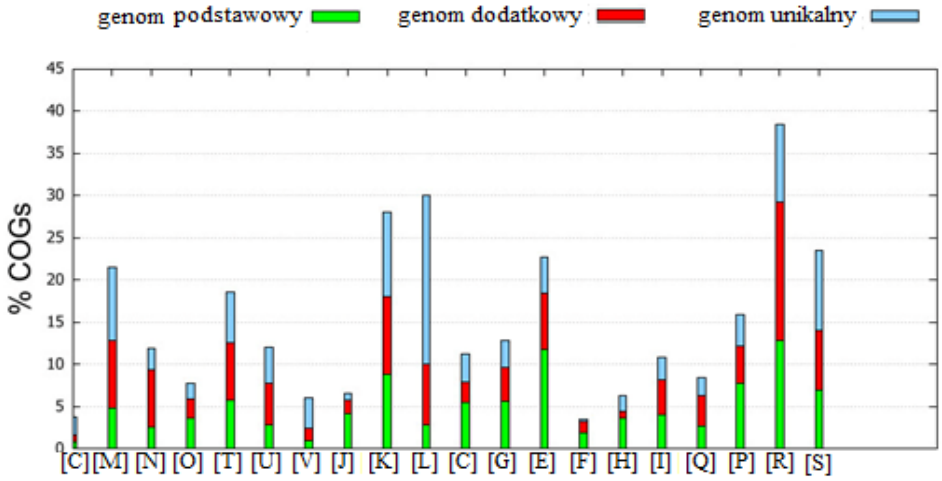

Rycina 5. Rozkład COG pangenomu *P. psychrophila*

[C] kontrola cyklu komórkowego, podział komórek; [M] biogeneza ściany komórkowej/błony komórkowej/osłony komórkowej; [N] ruchliwość komórek; [O] modyfikacje potranslacyjne, synteza białek opiekuńczych; [T] mechanizm transdukcji sygnału; [U] wymiana wewnątrzkomórkowa; [V] mechanizmy obronne; [J] translacja, biogeneza i struktura rybosomalna; [K] transkrypcja; [L] replikacja, rekombinacja i naprawa; [C] wytwarzanie i konwersja energii; [G] metabolizm i transport węglowodanów; [E] metabolizm i transport aminokwasów [F] metabolizm i transport nukleotydów; [H] metabolizm i transport koenzymów; [I] metabolizm i transport lipidów; [Q] biosynteza, transport i katabolizm metabolitów wtórnych; [P] metabolizm i transport jonów nieorganicznych; [R] prawdopodobna funkcja ogólna; [S] funkcja nieznana.

W niniejszej pracy, w genomie *P. psychrophila* KM02 udział genów ortologicznych związanych z metabolizmem i transportem aminokwasów i lipidów wynosił 9 i 3% odpowiednio. Uzyskane wyniki są zbieżne z rezultatami badań nad *Shewanella baltica*, gdzie obecność genów metabolizmu i transportu aminokwasów i lipidów został odnotowany na poziomach odpowiednio 8,66 i 3,8% (Li i in., 2020). Komórki *Shewanella baltica* należą do psychrotrofów i dominują w procesie psucia ryb przechowywanych w warunkach chłodniczych (Ge i in., 2017; Sterniša i in., 2020a). Adnotacja genomu *P. psychrophila* KM02 umożliwiła identyfikację genów kodujących m.in. dehydrogenazy o różnej specyficzności (COG1028) transport aminokwasów typem sekrecyjnym ABC/systemu transdukcji sygnału (COG0834), oksydazy D-aminokwasowe, glicyny (COG06685), przewidywane białko wypływowe treoniny (COG012), przewidywaną peptydazę zależną od cynku (COG0016), aminopeptydazę XAA – PRO (COG0006), karboksypeptydazę D-alanylo-D-alaniny (COG1686) i aminopetydazę metioninnową (COG0024). Na powyższe czynniki zwrócono szczególną uwagę, ponieważ determinują aktywności metaboliczne komórek, warunkujące psucie się żywności. Podobnie w genomie *P. fluorescens* SRM1 wyizolowanego z zepsutego mleka, zidentyfikowano operon zaangażowany w rozkład białek i lipidów oraz sekrecję enzymów za pomocą transportera błonowego ABC (Lo i in., 2015).

W niniejszej pracy, system GO wykorzystano w adnotacji funkcjonalnej transkryptów; genom/produktom genów przypisywano funkcje przy pomocy terminologii GO. Wybrane wyniki przeprowadzonej analizy przedstawiono w Tabeli 8. W genomie *P. psychrophila* KM02 870 sekwencjom przypisano termin GO „proces biologiczny", 77 sekwencjom termin GO „składnik komórkowy" oraz 680 sekwencjom termin GO „funkcja molekularna". W obrębie terminu GO "proces biologiczny" stwierdzono obecność przede wszystkim genów zaangażowanych w metabolizm (GO:0008152) oraz procesy komórkowe (GO:0009987). W grupie terminu GO:1901575 „proces kataboliczny substancji organicznych" największej liczbie transkryptów przypisano role w reakcjach chemicznych i szlakach rozkładu organicznych związków azotowych, kwasów organicznych, organicznych związków cyklicznych, węglowodanów, organicznych związków fosforanowych oraz rozkładu białek i lipidów. Terminy z kategorii GO „komórkowy proces kataboliczny" obejmowały głównie geny związane ze szlakami degradacji związków aromatycznych, związków azotowych, leków, neuroprzekaźników, makrocząsteczek, peptydów czy

związków siarki. Praca Liu i in. (2019) wskazuje, że im wyższa liczba terminów GO w kategorii „proces biologiczny", tym silniejsze zaangażowanie komórek w procesy psucia się żywności. Takie prawidłowości zaobserwowano przeprowadzając adnotację funkcjonalną transkryptów *P. fluorescens* wyizolowanego z żywności oraz *P. fluorescens* z delecją regulonu RpoS (czynnika związanego z odpowiedzią komórek na stres środowiskowy) (Liu i in., 2019).

W niniejszej pracy, w kategorii GO „składnik komórkowy" w genomie *P. psychrophila* KM02 wyróżniono obecność kompleksu T2SS, natomiast w kategorii GO „funkcja molekularna" aktywność transportera transbłonowego. Wśród innych terminów GO dotyczących funkcji molekularnej, najbardziej rozpowszechniona w genomie *P. psychrophila* KM02 była „aktywność katalityczna", „aktywność hydrolazy", „aktywność katalityczna, działająca na białko" oraz „aktywność hydrolazy działająca na wiązania estrowe".

Bazę danych Pfam wykorzystano również do przypisania odczytom przypuszczalnych funkcji (El-Gebali i in., 2019). W Tabeli 9 zaprezentowano wybrane wyniki profilowania Pfam związane z aktywnością hydrolazy, sekrecją białek oraz degradacją lipidów. Powyższe aktywności decydują o zdolności *P. psychrophila* KM02 do psucia ryb. Uzyskane odczyty w ilości odpowiednio 11828 i 7768 przypisano do klanów Aminohydro_1 i Abhydrolase_1. Otrzymane rezultaty przypisano również do rodzin peptydaz (głównie Peptidase_M20, Peptidase_M24, Peptidase_M23). Większość z tych enzymów jest klasyfikowana jako metalopeptydazy. W obrębie klanu ELFV_dehydrog najwięcej odczytów przypisano do białek dehydrogenaz aminokwasów, katalizujących przeniesienie grupy aminowej do ketokwasów. Powyższe związki odpowiadają za zmiany sensoryczne ryb (Zhuang i in., 2021). U *P. psychrophila* KM02 zidentyfikowano klany białek zaangażowane w rozkład tłuszczu; były to Lipase_3 i Lipase_GDSL, o wartościach odpowiednio 2131 i 1246. Termostabilne lipazy uczestniczące w psuciu żywności kodowane są przez geny *lipA* i *lipB*. Powyższe geny zidentyfikowano również u *P. fluorescens* SRM1 (Lo i in., 2015).

Ocena całego genomu *P. psychrophila* KM02 wskazała potencjał fizjologiczny drobnoustrojów do psucia ryb. Dane po sekwencjonowaniu zdeponowano w bazie NCBI pod numerem NZ_CP049044. Powyższe dane uznane zostały przez Zespół NCBI za materiał referencyjny.

Tabela 8. Wybrane terminy GO genomu *P. psychrophila* KM02

Domena biologiczna	Termin GO	Definicja wg bazy QuickGO (https://www.ebi.ac.uk/QuickGO/)	Ilość odczytów (analiza WGS)	Ilość odczytów (analiza RNA-seq)
Składnik molekularny GO	1902494 // kompleks katalityczny	Białka o aktywności katalitycznej	23765	86
	0098796 // kompleks białka błonowego	Białka strukturalne błony komórkowej	20030	297
	1902495 // kompleks transportu transbłonowego	Kompleks białek transbłonowych pozwalających na transfer substancji	15286	24
Funkcja molekularna GO	0016787 // aktywność hydrolazy	Hydroliza wiązań C-O, C-N, C-C, wiązań fosforowych.	284201	1809
	0008233 // aktywność peptydazy	hydroliza wiązania peptydowego	39142	296
	0022857 // aktywność transportera transbłonowego	uczestnictwo w wymianie substancji	207467	927
	0140096 // aktywność katalityczna wobec białka	Modyfikacja białka	85264	384
	0016788 // aktywność hydrolazy, hydroliza wiązań estrowych	hydroliza wiązania estrowego	44622	147

Tabela 9. Wybrane klany białek *P. psychrophila* KM02 związane z procesem psucia ryb

Identyfikator Pfam/Nazwa	Opis/przewidywana funkcja	Ilość odczytów (WGS)	Ilość odczytów (RNA-seq)
Amidohydro_1	Rodzina metalopeptydaz	11828	30
Abhydrolase_1	Rodzina enzymów hydrolitycznych obejmujących proteazy, lipazy, peroksydazy, esterazy, hydrolazy epoksydowe i dehydrogenazy	7768	10
AA_permease_2	Integralne białka błonowe zaangażowane w transport aminokwasów	6643	117
Abhydrolase_6	Rodzina enzymów hydrolitycznych alfa/beta, o szerokiej specyficzności	6099	0
MMPL	Białka strukturalne błony komórkowej związane z transportem lipidów	5848	2
Peptidase_M20	Rodzina metalopeptydaz wiążących jony cynku	5763	10
CN_hydrolase	Hydrolazy rozkładające wiązania C-N	5612	16
Amidase	Hydroliza wiązań amidowych	5466	6
T2SSE	Rodzina zawierająca komponenty T2SS oraz systemu sekrecyjnego typu IV	5142	0
Hydrolase_4	Egzopeptydazy	4896	16
MotA_ExbB	Białka błonowe zaangażowane w sekrecję enzymów	4393	23
Peptidase_M24	Rodzina metalopeptydaz należąca do rodziny MEROPS peptydaz M24	3955	41
M20_dimer	Rodzina peptydaz M20	3075	1
Peptidase_M23	Rodzina metalopeptydaz wiążących jon cynku	2758	26
Lon_C	Rodzina proteaz sklasyfikowanych jako S16 MEROPS	2446	11

Tabela 9. Wybrane klany białek *P. psychrophila* KM02 związane z procesem psucia ryb (c.d.)

Zn_protease	Proteazy wiążące jon cynku zależne od ATP	2408	3
ELFV_dehydrog	rodzina białek, które katalizują deaminację oksydacyjną aminokwasu do ketokwasów	2372	6
Peptidase_S11	egzopeptydazy, endopeptydazy, oligopeptydazy i omega-peptydazy	2249	29
Cys_Met_Meta_PP	Obejmuje enzymy zaangażowane w metabolizm cysteiny i metioniny; koenzymy w reakcjach dekarboksylacji, deaminacji i transaminacji	2191	18
Lipase_3	Hydroliza wiązań estrowych	2131	*
Amidohydro_2	Rodzina obejmująca deaminazę adeninową hydrolizującą adeninę do hipoksantyny i amoniaku	2066	0
Peptidase_M3	grupa metalopeptydaz (oligopeptydaz)	1757	21
Ser_hydrolase	hydrolazy seryny	1683	2
Peptidase_C13	rodzina proteaz cysteinowych hydrolizująca wiązanie peptydowe	1623	0
Peptidase_S9	rodzina peptydaz serynowych	1622	2
Aminopep	rodzina peptydaz z zachowanym motywem HEXXH	1550	3
Abhydrolase_2	Rodzina fosfolipaz i karboksyloesteraz o szerokiej specyficzności substratowej	1527	4
Lipase_GDSL	Esterazy i lipazy GDSL	1246	2
FA_desaturase	enzymy katalizujące insercję podwójnego wiązania w pozycji delta kwasów tłuszczowych	1240	5

* – w zastosowanych warunkach hodowli dedykowanych analizie RNA-seq nie odnotowano transkrypcji CDS, ponieważ tłuszcz nie był składnikiem pożywki

Obecność genów nie zawsze oznacza ich ekspresję w określonych warunkach środowiska (Camiade i in., 2020). Zastosowanie techniki RNA-seq umożliwiło dokonanie ilościowego pomiaru transkryptów *P. psychrophila* KM02. Hodowlę badanych drobnoustrojów prowadzono na zmodyfikowanej pożywce TSB z peptonem z ryby. Zastąpienie hydrolizatu białek roślinnych i kazeinowych peptonem z ryby pozwoliło na odwzorowanie źródła związków azotowych występujących w surowcu. W celu normalizacji danych wykorzystano współczynnik RPKM. Wartości RPKM umożliwiają porównanie poziomu transkrypcji genów w obrębie jednej próby (Liu i in., 2019).

W zastosowanych warunkach hodowli spośród 4719 CDS ekspresji uległo 1865 (około 40%). Najwyższym poziomem transkrypcji odznaczały się geny metabolizmu podstawowego, kodujące: białka rybosomalne, regulatory translacji, białka wiążące DNA oraz białka i lipoproteiny błony zewnętrznej (Rycina 6). Wykorzystując informacje z bazy danych Pfam, otrzymanym odczytom przypisano przewidywane funkcje, grupując dane w klany białek. W transkryptomie *P. psychrophila* KM02 najwięcej odczytów uzyskano dla klanu CL0023, do którego należą białka wiążące nukleotydy oraz dla klanu CL0063 obejmującego białka zawierające tzw. pofałdowanie Rossmanna wiążące FAD/NAD(P) (Rycina 7). Zgodnie z pracą Medvedev i in. (2021) białka z powyższym motywem są powszechne i pokrywają 38% referencyjnych szlaków metabolicznych. Na podstawie adnotacji z bazy danych GO, dominującym odczytom przypisano pełnioną funkcję w komórce. Wysoki udział w transkryptomie miały produkty genów przypisanych do funkcji molekularnych – wiązania oraz aktywności katalitycznej (Rycina 8). Ponieważ są to terminy obejmujące szeroki zakres funkcji komórkowych, dla wyodrębnionych terminów ontologii genów (Tabela 8) oraz klanów białek (Tabela 9) związanych z metabolizmem białek, lipidów oraz syntezą EPS przypisano poziomy transkrypcji w zastosowanych warunkach hodowli. Terminami ontologii genów ściśle powiązanymi z „aktywnością katalityczną" są m. in. aktywność hydrolazy oraz aktywność katalityczna wobec białka. Dla powyższych terminów oznaczono odpowiednio 1809 i 384 odczyty. Wyniki profilowania Pfam wykazały, że klany białek związane z aktywnością proteolityczną *P. psychrophila* KM02 ulegają ekspresji w pożywce imitującej produkt z ryb. Wysoką ilość odczytów otrzymano dla czynników należących do klanu Peptidase_M3 (21) oraz klanu Peptidase_S11 (29).

Przeprowadzona analiza całego transkryptomu *P. psychrophila* KM02 hodowanych w warunkach imitujących produkt na bazie ryb, pozwoliła na uzupełnienie

danych WGS. Do oznaczeń RNA-seq zastosowano pepton z ryb, dlatego największą liczbę odczytów przypisano do CDS związanych z metabolizmem białek/substancji azotowych.

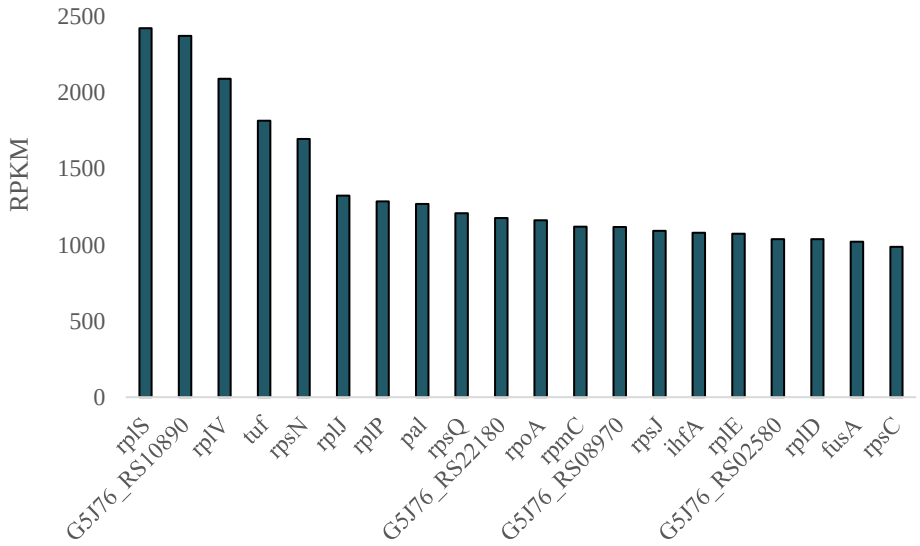

Rycina 6. Zidentyfikowane CDS o najwyższym poziomie transkrypcji u *P. psychrophila* KM02

rplS, G5J76_RS10890, rplV, rpsN, rplJ, rplP, rpsQ, rpmC, rpsJ, rplE, rplD, rpsC – białko rybosomalne, tuf, fusA – czynnik elongacyjny, pal – lipoproteina błony zewnętrznej, G5J76_RS22180, ihfA– białko wiążące DNA, rpoA – podjednostka alfa polimerazy RNA, G5J76_RS08970 – białko błony zewnętrznej, G5J76_RS02580 - białko zawierające domenę DUF1127; funkcja nieznana

Rycina 7. Klany białek o największej ilości przyporządkowanych odczytów transkryptomu *P. psychrophila* KM02

CL0021 – białka zwierające domenę wiążącą oligonukleotydy lub oligosacharydy; CL0023 – zawierające pętlę P hydrolazy trifosforanów nukleozydów; CL0036 – enzymy zwierające strukturę baryłki hydrolazy triozofosforanowej wiążącą fosforany; CL0063 – białka zawierające tzw. pofałdowanie Rossmanna wiążące FAD/NAD(P); CL0108 – ATPazy aktynopodobne; CL0123 – białka zawierające motyw helisa-zwrot-helisa; CL0193 – białka błony zewnętrznej zawierające motyw beta-baryłki

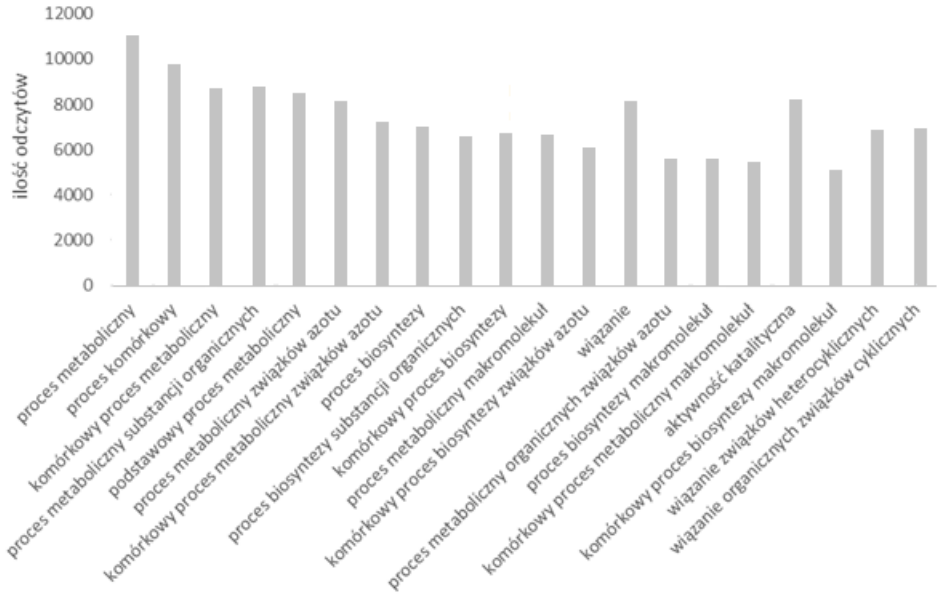

Rycina 8. Funkcje produktów genów o największej ilości dopasowanych odczytów w transkryptomie *P. psychrophila* KM02

4.6. Wpływ subMIC TEO, BPEO, ME, PHE, LIM i CAR na system efflux oraz T2SS u *P. psychrophila* KM02

Sposobem ingerencji w system quorum sensing jest również dezaktywacja jego czynników regulacyjnych, związanymi z systemami efflux i T2SS. Białka systemu efflux uczestniczą w transporcie cząsteczek AI; T2SS jest zaangażowany w proces sekrecji enzymów i innych produktów regulowanych przez quorum sensing (Moradali i in., 2017). System efflux, warunkując wydalanie czynników toksycznych (antybiotyków, metali ciężkich, związków organicznych, aktywnych składników środków dezynfekcyjnych) z wnętrza komórek, kształtuje oporność drobnoustrojów na powyższe czynniki (Rampioni i in., 2017).

W niniejszej pracy w złożonym *de novo* genomie *P. psychrophila* KM02 zidentyfikowano sekwencje kodujące białka systemu efflux oraz T2SS (publikacja P-3 i P-4). Do kolejnych etapów pracy wytypowano następujące geny: *mfs, mexAB-oprM, muxABC-ompB* (geny-operony systemu efflux) oraz *tadB1, tadC1, gspH1, gspH2, pulG, gspG, pulF2* (geny T2SS). Funkcje badanych genów opisano w Tabeli 1.

W niniejszej pracy wpływ olejków eterycznych i ich pojedynczych składników na białka systemu efflux *P. psychrophila* KM02 weryfikowano dwuaspektowo; oceniając

zmiany poziomu ekspresji genów kodujących białka fuzyjne *(mexA, muxA)* i białka zewnątrzbłonowe *(oprM, opmB)* oraz analizując potencjał ME, PHE, LIM i CAR do łączenia się w miejscu aktywnym białek transportujących Mfs, MexB, MuxB.

Białka Mfs, MexB i MuxB są związane z błoną cytoplazmatyczną drobnoustrojów i wiążą transportowany substrat (Li i Plésiat, 2016). Na podstawie sekwencji aminokwasowych w serwerze I-Tasser (Roy i in., 2010) przygotowano modele białek. Zmiany w poziomie mRNA badanych genów u *P. psychrophila* KM02 przedstawiono na Rycinie 9 oraz w publikacji P-2. Indukcję systemu efflux dokonano wprowadzając do hodowli komórek *P. psychrophila* KM02 antybiotyk (kwas nalidyksowy) w stężeniu 30 μg/mL, wobec którego testowane drobnoustroje nie wykazują wrażliwości. Następnie do hodowli wprowadzano olejki eteryczne i ich związki bioaktywne w stężeniu subMIC. Po narażeniu komórek na wybrane stężenie kwasu nalidyksowego, odnotowano wzrost poziomu mRNA genów *muxA, mexA* i *oprM*. Powyższa prawidłowość jest spójna z rezultatami uzyskanymi przez Takrami i in. (2017) i wskazuje na udział białek MuxA, MexA i OprM w procesie oporności *Pseudomonas* spp. na kwas nalidyksowy. Inkubacja komórek z subMIC TEO doprowadziła do istotnego obniżenia poziomu mRNA genów systemu efflux. Uzyskane wyniki potwierdzają zdolność TEO do ingerencji w system efflux. Zdolność stężeń subMIC ME, i PHE do zmian w poziomie mRNA genów systemu efflux była niższa niż olejku eterycznego. Podobną zależność zauważono w pracy Limaverde i in. (2017), gdzie zastosowanie subMIC olejku eterycznego z *Chenopodium ambrosioides* (komosy piżmowej) skutecznie hamowało działanie systemu efflux TetK u *Staphylococcus aureus*, podczas gdy jego główny związek, α-terpinen nie wykazywał żadnej aktywności. W niniejszej pracy wykazano, że BPEO mniej efektywnie wpływa na poziom mRNA genów systemu efflux u *P. psychrophila* KM02 niż jeden z jego głównych komponentów, CAR. Powyższa prawidłowość może wynikać z wpływu drugiego głównego składnika BPEO – LIM, którego zastosowanie nie skutkowało redukcją poziomu mRNA genów systemu efflux u *P. psychrophila* KM02. Odmienne rezultaty uzyskali de Araújo i in. (2021), udowadniając wpływ LIM na syntezę białka MrsA i TetK u *Staphylococcus aureus*. Rozbieżności te mogą wynikać z różnic w zastosowanym stężeniu LIM, który w prezentowanej pracy mógł być niewystarczający do hamowania systemu efflux.

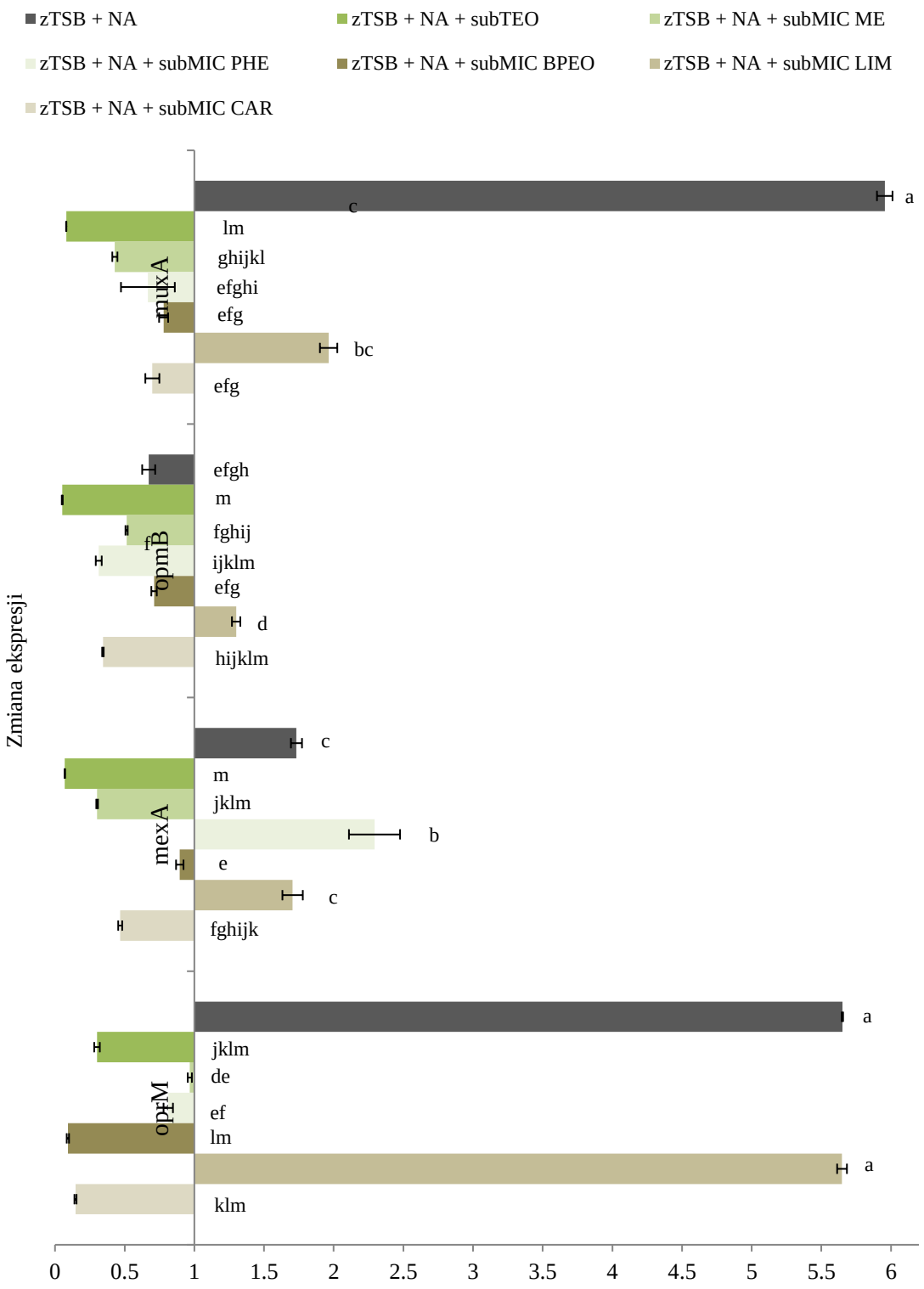

Rycina 9. Zmiana poziomu ekspresji genów systemu efflux (F=2629; p < 2e-16 ***) w komórkach *P. psychrophila* KM02 inkubowanych na pożywce zTSB z NA, suplementowanej subMIC TEO, BPEO, ME, PHE, LIM i CAR

Wyniki dokowania molekularnego składników bioaktywnych TEO i BPEO z białkami transportującymi systemu efflux (Mfs, MexB, MuxB) przedstawiono w Tabeli 10 oraz w publikacji P-3. Wizualizacje sposobu dokowania białek efflux z bioaktywnymi składnikami TEO w postaci rzutu kartonowego 2D oraz 3D przedstawiono na Rycinie 10-12.

Białko Mfs wpływa na ekspresję czynników wirulencji i odpowiada za wrażliwość na antybiotyki *P. aeruginosa*. W niniejszej pracy oddziaływania hydrofobowe z resztami ARG30 i ALA347 białka Mfs warunkowały tworzenie kompleksów z bioaktywnymi składnikami TEO i BPEO. Wartości dokowania wahały się w zakresie od -2,332 kcal/mol (Mfs-LIM) do -4,170 kcal/mol (Mfs-PHE). Dla kompleksu białka Mfs z kemferolem (udokumentowanym inhibitorem systemu efflux typu Mfs) wartość dokowania wynosiła -8,011 kcal/mol. Powyższy kompleks utworzony został za pomocą stabilizującego wiązania typu „π – stacking" z resztą PHE120. W pracy Zárate i in. (2019) również wykazano, że decydującą resztą wiążącą ligandy w miejscu aktywnym białka typu Mfs jest PHE. Z tą resztą aminokwasową, naturalny inhibitor kapsaicyna również tworzyła wiązanie typu „π – stacking", generując wartości dokowania -7,19 kcal/mol.

Kolejnym analizowanym białkiem systemu efflux był MexB. Powyższe białko bierze udział w aktywnym transporcie 3-okso-C12-HSL oraz reguluje dostęp cząsteczek AI do receptora systemu quorum sensing (Minagawa i in., 2012). Spośród analizowanych związków olejków eterycznych, najwyższą wartość dokowania otrzymano dla układu MexB-CAR, co mogło wynikać z oddziaływań elektrostatycznych z resztami ASN33 i PRO36. Według Klebe (2013) oddziaływania elektrostatyczne są dominującym czynnikiem w wiązaniu białko-ligand. Syntetyczny inhibitor Phe-Arg-β-naftyloamidu (PaβN) (Rampioni i in., 2017) wykazywał silną interakcję (-6,414 kcal/mol) za pośrednictwem reszt PHE388, GLU672, PRO36, GLY296 i ASN33. Powyższe wyniki są zgodne z badaniami Aparna i in. (2014), które wykazały, że miejscem aktywnym białka MexB u *P. aeruginosa* są reszty PRO36, PHE388 i GLN46.

Białko MuxB jest składnikiem kompleksu MuxABC-OpmB, odpowiedzialnego za oporność drobnoustrojów na antybiotyki: głównie nowobiocynę, tetracyklinę, erytromycynę, kitasamycynę i rokitamycynę (Mima i in., 2007). Dezaktywacja systemu efflux MuxABC-OpmB doprowadza do zmian w ekspresji sygnałów quorum sensing i do akumulacji AI PQS i AHL (Adamiak i in., 2021).

Tabela 10. Wyniki dokowania molekularnego inhibitorów oraz ME, PHE, LIM i CAR z białkami efflux komórek *P. psychrophila* KM02

Wariant kompleksu	Wartość dokowania [kcal/mol]	Energia kompleksu [kcal/mol]	Reszty aminokwasowe wchodzące w interakcje	Długość wiązania/ odległość [Å]	Typ interakcji
MFS – ME	-3,585	-24,801	ARG30 PHE119, PHE120, PHE59, TYR62	1,80; 2,48 -	Wodorowe hydrofobowe
MFS – PHE	-4,170	-15,217	TYR248, ILE144, PHE119, TRP350	-	Hydrofobowe
MFS – LIM	-2,332	-12,689	ARG30, ALA347, TYR248	-	Hydrofobowe
MFS – CAR	-4,092	-17,903	PHE120, ARG30, ALA347	- -	Polarne Hydrofobowe
MFS – kaempferol	-8,011	-39,001	PHE120 ARG30 ALA347 ASN374 TYR248	4,75 1,95 1,98 2,36 2,73	π – stacking aromatyczne wodorowe aromatyczne wodorowe aromatyczne wodorowe wodorowe
MEXB – ME	-4,369	-26,719	TYR35 ILE38, ALA39 GLU672	1,96 - -	Wodorowe hydrofobowe polarne
MEXB – PHE	-3,604	-18,009	ILE38, ALA39, VAL670, LEU137 ASN33, SER297	- -	hydrofobowe polarne
MEXB – LIM	-3,034	-17,814	ASN33, PRO36, GLU672	- -	Hydrofobowe Polarne
MEXB – CAR	-4,434	-26,716	AL39, VAL133 SER37, GLN34, ASN33	- -	Hydrofobowe polarne
MEXB – PaβN	-6,414	-7,131	PHE388 GLN469 GLY296 GLY296 ASN33 PRO36 GLU672 GLU672 GLU672	4,52 2,70 2,77 2,20 2,16 2,27 2,28 2,05 4,40	π – stacking wodorowe wodorowe aromatyczne wodorowe aromatyczne wodorowe aromatyczne wodorowe aromatyczne wodorowe aromatyczne wodorowe mostek solny

Tabela 10. Wyniki dokowania molekularnego inhibitorów oraz ME, PHE, LIM i CAR z białkami efflux komórek *P. psychrophila* KM02 (c.d.)

MUXB – ME	-4,125	-23,186	GLN563 SER663 ASN284	3,85 - -	Wodorowe polarne naładowane ujemnie
MUXB – PHE	-3,442	-17,175	ARG323, THR657 GLN563	- -	naładowane dodatnio polarne
MUXB – LIM	-3,311	-13,627	ARG323, THR657 ASP136	- -	naładowane dodatnio naładowane ujemnie
MUXB – CAR	-2,826	-10,665	GLN654, ALA135, VAL653, PRO134, THR137, SER663	- -	Hydrofobowe Polarne
MUXB – theobromine	-4,365	-27,255	GLN654 GLN563 ARG323, THR657	1,68 2,06 -	aromatyczne wodorowe aromatyczne wodorowe naładowane dodatnio

W niniejszej pracy najwyższą wartość dokowania odnotowano dla ME (-4,125 kcal/mol). Prawidłowość wynika z oddziaływań ME z resztami ARG323 i THR657 oraz wiązania wodorowego z GLN563, które stabilizuje utworzony układ. Ponieważ w literaturze nie opisano dotąd specyficznego inhibitora białka MuxB, przeprowadzono serię eksperymentów dokowania molekularnego (Ghosh i in., 2020) i na ich podstawie wybrano teobrominę, dla której wartość dokowania wyniosła -4,365 kcal/mol. Odnotowano obecność wiązań wodorowych z GLN654 i GLN563 oraz oddziaływań elektrostatycznych z dodatnio naładowanymi ARG323 i THR657.

Uzyskane wyniki analiz RT-qPCR oraz dokowania molekularnego potwierdziły potencjał TEO i BPEO do modulowania aktywności systemu efflux, który determinuje zarówno działanie mechanizmu quorum sensing oraz oporność na działanie związków toksycznych u *P. psychrophila* KM02.

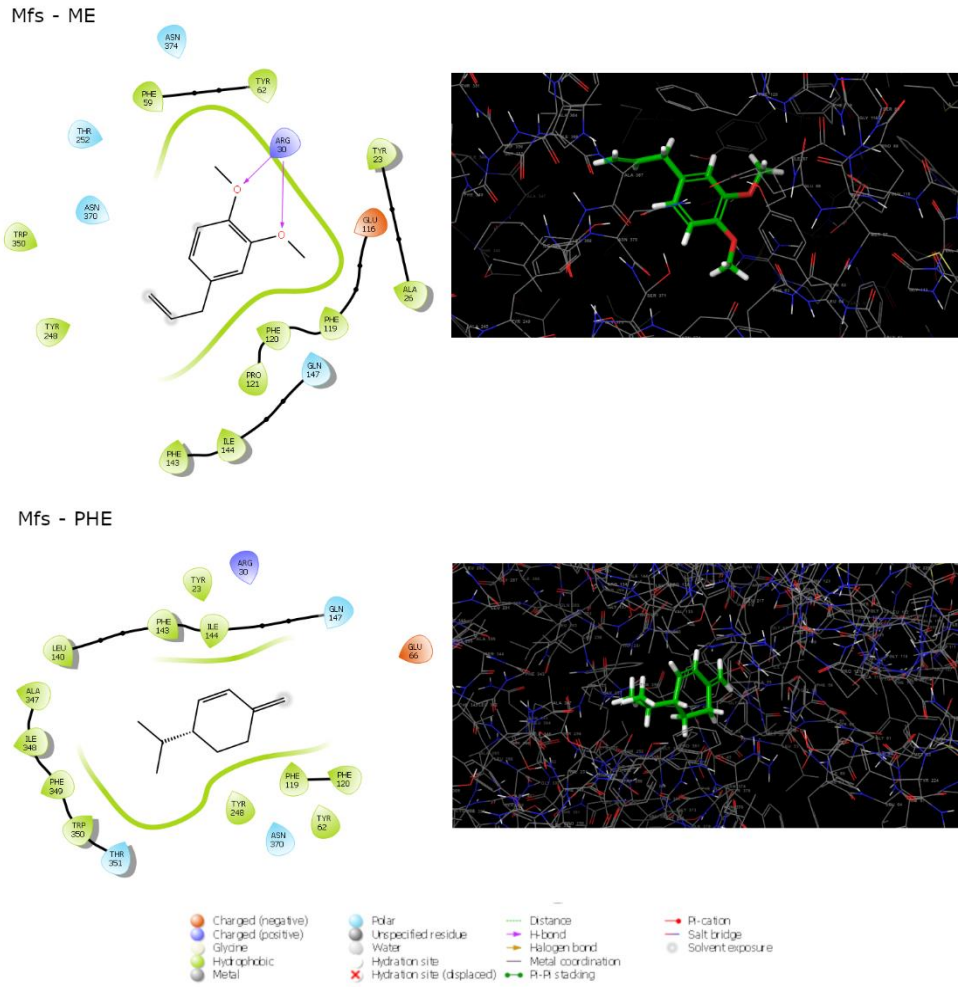

Rycina 10. Sposób dokowania białka efflux Mfs z ME i PHE

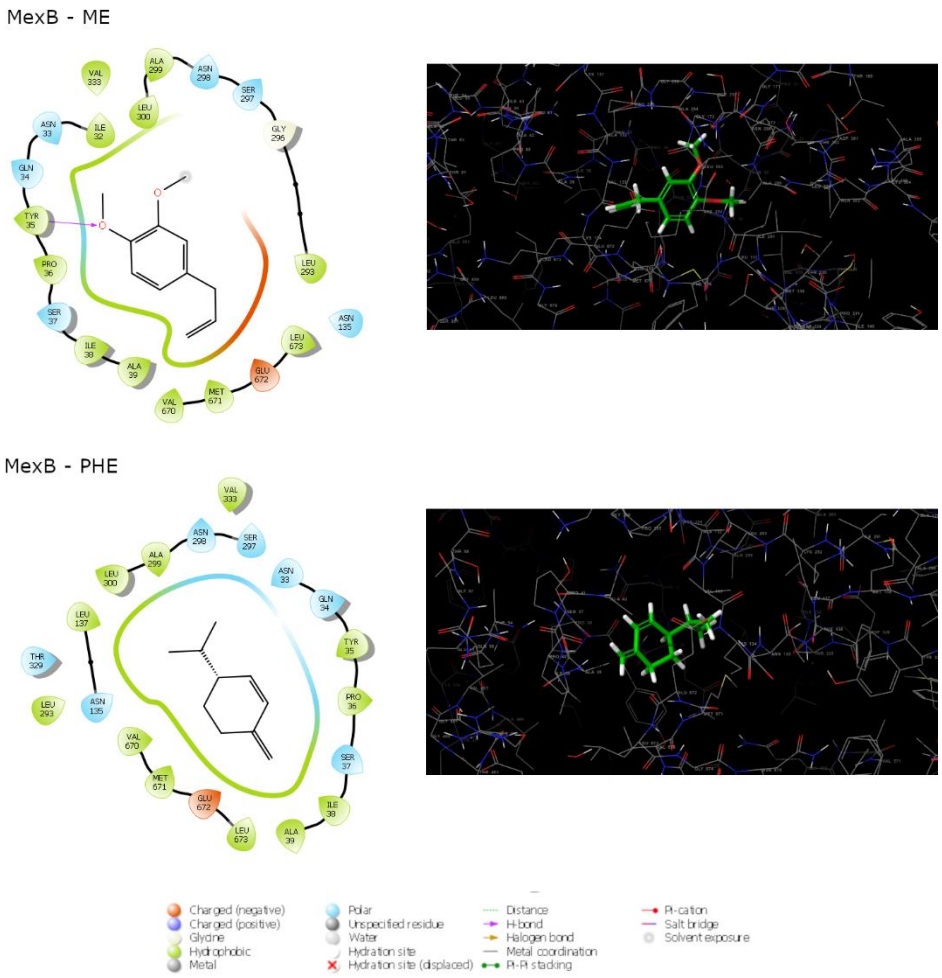

Rycina 11. Sposób dokowania białka efflux MexB z ME i PHE

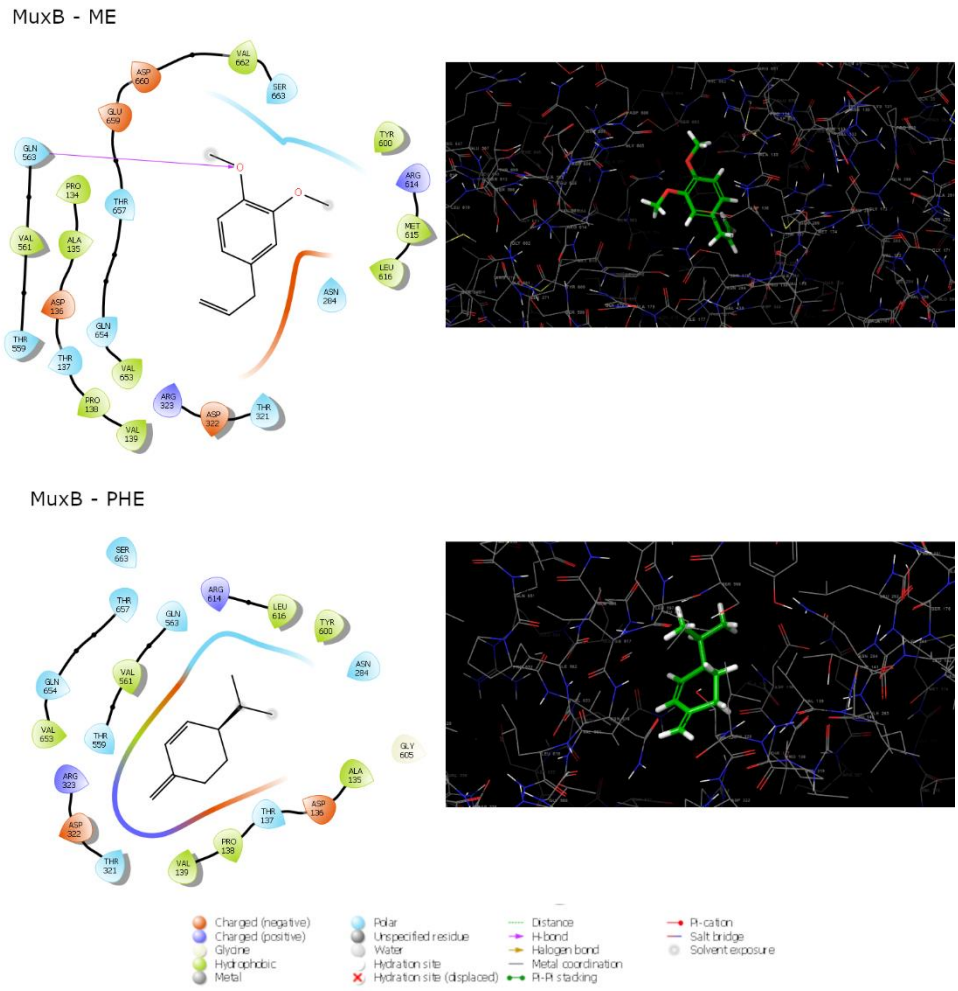

Rycina 12. Sposób dokowania białka efflux MuxB z ME i PHE

W niniejszej pracy zweryfikowano również wpływ TEO i BPEO na ekspresję genów kodujących białka systemu T2SS. Wpływ ten oceniano jako zmianę poziomu mRNA genów po inkubacji z subMIC TEO, BPEO, ME, PHE, LIM i CAR. Rezultaty analiz RT-qPCR przedstawiono na Rycinie 13 oraz w publikacji P-4. W genomie *P. psychrophila* KM02 zidentyfikowano geny związane z T2SS: geny *pulG* i *gspG* kodujące pseudopiliny PulG i GspG; *tadB1* i *tadC1* kodujące integralne białka błony wewnętrznej zaangażowane w ogólny szlak sekrecyjny (GSP); geny *gspH2* i *gspH1* kodujące białka zaangażowane w proces wydzielania; i *pulF* gen kodujący białko zaangażowane w eksport lipaz. Poziom ekspresji genów T2SS po inkubacji z analizowanymi czynnikami wahał się od 0,9 do 0,02. Największe redukcje poziomów mRNA genów T2SS odnotowano po ekspozycji komórek na TEO i jego pojedyncze składniki (ME i PHE). Poziom mRNA genów *gspH1* oraz *gspH2* wyniósł odpowiednio 0,05 i 0,02. Niniejsze wyniki są zgodne z pracą Jain i in. (2018), w której odpowiedź komórek *Pseudomonas* spp. na środki przeciwdrobnoustrojowe pochodzenia naturalnego oceniona została na poziomie proteomu. Zastosowanie wodnych ekstraktów katechin pozyskanych z kwiatów *Saraca asoca* doprowadziło u *P. aeruginosa* do obniżenia syntezy białek zaangażowanych w układy sekrecyjne (np. xcp, PilS). Dodatkowo w pracy Singh i in. (2017) odnotowano rolę olejku eterycznego tymianku w zwalczaniu czynników wirulencji regulowanych przez T2SS u *Xanthomonas oryzae*. Ekspresja czynników wirulencji *Xanthomonas* spp. uległa nieznacznym zmianom, gdy bakterie były traktowane samym tymolem.

Uzyskane wyniki potwierdziły zdolność badanych czynników do dezaktywacji systemu sekrecyjnego zidentyfikowanego w komórkach *P. psychrophila* KM02. Powyższe zmiany zaburzają funkcjonowanie systemu quorum sensing *P. psychrophila* KM02.

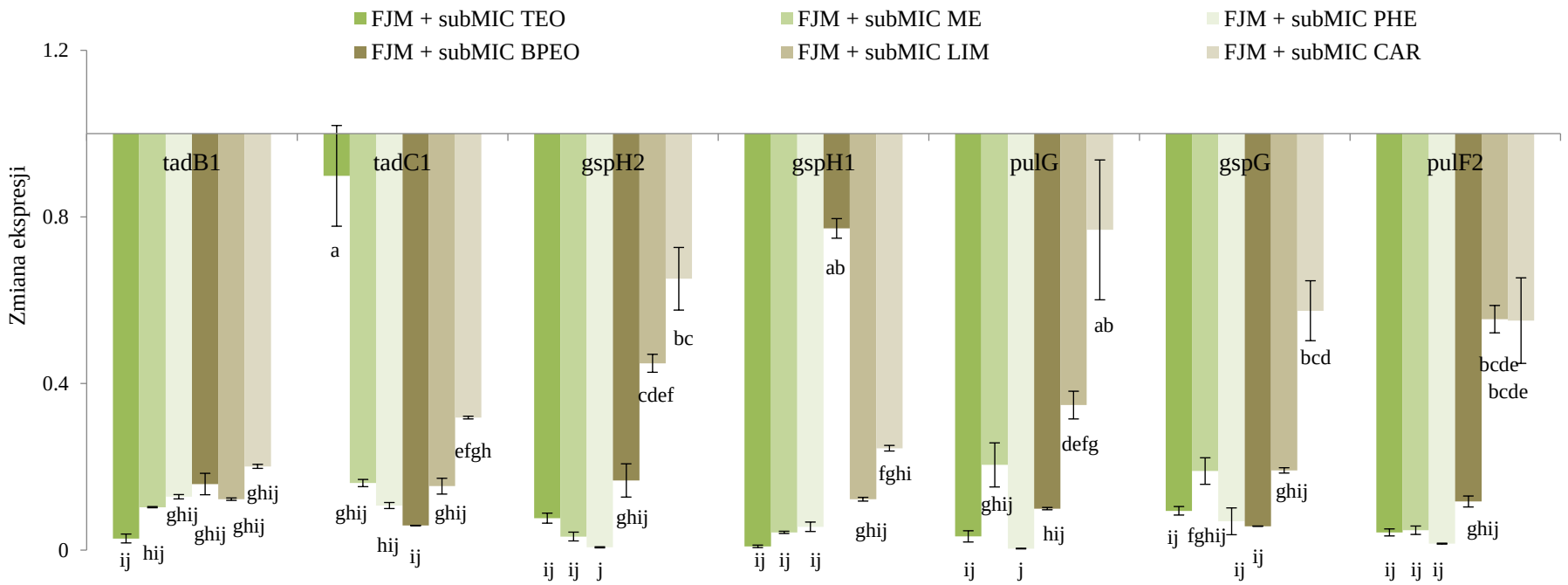

Rycina 13. Zmiana poziomu ekspresji genów systemu T2SS (F=41,32; p<2e-16 ***) w komórkach *P. psychrophila* KM02 inkubowanych na pożywce FJM suplementowanej subMIC TEO, ME, PHE, BPEO, LIM i CAR

4.7. Wpływ stężeń subMIC TEO, BPEO, ME, PHE, LIM i CAR na aktywność proteolityczną, lipolityczną oraz syntezę EPS zależnych od systemu quorum sensing u *P. psychrophila* KM02

Mikrobiologiczne psucie ryb objawia się przede wszystkim zmianami właściwości fizykochemicznych tkanki, obecnością na jej powierzchni warstwy śluzu oraz wytworzeniem nieprzyjemnego zapachu (Comi, 2017). Objawy te są wynikiem rozkładu białek i lipidów oraz syntezy EPS przez komórki bakteryjne. Powyższe aktywności metaboliczne *Pseudomonas* spp. regulowane są mechanizmem quorum sensing (Ding i in., 2019). W niniejszej pracy zbadano wpływ stężeń subMIC TEO i BPEO oraz ich głównych składników na aktywność proteolityczną, lipolityczną oraz syntezę EPS przez *P. psychrophila* KM02 hodowanego w pożywce TSB i w pożywce FJM. W tym celu przeprowadzono analizy spektrofotometryczne oraz analizy RT-qPCR. Jako próby kontrolne zastosowano hodowle drobnoustrojów prowadzone na podłożach bez dodatku testowanego czynnika przeciw-quorum sensing.

Wyniki wpływu stężeń subMIC TEO, BPEO i ich głównych składników na aktywność proteolityczną zawarto w publikacji P-2 i P-3 oraz przedstawiono na Rycinie 14-16. Zgodnie z wynikami doświadczeń spektrofotometrycznych, wszystkie analizowane substancje istotnie obniżyły aktywność proteolityczną komórek *P. psychrophila* KM02. Największe obniżenie powyższych własności (w zakresie od 36 do 41%) wywołał BPEO, LIM i CAR dodany do pożywki TSB. Podobną zależność odnotowano u komórek hodowanych w pożywce imitującej produkt z ryb. W danych warunkach aktywność proteolityczna została obniżona w zakresie od 27 do 36%. Testowane czynniki efektywniej ingerowały we własności proteolityczne *P. psychrophila* KM02 w warunkach *in vitro* niż *in situ*. Powyższa zależność może być rezultatem obecności głównie wysokocząsteczkowych białek w FJM (Burt, 2004). Suplementacja pożywek stężeniami subMIC PHE skutkowała obniżeniem aktywności proteolitycznej o 20 % (hodowla komórek na pożywce TSB) i o 16% (hodowla komórek na pożywce FJM). W profilu AI quorum sensing badanego mikroorganizmu syntetyzowanych w tych warunkach odnotowano obecność cząsteczek 3-okso-C8-HSL. Zależność między syntezą AI quorum sensing a aktywnością proteolityczną u *Pseudomonas* spp. oceniali również Ding i in., (2019), Li i in. (2019), Pattnaik i in. (2018) oraz Zhao i in. (2018). We wszystkich pracach ingerencja w mechanizm quorum

sensing drobnoustrojów skutkowała zmianami wydajności syntezy enzymów proteolitycznych.

Wpływ analizowanych substancji na aktywność proteolityczną *P. psychrophila* KM02 zbadano także na poziomie molekularnym; oceniano zmiany w poziomie ekspresji wybranych genów kodujących proteazy. Wyniki odnoszono do poziomów mRNA komórek hodowanych na podłożu bez dodatku czynnika przeciwdrobnoustrojowego. W niniejszej pracy, stężenia subMIC badanych czynników wpłynęły na poziom ekspresji genów kodujących proteazy. Było to widoczne we wszystkich wariantach doświadczenia; szczególnie po narażeniu *P. psychrophila* KM02 na stężenia subMIC BPEO i LIM. Rezultaty są zgodne z wynikami przesiewowymi, wykorzystującymi metodę spektrofotometryczną w ocenie zmian aktywności proteolitycznej drobnoustrojów. Powyższej zależności nie odnotowano dla wariantu doświadczenia subMIC ME-pożywka FJM oraz dla wariantu subMIC TEO i subMIC PHE w obu pożywkach.

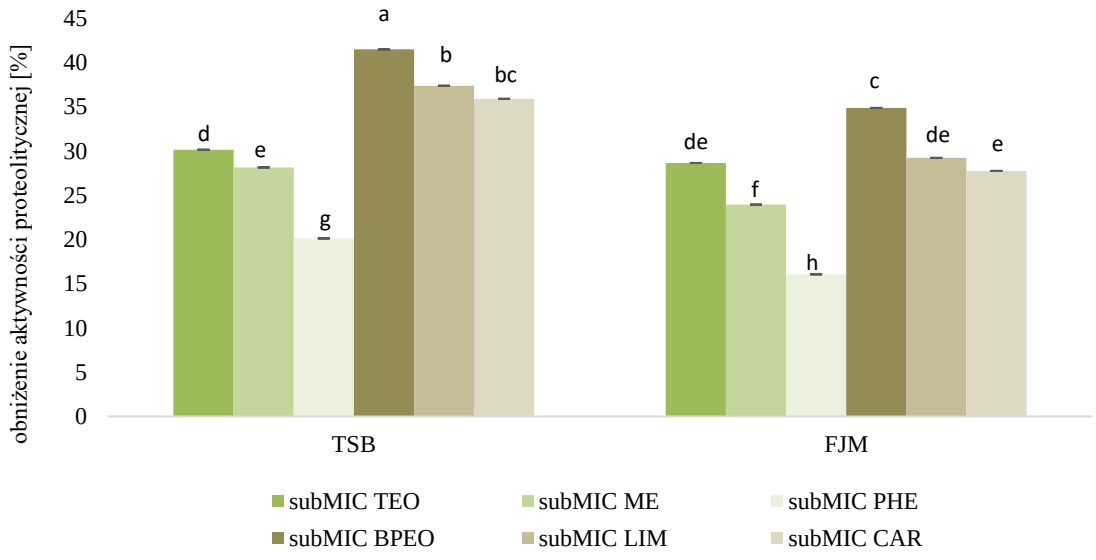

Rycina 14. Zmiana aktywności proteolitycznej (F=1054; p<2e-16 ***) komórek *P. psychrophila* KM02 inkubowanych na pożywkach TSB i FJM suplementowanych subMIC TEO, ME, PHE, BPEO, LIM i CAR

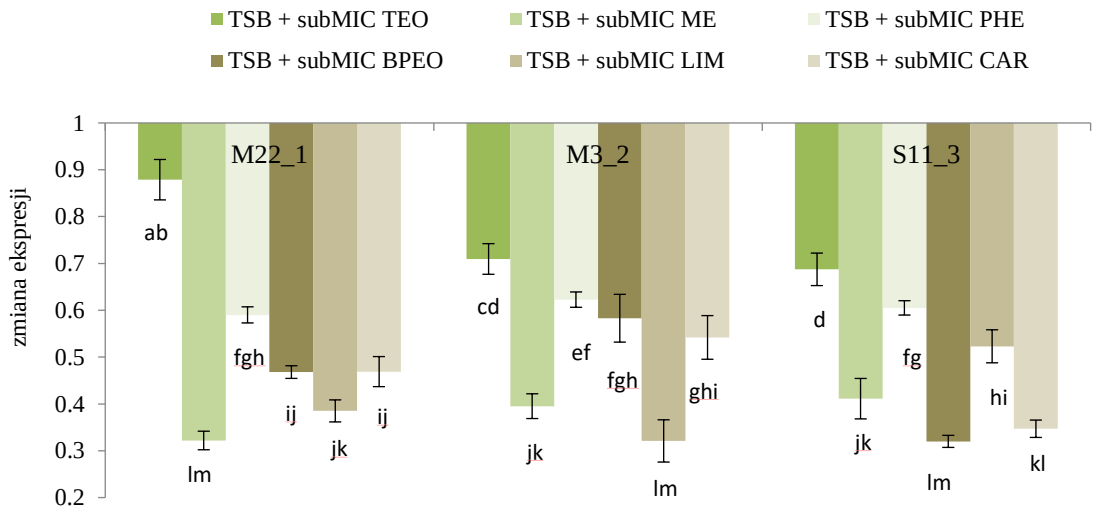

Rycina 15. Zmiana poziomu ekspresji wybranych genów kodujących proteazy (F=98.8, p<2e-16 ***) w komórkach *P. psychrophila* KM02 inkubowanych na pożywce TSB suplementowanej subMIC TEO, ME, PHE, BPEO, LIM i CAR

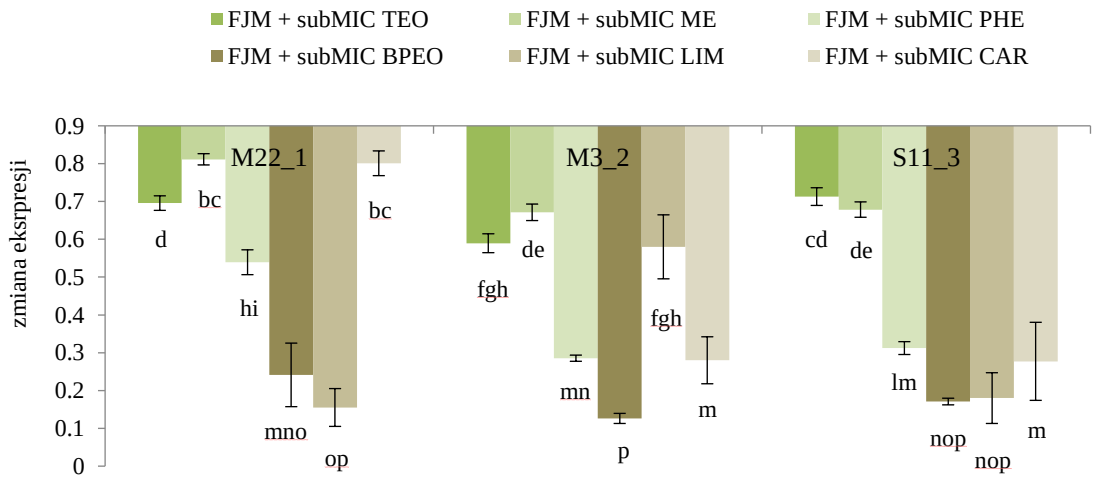

Rycina 16. Zmiana poziomu ekspresji wybranych genów kodujących proteazy (F=98.8; p<2e-16 ***) w komórkach *P. psychrophila* KM02 inkubowanych na pożywce FJM suplementowanej subMIC TEO, ME, PHE, BPEO, LIM i CAR

Wyniki wpływu analizowanych substancji na aktywność lipolityczną przedstawiono w publikacji P-4 oraz na Ryc. 17-19. Wyniki oznaczeń przesiewowych wykorzystujących metodę spektrofotometryczną wykazały wpływ testowanych czynników na aktywność lipolityczną *P. psychrophila* KM02; redukcja aktywności lipolitycznej drobnoustrojów mieściła się w zakresie od 11 do 46% w zależności od zastosowanego układu. Znaczna inhibicja aktywności lipolitycznej *P. psychrophila* KM02 odnotowana została po narażeniu komórek na subMIC TEO i BPEO. Redukcję aktywności lipolitycznej odnotowano również u komórek hodowanych w obecności subMIC ME, PHE, LIM i CAR. Przykładowo suplementacja pożywki TSB przez subMIC ME skutkowała obniżeniem lipolizy *P. psychrophila* KM02 o 17%. W podłożu FJM redukcję aktywności lipolitycznej (o 11%) odnotowano dla wariantu z subMIC CAR. Powyższe obserwacje są zgodne z rezultatami zmian aktywności lipolitycznej u *P. fluorescens* narażonego na działanie olejku eterycznego otrzymanego z jałowca (Myszka i in., 2021). W cytowanej pracy, dla wariantów hodowli suplementowanych olejkiem eterycznym z jałowca odnotowano zahamowanie produkcji lipaz o 45%, podczas gdy jego główne związki, tj. α-pinen i sabinen, były znacznie mniej skuteczne w badanym zakresie. Powyższa zależność może być związana z niższą aktywnością przeciwdrobnoustrojową związków terpenowych w stosunku do roztworów olejków eterycznych (Hyldgaard i in., 2012). Addytywne lub synergistyczne działanie przeciwdrobnoustrojowe obserwuje się podczas stosowania roztworów dwóch lub większej liczby związków terpenowych (Bassolé i Juliani, 2012). Na przykład w pracy Vuuren i Viljoen (2007) hamujący wpływ LIM na wzrost *P. aeruginosa* został wzmocniony przez dodanie równej objętości eukaliptolu.

Dla wariantów eksperymentów prowadzonych w pożywce FJM uzyskano istotnie niższe ($p < 0,05$) wyniki niż w warunkach *in vitro*, z wyjątkiem subMIC ME. Zgodnie z pracą Myszka i in., (2021), w pożywce pozyskanej z ryby odnotowano 1,8 mg/g białka oraz 0,0635 mg/g lipidów, co odwzorowuje produkt. Powyższe składniki zmniejszają aktywność przeciwdrobnoustrojową olejków eterycznych wobec komórek drobnoustrojów (Perricone i in., 2015). Podobnie Sterniša i in. (2020b) wykazali, niewielką wrażliwość komórek *P. psychrophila* na działanie olejku eterycznego z rozmarynu. W cytowanej pracy zastosowanie ekstraktu z rozmarynu w filetach z karpia skutkowało zatrzymaniem procesu lipolizy przez *P. psychrophila* o jeden dzień w stosunku do próby kontrolnej.

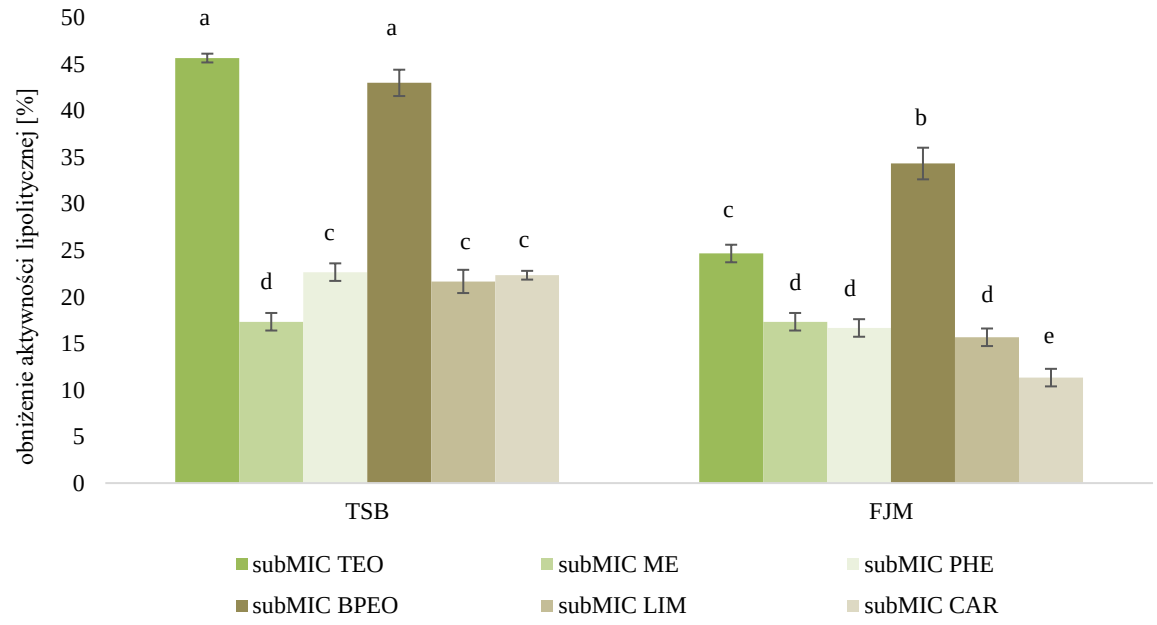

Rycina 17. Zmiana aktywności lipolitycznej (F=308,6; p<2e-16 ***) komórek *P. psychrophila* KM02 inkubowanych na pożywkach TSB i FJM suplementowanych subMIC TEO, ME, PHE, BPEO, LIM i CAR

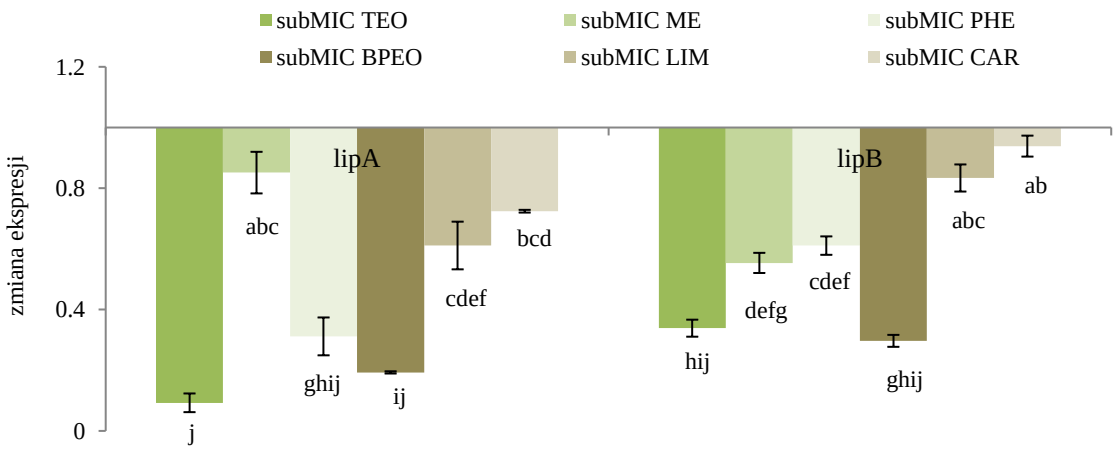

Rycina 18. Zmiana poziomu ekspresji wybranych genów kodujących lipazy (F=41.97; p<2.7e-15 ***) w komórkach *P. psychrophila* KM02 inkubowanych na pożywce TSB suplementowanej subMIC TEO, ME, PHE, BPEO, LIM i CAR

W niniejszej pracy ingerencję w syntezę lipaz przez testowane czynniki w stężeniach subMIC zweryfikowano również oceniając poziom ekspresji genów kodujących lipazy (*lipA*, *lipB*). Najwyższe obniżenie transkrypcji genu *lipA* odnotowano w komórkach *P. psychrophila* KM02 traktowanych subMIC BPEO i subMIC TEO, co potwierdziło obserwacje fenotypowe. Ponieważ geny *lipA i lipB* są połączone w jednym operonie, dlatego zakłócenie ekspresji choćby jednego z nich skutkuje zmianami fizjologicznymi (Frenken i in., 1993). W pracy Myszka i in. (2021), poziom mRNA genu *lipB* również ulegał obniżeniu w największym stopniu po inkubacji komórek *P. fluorescens* z subMIC olejku eterycznego z jałowca potwierdzając wcześniejsze obserwacje. Christensen i in. (2003) wykazali, że szczepy saprofityczne *Serratia proteamaculans* niezdolne do syntezy białka LipB nie zmieniają cech organoleptycznych produktów mlecznych.

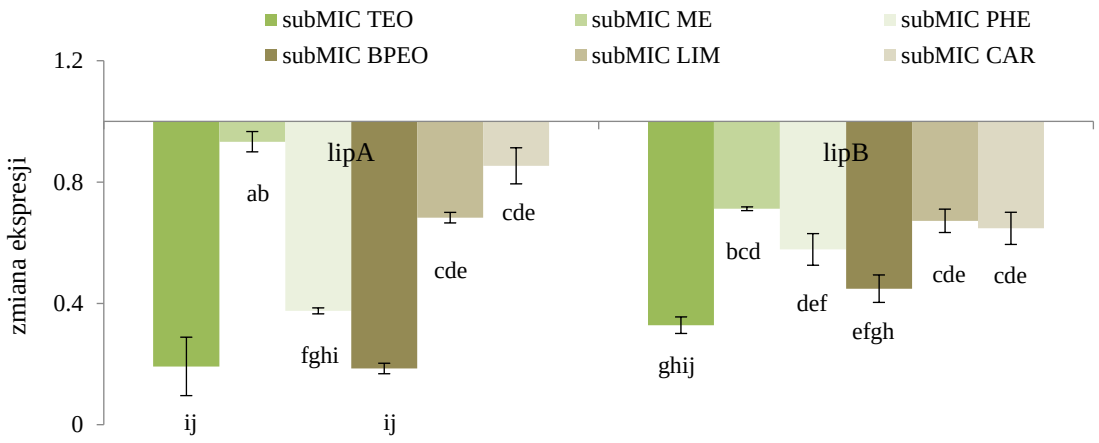

Rycina 19. Zmiana poziomu ekspresji wybranych genów kodujących lipazy (F=41.97; p<2.7e-15 ***) w komórkach *P. psychrophila* KM02 inkubowanych na pożywce FJM suplementowanej subMIC TEO, ME, PHE, BPEO, LIM i CAR

Wyniki wpływu analizowanych czynników na zdolność syntezy przez testowane drobnoustroje EPS przedstawiono w publikacji P-3 oraz na Rycinie 20-22. Syntezę EPS u *P. psychrophila* KM02 inkubowanych bez dodatku badanych czynników oszacowano średnio na poziomie 30,6 µg/10^7 jtk. Po suplementacji środowiska testowanymi czynnikami, efektywność syntezy EPS obniżyła się średnio o 48%. Było to szczególnie

widoczne po narażeniu komórek na działanie subMIC TEO i BPEO. W tych wariantach doświadczenia stwierdzono ponad 60% redukcję syntezy EPS w warunkach *in vitro* oraz ponad 50% redukcję syntezy EPS w warunkach *in situ*. Zastosowanie pojedynczych związków bioaktywnych badanych olejków eterycznych skutkowało inhibicją syntezy EPS od 25% (dla subMIC PHE w pożywce FJM) do 50% (dla subMIC ME w pożywce TSB).

Powyższe obserwacje weryfikowano eksperymentami RT-qPCR, oceniającymi zmiany ekspresji genów odpowiedzialnych za syntezę alginianu, tj. *algA*, kodującego liazę alginianową, *algU* kodującego czynnik sigma α oraz *mucA* kodującego czynnik anty-sigma α (Muhammadi i Ahmed, 2007). Wszystkie czynniki doprowadziły do istotnego obniżenia poziomu mRNA genów *algA* i *algU*. Największą redukcję transkrypcji genów *algA* i *algU* odnotowano w komórkach inkubowanych w pożywce TSB suplementowanej subMIC BPEO, LIM oraz CAR. Dla powyższych czynników odnotowano obniżenie mRNA genu *algA* odpowiednio o 82, 71 i 74%, natomiast genu *algU* o odpowiednio 36, 57 i 79%. Jedynym czynnikiem, dla którego zaobserwowano zwiększenie poziomu ekspresji genu *mucA* był subMIC LIM. Podobne wyniki uzyskano dla komórek *P. fluorescens* KM48 i *P. orientalis* KM149 narażonych na działanie olejku eterycznego z mirtu (Myszka i in., 2020). Powyższa zależność mogła być spowodowana zbliżonym mechanizmem działania LIM oraz głównych związków olejku eterycznego z mirtu: eukaliptolu, alfa-pinenu i octanu mirtenylu. Według Muhammadi i Ahmed, (2007), regulowanie poziomu ekspresji genu *algU* przez geny *muc* doprowadza do obniżenia syntezy EPS.

Uzyskane w niniejszej pracy wyniki wskazują, że TEO i BPEO to wartościowe źródła związków regulujących aktywności metaboliczne bakterii.

.

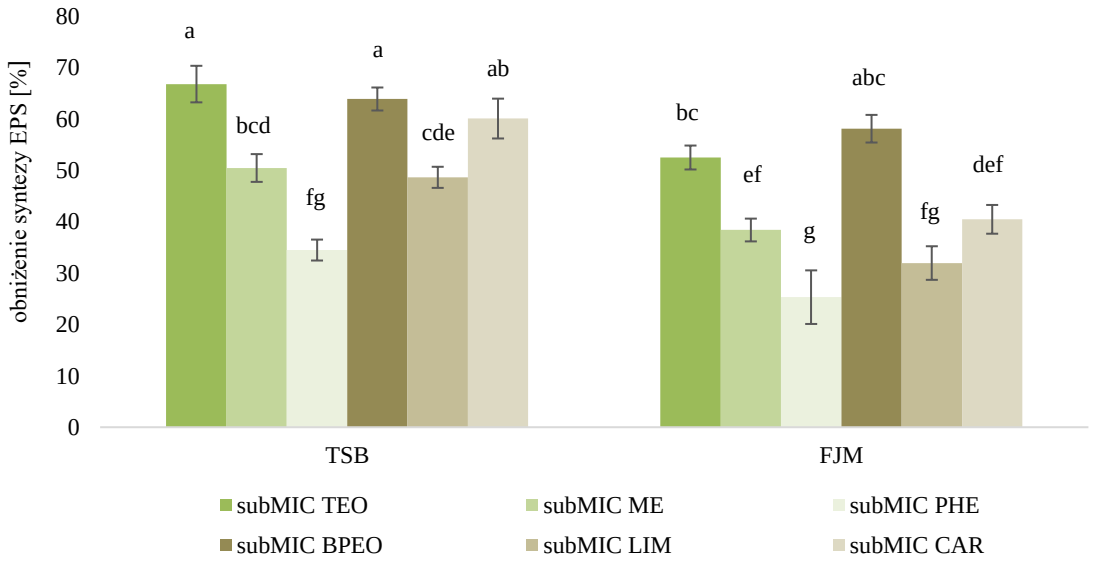

Rycina 20. Zmiana syntezy EPS (F=79,03; p<2e-16 ***) przez komórki *P. psychrophila* KM02 inkubowane na pożywkach TSB i FJM suplementowanych subMIC TEO, ME, PHE, BPEO, LIM i CAR

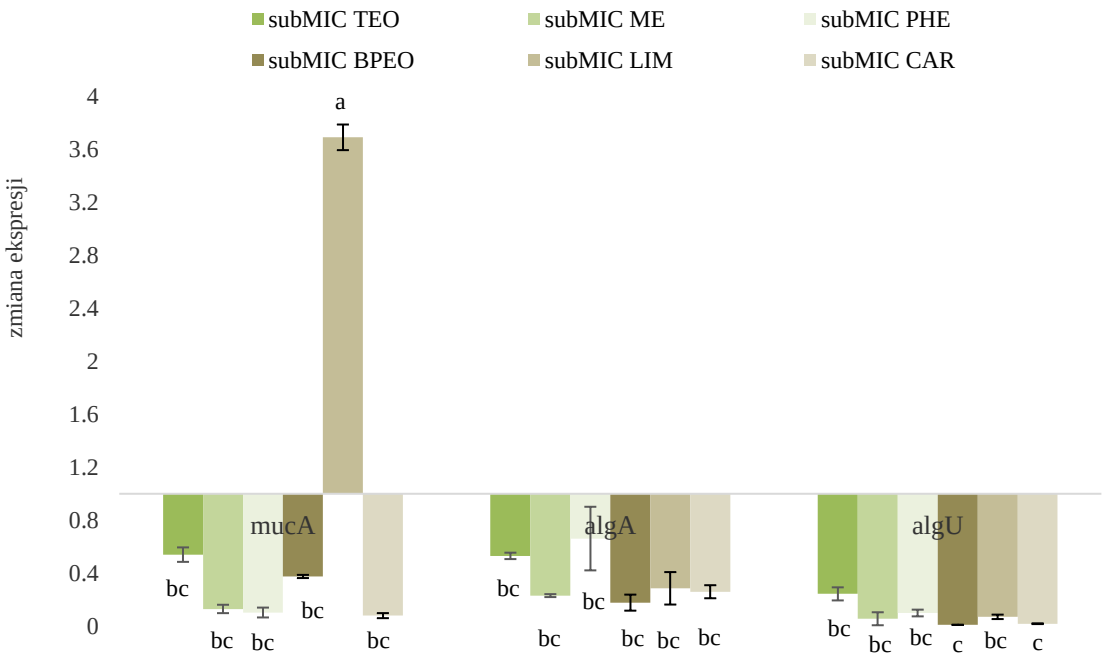

Rycina 21. Zmiana poziomu ekspresji wybranych genów regulujących syntezę EPS (F=25,16; p<2e-16 ***) w komórkach *P. psychrophila* KM02 inkubowanych na pożywce TSB suplementowanej subMIC TEO, ME, PHE, BPEO, LIM i CAR

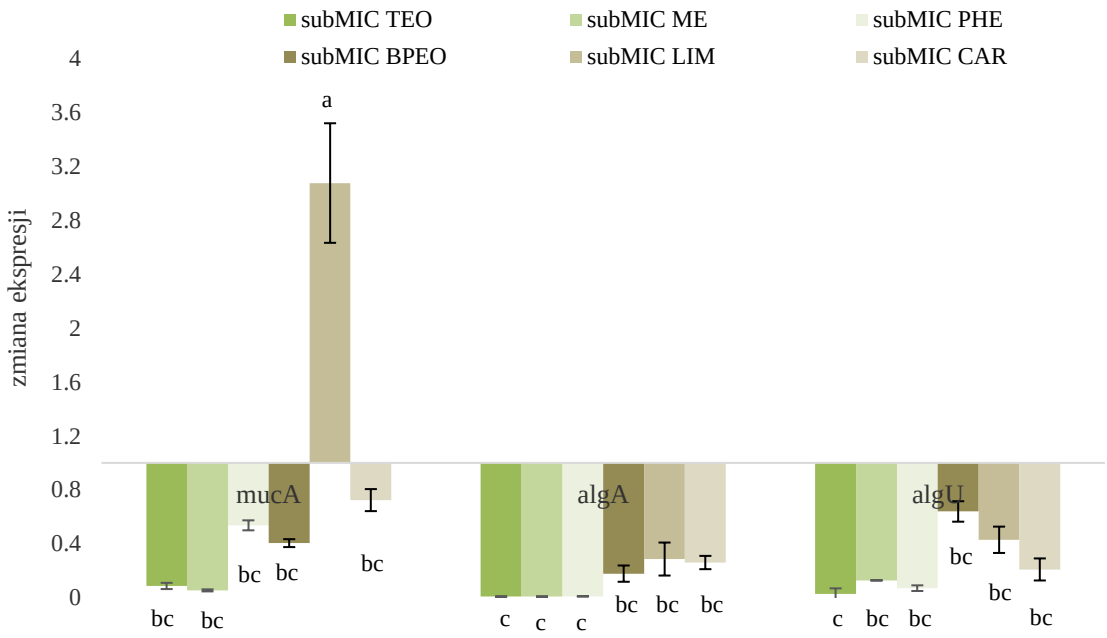

Rycina 22. Zmiana poziomu ekspresji wybranych genów regulujących syntezę EPS (F=25,16; p<2e-16 ***) w komórkach *P. psychrophila* KM02 inkubowanych na pożywce FJM suplementowanej subMIC TEO, ME, PHE, BPEO, LIM i CAR

4.8. Wzrost *P. psychrophila* KM02 w modelowym produkcie spożywczym

W niniejszej pracy zweryfikowano również aktywność przeciwdrobnoustrojową TEO i BPEO w produkcie modelowym. Porcje świeżego łososia atlantyckiego inokulowano wystandaryzowaną ilością komórek *P. psychrophila* KM02 (wartość początkowa 4 log jtk/g), traktowano marynatą octowo-olejową suplementowaną stężeniami subMIC TEO i BPEO, a następnie pakowano w warunkach próżniowych. Próby przechowywano w temperaturze 4°C przez 5 dni. Wyniki zmian liczby *P. psychrophila* KM02 w produkcie po 1, 3 i 5 dniach jego przechowywania zaprezentowano w publikacji P-4 oraz na Ryc.21.

Po 1 dniu przechowywania w próbie kontrolnej odnotowano liczbę komórek *P. psychrophila* KM02 na poziomie 4,8 log jtk/g, natomiast w próbach z marynatą suplementowaną stężeniami subMIC TEO i BPEO, odpowiednio 4,2 i 4,3 log jtk/g. Po 3 dobach przechowywania w próbach z dodatkiem subMIC TEO i BPEO, liczba komórek *P. psychrophila* KM02 wyniosła odpowiednio 4,9 log jtk/g i 5,2 log jtk/g. Dla ostatniego punktu pomiarowego odnotowano liczbę komórek na poziomie 5,2 log jtk/g (w próbie z subMIC TEO) i 5,4 log jtk/g (w próbie z subMIC BPEO). W próbach

kontrolnych liczba komórek świadcząca o rozpoczętym procesie psucia produktu (6 log jtk/g) osiągnięta została pomiędzy 3 a 5 dniem przechowywania. Takiej zależności nie stwierdzono w próbach traktowanych subMIC TEO i BPEO, co wskazuje na skuteczne działanie przeciwdrobnoustrojowe przygotowanej marynaty. Zastosowanie samego opakowania próżniowego nie zahamowało proliferacji komórek *P. psychrophila* KM02. W pracy Frangos i in. (2010), oceniającej jakość mikrobiologiczną pstrąga pakowanego w warunkach próżniowych, również zaobserwowano udział komórek *Pseudomonas* spp. w procesie psucia produktu. Zdaniem autorów powyższe zjawisko wynika z nieodpowiedniej bariery materiału użytego do pakowania lub niecałkowitego odprowadzenia gazu z prób. Ponadto, zgodnie ze wskazaniami literaturowymi, *Pseudomonas* spp. to fakultatywne beztlenowce (Kampers i in., 2021). Wpływ marynat wzbogaconych olejkami eterycznymi z oregano, rozmarynu i jałowca na kinetykę wzrostu bakterii psychrotrofowych w żywności badali również Siroli i in. (2020). W cytowanej pracy zabieg marynowania hamował wzrost bakterii z rodzaju *Pseudomonas* i bakterii z grupy coli. Badania molekularne przeprowadzone przez Wu i in. (2013) wykazały, że składniki olejków eterycznych mogą hamować syntezę DNA poprzez supresję aktywności gyrazy B lub hamować syntezę ATP. Niektóre środki mogą powodować również reorganizację łańcucha kwasu nukleinowego, co wpływa na metabolizm bakterii (Pan i in., 2020). Co więcej, poza poprawą bezpieczeństwa i okresu trwałości marynowanych ryb, stosowanie olejków eterycznych może również zwiększyć chęć konsumentów do zakupów takich produktów w świetle rosnącego popytu na żywność z tzw. czystą etykietą (Asioli i in., 2017).

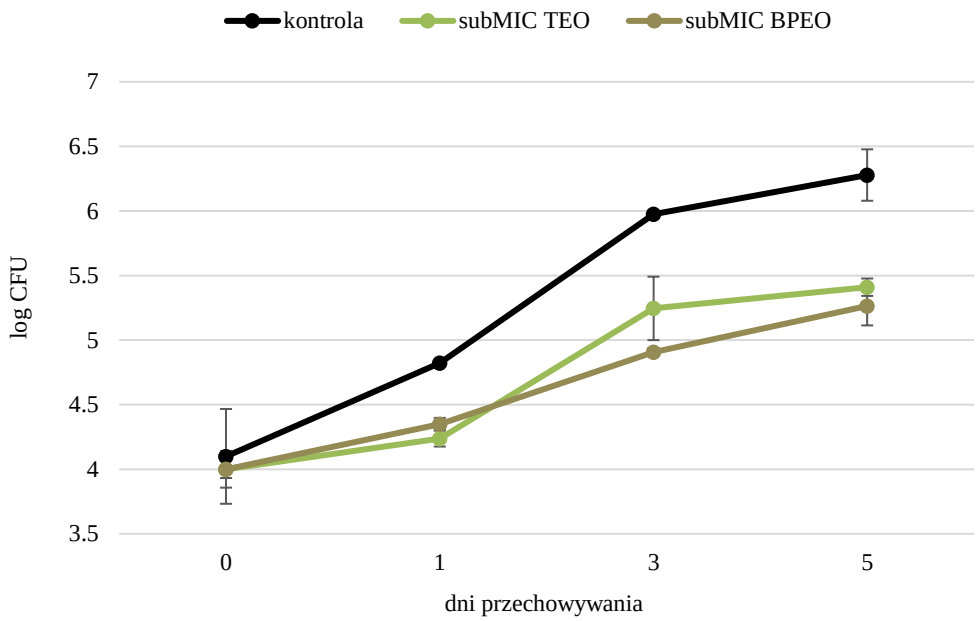

Rycina 23. Przeciwdrobnoustrojowa aktywność marynaty octowo-olejowej (F=50,34; p=2.65e-08 ***) suplementowanej subMIC TEO i subMIC BPEO wobec komórek *P. psychrophila* KM02, zastosowanej w filetach z łososia atlantyckiego przechowywanych w warunkach próżniowych w 4°C

5. Podsumowanie

W niniejszej pracy oceniano wpływ subMIC TEO i BPEO oraz ich głównych składników na metabolizm zależny od systemu *quorum sensing* u bakterii *P. psychrophila* KM02. Prowadzono hodowle komórek *Pseudomonas* spp. w pożywce TSB (warunkach *in vitro*) oraz w pożywce FJM (imitującej produkt z ryb; w warunkach *in situ*) suplementowanych badanymi czynnikami, a następnie wykonaniu posiewów mikrobiologicznych oraz ocen spektrofotometrycznych, chromatograficznych i genetycznych. Dodatkowo przeprowadzono analizy *in silico* dokowania molekularnego głównych składników badanych olejków eterycznych z wybranymi białkami *Pseudomonas* spp.

Pracę rozpoczęto od analiz przesiewowych ukierunkowanych na ocenę działania przeciwdrobnoustrojowego oraz przeciw-quorum sensing subMIC TEO i BPEO oraz ich głównych składników wobec trzech szczepów *Pseudomonas* spp. wyizolowanych z ryb – *P. psychrophila* KM02, *P. orientalis* KM149 oraz *P. fluorescens* KM248.

W pierwszym etapie badań pozyskano olejki eteryczne metodą hydrodestylacji oraz oznaczono ich składy chemiczne. W składzie TEO dominowały: ME (24,5 %) i PHE (19,3%), a u BPEO był to: CAR (19,6 %) i LIM (19,1 %). Korzystając z metody szeregu seryjnych rozcieńczeń wyznaczono wartości indeksów subMIC badanych czynników wobec komórek *Pseudomonas* spp. Odnotowano zbliżoną wrażliwość drobnoustrojów na testowane czynniki. Wartości indeksów subMIC TEO i BPEO mieściły się w zakresie 70 – 75 µL/mL i 100 – 135 µL/mL odpowiednio. Wartości indeksów subMIC: ME, PHE, LIM i CAR wynosiły odpowiednio: 10 – 12 µL/mL, 8 – 10 µL/mL, 60 – 65 µL/mL oraz 20 – 35 µL/mL Ponieważ jednym z mechanizmów działania przeciwdrobnoustrojowego związków terpenowych jest zmiana właściwości fizykochemicznych osłon komórkowych drobnoustrojów, w następnym etapie badań oceniono wpływ stężeń subMIC TEO i BPEO na profil estrów metylowych kwasów tłuszczowych *Pseudomonas* spp. Stwierdzono m.in. istotne obniżenie udziału nienasyconych kwasów tłuszczowych oraz istotny wzrost udziału nasyconych kwasów tłuszczowych u badanych szczepów *Pseudomonas* spp. Wyjątek stanowił *P. fluorescens* KM148, u którego powyższa zmiana nie była istotna statystycznie; w tym wariancie doświadczenia stwierdzono natomiast istotne obniżenie udziału kwasów tłuszczowych o rozgałęzionej budowie. Zarówno nienasycone i rozgałęzione kwasy tłuszczowe odpowiadają za płynność osłon komórkowych bakterii.

W następnym etapie pracy oceniono wpływ stężeń subMIC badanych czynników na system quorum sensing *Pseudomonas* spp. Badania polegały na analizie zmian w syntezie cząsteczek AI oraz ocenie oddziaływania czynników z białkami receptorowymi systemu quorum sensing. Profil AI *Pseudomonas* spp. składał się następujących cząsteczek: 3-okso-C12-HSL, 3-okso-C14-HSL, 3-okso-C6-HSL, 3-okso-C8-HSL, C12-HSL, C4-HSL i C6-HSL oraz PQS. Wśród zidentyfikowanych cząsteczek AHL, najwyższymi udziałami odznaczały się: 3-okso-C12-HSL, 3-okso-C8-HSL oraz C4-HSL. Występowały one w zakresach odpowiednio od 1,908 do 2,028 μg/mL, 1,119 do 1,953 μg/mL oraz od 1,217 do 1,312 μg/mL. Udział autoinduktora PQS wyniósł 0,0076 i 0,0030 μg/mL dla *P. psychrophila* KM02 oraz *P. fluorescens* KM148 odpowiednio. Zastosowanie subMIC TEO i BPEO oraz ich składników bioaktywnych doprowadziło do redukcji syntezy AI, co wskazało na ingerencję badanych czynników w system quorum sensing. Drugi kierunek analizy ingerencji w system quorum sensing dotyczył oceny potencjału bioaktywnych związków olejków eterycznych do wiązania się z białkami receptorowymi (LasR, RhlR, TraR i PqsR). Porównanie wartości dokowania oraz sposobu wiązania z natywnymi AI i znanymi inhibitorami quorum sensing dało wgląd w przypuszczalny mechanizm działania olejków eterycznych wobec systemu quorum sensing *Pseudomonas* spp.

Na podstawie doświadczeń, spośród trzech badanych gatunków *Pseudomonas* spp. do dalszych etapów pracy wytypowano szczep *P. psychrophila* KM02. Dla badanego mikroorganizmu przeprowadzono analizy WGS i RNA-seq celem identyfikacji czynników świadczących o zaangażowaniu komórek w procesy psucia żywności. Dodatkowo w złożonym *de novo* genomie *P. psychrophila* KM02, za pomocą narzędzia CARD, RAST oraz bazy NCBI zidentyfikowano sekwencje kodujące białka systemów: efflux oraz T2SS, zależnych od quorum sensing.

Biorąc pod uwagę możliwość blokowania białek systemu efflux przez związki terpenowe i tym samym zaburzanie procesu transportu komórkowego, przeprowadzono analizy dokowania molekularnego głównych składników TEO i BPEO z białkami systemu efflux. Wyniki dokowania molekularnego dostarczyły dowodów na to, że ME, PHE, CAR i LIM tworzą stabilne kompleksy z analizowanymi białkami i tym samym mogą wywoływać zmiany w funkcjonowaniu systemów transportu komórkowego u *P. psychrophila* KM02. Powyższą prawidłowość potwierdziły również wyniki analiz RT-qPCR genów związanych z systemem T2SS.

Biorąc pod uwagę dotychczasowe wyniki ukazujące wpływ badanych czynników na system quorum sensing, w dalszym etapie badań przeprowadzono eksperymenty oceniające zmiany w metabolizmie *P. psychrophila* KM02. Wyniki oznaczeń spektrofotometrycznych wykazały redukcję aktywności proteolitycznej, lipolitycznej oraz syntezy EPS u *P. psychrophila* KM02 po ekspozycji komórek na testowane czynniki. Powyższe obserwacje potwierdzono wynikami zmian poziomu mRNA genów kodujących proteazy i lipazy oraz genów warunkujących syntezę EPS.

W ostatnim etapie badań podjęto próbę praktycznego wykorzystania właściwości przeciwdrobnoustrojowych badanych olejków eterycznych. TEO i BPEO wprowadzano w stężeniach subMIC do marynat filetów świeżego łososia atlantyckiego. Wyniki zmian liczebności komórek *P. psychrophila* KM2 w czasie przechowywania produktu modelowego potwierdziły aktywność przeciwdrobnoustrojową badanych czynników.

Podsumowując, niniejsza praca wykazała wpływ TEO i BPEO oraz ich głównych składników, tj. ME, PHE, CAR i LIM na system quorum sensing i aktywności fizjologiczne *P. psychrophila* KM02 zależne od tego systemu. Powyższa prawidłowość może spowalniać proces psucia ryb przechowywanych w warunkach chłodniczych, w który zaangażowany jest *P. psychrophila* KM02. Tym samym potwierdzono postawione hipotezy badawcze. Uzyskane w niniejszej pracy wyniki uzupełniają wiedzę dotyczącą systemu quorum sensing u bakterii saprofitycznych wyizolowanych z żywności i stanowią obiecujący wstęp do kolejnych badań nad zastosowaniem olejków eterycznych.

6. Wnioski

I. Stężenia subMIC TEO i BPEO w warunkach *in vitro* ingerują w system quorum sensing i zmieniają aktywność metaboliczną komórek *P. psychrophila* KM02.

II. Ekspozycja komórek *P. fluorescens* KM148, *P. orientalis* KM249 oraz *P. psychrophila* KM02 na stężenia subMIC TEO i BPEO w warunkach *in vitro* skutkuje obniżeniem udziału nienasyconych kwasów tłuszczowych oraz kwasów tłuszczowych o budowie rozgałęzionej w osłonach komórkowych.

III. *P. fluorescens* KM148, *P. orientalis* KM249 oraz *P. psychrophila* KM02 w warunkach *in vitro* syntetyzują AI systemu quorum sensing należące do grupy AHL (tj. 3-okso-C12-HSL, 3-okso-C14-HSL, 3-okso-C6-HSL, 3-okso-C8-HSL, C12-HSL, C4-HSL, C6-HSL) oraz związek chinolowy – PQS.

IV. Stężenia subMIC TEO, BPEO, ME, PHE, LIM i CAR hamują syntezę cząsteczek AI w warunkach *in vitro* oraz oddziałują z białkami receptorowymi LasR, RhlR, TraR oraz PqsR systemu quorum sensing *Pseudomonas* spp.

V. W genomie *P. psychrophila* KM02 odnotowano obecność czynników świadczących o zdolności bakterii do rozkładu białek i tłuszczu oraz sekrecji enzymów. Są to m.in. terminy GO: GO:0016787//aktywność hydrolazy, GO:0022857//aktywność transportera transbłonowego, klany białek: AA_permease_2, Amidohydro_1, czy Peptidase_M24.

VI. W ocenie całego transkryptomu *P. psychrophila* KM02 największą liczbę odczytów przypisano do CDS związanych z metabolizmem białek/substancji azotowych.

VII. Cząsteczki ME, PHE, LIM i CAR wykazują zdolność wiązania do białek systemu efflux (Mfs, MexB, MuxB) *P. psychrophila* KM02.

VIII. Stężenia subMIC TEO, BPEO, ME, PHE, LIM i CAR obniżają poziom mRNA genów kodujących białka systemu efflux (*mexA, muxA, oprM, opmB*) oraz T2SS (*pulG, pulF, gspG, gpsH, tadB1, tadC1*) w warunkach *in vitro* oraz *in situ*.

IX. Stężenia subMIC TEO, BPEO, ME, PHE, LIM i CAR hamują aktywność proteolityczną, lipolityczną oraz syntezę EPS u *P. psychrophila* KM02 w warunkach *in vitro*. Powyższe wynika ze zmian ekspresji genów kodujących proteazy: *M22_1, M3_2, S11_3,* lipazy: *lipA* i *lipB* oraz białek regulujących syntezę EPS: *algA, algU* i *mucA*.

X. Stężenia subMIC TEO i BPEO wprowadzone do marynaty octowo-olejowej hamują wzrost komórek *P. psychrophila* KM02 w rybnym produkcie modelowym w czasie przechowywania w warunkach chłodniczych.

7. Bibliografia

Abraham, W. P., & Thomas, S. (2015). Draft Genome Sequence of Pseudomonas psychrophila MTCC 12324, Isolated from the Arctic at 79°N. *Genome Announcements*. https://doi.org/10.1128/genomeA.00578-15

Adamiak, J. W., Jhawar, V., Bonifay, V., Chandler, C. E., Leus, I. V., Ernst, R. K., Schweizer, H. P., & Zgurskaya, H. I. (2021). Loss of RND-Type Multidrug Efflux Pumps Triggers Iron Starvation and Lipid A Modifications in Pseudomonas aeruginosa. *Antimicrobial Agents and Chemotherapy*, *65*(10), e0059221. https://doi.org/10.1128/AAC.00592-21

Agreles, M. A. A., Cavalcanti, I. D. L., & Cavalcanti, I. M. F. (2021). The Role of Essential Oils in the Inhibition of Efflux Pumps and Reversion of Bacterial Resistance to Antimicrobials. *Current Microbiology*, *78*(10), 3609–3619. https://doi.org/10.1007/s00284-021-02635-1

Alcock, B. P., Raphenya, A. R., Lau, T. T. Y., Tsang, K. K., Bouchard, M., Edalatmand, A., Huynh, W., Nguyen, A.-L. V., Cheng, A. A., Liu, S., Min, S. Y., Miroshnichenko, A., Tran, H.-K., Werfalli, R. E., Nasir, J. A., Oloni, M., Speicher, D. J., Florescu, A., Singh, B., … McArthur, A. G. (2019). CARD 2020: Antibiotic resistome surveillance with the comprehensive antibiotic resistance database. *Nucleic Acids Research*. https://doi.org/10.1093/nar/gkz935

Ammor, M. S., Michaelidis, C., & Nychas, G.-J. E. (2008). Insights into the Role of Quorum Sensing in Food Spoilage. *Journal of Food Protection*, *71*(7), Article 7. https://doi.org/10.4315/0362-028X-71.7.1510

Annapoorani, A., Umamageswaran, V., Parameswari, R., Pandian, S. K., & Ravi, A. V. (2012). Computational discovery of putative quorum sensing inhibitors against LasR and RhlR receptor proteins of Pseudomonas aeruginosa. *Journal of Computer-Aided Molecular Design*, *26*(9), 1067–1077. https://doi.org/10.1007/s10822-012-9599-1

Aparna, V., Dineshkumar, K., Mohanalakshmi, N., Velmurugan, D., & Hopper, W. (2014). Identification of Natural Compound Inhibitors for Multidrug Efflux Pumps of Escherichia coli and Pseudomonas aeruginosa Using In Silico High-Throughput Virtual Screening and In Vitro Validation. *PLoS ONE*, *9*(7), Article 7. https://doi.org/10.1371/journal.pone.0101840

Asioli, D., Aschemann-Witzel, J., Caputo, V., Vecchio, R., Annunziata, A., Næs, T., & Varela, P. (2017). Making sense of the „clean label" trends: A review of consumer food choice behavior and discussion of industry implications. *Food Research International (Ottawa, Ont.)*, *99*(Pt 1), 58–71. https://doi.org/10.1016/j.foodres.2017.07.022

Aziz, R. K., Bartels, D., Best, A. A., DeJongh, M., Disz, T., Edwards, R. A., Formsma, K., Gerdes, S., Glass, E. M., Kubal, M., Meyer, F., Olsen, G. J., Olson, R., Osterman, A. L., Overbeek, R. A., McNeil, L. K., Paarmann, D., Paczian, T., Parrello, B., … Zagnitko, O. (2008). The RAST Server: Rapid Annotations using Subsystems Technology. *BMC Genomics*, *9*(1), 75. https://doi.org/10.1186/1471-2164-9-75

Bai, A. J., & Rai, V. R. (2011). Bacterial Quorum Sensing and Food Industry. *Comprehensive Reviews in Food Science and Food Safety*, *10*(3), Article 3. https://doi.org/10.1111/j.1541-4337.2011.00150.x

Bai A, J., & Rai V. R. (2014). Quorum Sensing Regulation and Inhibition of Exoenzyme Production and Biofilm Formation in the Food Spoilage Bacteria *Pseudomonas psychrophila* PSPF19. *Food Biotechnology*, *28*(4), Article 4. https://doi.org/10.1080/08905436.2014.963601

Bassolé, I. H. N., & Juliani, H. R. (2012). Essential Oils in Combination and Their Antimicrobial Properties. *Molecules*, *17*(4), 3989–4006. https://doi.org/10.3390/molecules17043989

Beven, C. A., Dieckelmann, M., & Beacham, I. R. (2001). A strain of Pseudomonas fluorescens with two lipase-encoding genes, one of which possibly encodes cytoplasmic lipolytic activity. *Journal of Applied Microbiology*, *90*(6), 979–987. https://doi.org/10.1046/j.1365-2672.2001.01333.x

Bijtenhoorn, P., Mayerhofer, H., Müller-Dieckmann, J., Utpatel, C., Schipper, C., Hornung, C., Szesny, M., Grond, S., Thürmer, A., Brzuszkiewicz, E., Daniel, R., Dierking, K., Schulenburg, H., & Streit, W. R. (2011). A novel metagenomic short-chain dehydrogenase/reductase attenuates Pseudomonas aeruginosa biofilm formation and virulence on Caenorhabditis elegans. *PloS One*, *6*(10), e26278. https://doi.org/10.1371/journal.pone.0026278

Bouyahya, A., Chamkhi, I., Balahbib, A., Rebezov, M., Shariati, M. A., Wilairatana, P., Mubarak, M. S., Benali, T., & El Omari, N. (2022). Mechanisms, Anti-Quorum-Sensing Actions, and Clinical Trials of Medicinal Plant Bioactive Compounds against Bacteria: A Comprehensive Review. *Molecules*, *27*(5), Article 5. https://doi.org/10.3390/molecules27051484

Brylinski, M. (2018). Aromatic interactions at the ligand-protein interface: Implications for the development of docking scoring functions. *Chemical Biology & Drug Design*, *91*(2), 380–390. https://doi.org/10.1111/cbdd.13084

Burt, S. (2004). Essential oils: Their antibacterial properties and potential applications in foods—a review. *International Journal of Food Microbiology*, *94*(3), Article 3. https://doi.org/10.1016/j.ijfoodmicro.2004.03.022

Calo, J. R., Crandall, P. G., O'Bryan, C. A., & Ricke, S. C. (2015). Essential oils as antimicrobials in food systems – A review. *Food Control*, *54*, 111–119. https://doi.org/10.1016/j.foodcont.2014.12.040

Camele, I., Elshafie, H. S., Caputo, L., & De Feo, V. (2019). Anti-quorum Sensing and Antimicrobial Effect of Mediterranean Plant Essential Oils Against Phytopathogenic Bacteria. *Frontiers in Microbiology*, *10*. https://www.frontiersin.org/articles/10.3389/fmicb.2019.02619

Camiade, M., Bodilis, J., Chaftar, N., Riah-Anglet, W., Gardères, J., Buquet, S., Ribeiro, A. F., & Pawlak, B. (2020). Antibiotic resistance patterns of Pseudomonas spp. Isolated from faecal wastes in the environment and contaminated surface water. *FEMS Microbiology Ecology*, *96*(2), fiaa008. https://doi.org/10.1093/femsec/fiaa008

Chang, C.-Y., Krishnan, T., Wang, H., Chen, Y., Yin, W.-F., Chong, Y.-M., Tan, L. Y., Chong, T. M., & Chan, K.-G. (2015). Non-antibiotic quorum sensing inhibitors acting against N-acyl homoserine lactone synthase as druggable target. *Scientific Reports*, *4*(1), Article 1. https://doi.org/10.1038/srep07245

Chao, J., Wolfaardt, G. M., & Arts, M. T. (2010). Characterization of Pseudomonas aeruginosa fatty acid profiles in biofilms and batch planktonic cultures. *Canadian Journal of Microbiology*, *56*(12), 1028–1039. https://doi.org/10.1139/W10-093

Chaudhari, N. M., Gupta, V. K., & Dutta, C. (2016). BPGA- an ultra-fast pan-genome analysis pipeline. *Scientific Reports*, *6*(1), 24373. https://doi.org/10.1038/srep24373

Chen, C. Y. S., & Tawan, C. (2020). Botany, Diversity, and Distribution of Black Pepper (Piper nigrum L.) Cultivars in Malaysia. *Borneo Journal of Resource Science and Technology*, *10*(1), Article 1. https://doi.org/10.33736/bjrst.1566.2020

Chen, F., Gao, Y., Chen, X., Yu, Z., & Li, X. (2013). Quorum Quenching Enzymes and Their Application in Degrading Signal Molecules to Block Quorum Sensing-Dependent

Infection. *International Journal of Molecular Sciences*, *14*(9), 17477–17500. https://doi.org/10.3390/ijms140917477

Cherepushkina, V. S., Mironova, T. E., Afonyushkin, V. N., Koptev, V. Yu., Nefedova, E. V., Donchenko, N. A., & Dimova, A. S. (2021). Study of the Dynamics of Biofilm Formation and Elastase Activity of Pseudomonas aeruginosa in the Presence of Dodecanoyl-Homoserine Lactone. *Bulletin of Experimental Biology and Medicine*, *171*(6), 741–744. https://doi.org/10.1007/s10517-021-05307-z

Christensen, A. B., Riedel, K., Eberl, L., Flodgaard, L. R., Molin, S., Gram, L., & Givskov, M. (2003). Quorum-sensing-directed protein expression in Serratia proteamaculans B5a. *Microbiology*, *149*(2), 471–483. https://doi.org/10.1099/mic.0.25575-0

Comi, G. (2017). Spoilage of Meat and Fish. W *The Microbiological Quality of Food* (s. 179–210). Elsevier. https://doi.org/10.1016/B978-0-08-100502-6.00011-X

Dalgaard, P. (1995). Qualitative and quantitative characterization of spoilage bacteria from packed fish. *International Journal of Food Microbiology*, *26*(3), Article 3. https://doi.org/10.1016/0168-1605(94)00137-U

Darling, A. C. E., Mau, B., Blattner, F. R., & Perna, N. T. (2004). Mauve: Multiple Alignment of Conserved Genomic Sequence With Rearrangements. *Genome Research*, *14*(7), 1394–1403. https://doi.org/10.1101/gr.2289704

Davies, D. G., Parsek, M. R., Pearson, J. P., Iglewski, B. H., Costerton, J. W., & Greenberg, E. P. (1998). The involvement of cell-to-cell signals in the development of a bacterial biofilm. *Science (New York, N.Y.)*, *280*(5361), 295–298. https://doi.org/10.1126/science.280.5361.295

de Araújo, A. C. J., Freitas, P. R., Dos Santos Barbosa, C. R., Muniz, D. F., Ribeiro-Filho, J., Tintino, S. R., Júnior, J. P. S., Filho, J. M. B., de Sousa, G. R., & Coutinho, H. D. M. (2021). Modulation of Drug Resistance by Limonene: Inhibition of Efflux Pumps in Staphylococcus aureus Strains RN-4220 and IS-58. *Current Drug Metabolism*, *22*(2), 110–113. https://doi.org/10.2174/1389200221999210104204718

Deryabin, D., Galadzhieva, A., Kosyan, D., & Duskaev, G. (2019). Plant-Derived Inhibitors of AHL-Mediated Quorum Sensing in Bacteria: Modes of Action. *International Journal of Molecular Sciences*, *20*(22), Article 22. https://doi.org/10.3390/ijms20225588

Di Pasqua, R., Hoskins, N., Betts, G., & Mauriello, G. (2006). Changes in Membrane Fatty Acids Composition of Microbial Cells Induced by Addiction of Thymol, Carvacrol, Limonene, Cinnamaldehyde, and Eugenol in the Growing Media. *Journal of Agricultural and Food Chemistry*, *54*(7), 2745–2749. https://doi.org/10.1021/jf052722l

Diggle, S. P., Matthijs, S., Wright, V. J., Fletcher, M. P., Chhabra, S. R., Lamont, I. L., Kong, X., Hider, R. C., Cornelis, P., Cámara, M., & Williams, P. (2007). The Pseudomonas aeruginosa 4-Quinolone Signal Molecules HHQ and PQS Play Multifunctional Roles in Quorum Sensing and Iron Entrapment. *Chemistry & Biology*, *14*(1), 87–96. https://doi.org/10.1016/j.chembiol.2006.11.014

Ding, T., Li, T., & Li, J. (2019). Virtual screening for quorum sensing inhibitors of *Pseudomonas fluorescens* P07 from a food-derived compound database. *Journal of Applied Microbiology*. https://doi.org/10.1111/jam.14333

Dosoky, Satyal, Barata, da Silva, & Setzer. (2019). Volatiles of Black Pepper Fruits (Piper nigrum L.). *Molecules*, *24*(23), 4244. https://doi.org/10.3390/molecules24234244

El-Gebali, S., Mistry, J., Bateman, A., Eddy, S. R., Luciani, A., Potter, S. C., Qureshi, M., Richardson, L. J., Salazar, G. A., Smart, A., Sonnhammer, E. L. L., Hirsh, L., Paladin, L., Piovesan, D., Tosatto, S. C. E., & Finn, R. D. (2019). The Pfam protein families

database in 2019. *Nucleic Acids Research*, *47*(D1), D427–D432. https://doi.org/10.1093/nar/gky995

FAO (Red.). (2018). *Meeting the sustainable development goals*.

Farsanipour, A. (2020). Effect of chitosan-whey protein isolated coatings incorporated with tarragon Artemisia dracunculus essential oil on the quality of Scomberoides commersonnianus fillets at refrigerated condition. *International Journal of Biological Macromolecules*, 6.

Fetzner, S. (2015). Quorum quenching enzymes. *Journal of Biotechnology*, *201*, 2–14. https://doi.org/10.1016/j.jbiotec.2014.09.001

Forde, A., & Fitzgerald, G. F. (1999). Analysis of exopolysaccharide (EPS) production mediated by the bacteriophage adsorption blocking plasmid, pCI658, isolated from Lactococcus lactis ssp. Cremoris HO2. *International Dairy Journal*, *9*(7), Article 7. https://doi.org/10.1016/S0958-6946(99)00115-6

Frangos, L., Pyrgotou, N., Giatrakou, V., Ntzimani, A., & Savvaidis, I. N. (2010). Combined effects of salting, oregano oil and vacuum-packaging on the shelf-life of refrigerated trout fillets. *Food Microbiology*, *27*(1), 115–121. https://doi.org/10.1016/j.fm.2009.09.002

Frenken, L. G. J., Groot, A., Tommassen, J., & Verrips, C. T. (1993). Role of the lipB gene product in the folding of the secreted lipase of Pseudomonas glumae. *Molecular Microbiology*, *9*(3), 591–599. https://doi.org/10.1111/j.1365-2958.1993.tb01719.x

Friesner, R. A., Banks, J. L., Murphy, R. B., Halgren, T. A., Klicic, J. J., Mainz, D. T., Repasky, M. P., Knoll, E. H., Shelley, M., Perry, J. K., Shaw, D. E., Francis, P., & Shenkin, P. S. (2004). Glide: A New Approach for Rapid, Accurate Docking and Scoring. 1. Method and Assessment of Docking Accuracy. *Journal of Medicinal Chemistry*, *47*(7), Article 7. https://doi.org/10.1021/jm0306430

Friesner, R. A., Murphy, R. B., Repasky, M. P., Frye, L. L., Greenwood, J. R., Halgren, T. A., Sanschagrin, P. C., & Mainz, D. T. (2006). Extra Precision Glide: Docking and Scoring Incorporating a Model of Hydrophobic Enclosure for Protein−Ligand Complexes. *Journal of Medicinal Chemistry*, *49*(21), Article 21. https://doi.org/10.1021/jm051256o

Ge, Y., Zhu, J., Ye, X., & Yang, Y. (2017). Spoilage potential characterization of Shewanella and Pseudomonas isolated from spoiled large yellow croaker (Pseudosciaena crocea). *Letters in Applied Microbiology*, *64*(1), 86–93. https://doi.org/10.1111/lam.12687

Ghaly. (2010). Fish Spoilage Mechanisms and Preservation Techniques: Review. *American Journal of Applied Sciences*, *7*(7), Article 7. https://doi.org/10.3844/ajassp.2010.859.877

Ghosh, A., Roymahapatra, G., Paul, D., & Mandal, S. M. (2020). Theoretical analysis of bacterial efflux pumps inhibitors: Strategies in-search of competent molecules and develop next. *Computational Biology and Chemistry*, *87*, 107275. https://doi.org/10.1016/j.compbiolchem.2020.107275

Gopu, V., Chandran, S., & Shetty, P. H. (2018). Significance and Application of Quorum Sensing in Food Microbiology. W V. C. Kalia (Red.), *Quorum Sensing and its Biotechnological Applications* (s. 193–219). Springer Singapore. https://doi.org/10.1007/978-981-13-0848-2_13

Gui, M., Liu, L., Wu, R., Hu, J., Wang, S., & Li, P. (2018). Detection of New Quorum Sensing N-Acyl Homoserine Lactones From Aeromonas veronii. *Frontiers in Microbiology*, *9*. https://doi.org/10.3389/fmicb.2018.01712

Harder, E., Damm, W., Maple, J., Wu, C., Reboul, M., Xiang, J. Y., Wang, L., Lupyan, D., Dahlgren, M. K., Knight, J. L., Kaus, J. W., Cerutti, D. S., Krilov, G., Jorgensen, W. L., Abel, R., & Friesner, R. A. (2016). OPLS3: A Force Field Providing Broad Coverage of

Drug-like Small Molecules and Proteins. *Journal of Chemical Theory and Computation*, *12*(1), Article 1. https://doi.org/10.1021/acs.jctc.5b00864

Hassoun, A., & Emir Çoban, Ö. (2017). Essential oils for antimicrobial and antioxidant applications in fish and other seafood products. *Trends in Food Science & Technology*, *68*, 26–36. https://doi.org/10.1016/j.tifs.2017.07.016

Hernando-Amado, S., Alcalde-Rico, M., Gil-Gil, T., Valverde, J. R., & Martínez, J. L. (2020). Naringenin Inhibition of the Pseudomonas aeruginosa Quorum Sensing Response Is Based on Its Time-Dependent Competition With N-(3-Oxo-dodecanoyl)-L-homoserine Lactone for LasR Binding. *Frontiers in Molecular Biosciences*, *7*, 25. https://doi.org/10.3389/fmolb.2020.00025

Hong, X., Wang, Y., Chen, S., & Zhu, J. (2021). Efficacy of Ten Structurally Related Essential Oil Components on Anti-biofilm and Anti-quorum Sensing against Fish Spoilers Pseudomonas and Aeromonas. *Journal of Aquatic Food Product Technology*, *30*(4), 462–473. https://doi.org/10.1080/10498850.2021.1895943

Hyldgaard, M., Mygind, T., & Meyer, R. L. (2012). Essential Oils in Food Preservation: Mode of Action, Synergies, and Interactions with Food Matrix Components. *Frontiers in Microbiology*, *3*. https://doi.org/10.3389/fmicb.2012.00012

Jain, P., Nale, A., & Dabur, R. (2018). Antimicrobial metabolites from Saraca asoca impairs the membrane transport system and quorum-sensing system in Pseudomonas aeruginosa. *Archives of Microbiology*, *200*(2), 237–253. https://doi.org/10.1007/s00203-017-1435-5

Jia, S., Li, Y., Zhuang, S., Sun, X., Zhang, L., Shi, J., Hong, H., & Luo, Y. (2019). Biochemical changes induced by dominant bacteria in chill-stored silver carp (Hypophthalmichthys molitrix) and GC-IMS identification of volatile organic compounds. *Food Microbiology*, *84*, 103248. https://doi.org/10.1016/j.fm.2019.103248

Jin, L., Chen, Y., Yang, W., Qiao, Z., & Zhang, X. (2020). Complete genome sequence of fish-pathogenic Aeromonas hydrophila HX-3 and a comparative analysis: Insights into virulence factors and quorum sensing. *Scientific Reports*, *10*(1), Article 1. https://doi.org/10.1038/s41598-020-72484-8

Kalia, V. C. (2013). Quorum sensing inhibitors: An overview. *Biotechnology Advances*, *31*(2), Article 2. https://doi.org/10.1016/j.biotechadv.2012.10.004

Kampers, L. F. C., Koehorst, J. J., van Heck, R. J. A., Suarez-Diez, M., Stams, A. J. M., & Schaap, P. J. (2021). A metabolic and physiological design study of Pseudomonas putida KT2440 capable of anaerobic respiration. *BMC Microbiology*, *21*(1), 9. https://doi.org/10.1186/s12866-020-02058-1

Klebe, G. (Red.). (2013). *Drug Design: Methodology, Concepts, and Mode-of-Action*. Springer Berlin Heidelberg. https://doi.org/10.1007/978-3-642-17907-5

Koh, C.-L., Sam, C.-K., Yin, W.-F., Tan, L. Y., Krishnan, T., Chong, Y. M., & Chan, K.-G. (2013). Plant-derived natural products as sources of anti-quorum sensing compounds. *Sensors (Basel, Switzerland)*, *13*(5), 6217–6228. https://doi.org/10.3390/s130506217

Kumar, L., Chhibber, S., Kumar, R., Kumar, M., & Harjai, K. (2015). Zingerone silences quorum sensing and attenuates virulence of Pseudomonas aeruginosa. *Fitoterapia*, *102*, 84–95. https://doi.org/10.1016/j.fitote.2015.02.002

Kuźma, Ł., Różalski, M., Walencka, E., Różalska, B., & Wysokińska, H. (2007). Antimicrobial activity of diterpenoids from hairy roots of Salvia sclarea L.: Salvipisone as a potential anti-biofilm agent active against antibiotic resistant Staphylococci. *Phytomedicine*, *14*(1), 31–35. https://doi.org/10.1016/j.phymed.2005.10.008

Land, M., Hauser, L., Jun, S.-R., Nookaew, I., Leuze, M. R., Ahn, T.-H., Karpinets, T., Lund, O., Kora, G., Wassenaar, T., Poudel, S., & Ussery, D. W. (2015). Insights from 20 years of

bacterial genome sequencing. *Functional & Integrative Genomics*, *15*(2), 141–161. https://doi.org/10.1007/s10142-015-0433-4

Lang, J., & Faure, D. (2014). Functions and regulation of quorum-sensing in Agrobacterium tumefaciens. *Frontiers in Plant Science*, *5*, 14. https://doi.org/10.3389/fpls.2014.00014

Lee, J., & Zhang, L. (2015). The hierarchy quorum sensing network in Pseudomonas aeruginosa. *Protein & Cell*, *6*(1), Article 1. https://doi.org/10.1007/s13238-014-0100-x

Leite de Souza, E. (2016). The effects of sublethal doses of essential oils and their constituents on antimicrobial susceptibility and antibiotic resistance among food-related bacteria: A review. *Trends in Food Science & Technology*, *56*, 1–12. https://doi.org/10.1016/j.tifs.2016.07.012

Li, J., Yu, H., Yang, X., Dong, R., Liu, Z., & Zeng, M. (2020). Complete genome sequence provides insights into the quorum sensing-related spoilage potential of Shewanella baltica 128 isolated from spoiled shrimp. *Genomics*, *112*(1), 736–748. https://doi.org/10.1016/j.ygeno.2019.05.010

Li, T., Cui, F., Bai, F., Zhao, G., & Li, J. (2016). Involvement of Acylated Homoserine Lactones (AHLs) of Aeromonas sobria in Spoilage of Refrigerated Turbot (Scophthalmus maximus L.). *Sensors*, *16*(7), 1083. https://doi.org/10.3390/s16071083

Li, T., Yang, B., Li, X., Li, J., Zhao, G., & Kan, J. (2018). Quorum sensing system and influence on food spoilage in Pseudomonas fluorescens from turbot. *Journal of Food Science and Technology*, *55*(8), 3016–3025. https://doi.org/10.1007/s13197-018-3222-y

Li, X.-Z., & Plésiat, P. (2016). Antimicrobial Drug Efflux Pumps in Pseudomonas aeruginosa. W X.-Z. Li, C. A. Elkins, & H. I. Zgurskaya (Red.), *Efflux-Mediated Antimicrobial Resistance in Bacteria: Mechanisms, Regulation and Clinical Implications* (s. 359–400). Springer International Publishing. https://doi.org/10.1007/978-3-319-39658-3_14

Limaverde, P. W., Campina, F. F., da Cunha, F. A. B., Crispim, F. D., Figueredo, F. G., Lima, L. F., Datiane de M Oliveira-Tintino, C., de Matos, Y. M. L. S., Morais-Braga, M. F. B., Menezes, I. R. A., Balbino, V. Q., Coutinho, H. D. M., Siqueira-Júnior, J. P., Almeida, J. R. G. S., & Tintino, S. R. (2017). Inhibition of the TetK efflux-pump by the essential oil of Chenopodium ambrosioides L. and α-terpinene against Staphylococcus aureus IS-58. *Food and Chemical Toxicology: An International Journal Published for the British Industrial Biological Research Association*, *109*(Pt 2), 957–961. https://doi.org/10.1016/j.fct.2017.02.031

Lin, J., Cheng, J., Wang, Y., & Shen, X. (2018). The Pseudomonas Quinolone Signal (PQS): Not Just for Quorum Sensing Anymore. *Frontiers in Cellular and Infection Microbiology*, *8*, 230. https://doi.org/10.3389/fcimb.2018.00230

Liu, M., Wang, H., & Griffiths, M. W. (2007). Regulation of alkaline metalloprotease promoter by N-acyl homoserine lactone quorum sensing in Pseudomonas fluorescens: Protease promoter regulation by AHLs in P. fluorescens. *Journal of Applied Microbiology*, *103*(6), Article 6. https://doi.org/10.1111/j.1365-2672.2007.03488.x

Liu, X., Xu, J., Zhu, J., Du, P., & Sun, A. (2019). Combined Transcriptome and Proteome Analysis of RpoS Regulon Reveals Its Role in Spoilage Potential of Pseudomonas fluorescens. *Frontiers in Microbiology*, *10*. https://www.frontiersin.org/article/10.3389/fmicb.2019.00094

Lo, R., Stanton-Cook, M. J., Beatson, S. A., Turner, M. S., & Bansal, N. (2015). Draft Genome Sequence of Pseudomonas fluorescens SRM1, an Isolate from Spoiled Raw Milk. *Genome Announcements*. https://doi.org/10.1128/genomeA.00138-15

Luciardi, M. C., Blázquez, M. A., Cartagena, E., Bardón, A., & Arena, M. E. (2016). Mandarin essential oils inhibit quorum sensing and virulence factors of Pseudomonas aeruginosa.

LWT - Food Science and Technology, *68*, 373–380. https://doi.org/10.1016/j.lwt.2015.12.056

Macwan, S., Dabhi, B., Aparnathi, K., & Prajapati, J. (2016). Essential Oils of Herbs and Spices: Their Antimicrobial Activity and Application in Preservation of Food. *International Journal of Current Microbiology and Applied Sciences*, *5*, 885–901. https://doi.org/10.20546/ijcmas.2016.505.092

Madhavi Sastry, G., Adzhigirey, M., Day, T., Annabhimoju, R., & Sherman, W. (2013). Protein and ligand preparation: Parameters, protocols, and influence on virtual screening enrichments. *Journal of Computer-Aided Molecular Design*, *27*(3), Article 3. https://doi.org/10.1007/s10822-013-9644-8

Medvedev, K. E., Kinch, L. N., Dustin Schaeffer, R., Pei, J., & Grishin, N. V. (2021). A Fifth of the Protein World: Rossmann-like Proteins as an Evolutionarily Successful Structural unit. *Journal of Molecular Biology*, *433*(4), 166788. https://doi.org/10.1016/j.jmb.2020.166788

Meliani, A., & Bensoltane, A. (2015). Review of Pseudomonas Attachment and Biofilm Formation in Food Industry. *Poultry, Fisheries & Wildlife Sciences*, *03*(01). https://doi.org/10.4172/2375-446X.1000126

Mima, T., Joshi, S., Gomez-Escalada, M., & Schweizer, H. P. (2007). Identification and Characterization of TriABC-OpmH, a Triclosan Efflux Pump of Pseudomonas aeruginosa Requiring Two Membrane Fusion Proteins. *Journal of Bacteriology*, *189*(21), 7600–7609. https://doi.org/10.1128/JB.00850-07

Minagawa, S., Inami, H., Kato, T., Sawada, S., Yasuki, T., Miyairi, S., Horikawa, M., Okuda, J., & Gotoh, N. (2012). RND type efflux pump system MexAB-OprM of Pseudomonas aeruginosa selects bacterial languages, 3-oxo-acyl-homoserine lactones, for cell-to-cell communication. *BMC Microbiology*, *12*, 70. https://doi.org/10.1186/1471-2180-12-70

Mireille Ayé, A., Bonnin-Jusserand, M., Brian-Jaisson, F., Ortalo-Magné, A., Culioli, G., Koffi Nevry, R., Rabah, N., Blache, Y., & Molmeret, M. (2015). Modulation of violacein production and phenotypes associated with biofilm by exogenous quorum sensing N-acylhomoserine lactones in the marine bacterium Pseudoalteromonas ulvae TC14. *Microbiology (Reading, England)*, *161*(10), 2039–2051. https://doi.org/10.1099/mic.0.000147

Moosavi-Nasab, M., Shad, E., Ziaee, E., Yousefabad, S. H. A., Golmakani, M. T., & Azizinia, M. (2016). Biodegradable Chitosan Coating Incorporated with Black Pepper Essential Oil for Shelf Life Extension of Common Carp (Cyprinus carpio) during Refrigerated Storage. *Journal of Food Protection*, *79*(6), 986–993. https://doi.org/10.4315/0362-028X.JFP-15-246

Moradali, M. F., Ghods, S., & Rehm, B. H. A. (2017). Pseudomonas aeruginosa Lifestyle: A Paradigm for Adaptation, Survival, and Persistence. *Frontiers in Cellular and Infection Microbiology*, *7*. https://www.frontiersin.org/articles/10.3389/fcimb.2017.00039

Mrozik, A., Piotrowska-Seget, Z., & Łabużek, S. (2004). Changes in whole cell-derived fatty acids induced by naphthalene in bacteria from genus Pseudomonas. *Microbiological Research*, *159*(1), 87–95. https://doi.org/10.1016/j.micres.2004.02.001

Muhammadi, & Ahmed, N. (2007). Genetics of Bacterial Alginate: Alginate Genes Distribution, Organization and Biosynthesis in Bacteria. *Current Genomics*, *8*(3), 191–202.

Myszka, K., & Czaczyk, K. (2010). Mechanizm quorum sensing jako czynnik regulujący wirulencję bakterii Gram-ujemnych. *Postępy higieny i medycyny doświadczalnej (Online)*, *64*, 582–589.

Myszka, K., Sobieszczańska, N., Olejnik, A., Majcher, M., Szwengiel, A., Wolko, Ł., & Juzwa, W. (2020). Studies on the anti-proliferative and anti-quorum sensing potentials of Myrtus communis L. essential oil for the improved microbial stability of salmon-based products. *LWT*, *127*, 109380. https://doi.org/10.1016/j.lwt.2020.109380

Myszka, K., Tomaś, N., Wolko, Ł., Szwengiel, A., Grygier, A., Nuc, K., & Majcher, M. (2021). In situ approaches show the limitation of the spoilage potential of Juniperus phoenicea L. essential oil against cold-tolerant Pseudomonas fluorescens KM24. *Applied Microbiology and Biotechnology*, *105*(10), 4255–4268. https://doi.org/10.1007/s00253-021-11338-3

Nazzaro, F., Fratianni, F., De Martino, L., Coppola, R., & De Feo, V. (2013). Effect of Essential Oils on Pathogenic Bacteria. *Pharmaceuticals*, *6*(12), Article 12. https://doi.org/10.3390/ph6121451

Pamp, S. J., & Tolker-Nielsen, T. (2007). Multiple roles of biosurfactants in structural biofilm development by Pseudomonas aeruginosa. *Journal of Bacteriology*, *189*(6), 2531–2539. https://doi.org/10.1128/JB.01515-06

Pan, Y., Deng, Z., & Shahidi, F. (2020). Natural bioactive substances for the control of food-borne viruses and contaminants in food. *Food Production, Processing and Nutrition*, *2*(1), 27. https://doi.org/10.1186/s43014-020-00040-y

Pandey, A. K., Kumar, P., Singh, P., Tripathi, N. N., & Bajpai, V. K. (2017). Essential Oils: Sources of Antimicrobials and Food Preservatives. *Frontiers in Microbiology*, *7*. https://doi.org/10.3389/fmicb.2016.02161

Papenfort, K., & Bassler, B. (2016). Quorum-Sensing Signal-Response Systems in Gram-Negative Bacteria. *Nature reviews. Microbiology*, *14*(9), Article 9. https://doi.org/10.1038/nrmicro.2016.89

Pattnaik, S. S., Ranganathan, S., Ampasala, D. R., Syed, A., Ameen, F., & Busi, S. (2018). Attenuation of quorum sensing regulated virulence and biofilm development in Pseudomonas aeruginosa PAO1 by Diaporthe phaseolorum SSP12. *Microbial Pathogenesis*, *118*, 177–189. https://doi.org/10.1016/j.micpath.2018.03.031

Pena, R. T., Blasco, L., Ambroa, A., González-Pedrajo, B., Fernández-García, L., López, M., Bleriot, I., Bou, G., García-Contreras, R., Wood, T. K., & Tomás, M. (2019). Relationship Between Quorum Sensing and Secretion Systems. *Frontiers in Microbiology*, *10*, 1100. https://doi.org/10.3389/fmicb.2019.01100

Perricone, M., Arace, E., Corbo, M. R., Sinigaglia, M., & Bevilacqua, A. (2015). Bioactivity of essential oils: A review on their interaction with food components. *Frontiers in Microbiology*, *6*. https://doi.org/10.3389/fmicb.2015.00076

Petkau, A., Stuart-Edwards, M., Stothard, P., & Van Domselaar, G. (2010). Interactive microbial genome visualization with GView. *Bioinformatics*, *26*(24), 3125–3126. https://doi.org/10.1093/bioinformatics/btq588

Pfaffl, M. W. (2001). A new mathematical model for relative quantification in real-time RT-PCR. *Nucleic Acids Research*, *29*(9), Article 9. https://doi.org/10.1093/nar/29.9.e45

Polychroniadou, A. (1988). A simple procedure using trinitrobenzenesulphonic acid for monitoring proteolysis in cheese. *Journal of Dairy Research*, *55*(4), Article 4. https://doi.org/10.1017/S0022029900033379

Rampioni, G., Pillai, C. R., Longo, F., Bondì, R., Baldelli, V., Messina, M., Imperi, F., Visca, P., & Leoni, L. (2017). Effect of efflux pump inhibition on Pseudomonas aeruginosa transcriptome and virulence. *Scientific Reports*, *7*(1), Article 1. https://doi.org/10.1038/s41598-017-11892-9

Rao, J., Chen, B., & McClements, D. J. (2019). Improving the Efficacy of Essential Oils as Antimicrobials in Foods: Mechanisms of Action. *Annual Review of Food Science and Technology*, *10*(1), 365–387. https://doi.org/10.1146/annurev-food-032818-121727

Raposo, A., Pérez, E., de Faria, C. T., Ferrús, M. A., & Carrascosa, C. (2017). Food Spoilage by *Pseudomonas* spp.-An Overview. W O. V. Singh (Red.), *Foodborne Pathogens and Antibiotic Resistance* (s. 41–71). John Wiley & Sons, Inc. https://doi.org/10.1002/9781119139188.ch3

Ravn, L., Christensen, A. B., Molin, S., Givskov, M., & Gram, L. (2001). Methods for detecting acylated homoserine lactones produced by Gram-negative bacteria and their application in studies of AHL-production kinetics. *Journal of Microbiological Methods*, *44*(3), Article 3. https://doi.org/10.1016/S0167-7012(01)00217-2

Rémy, B., Plener, L., Decloquement, P., Armstrong, N., Elias, M., Daudé, D., & Chabrière, É. (2020). Lactonase Specificity Is Key to Quorum Quenching in Pseudomonas aeruginosa. *Frontiers in Microbiology*, *11*, 762. https://doi.org/10.3389/fmicb.2020.00762

Riedel, K., Ohnesorg, T., Krogfelt, K. A., Hansen, T. S., Omori, K., Givskov, M., & Eberl, L. (2001). *N* -Acyl- L -Homoserine Lactone-Mediated Regulation of the Lip Secretion System in *Serratia liquefaciens* MG1. *Journal of Bacteriology*, *183*(5), 1805–1809. https://doi.org/10.1128/JB.183.5.1805-1809.2001

Roos, K., Wu, C., Damm, W., Reboul, M., Stevenson, J. M., Lu, C., Dahlgren, M. K., Mondal, S., Chen, W., Wang, L., Abel, R., Friesner, R. A., & Harder, E. D. (2019). OPLS3e: Extending Force Field Coverage for Drug-Like Small Molecules. *Journal of Chemical Theory and Computation*, *15*(3), 1863–1874. https://doi.org/10.1021/acs.jctc.8b01026

Roy, A., Kucukural, A., & Zhang, Y. (2010). I-TASSER: A unified platform for automated protein structure and function prediction. *Nature Protocols*, *5*(4), Article 4. https://doi.org/10.1038/nprot.2010.5

Ruijter, J. M., Ramakers, C., Hoogaars, W. M. H., Karlen, Y., Bakker, O., van den Hoff, M. J. B., & Moorman, A. F. M. (2009). Amplification efficiency: Linking baseline and bias in the analysis of quantitative PCR data. *Nucleic Acids Research*, *37*(6), Article 6. https://doi.org/10.1093/nar/gkp045

Sadiq, S., Rana, N. F., Zahid, M. A., Zargaham, M. K., Tanweer, T., Batool, A., Naeem, A., Nawaz, A., Rizwan-Ur-Rehman, null, Muneer, Z., & Siddiqi, A. R. (2020). Virtual Screening of FDA-Approved Drugs against LasR of Pseudomonas aeruginosa for Antibiofilm Potential. *Molecules (Basel, Switzerland)*, *25*(16), 3723. https://doi.org/10.3390/molecules25163723

Schuster, M., Lostroh, C. P., Ogi, T., & Greenberg, E. P. (2003). Identification, Timing, and Signal Specificity of Pseudomonas aeruginosa Quorum-Controlled Genes: A Transcriptome Analysis. *Journal of Bacteriology*, *185*(7), 2066–2079. https://doi.org/10.1128/JB.185.7.2066-2079.2003

Schuster, M., & Peter Greenberg, E. (2006). A network of networks: Quorum-sensing gene regulation in Pseudomonas aeruginosa. *International Journal of Medical Microbiology*, *296*(2–3), 73–81. https://doi.org/10.1016/j.ijmm.2006.01.036

Sendra, E. (2016). Essential Oils in Foods: From Ancient Times to the 21st Century. *Foods (Basel, Switzerland)*, *5*(2), 43. https://doi.org/10.3390/foods5020043

Seukep, A. J., Kuete, V., Nahar, L., Sarker, S. D., & Guo, M. (2019). Plant-derived secondary metabolites as the main source of efflux pump inhibitors and methods for identification. *Journal of Pharmaceutical Analysis*. https://doi.org/10.1016/j.jpha.2019.11.002

Shadman, S., Hosseini, S. E., Langroudi, H. E., & Shabani, S. (2017). Evaluation of the effect of a sunflower oil-based nanoemulsion with Zataria multiflora Boiss. Essential oil on the

physicochemical properties of rainbow trout (Oncorhynchus mykiss) fillets during cold storage. *LWT - Food Science and Technology*, *79*, 511–517. https://doi.org/10.1016/j.lwt.2016.01.073

Sikkema, J., de Bont, J. A., & Poolman, B. (1995). Mechanisms of membrane toxicity of hydrocarbons. *Microbiological Reviews*, *59*(2), 201–222. https://doi.org/10.1128/mr.59.2.201-222.1995

Singh, A., Gupta, R., Tandon, S., & Pandey, R. (2017). Thyme Oil Reduces Biofilm Formation and Impairs Virulence of Xanthomonas oryzae. *Frontiers in Microbiology*, *8*, 1074. https://doi.org/10.3389/fmicb.2017.01074

Sionov, R. V., & Steinberg, D. (2022). Targeting the Holy Triangle of Quorum Sensing, Biofilm Formation, and Antibiotic Resistance in Pathogenic Bacteria. *Microorganisms*, *10*(6), 1239. https://doi.org/10.3390/microorganisms10061239

Siroli, L., Baldi, G., Soglia, F., Bukvicki, D., Patrignani, F., Petracci, M., & Lanciotti, R. (2020). Use of Essential Oils to Increase the Safety and the Quality of Marinated Pork Loin. *Foods*, *9*(8), Article 8. https://doi.org/10.3390/foods9080987

Skandamis, P. N., & Nychas, G.-J. E. (2012). Quorum Sensing in the Context of Food Microbiology. *Applied and Environmental Microbiology*, *78*(16), Article 16. https://doi.org/10.1128/AEM.00468-12

Smith, J. L., Fratamico, P. M., & Novak, J. S. (2004). Quorum Sensing: A Primer for Food Microbiologists†. *Journal of Food Protection*, *67*(5), 1053–1070. https://doi.org/10.4315/0362-028X-67.5.1053

Socaciu, M.-I., Fogarasi, M., Simon, E. L., Semeniuc, C. A., Socaci, S. A., Podar, A. S., & Vodnar, D. C. (2021). Effects of Whey Protein Isolate-Based Film Incorporated with Tarragon Essential Oil on the Quality and Shelf-Life of Refrigerated Brook Trout. *Foods*, *10*(2), 401. https://doi.org/10.3390/foods10020401

Soheili, V., Tajani, A. S., Ghodsi, R., & Bazzaz, B. S. F. (2019). Anti-PqsR compounds as next-generation antibacterial agents against Pseudomonas aeruginosa: A review. *European Journal of Medicinal Chemistry*, *172*, 26–35. https://doi.org/10.1016/j.ejmech.2019.03.049

Sonbol, F., El-Banna, T., Elgaml, A., & Aboelsuod, K. M. (2022). Impact of Quorum Sensing System on Virulence Factors Production in Pseudomonas aeruginosa. *Journal of Pure and Applied Microbiology*, *16*(2), 1226–1238. https://doi.org/10.22207/JPAM.16.2.51

Sruthi, D., Zachariah, T. J., Leela, N. K., & Jayarajan, K. (2013). Correlation between chemical profiles of black pepper (Piper nigrum L.) var. Panniyur-1 collected from different locations. *Journal of Medicinal Plants Research*, *7*(31), 2349–2357. https://doi.org/10.5897/JMPR2013.4493

Stanborough, T., Fegan, N., Powell, S. M., Singh, T., Tamplin, M., & Chandry, P. S. (2018). Genomic and metabolic characterization of spoilage-associated Pseudomonas species. *International Journal of Food Microbiology*, *268*, 61–72. https://doi.org/10.1016/j.ijfoodmicro.2018.01.005

Sterniša, M., Bucar, F., Kunert, O., & Smole Možina, S. (2020a). Targeting fish spoilers Pseudomonas and Shewanella with oregano and nettle extracts. *International Journal of Food Microbiology*, *328*, 108664. https://doi.org/10.1016/j.ijfoodmicro.2020.108664

Sterniša, M., Klančnik, A., & Smole Možina, S. (2019). Spoilage *Pseudomonas* biofilm with *Escherichia coli* protection in fish meat at 5 °C. *Journal of the Science of Food and Agriculture*, *99*(10), 4635–4641. https://doi.org/10.1002/jsfa.9703

Sterniša, M., Purgatorio, C., Paparella, A., Mraz, J., & Smole Možina, S. (2020b). Combination of rosemary extract and buffered vinegar inhibits *PSEUDOMONAS* and *SHEWANELLA*

growth in common carp (*CYPRINUS CARPIO*). *Journal of the Science of Food and Agriculture*, *100*(5), 2305–2312. https://doi.org/10.1002/jsfa.10273

Stuer, W., Jaeger, K. E., & Winkler, U. K. (1986). Purification of extracellular lipase from Pseudomonas aeruginosa. *Journal of Bacteriology*, *168*(3), 1070–1074. https://doi.org/10.1128/jb.168.3.1070-1074.1986

Sybiya Vasantha Packiavathy, I. A., Agilandeswari, P., Musthafa, K. S., Karutha Pandian, S., & Veera Ravi, A. (2012). Antibiofilm and quorum sensing inhibitory potential of Cuminum cyminum and its secondary metabolite methyl eugenol against Gram negative bacterial pathogens. *Food Research International*, *45*(1), Article 1. https://doi.org/10.1016/j.foodres.2011.10.022

Szczepanik, M., Walczak, M., Zawitowska, B., Michalska-Sionkowska, M., Szumny, A., Wawrzeńczyk, C., & Brzezinska, M. S. (2018). Chemical composition, antimicromicrobial activity and insecticidal activity against the lesser mealworm *ALPHITOBIUS DIAPERINUS* (Panzer) (Coleoptera: Tenebrionidae) of *ORIGANUM VULGARE* L. ssp. *Hirtum* (Link) and *ARTEMISIA DRACUNCULUS* L. essential oils. *Journal of the Science of Food and Agriculture*, *98*(2), Article 2. https://doi.org/10.1002/jsfa.8524

Takrami, S. R., Ranji, N., & Hakimi, F. (2017). New Mutations in Ciprofloxacin Resistant Strains of Pseudomonas aeruginosa Isolated from Guilan Province, Northern Iran. *Molecular Genetics, Microbiology and Virology*, *32*(4), 218–223. https://doi.org/10.3103/S089141681704005X

Tang, R., Zhu, J., Feng, L., Li, J., & Liu, X. (2019). Characterization of LuxI/LuxR and their regulation involved in biofilm formation and stress resistance in fish spoilers Pseudomonas fluorescens. *International Journal of Food Microbiology*, *297*, 60–71. https://doi.org/10.1016/j.ijfoodmicro.2018.12.011

Truchado, P., Larrosa, M., Castro-Ibáñez, I., & Allende, A. (2015). Plant food extracts and phytochemicals: Their role as Quorum Sensing Inhibitors. *Trends in Food Science & Technology*, *43*(2), Article 2. https://doi.org/10.1016/j.tifs.2015.02.009

Udine, C., Brackman, G., Bazzini, S., Buroni, S., Van Acker, H., Pasca, M. R., Riccardi, G., & Coenye, T. (2013). Phenotypic and genotypic characterisation of Burkholderia cenocepacia J2315 mutants affected in homoserine lactone and diffusible signal factor-based quorum sensing systems suggests interplay between both types of systems. *PloS One*, *8*(1), e55112. https://doi.org/10.1371/journal.pone.0055112

Van de Vel, E., Sampers, I., & Raes, K. (2019). A review on influencing factors on the minimum inhibitory concentration of essential oils. *Critical Reviews in Food Science and Nutrition*, *59*(3), 357–378. https://doi.org/10.1080/10408398.2017.1371112

Venturi, V. (2006). Regulation of quorum sensing in *Pseudomonas*. *FEMS Microbiology Reviews*, *30*(2), 274–291. https://doi.org/10.1111/j.1574-6976.2005.00012.x

Venugopal, V. (1990). Extracellular Proteases of Contaminant Bacteria in Fish Spoilage: A Review. *Journal of Food Protection*, *53*(4), 341–350. https://doi.org/10.4315/0362-028X-53.4.341

Verma, M. K., Anand, R., Chisti, A. M., Kitchlu, S., Chandra, S., Shawl, A. S., & Khajuria, R. K. (2010). Essential Oil Composition of *Artemisia dracunculus* L. (Tarragon) Growing in Kashmir -India. *Journal of Essential Oil Bearing Plants*, *13*(3), Article 3. https://doi.org/10.1080/0972060X.2010.10643830

Vetrivel, A., Ramasamy, M., Vetrivel, P., Natchimuthu, S., Arunachalam, S., Kim, G.-S., & Murugesan, R. (2021). Pseudomonas aeruginosa Biofilm Formation and Its Control. *Biologics*, *1*(3), Article 3. https://doi.org/10.3390/biologics1030019

Vieira, B. B., Mafra, J. F., Bispo, A. S. da R., Ferreira, M. A., Silva, F. de L., Rodrigues, A. V. N., & Evangelista-Barreto, N. S. (2019). Combination of chitosan coating and clove essential oil reduces lipid oxidation and microbial growth in frozen stored tambaqui (Colossoma macropomum) fillets. *LWT*, *116*, 108546. https://doi.org/10.1016/j.lwt.2019.108546

Vital, A. C. P., Guerrero, A., Ornaghi, M. G., Kempinski, E. M. B. C., Sary, C., Monteschio, J. de O., Matumoto-Pintro, P. T., Ribeiro, R. P., & do Prado, I. N. (2018). Quality and sensory acceptability of fish fillet (Oreochromis niloticus) with alginate-based coating containing essential oils. *Journal of Food Science and Technology*, *55*(12), 4945–4955. https://doi.org/10.1007/s13197-018-3429-y

Vuuren, S. F. van, & Viljoen, A. M. (2007). Antimicrobial activity of limonene enantiomers and 1,8-cineole alone and in combination. *Flavour and Fragrance Journal*, *22*(6), 540–544. https://doi.org/10.1002/ffj.1843

Wahjudi, M., Papaioannou, E., Hendrawati, O., van Assen, A. H. G., van Merkerk, R., Cool, R. H., Poelarends, G. J., & Quax, W. J. (2011). PA0305 of Pseudomonas aeruginosa is a quorum quenching acylhomoserine lactone acylase belonging to the Ntn hydrolase superfamily. *Microbiology (Reading, England)*, *157*(Pt 7), 2042–2055. https://doi.org/10.1099/mic.0.043935-0

Warrier, A., Satyamoorthy, K., & Murali, T. S. (2021). Quorum-sensing regulation of virulence factors in bacterial biofilm. *Future Microbiology*, *16*(13), 1003–1021. https://doi.org/10.2217/fmb-2020-0301

Whittaker, P., Fry, F. S., Curtis, S. K., Al-Khaldi, S. F., Mossoba, M. M., Yurawecz, M. P., & Dunkel, V. C. (2005). Use of Fatty Acid Profiles to Identify Food-Borne Bacterial Pathogens and Aerobic Endospore-Forming Bacilli. *Journal of Agricultural and Food Chemistry*, *53*(9), 3735–3742. https://doi.org/10.1021/jf040458a

Wu, S., Zhu, Z., Fu, L., Niu, B., & Li, W. (2011). WebMGA: A customizable web server for fast metagenomic sequence analysis. *BMC Genomics*, *12*, 444. https://doi.org/10.1186/1471-2164-12-444

Wu, T., Zang, X., He, M., Pan, S., & Xu, X. (2013). Structure-activity relationship of flavonoids on their anti-Escherichia coli activity and inhibition of DNA gyrase. *Journal of Agricultural and Food Chemistry*, *61*(34), 8185–8190. https://doi.org/10.1021/jf402222v

Xia, S., Zhou, L., Zhang, Z., & Li, J. (2012). Influence and mechanism of N-(3-oxooxtanoyl)-L-homoserine lactone (C8-oxo-HSL) on biofilm behaviors at early stage. *Journal of Environmental Sciences*, *24*(12), 2035–2040. https://doi.org/10.1016/S1001-0742(11)61060-7

Xie, J., Zhang, Z., Yang, S.-P., Cheng, Y., & Qian, Y.-F. (2018). Study on the spoilage potential of Pseudomonas fluorescens on salmon stored at different temperatures. *Journal of Food Science and Technology*, *55*(1), 217–225. https://doi.org/10.1007/s13197-017-2916-x

Yang, J., Yan, R., Roy, A., Xu, D., Poisson, J., & Zhang, Y. (2015). The I-TASSER Suite: Protein structure and function prediction. *Nature Methods*, *12*(1), Article 1. https://doi.org/10.1038/nmeth.3213

Ye, J., Coulouris, G., Zaretskaya, I., Cutcutache, I., Rozen, S., & Madden, T. L. (2012). Primer-BLAST: A tool to design target-specific primers for polymerase chain reaction. *BMC Bioinformatics*, *13*(1), 134. https://doi.org/10.1186/1471-2105-13-134

Yu, H., Liu, Y., Yang, F., Xie, Y., Guo, Y., Cheng, Y., & Yao, W. (2022). The combination of hexanal and geraniol in sublethal concentrations synergistically inhibits quorum sensing in Pseudomonas fluorescens—In vitro and in silico approaches. *Journal of Applied Microbiology*, *133*(4), 2122–2136. https://doi.org/10.1111/jam.15446

Yu, Z., Tang, J., Khare, T., & Kumar, V. (2020). The alarming antimicrobial resistance in ESKAPEE pathogens: Can essential oils come to the rescue? *Fitoterapia*, *140*, 104433. https://doi.org/10.1016/j.fitote.2019.104433

Zhang, Y. (2008). I-TASSER server for protein 3D structure prediction. *BMC Bioinformatics*, *9*(1), Article 1. https://doi.org/10.1186/1471-2105-9-40

Zhao, D., Lyu, F., Liu, S., Zhang, J., Ding, Y., Chen, W., & Zhou, X. (2018). Involvement of bacterial quorum sensing signals in spoilage potential of *Aeromonas veronii* bv. *Veronii* isolated from fermented surimi. *Journal of Food Biochemistry*, *42*(2), e12487. https://doi.org/10.1111/jfbc.12487

Zhou, L., Zhang, Y., Ge, Y., Zhu, X., & Pan, J. (2020). Regulatory Mechanisms and Promising Applications of Quorum Sensing-Inhibiting Agents in Control of Bacterial Biofilm Formation. *Frontiers in Microbiology*, *11*. https://www.frontiersin.org/articles/10.3389/fmicb.2020.589640

Zhou, L., Zheng, H., Tang, Y., Yu, W., & Gong, Q. (2013). Eugenol inhibits quorum sensing at sub-inhibitory concentrations. *Biotechnology Letters*, *35*(4), 631–637. https://doi.org/10.1007/s10529-012-1126-x

Zhuang, S., Hong, H., Zhang, L., & Luo, Y. (2021). Spoilage-related microbiota in fish and crustaceans during storage: Research progress and future trends. *Comprehensive Reviews in Food Science and Food Safety*, *20*(1), 252–288. https://doi.org/10.1111/1541-4337.12659

Spis rycin

Spis tabel

Oświadczenia współautorów publikacji stanowiących przedmiot rozprawy doktorskiej

OŚWIADCZENIE

Oświadczam, że jestem współautorem pracy:

Tomaś N., Myszka K.* Current advances in the concept of quorum sensing - based prevention of spoilage of fish products by Pseudomonads. Applied Sciences 12, 6719 (2022). https://doi.org/10.3390/app12136719

będącej częścią monotematycznego cyklu publikacji, stanowiącego rozprawę doktorską mgr inż. Natalii Małgorzaty Tomaś. Jednocześnie oświadczam, że indywidualny wkład w powstanie pracy był następujący:

Mgr inż. Natalia Małgorzata Tomaś	60%	Zebranie literatury. Napisanie części manuskryptu.	Natalia Tomaś
Prof. UPP dr hab. Kamila Myszka	40%	Napisanie części manuskryptu, korekta manuskryptu.	Kamila Myszka

OŚWIADCZENIE

Oświadczam, że jestem współautorem pracy:

Sobieszczańska N.*, Myszka K., Szwengiel A., Majcher M., Grygier A., Wolko Ł. Tarragon essential oil as a source of bioactive compounds with anti-quorum sensing and anti-proteolytic activity against *Pseudomonas* spp. isolated from fish – *in vitro, in silico* and *in situ* approaches. International Journal of Food Microbiology 331, 108732 (2020). https://doi.org/10.1016/j.ijfoodmicro.2020.108732

będącej częścią monotematycznego cyklu publikacji, stanowiącego rozprawę doktorską mgr inż. Natalii Małgorzaty Tomaś. Jednocześnie oświadczam, że indywidualny wkład w powstanie pracy był następujący:

Mgr inż. Natalia Małgorzata Tomaś (wówczas Sobieszczańska)	65%	Opracowanie koncepcji manuskryptu, prowadzenie hodowli mikroorganizmów, ekstrakcja kwasów tłuszczowych, przeprowadzenie analizy GC-FID, ekstrakcja autoinduktorów quorum sensing i przygotowanie prób, przeprowadzenie analiz dokowania molekularnego, analiz spektrofotometrycznych i RT-qPCR, przygotowanie pożywki do analiz *in situ*, współudział w opracowaniu wyników i ich analiza statystyczna, napisanie manuskryptu.	Natalia Tomaś
Prof. UPP dr hab. Kamila Myszka	10%	Opracowanie koncepcji badań, izolacja szczepów do badań, wyznaczenie indeksów subMIC, korekta manuskryptu.	Kamila Myszka
Prof. UPP dr hab. Artur Szwengiel	10%	Przeprowadzenie analiz UHPLC-MS/MS i opracowanie wyników.	Szwengiel
Prof. dr hab. Małgorzata Majcher	5%	Przeprowadzenie procesu hydrodestylacji i analizy GC-MS i opracowanie wyników.	MMajcher 25/05/23
Dr Anna Grygier	5%	Przeprowadzenie analizy GC-FID i opracowanie wyników.	A. Grygier 25.05.23
Prof. UPP dr hab. Łukasz Wolko	5%	Zaprojektowanie starterów do reakcji RT-qPCR.	Łukasz Wolko

OŚWIADCZENIE

Oświadczam, że jestem współautorem pracy:

Tomaś N.*, Myszka K., Wolko Ł, Nuc K., Szwengiel A., Grygier A., Majcher M. Effect of black pepper essential oil on quorum sensing and efflux pump systems in the fish-borne spoiler *Pseudomonas psychrophila* KM02 identified by RNA-seq, RT-qPCR and molecular docking analyses. Food Control 130, 108284 (2021). https://doi.org/10.1016/j.foodcont.2021.108284

będącej częścią monotematycznego cyklu publikacji, stanowiącego rozprawę doktorską mgr inż. Natalii Małgorzaty Tomaś. Jednocześnie oświadczam, że indywidualny wkład w powstanie pracy był następujący:

Mgr inż. Natalia Małgorzata Tomaś	55%	Opracowanie koncepcji manuskryptu, prowadzenie hodowli mikroorganizmów, ekstrakcja kwasów tłuszczowych, przeprowadzenie analizy GC-FID, ekstrakcja autoinduktorów quorum sensing i przygotowanie prób, przeprowadzenie analiz dokowania molekularnego, analiz spektrofotometrycznych i RT-qPCR, identyfikacja genów, przygotowanie pożywki do analiz *in situ*, współudział w opracowaniu wyników i ich analiza statystyczna, napisanie manuskryptu.	Natalia Tomaś
Prof. UPP dr hab. Kamila Myszka	10%	Opracowanie koncepcji badań, izolacja szczepów do badań, wyznaczenie indeksów subMIC, korekta manuskryptu.	Kamila M, h
Prof. UPP dr hab. Łukasz Wolko	10%	Analiza transkryptomu i obróbka bioinformatyczna wyników	Łukasz Wolko
Prof. dr hab. Katarzyna Nuc	5%	Analiza transkryptomu.	Katarzyna Nuc
Prof. UPP dr hab. Artur Szwengiel	5%	Przeprowadzenie analiz UHPLC-MS/MS i opracowanie wyników.	Szwengiel
Dr Anna Grygier	5%	Przeprowadzenie analizy GC-FID i opracowanie wyników.	A. Grygier 25.05.23
Prof. dr hab. Małgorzata Majcher	5%	Przeprowadzenie procesu hydrodestylacji i analizy GC-MS i opracowanie wyników.	MMajcher 25/05/23

OŚWIADCZENIE

Oświadczam, że jestem współautorem pracy:

Tomaś N.*, Myszka K. & Wolko Ł. Black pepper and tarragon essential oils suppress the lipolytic potential and the type II secretion system of *P. psychrophila* KM02. Scientific Reports 12, 5487 (2022). https://doi.org/10.1038/s41598-022-09311-9

będącej częścią monotematycznego cyklu publikacji, stanowiącego rozprawę doktorską mgr inż. Natalii Małgorzaty Tomaś. Jednocześnie oświadczam, że indywidualny wkład w powstanie pracy był następujący:

Mgr inż. Natalia Małgorzata Tomaś	60%	Opracowanie koncepcji manuskryptu, prowadzenie hodowli mikroorganizmów, przeprowadzenie analiz RT-qPCR, przeprowadzenie analiz spektrofotometrycznych i modelowych, przeprowadzenie analizy genomu, współudział w opracowaniu wyników i ich analiza statystyczna, napisanie manuskryptu.	Natalia Tomaś
Prof. UPP dr hab. Kamila Myszka	20%	Opracowanie koncepcji badań, przeprowadzenie analiz spektrofotometrycznych i modelowych, korekta manuskryptu.	Kamila Myszka
Prof. UPP dr hab. Łukasz Wolko	20%	Obróbka bioinformatyczna genomu, wyznaczenie starterów do reakcji RT-qPCR.	Łukasz Wolko

Publikacje stanowiące przedmiot rozprawy doktorskiej

applied sciences

MDPI

Review

Current Advances in the Concept of Quorum Sensing-Based Prevention of Spoilage of Fish Products by Pseudomonads

Natalia Tomaś and Kamila Myszka *

Department of Biotechnology and Food Microbiology, Poznan University of Life Sciences, Wojska Polskiego 48, 60-627 Poznan, Poland; natalia.tomas@up.poznan.pl
* Correspondence: kamila.myszka@up.poznan.pl

Abstract: Microbial spoilage of fish is attributed to quorum sensing (QS)-based activities. QS is a communication process between the cells in which microorganisms secrete and sense the specific chemicals (autoinductors, AIs) that regulate proteolysis, lipolysis, and biofilm formation. These activities change the organoleptic characteristics and reduce the safety of the products. Although the microbial community of fish is diverse and may consist of a range of bacterial strains, the deterioration of fish-based products is attributed to the growth and activity of *Pseudomonas* spp. This work summarizes recent advancements to assess the influence of QS mechanisms on seafood spoilage by *Pseudomonas* spp. The quorum sensing inhibition (QSI) in the context of fish preservation has also been discussed. Detailed recognition of this phenomenon is crucial in establishing effective strategies to prevent the premature deterioration of fish-based products.

Keywords: *Pseudomonas* spp.; quorum sensing (QS); autoinductors (AIs); quorum sensing inhibition; spoilage of fish-based products; fish preservation

Citation: Tomaś, N.; Myszka, K. Current Advances in the Concept of Quorum Sensing-Based Prevention of Spoilage of Fish Products by Pseudomonads. *Appl. Sci.* **2022**, *12*, 6719. https://doi.org/10.3390/app12136719

Academic Editors: Jesus Simal-Gandara, Jianbo Xiao and Md Afjalus Sira

Received: 26 May 2022
Accepted: 30 June 2022
Published: 2 July 2022

1. Introduction

The nutritional and health value of fish, as well as their relatively low price and availability, affect global production, which is projected to reach 200 Mt by 2029, increasing by 25 Mt from the base period (average of 2017–2019) [1]. As reported by FAO [1], 44% of total fish production is utilized in the fresh/chilled form, which are usually more perishable than most other foodstuffs [2]. The high content of free amino acids, high post-mortem pH, high water content, and presence of trimethylamine oxide (TMAO) promote the growth of microorganisms in fish-based products. Psychrotolerant species of the genera *Pseudomonas* mainly contribute to seafood deterioration; the bacteria may decompose nitrogenous/lipid substances [3], which can result in greater weight loss, a reduction in water-holding capacity, textural changes, and off-odor effects of products [4,5]. *Pseudomonas* spp. have successfully evolved genotypic and phenotypic traits enabling growth and defeating the negative effects of conventional seafood antimicrobials and temperature stress [4,6–8] (Figure 1). Despite implementing quality control programs in the seafood industry, about one-fourth of the world's supply and 30% of landed fish are lost due to microbial activity [8]. Therefore, it is necessary to develop new solutions to prevent spoilage of fish-based products caused by *Pseudomonas* spp.

The metabolic activities of *Pseudomonas* spp. are regulated via a quorum sensing (QS) system, which was perfectly described in the work of Venturi [9]. In that system, small-signal molecules (autoinductors, AIs), followed by interaction with cognate receptor proteins, lead to a coordinated regulation of specific gene expression [9]. Two acyl-homoserine lactone (AHL) QS systems, LasI-LasR and RhlI-RhlR, were identified in *P. aeruginosa*; these two systems also interact with a 2-heptyl-3-hydroxy-4-quinolone signal (PQS) and 2-2-hydroxyphenyl)-thiazole-4-carbaldehyde (IQS) systems [10].

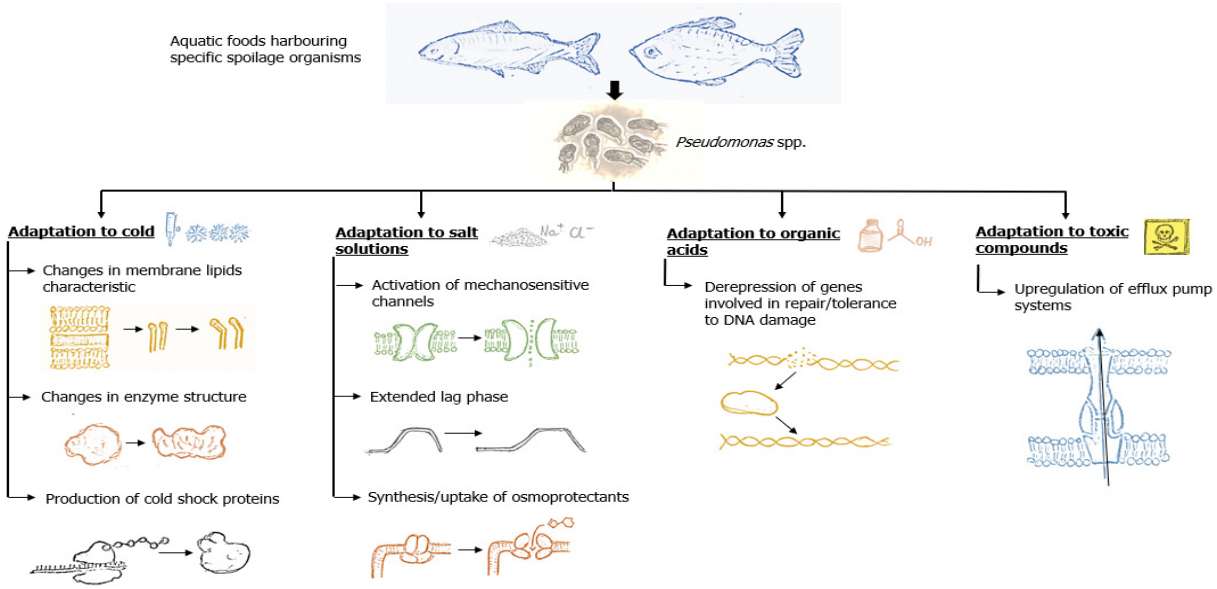

Figure 1. Schematic explanation of *Pseudomonas* spp. adaptation strategies to environmental conditions.

Numerous articles are available in which the background of food-associated stresses and their impact on the cellular response of bacteria are expertly described [9,11]. However, few of them address the effect of inhibition of QS mechanisms on seafood quality. Due to the resistance of *Pseudomonas* spp. to conventional food preservation systems, QS-based control methods are often considered [12]. Their application to the food industry would greatly aid efforts to eradicate undesirable microflora from food processing environments and, ultimately, from food products. These approaches, in contrast to bactericidal treatments, exert less selective pressure, which in turn reduces the likelihood of resistance development. QS inhibitors would help design approaches for reducing or preventing spoilage reactions or even controlling the expression of virulence factors of *P. aeruginosa* [13].

This review summarizes recent research reports on the QS phenomenon in *Pseudomonas* spp. We present the role of QS in regulating the metabolic activity of *Pseudomonas* spp. (i) and review of the current applications of QS inhibitors in preventing bacterial food spoilage (ii). Our goal is to provide a new perspective for the search for more effective food antimicrobials through the use of QS inhibitory agents.

2. QS System in Pseudomonads

The AHLs-depended QS networks studied are the best so far and the focus of this review will be on the structural basis of that systems in pseudomonads [9]. Moreover, transcriptomic studies have revealed that the AHL-regulated genes and operons constitute over 6% of the genome and are scattered through the chromosome [14,15]. That supports the view that the AHL system in bacteria constitutes a global regulatory system [16].

AHL signals differ in the chemical structure; the differences are in the length of the acyl chain and the substituents (usually 3-oxo or 3-hydroxy groups) at the 3 position of the acyl chain [17,18].

In *P. aeruginosa*, two AI synthase genes, *lasI and rhlI*, are involved in the synthesis of AHLs; they share significant sequence homologies to *luxI* of *Vibrio fisheri* [10]. AHLs accumulate both in the cells and in the environment. As the bacteria grow, the concentration of secreted AHL molecules increases [19]. When the population density reaches the "quorum", AIs exceed the critical threshold and are recognized by specific receptors that belong to a large class of DNA-binding transcription factors named "R-proteins" [18]. In

P. aeruginosa, the LasR, upon binding to the specific AHL, directly regulates the transcription of target genes by binding to or dissociating from corresponding promoters [10,18].

In *P. aeruginosa*, there are also two other types of AHL-mediated systems, the *pqs* system and the *iqs* system. These networks work in a manner similar to the *las* and *rhl* systems, though their AIs are PQS and IQS [20,21].

PQS is synthesized via a "head to head" condensation of anthranilate and β-keto dodecanoate and requires the products of the *pqsA*, *pqsB*, *pqsC*, and *pqsD* genes, which generate over 50 other 2-alkyl-4-quinolones including 2-heptyl-4-quinolone (HHQ) [22]. Many of these signals are produced at low levels; thus, their biological function is not yet clear [16]. In addition to their regulatory role in the pathogenicity of *P. aeruginosa*, it is believed that PQS can also induce outer membrane vesicle formation, activate the oxidative stress response, act as a stress warning signal, and modulate the host immune response [16,23,24].

The role of the last gene of the *pqs* operon (*pqsE*) is not known, but while *pqsE* mutants produce parental levels of PQSs, the strains do not exhibit any PQS-related phenotypes; consequently, PqsE is considered to facilitate the response to PQS [25]. The immediate precursors of PQS are HHQ, and its conversion to PQS depends on the activation of PqsH, a putative mono-oxygenase [22] that is LasR regulated, so linking AHL and PQS regulatory networks.

IQS belongs to a new class of AIs of the QS system. The genes that are involved in IQS synthesis are a non-ribosomal peptide synthase gene cluster *ambBCDE*. When inhibited, it caused a decrease in the production of PQS and C4-HSL AIs, as well as QS-regulated activities of bacteria [21]. IQS has been shown to contribute to the full virulence of *P. aeruginosa* in different animal models, highlighting the function of this new QS system in the modulation of bacterial pathogenesis. Importantly, upon phosphate depletion in the culture medium, IQS was demonstrated to be able to partially take over the function of the central *las* system in pseudomonads [26].

There are interconnections between the aforementioned QS systems in pseudomonads. The *las* system is activated by 3-oxo-C12-HSL. Next, the LasR-3-oxo-C12-HSL complex multimerizes and stimulates the transcription of *rhlR*, *rhlI*, *lasI* (hence a positive feedback loop), and other genes that are part of this regulon [27]. The RhlR-C4-HSL also multimerizes and activates its own regulon; *rhlI* forms the second positive feedback loop [10,28]. LasR-3-oxo-C12-HSL positively controls PqsR, a transcriptional regulator of operon *pqsABCD,* and the expression of *pqsH,* the gene encoding the final converting enzyme of PQS from precursor HHQ [10]. Interestingly, *pqsR* and *pqsABCDE* expression can be inhibited by RhlR-C4-HSL, suggesting that the ratio of the concentration of 3-oxo-C12-HSL and C4-HSL plays a crucial role in the dominance of the *pqs* signaling system [29]. As stated above, LasR-3-oxo-C12-HSL regulates the onset and activation of both the *pqs* and *rhl* systems in *P. aeruginosa*. These networks represent a step-wise activation cascade that is triggered by the attainment of the "quorum" in pseudomonads [10]. Recently detected IQS is also controlled by LasRI; disruption of either *lasR* or *lasI* limits the expression of *ambBCDE* and production of IQS [26].

3. Examples of QS-Based Activities of *Pseudomonas* spp. Affecting Spoilage of Fish

Extracellular enzyme biosynthesis and biofilm development are regulated by the QS system. The above microbial activities play a major role in the fish spoilage process [13,30–32]. AIs of the QS system have been detected in spoiled fish filets, cold-smoked, and minced fish products [13]. The degree of fish spoilage was correlated with the concentration of AIs [30]. Examples of the effects of AIs on fish spoilage are presented in Table 1.

Table 1. Examples of *Pseudomonas* spp. phenotypes regulated by AHLs-mediated system.

Microorganism	AHL	Phenotypes Regulated by QS	Reference
P. aeruginosa	3-oxo-C12-HSL	Pyoverdine production	[33]
P. psychrophila	C4-HSL	Exoenzyme production	[34]
P. fluorescens, *P. putida*	3-oxo-C6-HSL, C6-HSL, C8-HSL, C12-HSL	Proteolytic activity	[34]
Pseudomonas spp.	C4-HSL, 3-oxo-C6-HSL, C6-HSL, C8-HSL, C12-HSL	Slime formation	[13]
P. fluorescens, *P. putida*	3-oxo-C6-HSL, C6-HSL, C8-HSL, C12-HSL	Proteolytic activity	[13]
P. fluorescens	C4-HSL	Biofilm formation, EPS production	[35]
P. fluorescens	C4-HSL	Biofilm formation	[19]
P. fluorescens	3-oxo-C14-HSL, 3-oxo-C6-HSL, C4-HSL	Lipolytic activity	[5]

3.1. QS and Proteolysis

Pseudomonas spp. isolated from fishery products displayed proteolytic activities accompanied by an increase in amino acids and volatile sulfur compounds such as mercaptans and H_2S [32]. The proteases of fish-borne *Pseudomonas* spp. are serine, thiol, or metalloproteases stabilized by Ca^{2+}. They exhibit low activation energies compared to the classical trypsin protease [36]. Proteolytic enzymes degrade the fish muscle and connective tissue, facilitating bacterial penetration to deeper structures and causing textural changes in fish [37].

AHLs have been identified in proteinaceous foods and were correlated with the proteolytic activity of microflora [34]. AHLs were found in rainbow trout fillets contaminated by *P. fluorescens* and *P. putida* [13]. Moreover, *P. fluorescens* exhibited significantly higher proteolytic activity when exogenous C4-HSL and C6-HSL were added to the culture [30]. A significant increase in total volatile basic nitrogen (TVB-N) (from 5.21 to approximately 60 mg N/100 g) during storage was observed with the addition of C4-HSL and C14-HSL. These AIs had a stimulatory effect on the *aprX* metalloprotease gene expression and proteolytic activity of *P. fluorescens* (by 63 and 52%, respectively) [38]. In *P. psychrophila*, *P. orientalis*, and *P. fluorescens*, changes in QS systems involving downregulation of AHL and the PQS molecules resulted in inhibition of proteolysis (approximately 15 to 30%) along with downregulation of genes encoding metalloproteases [39]. A significant inhibition by about 40% of extracellular protease activity was finally confirmed by Tang et al. [35] in ΔluxI and ΔluxR mutants of *P. fluorescens*.

3.2. QS and Lipolysis

Fish muscle is characterized by a relatively higher content of lipids that accounts for 16% [4]. *Pseudomonas* spp. produce lipolytic enzymes that catalyze the hydrolysis of triglycerides to glycerol and free fatty acids, resulting in unpleasant odors related to the development of aldehydes [2]. The lipolytic activity of fish-borne spoilers *Pseudomonas* spp. was described by Myszka et al. [5] and Sterniša et al. [37]. It has been established that QS-regulated *lipA* and *lipB* genes are responsible for fish spoilage [40]. The lipase encoded by *lipB* is solely responsible for "lipolytic phenotype" of *P. fluorescens*, which leads to rancidity, a soapy off-flavor, and other quality defects of fish [41]. *lipA* is located at the end of a polycistronic operon in the *apr* gene cluster; its downregulation results in the loss or relatively low lipolytic activity of bacteria [42]. Moreover, studies performed by Riedel et al. [43] demonstrated that Lip exporter is regulated by the QS system; its function is essential for lipase secretion. Supplementation of the culture medium with AHLs increased transcription of *lipA* and *lipB* of bacteria [44]; the bacteria lost the ability to synthesize lipase since they contained a nonfunctional AHL of the QS system [45].

3.3. QS and Biofilm Formation

The formation of biofilms is a stepwise process involving the initial attachment of bacteria to surfaces, microcolonies growth and maturation into expanding structures, and further detachment of aged microorganisms [46]. It has been proposed that

AHL-mediated QS is involved in all stages of biofilm formation. The influence of the *las* AI, 3-oxo-C12-HSL on biofilm maturation in *P. aeruginosa* has been described by Davies et al. [47]. Strain deficient in the production of 3-oxo-C12-HSL formed very thin biofilms that lacked the three-dimensional architecture observed with the parent. In addition, while the wild-type biofilm was resistant to sodium dodecyl sulfate (SDS), the biofilm formed by the *lasI* mutant was easily dispersed upon exposure to SDS [47].

The relationship between QS and biofilm formation was also described indirectly by evaluating the effects of AIs on twitching and swarming motilities, rhamnolipids, and exopolysaccharides (EPS) production [33]. Swarming motility, which is an organized form of structure translocation, is useful in the early stages of biofilm development and is regulated by the *rhl* system similarly to twitching motility—a flagella-independent way of translocation necessary for microcolony development [48]. EPS holds all cells of biofilm in the near vicinity to enable QS interactions [49]. Rhamnolipid production is involved in several aspects of biofilm formation, such as the formation of microcolonies, maintaining the open channel structure, facilitating mushroom-shaped structures, and aiding cell dispersion [50].

In general, the addition of AHLs to the culture medium was shown to affect EPS (alginate)/rhamnolipid production, twitching and swarming motilities, and biofilm maturity by *Pseudomonas* spp. [30,51]. Inhibiting OS would be, therefore, an alternative to combat the biofilm problems [51,52]. Adhered *Pseudomonas* spp. are found in many locations on seafood processing lines, despite the fact that thorough cleaning and disinfection are carried out regularly. Moreover, biofilms of *Pseudomonas* spp. enhanced the colonization of *Listeria monocytogenes* on food contact materials which promoted food contamination [53].

4. QS Inhibition in the Context of Fish Preservation

As researchers correlated metabolic activities with the QS mechanism [13,54], the search for QS inhibiting agents as an alternative approach for fish preservation has been extensively studied [55]. Disrupting the bacterial QS network is a reverse bactericidal strategy that will not exert selection pressure, leading, as with conventional preservatives, to the development of resistance [56]. Moreover, blocking QS renders the bacteria less virulent [9]. In general, QS inhibitors (QSIs) and quorum quenching enzymes (QQ) can be successfully used for food safety control. QS inhibiting agents can target AIs, and QS receptors and interfere with signaling cascades [54]. All of these mechanisms are present in *Pseudomonas* spp.; a detailed description is given below.

4.1. QS Inhibiting Agents

The agents that target pseudomonads AIs include mainly lactonases, acylases (also known as amidases or aminohydrolases), and oxidoreductases. Enzymes can lead to one of the following effects: (i) AI-degradation for fine-tuning the endogenous QS system, (ii) AI-degradation for modulating the QS system, and (iii) AI-degradation as a mechanism to use AIs for nutrient sources. Inactivation of AI synthases and modification/degradation of AIs affect the QS system of pseudomonads [57].

Among lactone-degrading enzymes, metallo-β-lactamase-like lactonases (MLL) and phosphotriesterase-like lactonases (PLL) are the main studied families [57,58]. They share a common catalytic mechanism and their differences in AHL substrate preference lie in how the acyl chain can be accommodated into the catalytic site [59]. PLL favors long aliphatic lactones as substrates, whereas MLL exhibits board AHL specificity. The work of Rémy et al. [60] confirms that levels of C4-HSL and 3-oxo-C12-HSL and low expression of *las* and *rhl* genes in *P. aeruginosa* were due to PLL and MLL activity.

Acylases hydrolase the amide bond between the acyl chain and the homoserine lactone ring [57]. Four AHL-acylases are present in *P. aeruginosa*: namely *pvdQ*, *quiP*, *hacB*, and PA1893 [61]. When *P. aeruginosa* is grown in a rich medium, the constitutive expression of these acylases shows a decreased level of 3-oxo-C12-HSL. Vice versa, disruption

of the acylase genes resulted in a higher concentration of AIs. In addition, a Δ*hacB* single mutant and a Δ*pvdQ*, Δ*hacB*, and Δ*quiP* triple mutant secrete more efficiently 3-oxo-C12-HSL in comparison to Δ*pvdQ*, Δ*quiP* double mutant that produced AHLs in the same level as wild-type pseudomonads. This observation indicates that HacB might be working as the main acylase in controlling 3-oxo-C12-HSL accumulation in pseudomonads [62].

Oxidoreductases modify AIs by oxidizing or reducing the acyl chain at the third or distal carbon without degrading the AHLs [58]. Such modification may also affect the specificity and recognition of the AIs, thus disturbing the activation of the QS-mediated genes [63]. BpiB09 oxidoreductase derived from a metagenomics library was found to be capable of inactivating 3-oxo-C12-HSL in *P. aeruginosa* [64]. Its expression in pseudomonads resulted in significantly reduced QS-controlled bacteria phenotypes.

QS inhibiting agents also target QS receptors that inactivate the receptor or compete with the receptor. Terpenes and flavonoids of plant essential oils (EOs), as well as halogenated furanones derived from algae, can bind to QS receptors [21]. Examples of natural QS inhibiting agents against *Pseudomonas* spp. are presented in Table 2. For instance, a plant flavonoid naringenin competes with the 3-oxo-C12-HSL by binding to the LasR receptor leading to inhibition of QS-regulated virulence factors in *Pseudomonas* spp. [65]. Methyl eugenol and β-phellandrene of tarragon EO [39] and quercetin [54] show similar anti-QS activities [66]. Methyl eugenol, β-phellandrene, and quercetin were successfully docked into the LasR of pseudomonads [54,66]. High docking score values of the examined agents-LasR receptor were due to the range of H-bones created with negatively charged residues of the proteins [66]. According to Klebe [67], hydrogen bonds provide stability to the complex ligand-receptor and play a key role in molecular recognition. Moreover, the effective binding of compounds of EOs results in conformational changes in the proteins [68].

Table 2. Impact of natural QS inhibiting agents on fish-associated *Pseudomonas* spp.

QS Inhibiting Agent	Target Microorganism	Impact on Bacterial QS-Controlled Processes	Reference
Piper nigrum L. EO	*P. psychrophila*	reduction of proteolytic and lipolytic activities	[66]
Ferula asafoetida EO	*P. aeruginosa*	Reduction of pyocyanin and elastase production; prevention of biofilm formation	[69]
Myrtus communis L. EO	*P. fluorescens*, *P. orientalis*	Reduction in the EPS production	[52]
Origanum majorana EO	*P. putida*	Prevention of biofilm formation	[70]
Juniperus phoenicea EO	*P. fluorescens*	Reduction of proteolytic and lipolytic activities	[5]
Cinnamaldehyde	*P. fluorescens*	Reduction of proteolytic activity; prevention of biofilm formation	[71]
Quercetin	*P. aeruginosa*	Reduction the EPS production and bacterial motility, prevention of biofilm formation	[54]
Garlic extract	*P. aeruginosa*	Reduction of rhamnolipid production	[72]

Selective metabolites produced by lactic acid bacteria can also bind simultaneously to different QS receptors. The affinity of 3-benzene lactic acids from *Lactobacillus* spp. for RhlR and PqsR receptors is higher compared to C4-HSL and PQS ligands in *P. aeruginosa* [73]. In addition, flavonoids can also non-competitively bind to the LasR receptor and prevent the protein from binding to DNA. The agents also cause the repression of QS-mediated activities [74].

The third mechanism of inactivation of the QS system in *Pseudomonas* spp. blocks the signaling cascade by deactivating the downstream response regulators or other regulatory factors [21]. For instance, an efflux pump inhibitor PAβN reduces the accumulation of AIs in supernatants and significantly decreases the relative expression of the QS cascade (*pqaA*, *pqsR*, *lasI*, *lasR*, *rhlI*, and *RhlR*) in *P. aeruginosa*. Limonene and β-caryophyllene from black pepper EO also exhibited the anti-QS and anti-efflux pumps of pseudomonads [66]. The mRNA transcript levels of autoinductor synthases, membrane fusion,

outer membrane proteins, and transcription of repressor regulators MarR and TetR were observed in *P. psychrophila*. In general, limonene and β-caryophyllene affected the functioning of the QS system in *P. psychrophila* and consequently reduced the spoilage potential [66].

4.2. Examples of Use Anti-QS Agents in Fish Preservation

To delay spoilage and extend the shelf life of fish, alternative preservation methods involving the addition of compounds with known anti-QS activity were proposed [75]. However, new preservative techniques require extensive research to be effectively applied to fish products due to the different sensitivity of microorganisms to QS inhibiting agents introduced directly into the food matrix compared to the sensitivity of cells to the above agents recorded in vitro [37,67].

The most convenient method of using anti-QS agents is to add them directly to marinades or brine. For instance, fresh salmon samples were immersed in marinade composed of 95% olive oil and 5% vinegar and enriched with pepper EO. After 72 h of incubation, the protease and elastase activities of *P. aeruginosa* were suppressed by 30–50% and 60–70%, respectively [76]. Moreover, Van Haute et al. [77] and Eskandari et al. [78] reported that the shelf life of salmon and silver carp could be extended when marinated with anti-QS agents. Both the addition of cinnamon EO and black cumin extract inhibited microbial proliferation. After 15 days of storage, total psychotropic pseudomonads content was low, lipid oxidation was delayed, and sensory quality (texture, color, and odor) was high compared to control samples [78]. In the work of Sterniša et al. [37], rosemary extract, buffered vinegar, and their combinations were used as dip treatments against *P. fragi*, *P. psychrophila*, *Shewanella putrefaciens*, and *Shewanella xiamenesis* in common carp meat. The results showed that *Pseudomonas* strains were more resistant to applied antimicrobials, and only a concentration of 3.13 mg/mL rosemary extract in vinegar resulted in growth inhibition and lowered lipolytic and proteolytic activity.

Although the direct application of anti-QS EOs to fish-based products is the most common application method, the technique has some disadvantages. Indeed higher concentrations of EOs are needed to achieve the same effect in food compared to in vitro approaches. In addition, even at low doses, some EOs could have a negative impact on the sensory attributes. Therefore, an alternative solution is to use edible coating/films enriched with anti-QS EOs.

The advantages of edible films are stabilizing volatiles entrapped into their structure, increasing the oxygen barrier, and maintaining sensory and texture attributes [79]. The application of the anti-QS myrtle EO to the chitosan-based nanomatrix of salmon-based products enhanced the activity of the agent against *Pseudomonas* spp. [52]. *Pseudomonas* population was maintained at approximately under 10^4 CFU/g relatives to the control, reaching 10^8 CFU after 5 days of storage. Chitosan coatings in combination with whey protein and tarragon EO were also tested for their preservative effects on *Scomberoides commersonnianus* fillets under refrigerated conditions. The applied treatment inhibited the growth of psychrotrophic bacteria, delayed the increase in TVB-N content and pH value while significantly reducing lipid oxidation [80]. Xu et al. [81] evaluated the preservative effect of two gelatin coatings, the first combined with ginger and the second with garlic EO for turbot fillets stored for 20 days at 4 °C. The results showed the ability of garlic EO coating to prolong the shelf life of fresh fish. After incubation, the total viable counts of bacteria did not exceed 10^6 CFU/g, the TVB-N concentration was approximately 20 mg/100 g of product, and the hardness decreased by approximately 53% compared to the control samples [81].

To the best of our knowledge, the use of an AHL-degrading enzyme for fish preservation has only been evaluated in the work of Gui et al. [82]. A combination of bacteriocin nisin, AiiAAI96 AHL-lactonase, and vacuum packaging was used to preserve chilled sturgeon fillets. The treatments acted synergistically in inhibiting the growth of

psychrotrophs and delaying food spoilage; they extended the shelf life of the fish samples by 5 days [82].

5. Future Work and Conclusions

QS plays a prime function in regulating fish spoilage by *Pseudomonas* spp. Thus a proper and in-depth understanding of the QS system in those bacteria is very much essential. Of particular interest are studies that will clarify the following issues related to QS inhibition: (i) what are the best conditions for QS inhibiting agents in controlling bacterial phenotypes? and (ii) whether QS inhibiting agents impact beneficial microflora in food ecosystems. In addition, more than one AHL-mediated QS system occurs in a particular strain, which are all involved in metabolic activity regulation. Some investigated QS inhibiting agents show high target specificity. These agents present a challenge in developing approaches that influence a broad range of AIs of *Pseudomonas* spp. Further investigations should focus on studying the "universal" anti-QS agent that targets a broad range of AIs to inhibit QS activity efficiently. A combination of the anti-QS approach with other biocontrol treatments to obtain a synergistic effect is a promising strategy that could increase the susceptibility of pseudomonads to the conventional preservative treatment of seafood.

In this minireview, a summary of the results related to the contribution of QS in the metabolic activities of *Pseudomonas* spp. is provided. QS inhibiting agents with examples of their application in seafood products were also described. With the increasing amount of information available, QS-based strategies can be used more effectively to extend the shelf life of perishable fish products and as innovative strategies for controlling foodborne *P. aeruginosa*.

Author Contributions: N.T. and K.M. conceived the concept and wrote the manuscript. All authors have read and agreed to the published version of the manuscript.

Funding: This study was funded by the National Science Centre, Poland (grant number 2016/23/D/NZ9/00028).

Institutional Review Board Statement: Not applicable.

Informed Consent Statement: Not applicable.

Conflicts of Interest: The authors declare no conflict of interest.

References

1. FAO. *The State of World Fisheries and Aquaculture (Sofia)—Meeting the Sustainable Development Goals*; FDA: Rome, Italy, 2018; p. pxiii-210.
2. Comi, G. Spoilage of meat and fish. In *The Microbiological Quality of Food*; Bevilacqua, A., Corbo, M.R., Sinigaglia, M., Eds.; Woodhead Publishing: Cambridge, UK, 2017; pp. 179–210.
3. Raposo, A.; Pérez, E.; de Faria, C.T.; Ferrús, M.A.; Carrascosa, C. Food spoilage by *Pseudomonas* spp.—An overview. In *Foodborne Pathogens and Antibiotic Resistance*; Singh, O.V., Ed.; John Wiley & Sons, Inc.: Hoboken, NJ, USA, 2017; pp. 41–71.
4. Xie, J.; Zhang, Z.; Yang, S.-P.; Cheng, Y.; Qian, Y.-F. Study on the spoilage potential of *Pseudomonas fluorescens* on salmon stored at different temperatures. *J. Food Sci. Technol.* **2018**, *55*, 217–225.
5. Myszka, K.; Tomaś, N.; Wolko, Ł.; Szwengiel, A.; Grygier, A.; Nuc, K.; Majcher, M. In situ approaches show the limitation of the spoilage potential of *Juniperus phoenicea* L. essential oil against cold-tolerant *Pseudomonas fluorescens* KM24. *Appl. Microbiol. Biotechnol.* **2021**, *105*, 4255–4268.
6. Freeman, B.C.; Chen, C.; Yu, X.; Nielsen, L.; Peterson, K.; Beattle, G.A. Physiological and transcriptional responses to osmotic stress of two *Pseudomonas syringae* strains that differ in epiphytic fitness and osmotolerance. *J. Bacteriol.* **2013**, *195*, 4742–4752.
7. Gram, L.; Ravn, L.; Rasch, M.; Bruhn, J.B.; Christensen, A.B.; Givskov, M. Food spoilage—Interactions between food spoilage bacteria. *Int. J. Food Microbiol.* **2002**, *78*, 79–97.
8. Ghaly, A.E.; Dave, D.; Budge, S.; Brooks, M.S. Fish spoilage mechanisms and preservation techniques: Review. *Am. J. Appl. Sci.* **2010**, *7*, 859–877.
9. Venturi, V. Regulation of quorum sensing in *Pseudomonas*. *FEMS Microbiol. Rev.* **2006**, *30*, 274–291.
10. Lee, J.; Zhang, L. The hierarchy quorum sensing network in *Pseudomonas aeruginosa*. *Protein Cell* **2015**, *6*, 26–41.
11. Tribelli, P.M.; López, N.I. Reporting key features in cold-adapted bacteria. *Life* **2018**, *8*, 8.

12. Machado, I.; Silva, L.R.; Giaouris, E.D.; Melo, L.F.; Simões, M. Quorum sensing in food spoilage and natural-based strategies for its inhibition. *Food Res. Int.* **2020**, *127*, 108754.
13. Bai, A.J.; Rai, V.R. Bacterial quorum sensing and food industry. *Compr. Rev. Food Sci. Food Saf.* **2011**, *10*, 183–193.
14. Wagner, V.E.; Bushnell, D.; Passador, L.; Brooks, A.I.; Iglewski, B.H. Microarray analysis of *Pseudomonas aeruginosa* quorum sensing regulons: Effects of growth phase and environment. *J. Bacteriol.* **2003**, *185*, 2066–2075.
15. Schuster, M.; Lostroh, C.P.; Ogi, T.; Greenberg, E.P. Identification, timing and signal specificity of *Pseudomonas aeruginosa* quorum-controlled genes: A transcriptome analysis. *J. Bacteriol.* **2003**, *185*, 2066–2079.
16. Diggle, S.P.; Matthijs, S.; Wright, V.J.; Fletcher, M.P.; Chhabra, S.R.; Lamont, I.L.; Kong, X.; Hider, R.C.; Cornelis, P.; Cámara, M.; et al. The *Pseudomonas aeruginosa* 4-quinolone signal molecules HHQ and PQS play multifunctional roles in quorum sensing and iron entrapment. *Chem. Biol.* **2007**, *14*, 87–96.
17. Skandamis, P.N.; Nychas, G.-J.E. Quorum sensing in the context of food microbiology. *Appl. Environ. Microbiol.* **2012**, *78*, 5473–5482.
18. Li, Z.; Nair, S.K. Quorum sensing: How bacteria can coordinate activity and synchronize their response to external signals? *Protein Sci.* **2012**, *21*, 1403–1417.
19. Li, T.; Wang, D.; Ren, L.; Mei, Y.; Ding, T.; Li, Q.; Chen, H.; Li, J. Involvement of exogenous N-Acyl-homoserine lactones in spoilage potential of *Pseudomonas fluorescens* isolated from refrigerated turbot. *Front. Microbiol.* **2019**, *10*, 2716.
20. Fuqua, C.; Parsek, M.R.; Greenberg, E.P. Regulation of gene expression by cell-to-cell communication: Acyl-homoserine lactone quorum sensing. *Annu. Rev. Genet.* **2001**, *35*, 439–468.
21. Zhou, L.; Zhang, Y.; Ge, Y.; Zhu, X.; Pan, J. Regulatory mechanisms and promising application of quorum sensing-inhibiting agents in control of bacterial biofilm formation. *Front. Microbiol.* **2020**, *11*, 589640.
22. Gallagher, L.A.; McKnight, S.L.; Kuznetsova, M.S.; Pesci, E.C.; Manoil, C. Functions required for extracellular quinolone signaling by *Pseudomonas aeruginosa*. *J. Bacteriol.* **2002**, *184*, 6472–6480.
23. Lin, J.; Cheng, J.; Wang, Y.; Shen, X. The *Pseudomonas* quinolone signal (PQS): Not just for quorum sensing any more. *Front. Cell. Infect. Microbiol.* **2018**, *8*, 230.
24. Bru, J.L.; Rawson, B.; Trinh, C.; Whiteson, K.; Høyland-Kroghsbo, N.M.; Siryaporn, A. PQS produced by the *Pseudomonas aeruginosa* stress response repels swarms away from bacteriophage and antibiotics. *J. Bacteriol.* **2019**, *201*, e00383-19.
25. Diggle, S.P.; Winzer, K.; Chhabra, S.R.; Worrall, K.E.; Cámara, M.; Williams, P. The *Pseudomonas aeruginosa* quinolone signal molecule overcomes the cell density-dependency of the quorum sensing hierarchy, regulates *rhl*-dependent genes at the onset of stationary phase and can be produced in the absence of LasR. *Mol. Microbiol.* **2003**, *50*, 29–43.
26. Lee, J.; Wu, J.; Deng, Y.; Wang, J.; Wang, C.; Wang, J.; Chang, C.; Dong, Y.; Williams, P.; Zhang, L.H. A cell-cell communication signal integrates quorum sensing and stress response. *Nat. Chem. Biol.* **2013**, *9*, 339–343.
27. Pesci, E.C.; Pearson, J.P.; Seed, P.C.; Iglewski, B.H. Regulation of las and rhl quorum sensing in *Pseudomonas aeruginosa*. *J. Bacteriol.* **1997**, *179*, 3127–3132.
28. Ventre, I.; Ledgham, F.; Prima, V.; Lazdunski, A.; Foglino, M.; Sturgis, J.N. Dimerization of the quorum sensing regulator RhlR: Development of a method using EGFP fluorescence anisotropy. *Mol. Microbiol.* **2003**, *48*, 187–198.
29. Cao, H.; Krishnan, G.; Goumnerov, B.; Tsongalis, J.; Tompkins, R.; Rahme, L.G. A quorum sensing-associated virulence genes of *Pseudomonas aeruginosa* encodes a LysR-like transcription regulator with a unique self-regulatory mechanism. *Proc. Natl. Acad. Sci. USA* **2001**, *98*, 14613–14618.
30. Li, T.; Yang, B.; Li, X.; Li, J.; Zhao, G.; Kan, J. Quorum sensing system and influence on food spoilage in *Pseudomonas fluorescens* from turbot. *J. Food Sci. Technol.* **2018**, *55*, 3016–3025.
31. Meliani, A.; Bensoltane, A. Review of *Pseudomonas* attachment and biofilm formation in food industry. *Poult. Fish. Wildl. Sci.* **2015**, *3*, 2–7.
32. Venugopal, V. Extracellular proteases of contaminant bacteria in fish spoilage: A review. *J. Food Prot.* **1990**, *53*, 341–350.
33. Rasamiravaka, T.; Labtani, Q.; Duez, P.; El Jaziri, M. The formation of biofilms by *Pseudomonas aeruginosa*: A review of the natural and synthetic compounds interfering with control mechanisms. *Biomed. Res. Int.* 2015, *2015*, 759348.
34. Ammor, M.S.; Michaelidis, C.; Nychas, G.-J.E. Insights into the role of quorum sensing in food spoilage. *J. Food Prot.* **2008**, *71*, 1510–1525.
35. Tang, R.; Zhu, J.; Feng, L.; Li, J.; Liu, X. Characterization of LuxI/LuxR and their regulation involved in biofilm formation and stress resistance in fish spoilers *Pseudomonas fluorescens*. *Int. J. Food Microbiol.* **2019**, *297*, 60–71.
36. Stepaniak, L.; Fox, P.F.; Daly, C. Isolation and general characterization of a heat-stable proteinase from *Pseudomonas fluorescens*. *Biochim. Biophys. Acta* **1982**, *717*, 376–383.
37. Sterniša, M.; Purgatorio, C.; Paparella, A.; Mraz, J.; Smole Možina, S. Combination of rosemary extract and buffered vinegar inhibits *Pseudomonas* and *Shewanella* growth in common carp (*Cypronus carpio*). *J. Sci. Food Agric.* **2020**, *100*, 2305–2312.
38. Liu, M.; Wang, H.; Griffiths, M.W. Regulation of alkaline metalloprotease promoter by N-acyl homoserine lactone quorum sensing in Pseudomonas fluorescens: Protease promoter regulation by AHLs in *Pseudomonas fluorescens*. *J. Appl. Microbiol.* **2007**, *103*, 2174–2184.
39. Sobieszczańska, N.; Myszka, K.; Szwengiel, A.; Majcher, M.; Grygier, A.; Wolko, Ł. Tarragon essential oil as a source of bioactive compounds with anti-quorum sensing and anti-proteolytic activity against *Pseudomonas* spp. isolated from fish—in vitro, in silico and in situ approaches. *Int. J. Food Microbiol.* **2020**, *331*, 108732.

40. Christensen, A.B.; Riedel, K.; Eberl, L.; Flodgaard, L.R.; Molin, S.; Gram, L.; Givskov, M. Quorum-sensing-directed protein expression in *Serratia proteamaculans* B5a. *Microbiology* **2003**, *149*, 471–483.
41. Beven, C.-A.; Dieckelmann, M.; Beacham, I.R. A strain of *Pseudomonas fluorescens* with two lipase-encoding genes, one of which possibly encodes cytoplasmic lipolytic activity. *J. Appl. Microbiol.* **2001**, *90*, 979–987.
42. Woods, R.G.; Burger, M.; Beven, C.-A.; Beachman, I.R. The *apX-lipA* operon of *Pseuodmonas fluorescens* B_{52}: A molecular analysis of metalloprotease and lipase production. *Microbiology* **2001**, *147*, 345–354.
43. Riedel, K.; Hentzer, M.; Geisenberger, O.; Huber, B.; Steidle, A.; Wu, H.; Høiby, N.; Givskov, M.; Molin, S.; Eberl., L. *N*-Acylhomoserine-lactone-mediated communication between *Pseudomonas aeruginosa* and *Brukholderia cepacia* in mixed biofilms. *Microbiology* **2001**, *147*, 3249–3262.
44. Udine, C.; Brackman, G.; Bazzini, S.; Buroni, S.; Van Acker, H.; Pasca, M.R.; Riccardi, G.; Coenye, T. Phenotypic and genotypic characterization of *Brukholderia cenocepacia* J2315 mutants affected in homoserine lactone and diffusible signal factor-based quorum sensing system suggests interplay between both types systems. *PLoS ONE* **2013**, *8*, e55112.
45. Devescovi, G.; Bigirimana, A.; Degrassi, G.; Cabrio, L.; LiPuma, J.J.; Kim, J.; Hwang, I.; Venturi, V. Involvement of a quorum sensing –regulated lipase secreted by a clinical isolate of *Brukholderia glumae* in severe disease symptoms in rice. *Appl. Environ. Microbiol.* **2007**, *73*, 4950–4958.
46. Hall-Stoodley, L.; Costerton, J.W.; Stoodley, P. Bacterial biofilms: From the natural environment to infectious diseases. *Nat. Rev. Microbiol.* **2004**, *2*, 95–108.
47. Davies, D.G.; Parsek, M.R.; Pearson, J.P.; Iglewski, B.H.; Costerton, J.W.; Greenberg, E.P. The involvement of cell-to-cell signals in the development of a bacterial biofilm. *Science* **1998**, *280*, 295–298.
48. Daniels, R.; Vanderleyden, J.; Michiels, J. Quorum sensing and swarming migration in bacteria. *FEMS Microbiol. Rev.* **2004**, *28*, 261–289.
49. Vetrivel, A.; Ramasamy, M.; Vetrivel, P.; Natchimuthu, S.; Arnuachalam, S.; Kim, G.-S.; Murugesan, R. *Pseudomonas aeruginosa* biofilm formation and its control. *Biologics* **2021**, *1*, 312–336.
50. Pamp, S.J.; Tolker-Nielsen, T. Multiple roles of biosurfactants in structural biofilm development by *Pseudomonas aeruginosa*. *J. Bacteriol.* **2007**, *189*, 2531–2539.
51. Bai, A.J.; Vittal, R. Quorum sensing regulation and inhibition of exoenzyme production and biofilm formation in the food spoilage bacteria *Pseudomonas psychrophila* PSPF19. *Food Biotechnol*. **2014**, *28*, 293–308.
52. Myszka, K.; Sobieszczańska, N.; Olejnik, A.; Majcher, M.; Szwengiel, A.; Wolko, Ł.; Juzwa, W. Studies on the anti-proliferative and anti-quorum sensing potentials of *Myrtus communis* L. essential oil for the improved microbial stability of salmon-based products. *LWT* **2020**, *127*, 109380.
53. Guðbjörnsdóttir, B.; Einarsson, H.; Thorkelsson, G. Microbial adhesion to processing lines for fish filets and cooked shrimp: Influence of stainless steel surface finish and presence of gram-negative bacteria on the attachment of *Listeria monocytogenes*. *Food Technol. Biotechnol.* **2005**, *43*, 55–61.
54. Gopu, V.; Meena, C.K.; Shetty, P.H. Quercetin influences quorum sensing in food borne bacteria: In-vitro and in-silico evidence. *PLoS ONE* **2015**, *10*, e0134684.
55. Li, T.; Cui, F.; Bai, F.; Zhao, G.; Li, J. Involvement of Acylaated Homoserine Lactones (AHLs) of *Aeromonas sorbia* in spoilage of refrigerated turbot (*Scophthalmus maximus* L.). *Sensors* **2016**, *16*, 1083.
56. Alvarez-Ordóñez, A. New weapons to fight old enemies: Novel strategies for the (bio)control of bacterial biofilms in the food industry. *Front. Microbiol.* **2016**, *7*, 1641.
57. Utari, P.D.; Vogel, J.; Quax, W.J. Deciphering physiological functions of AHL quorum quenching acylases. *Front. Microbiol.* **2017**, *8*, 1123.
58. Teiber, J.F.; Horke, S.; Haines, D.C.; Chowdhary, P.K.; Xiao, J.; Kramer, G.L.; Haley, R.W.; Draganov, D.I. Dominant role of paraoxonases in inactivation of the *Pseudomonas aeruginosa* quorum-sensing signal *N*-(3-oxododecanoyl)-L-homoserine lactone. *Infect. Immun.* **2008**, *76*, 2512–2519.
59. Bergonzi, C.; Schwab, M.; Naik, T.; Elias, M. The structural determinants accounting for the board substrate specificity of the quorum quenching lactonase Gcl. *Chem. Bio. Chem.* **2019**, *20*, 1848–1855.
60. Rémy, B.; Plener, L.; Decloquement, P.; Armstrong, N.; Elias, M.; Daudé, D.; Chabrère, E. Lactonase specificity is key to quorum quenching in *Pseudomonas aeruginosa*. *Front. Microbiol.* **2020**, *11*, 762.
61. Huang, J.J.; Petersen, A.; Whiteley, M.; Leadbetter, J.R. Identification of QuiP, the product of gene PA1032, as the second acyl-homoserine lactone acylase of *Pseudomonas aeruginosa* PAO1. *Appl. Environ. Microbiol.* **2006**, *72*, 1190–1197.
62. Wahjudi, M.; Papaioannou, E.; Hendrawati, O.; van Assen, A.H.G.; van Merkerk, R.; Cool, R.H.; Poelarends, G.J.; Quax, W.J. PA0305 of *Pseudomonas aeruginosa* is a quorum quenching acylhomoserine lactone acylase belonging to the Ntn hydrolase superfamily. *Microbiology* **2011**, *157*, 2042–2055.
63. Chen, F.; Gao, Y.; Chen, X.; Yu, Z.; Li, X. Quorum quenching enzymes and their application in degrading signal molecules to block quorum sensing-dependent infection. *Int. J. Mol. Sci.* **2013**, *14*, 17477–17500.
64. Bijtenhoorn, P.; Mayerhofe, H.; Müller-Dieckman, J.; Utpatel, C.; Schippe, C.; Hornung, C.; Szesny, M.; Grond, S.; Thürmer, A.; Brzuszkiewicz, E.; et al. A novel metagenomics short-chain dehydrogenase/reductase attenuates *Pseudomonas aeruginosa* biofilm formation and virulence on *Caenorhabditis elegans*. *PLoS ONE* **2011**, *6*, e26278.

65. Hernando-Amado, S.; Alcalde-Rico, M.; Gil-Gil, T.; Valverde, J.R.; Martinez, J.I. Naringenin inhibition of the *Pseudomonas aeruginosa* quorum sensing response is based on its time-dependent competition with N-(3-oxo-dodecanoyl)-L-homoserine lactone for LasR binding. *Front. Mol. Biosci.* **2020**, *7*, 25.
66. Tomaś, N.; Myszka, K.; Wolko, Ł.; Nuc, K.; Szwengiel, A.; Grygier, A.; Majcher, M. Effect of black pepper essential oil on quorum sensing and efflux pump systems in the fish-borne spoiler *Pseudomonas psychrophila* KM02 identified by RNA-seq, RT-qPCR and molecular docking analyses. *Food Cont.* **2021**, *130*, 108284.
67. Klebe, G. *Drug Design: Methodology, Concepts, and Mode-of-Action*; Springer: Berlin/Heidelberg, Germany, 2003; p. 71.
68. Kumar, L.; Chhibber, S.; Kumar, R.; Kumar, M.; Harjai, K. Zingerone silences quorum sensing and attenuates virulence of *Pseudomonas aeruginosa*. *Fitoterapia* **2015**, *102*, 84–95.
69. Sepahi, E.; Tarighi, S.; Ahmadi, F.S.; Bagheri, A. Inhibition of quorum sensing in *Pseudomonas aeruginosa* by two herbal essential oils from *Apiaceae* family. *J. Microbiol.* **2015**, *53*, 176–180.
70. Kerekes, E.-B.; Deák, É.; Takó, M.; Tserennadmid, R.; Petkovits, T.; Vágvölgyi, C.; Krisch, J. Anti-biofilm forming and anti-quorum sensing activity of selected essential oils and their main components on food-related microorganisms. *J. Appl. Microbiol.* **2013**, *115*, 933–942.
71. Li, T.; Wang, D.; Liu, N.; Ma, Y.; Ding, T.; Mei, Y.; Li, J. Inhibition of quorum sensing-controlled virulence factors and biofilm formation in *Pseudomonas fluorescens* by cinnamaldehyde. *Int, J. Food Microbiol.* **2018**, *269*, 98–106.
72. Jakobsen, T.H.; van Gennip, M.; Phipps, R.K.; Shanmugham, M.S.; Christensen, L.D.; Alhede, M.; Skindersoe, M.E.; Rasmussen, T.B.; Friedrich, K.; Uthe, F.; et al. Ajoene, a sulfur-rich molecule from garlic, inhibits genes controlled by quorum sensing. *Antimicrob. Agents Chemother.* **2012**, *56*, 2314–2325.
73. Chatterjee, M.; D'Morris, S.; Paul, V.; Warrier, S.; Vasudevan, A.K.; Vanuopadath, M.; Nair, S.S.; Paul-Prasanth, B.; Mohan, C.G.; Biwas, R. Mechanistic understanding of phenyllactic acid mediated inhibition of quorum sensing and biofilm development in *Pseudomonas aeruginosa*. *Appl. Microbiol. Biotechnol.* **2017**, *101*, 8223–8236.
74. Paczkowski, J.E.; Mukherjee, S.; McCready, A.R.; Cong, J.P.; Aquino, C.J.; Kim, H.; Henke, B.R.; Smith, C.D.; Bassler, B.L. Flavonoids suppress *Pseudomonas aeruginosa* virulence through allosteric inhibition of quorum sensing receptors. *J. Biol. Chem.* **2017**, *292*, 4064–4076.
75. Zhu, J.; Zhang, Y.; Deng, J.; Jiang, H.; Zhuang, L.; Ye, W.; Ma, J.; Jiang, J.; Feng, L. Diketopiperazines synthesis gene in *Shewanella baltica* and roles of diketopiperazines and resveratrol in quorum sensing. *J. Agric. Food Chem.* **2019**, *67*, 12013–12025.
76. Myszka, K.; Olejnik, A.; Majcher, M.; Sobieszczańska, N.; Grygier, A.; Powierska-Czarny, J.; Rudzińska, M. Green pepper essential oil as a biopreservative agent for fish-based products: Antimicrobial and antivirulence activities against *Pseudomonas aeruginosa* KM01. *LWT* **2019**, *108*, 6–13.
77. Van Haute, S.; Raes, K.; Van der Meeren, P.; Sampers, I. The effect of cinnamon, oregano and thyme essential oils in marinade on the microbial shelf life of fish and meat products. *Food Control* **2016**, *68*, 30–39.
78. Eskandari, S.; Hosseini, H.; Gholamzadeh, M.; Mousavi Khaneghah, A.; Hosseini, E. The effects of black cumin, black caraway extracts and their combination on shelf life extension of silver carp (*Hypophthalmichthys molitrix*) during refrigerated storage. *J. Food Saf.* **2014**, *35*, 154–160.
79. Alvarez, M.V.; Ortega-Ramirez, L.A.; Gutierrez-Pacheco, M.M.; Bernal-Mercado, A.T.; Rodriguez-Garcia, I.; Gonzalez-Aguilar, G.A.; Ponce, A.; Moreira, M.; del Roura, S.I.; Ayala-Zavala, J.F. Oregano essential oil-pectin edible films as anti-quorum sensing and food antimicrobial agents. *Front. Microbiol.* **2014**, *5*, 699.
80. Farsanipour, A.; Khodanazary, A.; Hosseini, S.M. Effect of chitosan-whey protein isolated coatings incorporated with tarragon *Artemisia dracunculus* essential oil on the quality of *Scomberoides commersonnianus* fillets at refrigerated condition. *Int. J. Biol. Macromol.* **2020**, *155*, 766–771.
81. Xu, Y.; Wang, R.; Zhao, H.; Zhao, J.; Zhang, J.; Li, J. Effects of gelatin combined with essential oils coating on storage quality of turbot (Psetta maxima) fillets. In Proceedings of the 2017 6th International Conference on Measurement, Instrumentation and Automation (ICMIA 2017), Zhuhai, China, 29–30 June 2017.
82. Gui, M.; Zhang, Y.; Gao, L.; Li, P. Effect of AHL-lactonase and nisin on microbiological, chemical and sensory quality of vacuum packaged sturgeon storage at 4 °C. *Int. J. Food Prop.* **2021**, *24*, 222–232.

International Journal of Food Microbiology 331 (2020) 108732

Contents lists available at ScienceDirect

International Journal of Food Microbiology

journal homepage: www.elsevier.com/locate/ijfoodmicro

Tarragon essential oil as a source of bioactive compounds with anti-*quorum sensing* and anti-proteolytic activity against *Pseudomonas* spp. isolated from fish – *in vitro*, *in silico* and *in situ* approaches

Natalia Sobieszczańska[a,*], Kamila Myszka[a], Artur Szwengiel[b], Małgorzata Majcher[c], Anna Grygier[c], Łukasz Wolko[d]

[a] Department of Biotechnology and Food Microbiology, Poznan University of Life Sciences, Wojska Polskiego 48, 60-637 Poznan, Poland
[b] Department of Fermentation and Biosynthesis, Poznan University of Life Sciences, Wojska Polskiego 31, 60-637 Poznan, Poland
[c] Department of Food Chemistry and Instrumental Analysis, Poznan University of Life Sciences, Wojska Polskiego 31, 60-637 Poznan, Poland
[d] Department of Biochemistry and Biotechnology, Poznan University of Life Sciences, Dojazd 11, 60-632 Poznan, Poland

ARTICLE INFO

Keywords:
Food spoilage
Molecular docking
Autoinductors
Gene expression
subMIC

ABSTRACT

The present study aimed to evaluate the anti-*quorum sensing* (anti-QS) and anti-proteolytic potentials of tarragon essential oil (TEO) and its major compounds against food-associated *Pseudomonas* spp. The activities were verified by *in vitro*, *in silico* and *in situ* approaches. In this work, methyl eugenol (ME)- and β-phellandrene (β-PH)-rich TEO was investigated. TEO at subMIC increased the percentage of saturated fatty acids in the bacterial membranes (from 7 to 22%) and exhibited anti-*quorum sensing via* decreasing the efficiency of QS autoinducer synthesis [3-oxo-C12-HSL (from 2.028 μg/mL to < LOD), C4-HSL (from 1.312 μg/mL to < LOD) and PQS (from 0.007625 μg/mL to < LOD)]. ME and β-PH were docked into LasR, RhlR and PqsR proteins, with docking scores comparable to native autoinductors. The subMICs of TEO, ME and β-PH decreased the proteolysis in the examined bacteria by 33, 29, and 21% (in TSB medium) and by 29, 26, and 19% (in fish juice medium), respectively. Almost all genes encoding proteases were downregulated by the applied agents. The ME- and β-PH-rich TEO acts as an anti-QS agent and significantly suppresses the proteolytic activity of food-associated pseudomonads. It might therefore increase the quality of fish-based products, where *Pseudomonas* spp. predominate.

1. Introduction

Cold-resistant *Pseudomonas* spp. are considered one of the specific spoilage organisms (SSOs) of fresh and/or aerobically stored refrigerated fish-based products (Caldera et al., 2016; Zhang et al., 2019). High water activity, high *post mortem* pH (> 6), and large amounts of easily assimilated proteins of seafoods significantly promote pseudomonads growth, leading to decreased organoleptic properties of products. In fish muscles, *Pseudomonas* spp. secrete metallopeptidases that hydrolyze proteins and cause the formation of unpleasant odors and flavors (Liu et al., 2006). These activities result in unacceptance by consumers and lead to economic loss of food producers (Sterniša et al., 2019).

The production and secretion of metallopeptidases by *Pseudomonas* spp. can be regulated by the *quorum sensing* (QS) mechanism. In that system, small signal molecules (autoinducers), followed by interaction with cognate receptor proteins cause a coordinated regulation of specific gene expression (Papenfort and Bassler, 2016). The QS of pseudomonads consists of four hierarchically functioning autoinducer synthesis/transcriptional receptor protein combinations (LasI/R, RhlI/R, PQS-controlled system and IQS system) involving signal molecules belonging to acyl-homoserine lactones (AHLs) and quinolone (PQS) groups (Lee and Zhang, 2015).

The blocking of the QS system can be regarded as a new preservation technique for seafoods (Truchado et al., 2015). To date, various methods of QS attenuation have been proposed, but the exploitation of natural plant-derived essential oils (EOs) as sources of QS inhibitors (QSIs) meets only the requirements of modern consumers, pending seafoods without synthetic preservatives (Calo et al., 2015). QSIs are structural analogs of QS autoinducers that disrupt the QS mechanism by interacting with cognate receptor proteins (Kalia, 2013). However, to date, such studies are very rare. The true prediction of the potential interaction between a bioactive molecule (ligand) from EO and the target bacterial QS receptor should be conducted only at the atomic

* Corresponding author.
E-mail address: natalia.sobieszczanska@up.poznan.pl (N. Sobieszczańska).

https://doi.org/10.1016/j.ijfoodmicro.2020.108732
Received 20 December 2019; Received in revised form 26 May 2020; Accepted 3 June 2020
Available online 05 June 2020

level, truly estimating the docking score for the generated complex (Friesner et al., 2006).

The potential source of pseudomonad QSIs might be tarragon (*Artemisia dracunculus* L.) EO (TEO). (Mokhetho et al., 2018). However, in the available literature, there is a lack of detailed knowledge explaining the molecular mechanism of this process (Skandamis and Nychas, 2012), especially towards SSOs of seafoods. The fish-based products, where tarragon leaves were used for flavoring purposes, exhibited high quality in general (Lopes-Lutz et al., 2008).

This study aimed to investigate the impact of the subinhibitory concentration (subMIC) of TEO and its major compounds on the QS system and proteolytic activity of *P. psychrophila* KM02, *P. orientalis* KM249 and *P. fluorescens* KM148. The strains isolated from commercially available fish-based products were used. We hypothesized that *(i)* subMICs of TEO and its major compounds alter QS-autoinducer synthesis; *(ii)* TEO major compounds competitively bind to QS receptors; *(iii)* subMICs of TEO and its major compounds significantly decrease proteolytic activity; and *(iv)* downregulation of the expression levels of genes encoding metalloproteases would be observed. Finally, to establish the effects of the analyzed compounds *in situ*, the proteolytic activity and gene expression were also evaluated in a fish-based model product.

2. Materials and methods

2.1. Tarragon essential oil extraction and identification of compounds

EOs were extracted from dried leaves of tarragon (*Artemisia dracunculus* L.) from Spain by hydro distillation in a Clevenger-type apparatus. The compounds were further identified using a Hewlett-Packard HP 7890A gas chromatograph instrument coupled to a 5975C mass spectrometer (Agilent Technologies, U.S.A.) as described in our previous study (Myszka et al., 2019). Mass spectra were obtained at 70 eV over the mass scanning range 33–350 *m/z*. TEO compounds were identified by comparing the peak retention indices (RI) and mass spectra with those of the standards of homologous series of n-alkanes (C7–C24) under the same operating conditions. The relative percentages of the constituents were calculated based on gas chromatography peak areas relative to the total essential oil.

2.2. Microorganisms and culture conditions

The *P. psychrophila*, *P. orientalis, and P. fluorescens* were isolated from commercially available fresh salmon (*Salmo salar*) fillets and deposited in the culture collection (culture deposition number: *Pseudomonas psychrophila* KM02, *Pseudomonas orientalis* KM249, *Pseudomonas fluorescens* KM148) at the Department of Biotechnology and Food Microbiology at the Poznan University of Life Sciences. Sequencing and analysis of restriction length polymorphisms of 16S rRNA gene amplicons were employed for its identification. The strains were preserved in cryovials (Medical Wire & Equipment, Corsham, UK) and stored at −80 °C.

The strains were revived as needed and cultured in tryptic soy broth (TSB) (BD Biosciences, USA) supplemented with selected concentrations of TEO and its major compounds. The incubation was carried out at 4 ± 2 °C for 72 h. The pH of the media was 7.0.

2.3. SubMIC determination

A broth macro dilution method according to Clinical and Laboratory Standards Institute (2012) was employed to evaluate the subMIC of TEO and major compounds against analyzed microorganisms. The turbidity of the culture suspensions was adjusted with sterile saline to an equivalent of 0.5 McFarland standard. TEO and its major compounds were diluted in dimethyl sulfoxide (DMSO) (Sigma-Aldrich, USA) to obtain a range of different concentrations. Uninoculated TSB media with and without TEO, ME (methyl eugenol) and β-PH (β-phellandrene) served as the controls. Samples were tested visually after a 72-h incubation at 4 °C. The concentrations that resulted in no significant growth inhibition were selected as subMIC for further experiments.

2.4. Cellular fatty acid methyl ester (FAME) determination

The effects of subMIC concentrations of TEO on the FAME profile of *P. psychrophila* KM02, *P. orientalis* KM249 and *P. fluorescens* KM148 were examined by GC-FID analysis according to the procedure described by Myszka et al., 2019. For separation and identification of FAMEs, the Trace 1300 system (Thermo Fisher Scientific, Waltham, MA, USA) with a 30 m × 0.25 mm × 0.25 μm column (HP-5MS; Agilent Technologies) and a flame ionization detector were used. Particular fatty acids (FAs) were identified by comparing the peak retention time (Rt) with the Bacterial Acid Methyl Esters Mix standard (Sigma-Aldrich, USA). The abundance of individual FAs was shown as a percentage of the total detected FAs.

2.5. QS autoinducers estimation

The procedure employed by Ravn et al. (2001) was used for the extraction of AHLs and alkyl quinolone molecules (HHQ and PQS). Briefly, cultures were centrifuged (3000 *g*, 10 min) and supernatants were passed through a Millex-GP 0.22-μm filter (Merck, Germany). The cell-free supernatants were treated twice with an equal volume of ethyl acetate (Sigma-Aldrich, USA) acidified with 0.5% formic acid (Sigma-Aldrich, USA). The extracts were evaporated to dryness and stored at −20 °C. The profile of AHLs and alkyl quinolone molecules: 2-Heptyl-3-hydroxy-4(1H)-quinolone (PQS) and 2-heptyl-4-quinolone (HHQ) were determined using reversed phase (RP) ultrahigh-performance liquid chromatography (Dionex UltiMate 3000 UHPLC, Thermo Fisher Scientific, Sunnyvale, CA, USA) with an ultrahigh-resolution orthogonal quadrupole time of flight (qTOF) mass spectrometer (maXis impact, Bruker Daltonik, Bremen, Germany) with an ESI source (ESI-MS), according to our previous study (Myszka et al., 2020).

The AHLs, HHQ and PQS were identified by comparing their retention times with those of the standards and based on molecular mass information from the MS detector or using MS and MS/MS data. The tandem mass spectrometric data (MS/MS) were carried out for searching molecular structure using two computational methods: CSI:FingerID, which combines fragmentation tree computation and machine learning (Shen et al., 2014) and the *in silico* fragmenter MetFrag (Ruttkies et al., 2016).

Quantitative analyses were conducted with calibration samples prepared in methanol as a surrogate matrix. The limit of detection (LOD, S/N < 3) for N-[(*RS*)-3-hydroxybutyryl]-HSL and C4-HSL was 0.040 μg/mL; for 3-oxo-C8-HSL, 3-oxo-C12-HSL, and 3-oxo-C14-HSL, it was 0.005 μg/mL. The limits of detection (LOD, S/N > 3) for HHQ and PQS were 0.0002 and 0.0001 μg/mL, respectively.

2.6. Molecular docking analysis

The crystallographic structures of the QS receptor proteins LasR (PDB ID: 2UV0) and PqsR (PDB ID: 4JVI) were imported from the RCSB Protein Data Bank (PDB) in Schrödinger Maestro software (Schrödinger LLC, New York, 2018). Due to the inaccessibility of the crystal structure of the RhR protein, the sequence was downloaded from the UniProt database (ID: P54292); subsequently, the protein was modeled and validated using the I-Tasser webserver (Roy et al., 2010).

All protein structures were prepared in Protein Preparation Wizard (Sastry et al., 2013) in the Schrodinger software suite: the bond orders were assigned, hydrogens were added, zero-order bonds to metals and disulfide bonds were created, followed by assigning missing side chains and setting up the pH value at 7 ± 2. Water molecules were removed (> 5.00 Å radius), and hydrogen bonds were optimized using sample

orientations. Finally, the OPLS3e force field (Harder et al., 2016) was used for restrained minimization to the default root mean square deviation (RMSD) value of 0.30 Å.

The three-dimensional structures of ME (CID:7127), β-PH (CID:11142) and the autoinducers 3-oxo-C12-HSL (CID:3246941), C4-HSL (CID:10130163), and PQS (CID:2763159) were retrieved in SD format from the PubChem database and processed in Ligand Preparation Panel (LigPrep, Schrödinger LLC, New York).

The molecular docking studies were conducted in Glide Ligand Docking Panel, version 11.7 (Glide, Schrödinger, LLC, New York, 2018) in the Schrödinger Maestro suite using Extra Precision mode (XP) (Friesner et al., 2006). Initially, the docking grids were generated in the receptor active sites of the LasR and PqsR proteins, whereas for RhlR protein, the sitemap was used. The ligands were flexible sampled on defined receptor grids. The constraints on ligand-receptor interactions were not set.

2.7. Proteolytic activity evaluation

Proteolytic activity after treatment with subMICs of TEO and its major compounds was examined according to the method described by Polychroniadou (1988), with modifications. Briefly, 1 mL of *P. psychrophila* KM02, *P. orientalis* KM249 and *P. fluorescens* KM148 cultures (concentrations of 10^8 CFU/mL) were centrifuged (3000 *g*, 10 min, 4 °C). Next, 0.5 mL of supernatant was mixed with 0.5 mL of borate buffer (0.1 M $Na_2B_4O_7$ in 0.1 M NaOH, pH 9.5) and 1 mL (1 mg/mL) of TNBS reagent (2,4,6-trinitrobenzenesulfonic acid) (Sigma-Aldrich, USA). Samples were then incubated at 37 °C for 60 min. The reaction was stopped with 2 mL of 0.1 M NaH_2PO_4 containing 1.5 mM Na_2SO_3. The sample prepared with 0.5 mL of H_2O served as the control probe.

The degree of protein hydrolysis was determined based on the released α-amino groups reacting with the TNBS reagent, which resulted in yellow-orange color development. The difference in its intensity was measured at 420 nm on a SPECORD® 205 UV-VIS spectrophotometer (Analytic Jena, Germany) and presented as the percentage inhibition (% PI) of proteolytic activity according to the following equation:

$$\%PI = 100 - \left(\frac{A_t}{A_c} * 100\right)$$

where:

A_t – absorbance value obtained for the sample with the given treatment

A_c – absorbance value obtained for the control sample (cells cultivated only in TSB medium)

2.8. RNA isolation and cDNA synthesis

The cultures were treated with the RNAprotect® Bacteria Reagent (Qiagen, Germany). Total RNA was isolated on a PureLink™ RNA Mini Kit (Thermo Fisher Scientific, USA) and purified using the PureLink™ DNase Set (Invitrogen, USA) according to the manufacturer's protocols. The quantity and quality of isolated RNA were analyzed by fluorescence-based Qubit™ XR RNA and Qubit™ IQ RNA Assay Kits (Thermo Fisher Scientific, USA) on a Qubit Fluorometer 4 (Invitrogen, USA). The first strand of + cDNA was synthesized from 1.0 µg of total RNA with the High Capacity RNA-to-cDNA Kit (Life Technologies, USA).

2.9. Quantitative Real-Time PCR experiment

The RT-qPCR analyses were performed in Stratagene Mx3005P (Applied Biosystems, USA) using the GoTaq® Master Mix (Promega, Germany). The primers used in the study are listed in Table 1. Primers were designed using the CLC Genomics Workbench (Qiagen, USA) based on the genome sequence of *Pseudomonas psychrophila* KM02 (GenBank accession no: CP049044). The whole-genome sequencing was outsourced in laboratory specialized in NGS (Genomed S.A., Warsaw). The specificity of primers was confirmed by PCR analysis using a Bio-Rad thermocycler and capillary electrophoresis of amplicons on a QIAxcel Advanced system (Qiagen, USA). In RT-qPCR analyses, the 16S rRNA gene was used as a reference gene. The cycling conditions were as follows: initial denaturation at 95 °C for 2 min and 45 cycles of denaturation at 95 °C for 15 s, annealing and extension at 58 °C for 1 min. The melting curve was also applied.

Table 1
Primers for RT-qPCR analysis.

Gene	Primer	Sequence (5′-3′)	Tm [°C]	Size [bp]
Housekeeping gene				
16S rRNA	Forward	AGAGTTTGATCMTGGCTCAG	52	1500
	Reverse	CGGTTACCTTGTTACGACTT		
Proteases				
M16–1	Forward	TGCCCTTGATCGTAACAG	54	130
	Reverse	TGAAAAGTCATCCAGCCC		
M16–2	Forward	GCAACTGTTCACCGAGAT	55	114
	Reverse	CGAGAATGTGGGGTTTCC		
M16–3	Forward	GCGAAATCATCAAAAACGAG	54	127
	Reverse	TGCATCCACCCGATTATC		
M22–1	Forward	CGTGCCTACCGAGATTGA	56	112
	Reverse	CGGAATACCCCAGGCAAA		
M3–2	Forward	GCTTTGCCCTTGATCGTA	55	132
	Reverse	AAAAGTCATCCAGCCCCA		
S11_3	Forward	TATCGTCATCGACTCAGG	51	134
	Reverse	GGTTCATAAAGTGGGTGT		

The impact of subMICs of TEO and its major compounds on the changes in the expression of genes encoding proteases (gene of interest = GOI) in food-related pseudomonads were calculated according to the Pfaffl method (Pfaffl, 2001). The efficiency of a particular amplicon group was estimated using LinRegPCR software (Ruijter et al., 2009). The results are presented as the ratio of gene expression in treated samples in relation to control samples (with expression equal to 1), normalized to the internal reference gene, according to the following equation:

$$ratio = \frac{E_{GOI}{}^{\Delta C_{t\ target}\ (control-sample)}}{E_{ref.}{}^{\Delta C_{t\ ref}\ (control-sample)}}$$

2.10. In situ fish-based model analysis

To study the inhibition attribute of subMICs of TEO and its major compounds on the food-related pseudomonads QS phenotype in fish-based model conditions, the fish juice media was developed according to a modified methodology of Dalgaard (1995). Briefly, 1000 g of fresh salmon fillets were dissolved in 500 mL of tap water and homogenized in a laboratory Stomacher. To separate the solids, the mixture was pressed through two layers of gauze and subsequently through paper filters. Fish juice was supplemented with 0.10 M phosphate buffer, 0.065 M H_2KPO_4, and 0.044 M HK_2PO_4. The pH value was adjusted to 6.6. Subsequently, fish juice was sterilized at 121 °C for 15 min, cooled and enriched with TMAO (1.6 g/L), L-cysteine (40 mg/L), and L-methionine (40 mg/L). Finally, 1 mL of fish juice aliquots was inoculated with 100 µL of bacterial cultures (10^8 CFU/mL) and supplemented with subMICs of TEO and its major compounds. After 72 h of incubation at 4 ± 2 °C, proteolytic activity and gene expression studies were performed as previously indicated.

2.11. Statistical analysis

The experiments were performed in triplicate, and the results are expressed as the mean ± standard deviation. To assess the differences between each class of FA in each strain, Student's *t*-test in Statistica

Table 2
GC/MS results of TEO composition with relative percentage values of individual compounds.

Compound	RI - Wax	RI - DB-5	[%] Composition
Alpha-pinene	1035	939	1.8
Alpha-terpinene	1184	1015	0.5
Limonene	1208	1030	1.2
1,8-Cineole (eucalyptol)	1222	1031	1.5
Beta ocimene E	1235	1041	3.5
Beta-phellandrene	1245	1042	19.3
Gama-terpinene	1249	1072	0.9
Beta ocimene Z	1250	1051	8.8
Beta-caryophyllene	1594	1414	0.9
Terpinen-4-ol	1606	1180	3.0
Methyl chavicol	1657	1199	1.1
Germacrene	1705	1487	0.8
Geranyl acetate	1761	1384	1.2
Elemicin	1862	1514	14.4
Isoelemicin	1944	1596	11.3
Methyl eugenol	2001	1404	24.5
Spathulenol	2108	1578	1.8
Thymol	2179	1283	1.7
Methyl isoeugenol	2188	1491	1.8

[%] Composition of individual compound were calculated from the chromatogram obtained in triplicate on the Supelcowax 10 column (normalized peak area %). Values in bold indicate the most abundant compounds. RI – Wax – retention index on Suplecowax 10 column. RI – DB-5 – retention index on DB-5 column.

software (Statsoft, Inc. 2012) was applied. Significant differences ($p < 0.05$) in proteolytic activity inhibition were established by two-way analysis of variance (ANOVA) followed by *post hoc* Tukey's test in R software (R Core Team, 2015).

3. Results

3.1. Chemical composition of TEO

The GC/MS results of the chemical composition of TEO and the relative percentage of 19 identified compounds are presented in Table 2. The major compounds, comprising > 15% of the total TEO volume, were methyl eugenol (ME) (24.5%) and β-phellandrene (β-PH) (19.3%). Elemicin, isoelemicin and β-ocimene-Z were present in minority, ranging from 14.4 to 8.8% of TEO. The remaining compounds occurred in trace amounts (< 4%). According to the chemical classification of individual TEO constituents, groups of monoterpenes (*e.g.*, β-PH), phenol and benzene derivatives (ME) were dominant in TEO and accounted for 42.5%, 26.8% and 26.3%, respectively.

3.2. MIC

To determine the antimicrobial effect of the selected dilutions of TEO, ME and β-PH against *P. psychrophila* KM02, *P. orientalis* KM249, and *P. fluorescens* KM148 the biomass buildup levels were evaluated (data not shown). In this work, concentrations below the sub-MIC of TEO (75.0 μL/mL for *P. psychrophila* KM02 and *P. fluorescens* KM148; 70.0 μL/mL for *P. orientalis* KM249), the sub-MIC of ME (10.0 μL/mL for *P. psychrophila* KM02; 12.0 μL/mL for *P. orientalis* KM249 and *P. fluorescens* KM148), and the sub-MIC of β-PH (8.0 μL/mL for *P. psychrophila* KM02 and *P. fluorescens* KM148 was; 10 μL/mL for *P. orientalis* KM249) were selected for further experiments.

3.3. Effect of the subMIC of TEO on the FAME profile of Pseudomonas spp.

The changes in membrane lipid composition were investigated using GC/MS analysis. The cellular FAME profiles of the *P psychrophila* KM02, *P. orientalis* KM249 and *P. fluorescens* KM148 cultivated in TSB medium and in the presence of the subMIC of TEO are shown in Table 3. Accordingly, 12 different fatty acid methyl esters were identified and calculated as a percentage of the total membrane lipid composition in analyzed microorganisms. In contrast to treated cells, in which 2-hydroxydodecanoic acid (2-OH C12) was present at a level of 8.3% (in *P. psychrophila* KM02), 6.9% (in *P. orientalis*), and 11.0% (in *P. fluorescens*), it was not detected in control samples.

In terms of *P. psychrophila* KM02, the 3-hydroxybutanoic acid (3-OH C14) and 9,12-octadecadienoic acid (C18:2 cis) were the majority and together accounted for > 50% (control cells) and 40% (treated cells) of the total fatty acids. However, a decrease in the level of 3-OH-C14 upon treatment with TEO was observed; thus, the overall level of fatty acids with hydroxyl groups remained constant and did not differ significantly (Fig. 1A). Conversely, the growth of *P. psychrophila* KM02 in the presence of the subMIC of TEO induced an increase in the level of butanoic acid (C12) (from 1.8 to 7.7%) and hexadecanoic acid (C16) (from 3.3 to 7.3%), resulting in a significant ($p < 0.05$) increase in the level of saturated fatty acids (SFA) upon treatment with the subMIC of TEO (Fig. 1A). Simultaneously, the content of the sum of unsaturated fatty acids (UFA) slightly decreased. The significant alteration concerned the sum of the branched fatty acids (Ante-C15 and Iso−C17), whose level decreased from 10.1 to 4.9% after incubation with the subMIC of TEO (Fig. 1A).

The major fatty acids in *P. orientalis* KM249 cultivated in TSB medium were C18:2 *cis*-9.12 and C19:0 *cyc*, the levels of which after treatment with subMIC of TEO decreased from 32.9 to 11.7% and from 16.2 to 4.4%, respectively. Such modifications affected the overall changes in the levels of particular groups of fatty acids: significant decreases in UFA (approximately 33%) and cyclopropane fatty acids (CFA) (approximately 61%) were observed and were coupled with an increase in SFA (approximately 67%) (Fig. 1B). In contrast to *P. psychrophila* KM02, the significant alterations also concerned fatty acids with hydroxyl groups, mostly as the result of increased 3-OH-C14:0 levels.

The treatment of *P. fluorescens* KM148 with subMIC of TEO did not result in significant changes between UFA and SFA as observed in previous microorganisms. In both culture conditions, the C16:1 *cis*-9 and C18:2 *cis*-9.12 belonging to UFA were in the majority. The most considerable variations concerned hydroxyl fatty acids, the levels of which increased from 6.4 to 27.3% (Fig. 1C). Simultaneously, significant decreases in cyclopropane and branched fatty acids were observed.

3.4. Effect of the subMICs of TEO, ME and β-PH on Pseudomonas spp. QS autoinducer synthesis

The effects of the subMICs of TEO, ME and β-PH on *P. psychrophila* KM02, *P. orientalis* KM249, and *P. fluorescens* KM148 QS autoinducer synthesis were examined by the RP-UHPLC-ESI-MS system. The reduction and/or lack of particular AHLs and alkyl quinolone molecules in the cultures incubated in media supplemented with the subMICs of TEO, ME and β-PH confirmed the anti-QS activity of the investigated agents (Table 4).

In extracts from *P. psychrophila* KM0 and *P. fluorescens* reference samples, 7 different AHLs (3-oxo-C12-HSL, 3-oxo-C14-HSL, 3-oxo-C6-HSL, 3-oxo-C8-HSL, C12-HSL, C4-HSL, C6-HSL) and one quinolone molecule (PQS) were detected. Among the AHLs, 3-oxo-C12-HSL and C4-HSL were the most important, as their concentrations in control samples were 1.908 (± 0.031) μg/mL and 1.217 (± 0.010) μg/mL, respectively. Moreover, in control samples, the PQS concentration was 0.0076 (± 3.5E−05) μg/mL and was decreased by approximately 95% after treatment with TEO and ME. HHQ molecules were not detected in any of the samples.

Table 3
Profile of cellular fatty acids of examined *Pseudomonas* spp. cultivated in presence of subMIC of TEO.

fatty acid	[%] Composition (± SD) of FAs under different growth conditions					
	Pseudomonas psychrophila KM02		Pseudomonas orientalis KM249		*Pseudomonas fluorescens* KM148	
	TSB medium	TSB + subMIC of TEO	TSB medium	TSB + subMIC of TEO	TSB medium	TSB + subMIC of TEO
C12:0	1.8 (± 0.4)	7.7 (± 0.6)	1.8 (± 0.2)	5.5 (± 0.5)	5.7 (± 0.6)	6.4 (± 1.5)
2-OH-C12:0	ND	8.3 (± 1.4)	ND	6.9 (± 0.2)	ND	11.0 (± 1.8)
C14:0	2.3 (± 0.3)	3.3 (± 0.7)	2.0 (± 0.4)	4.7 (± 0.6)	2.1 (± 0.3)	4.6 (± 1.1)
Ante-C15:0	4.0 (± 0.1)	2.0 (± 1.0)	1.0 (± 0.9)	1.3 (± 0.4)	3.7 (± 0.3)	2.1 (± 0.4)
3-OH-C14:0	30.8 (± 21)	21.7 (± 0.7)	15.9 (± 1.8)	22.6 (± 1.2)	6.4 (± 0.8)	16.3 (± 2.4)
C16:1 *cis*-9	7.5 (± 1.2)	13.2 (± 2.2)	14.4 (± 1.2)	15.6 (± 1.0)	21.9 (± 1.3)	19.5 (± 2.6)
C16:0	3.3 (± 0.7)	7.3 (± 0.4)	3.5 (± 0.4)	11.9 (± 0.8)	13.9 (± 0.5)	9.2 (± 2.7)
Iso-C17:0	6.1 (± 0.3)	2.9 (± 0.4)	1.8 (± 0.1)	2.7 (± 0.5)	5.7 (± 0.8)	2.1 (± 0.7)
C17:0 *cyc*	1.4 (± 0.2)	2.2 (± 0.5)	1.8 (± 0.2)	2.5 (± 0.2)	6.8 (± 0.4)	2.7 (± 0.7)
C18:2 *cis*-9.12	24.5 (± 1.0)	20.6 (± 1.2)	32.9 (± 2.4)	11.7 (± 0.8)	22.8 (± 1.2)	17.9 (± 2.9)
C18:1 *trans*-9	13.8 (± 0.7)	7.2 (± 1.1)	8.8 (± 2.2)	10.3 (± 0.7)	5.7 (± 0.9)	6.6 (± 3.2)
C19:0 *cyc*	4.5 (± 0.6)	3.7 (± 0.6)	16.2 (± 2.5)	4.4 (± 0.7)	5.5 (± 0.6)	1.6 (± 0.5)
Total	100.0	100.0	100.0	100.0	100.0	100.0

[%] Composition of particular FA was calculated as a mean percentage value (± SD) of total FAs from chromatograph obtained in triplicate. ND – not detected.

3.5. Interactions of the main TEO components with Pseudomonas spp. QS receptor proteins

To evaluate the anti-QS activity of the TEO main components, molecular docking studies were employed. This computational analysis provided insight into the binding affinity of the TEO major compounds (ME, β-PH) and native autoinducers (3-oxo-C12-HSL, C4-HSL, and PQS) with the corresponding QS-transcriptional regulatory proteins. All compounds were successfully docked to the LasR, RhlR and PqsR proteins in Glide (Schrödinger, LLC, New York, 2018). The docking Glide results for a particular complex and the detailed characterization of bonding interactions are presented in Tables 5 and 6, respectively. Two- and three-dimensional structures of ligand-protein interactions are shown in Figs. 2 to 4.

For LasR protein, the highest docking score (−9.750 kcal/mol) and Glide energy (−60.513 kcal/mol) were for the native autoinducer 3-oxo-C12-HSL. As shown in Fig. 2A, it formed a stable complex with LasR protein, particularly by 4 hydrogen bonds with the TYR56, TRP60, ASP73 and ARG61 residues. In the case of the LasR-ME complex with a docking score of −6.145 kcal/mol, the same residues were involved in the interaction. The aromatic group of ME showed π-π interactions with TYR56 (Fig. 2B). β-PH performed no hydrogen bonding with the LasR active site; only hydrophobic interactions with common surrounding residues, such as VAL76, ALA127, LEU125, LEU36, and LEU39, were observed (Fig. 2C).

In contrast to the LasR docking results, β-PH exhibited the highest binding energy (−6.566 kcal/mol) when bound to the RhlR protein (Fig. 3C), and it was even greater than the native autoinducer C4-HSL (−5.990 kcal/mol), which created one hydrogen bond with TRP68 (Fig. 3A). This residue was also involved in forming a hydrogen bond with the oxygen of ME (Fig. 3B). All docked ligands engaged in hydrophobic interactions with RhlR residues as follows: LEU69, TYR72, and TYR77. Additionally, as it is shown in the Fig. 3, ASP81, a negatively charged residue, was also in surrounding of docked ligands, which indicated the occupation of the same active site of RhlR receptor.

Molecular docking analyses with PqsR revealed the highest docking score for the native autoinducer (−7.772 kcal/mol), which formed one hydrogen bond with LEU207 at a distance of 1.73 Å (Table 6) and interacted with hydrophobic residues of LEU208, ILE236, ALA237, and PRO238. (Fig. 4A). Although the docking score of ME was only −4.921 kcal/mol, the complex with PqsR protein was stabilized by a high van der Waals energy value (Table 5), and the same residues were involved in the binding (Fig. 4B). β-PH showed a docking score on the level of −5.263 kcal/mol and hydrophobically interacted with ILE263, ILE236, TRP234 and TYR258 residues. Additionally, only this compound was in contact with the negatively charged residues of GLU256 and GLU259, which differentiated it from the other docked ligands.

3.6. Effect of the subMICs of TEO, ME and β-PH on Pseudomonas spp. proteolytic activity

The changes in the proteolytic activity of *P. psychrophila* KM02, *P. orientalis* KM249, and *P. fluorescens* KM148 by the subMICs of TEO, ME, and β-PH were investigated by spectrophotometric analysis with TNBS reagent. The percentages of inhibition of the proteolysis after treatment with subMICs of TEO, ME and β-PH are presented in Fig. 5.

As shown, all of the applied treatments considerably ($p < 0.05$) decreased the proteolytic activity of *Pseudomonas* spp. cells, but the extent varied according to the type of treatment and the variant of experiment. The highest reduction was observed for *P. fluorescens* KM148 treated with TEO applied in TSB medium (32.5%), while the β-PH treatment had the lowest inhibitory effect on *P. psychrophila* KM02 proteolytic activity when cultured in fish juice medium (16.0%). The overall results for *in situ* conditions were significantly lower ($p < 0.05$) than those obtained *in vitro*, except for TEO in *P. psychrophila* KM02, and for β-PH in *P. fluorescens* KM148. DMSO, as the solvent of the analyzed compounds, did not influence the proteolytic activity (data not shown), confirming the effectiveness of TEO, ME and β-PH in proteolytic activity inhibition.

3.7. Effect of the subMICs of TEO, ME and β-PH on Pseudomonas spp. gene expression levels

The effect on the expression of genes encoding proteases in the *P. psychrophila* KM02, *P. orientalis* KM249 and *P. fluorescens* KM148 was evaluated by RT-qPCR. The transcriptional levels of M16_1, M16_2, M16_3, M22_1, M3_2, and S11_3 were normalized to the non-differentially expressed reference gene 16S RNA and were calculated as the ratio of expression (expression in control cultures equaled 1). The results for *in vitro* (TSB medium) and *in situ* (fish juice medium) conditions are presented in Figs. 6 and 7, respectively. As shown, the gene expression was altered divergently, but most of the genes were downregulated by the applied treatments.

Compared to the mRNA isolated from *P. psychrophila* KM02 (A) cells cultivated in TSB medium (control), the highest reduction was observed for the M16_2 and M16_3 genes after treatment with the subMIC of TEO (75% and 73%, respectively). ME applied to TSB medium decreased the expression of all analyzed genes at least by 50%. The last analyzed compound, β-PH, downregulated all of the proteases, but the mean

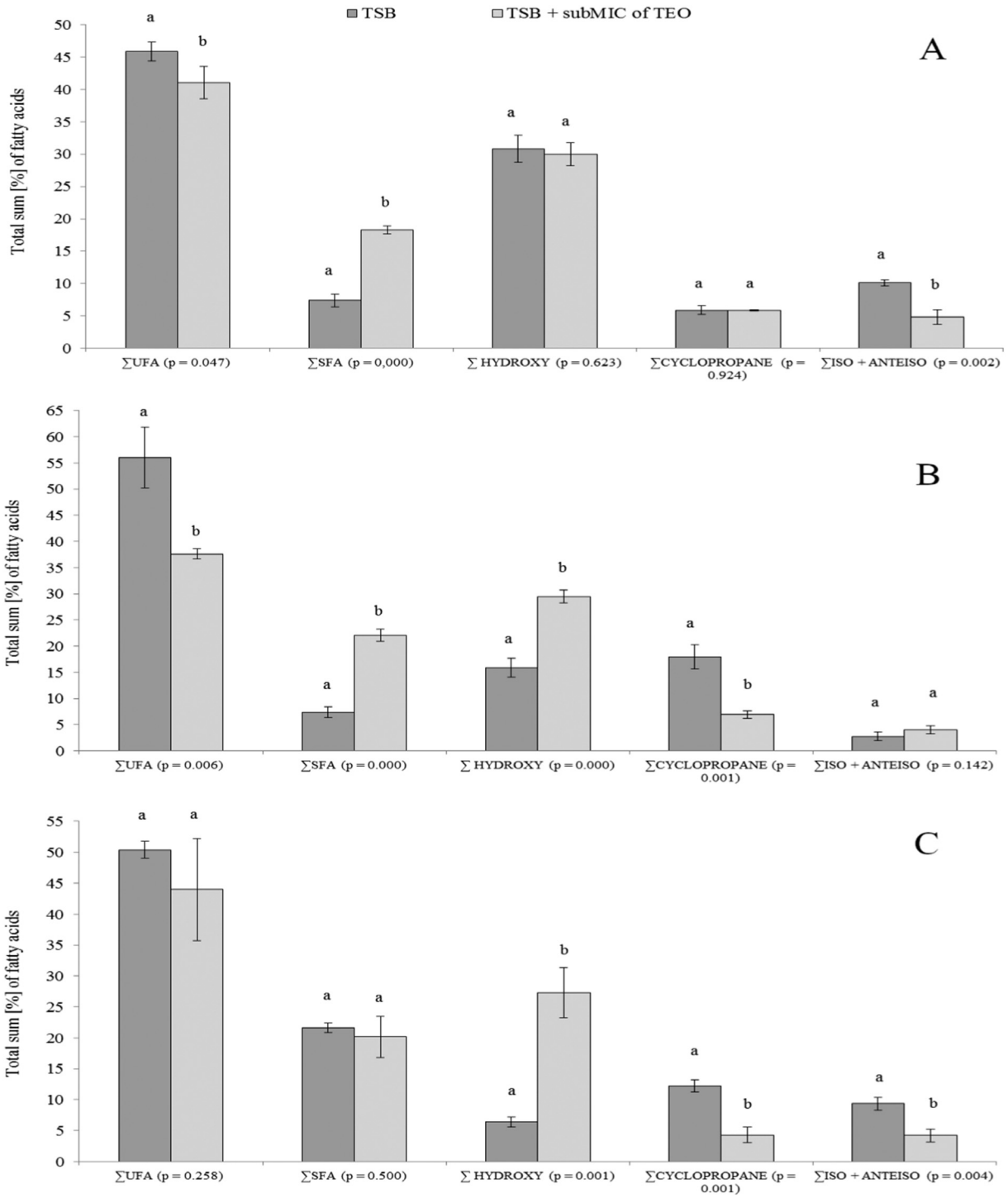

Fig. 1. Percentage sum of different class of fatty acids and changes occurring in response to treatment with subMIC of TEO in *P. psychrophila* KM02 (A), *P. orientalis* KM249 (B), and *P. fluorescens* KM148 (C). Means in the same column followed by the same letter not differ significantly ($P < 0.05$) according to t-student tests. Values are means of triplicate determinations. UFA – unsaturated fatty acids. SFA – saturated fatty acids. HYDROXY – hydroxy fatty acids. CYCLOPROPANE - cyclopropane fatty acids. ISO + ANTEISO - iso- and anteiso-methyl-branched fatty acids.

inhibition was only on average 35%. This was in contrast to *in situ* conditions, where β-PH was the most effective in gene inhibition; for instance, the M16_2 and M16_4 transcription levels were decreased by approximately 85 and 87%, respectively. In *P. orientalis* KM249 (B) cells cultivated in TSB medium supplemented with subMIC of TEO, upregulation of the expression of the S11_3 gene was observed (ratio 1.2), but the rest of the genes were downregulated, with the highest reduction in the M3_2 gene (by 68%). Treatment with subMIC of ME resulted in similar changes in both types of experiments, but for TSB medium, the greatest inhibition of the M22_1 gene (68%) was observed, while for fish juice medium, the M3_2 gene was inhibited to the greatest extent (55%). The incubation of *P. orientalis* KM249 with subMIC of β-PH resulted in completely inverse changes in gene expression depending on the type of medium; in TSB, the most considerable inhibition concerned the M3_2 gene (65%), while in fish juice medium, the M16_1 gene was the most downregulated (66%). Regarding to *P. fluorescens* KM148 (C),

Table 4
RP-UHPLC-ESI-MS results of quality and quantity of autoinducers synthesized by examined *Pseudomonas* spp. under different conditions.

Culture variant		Concentration [μg/mL] (± SD) of signal molecules under different growth conditions								
		Acyl homoserine lactones							Alkyl quinolone molecules	
		3-Oxo-C12-HSL	3-Oxo-C14-HSL	3-Oxo-C6-HSL	3-Oxo-C8-HSL	C12-HSL	C4-HSL	C6-HSL	PQS	
TSB medium	P. psychrophila KM02	1.908 (± 0.031)	0.007 (± 0.000)	0.015 (± 0.000)	1.119 (± 0.063)	0.136 (± 0.004)	1.217 (± 0.010)	0.017 (± 0.000)	0.0076 (± 0.0000)	
	P. orientalis KM249	2.028 (± 0.049)	< LOD	0.022 (± 0.001)	1.953 (± 0.006)	< LOD	1.312 (± 0.021)	0.021 (± 0.001)	ND	
	P. fluorescens KM148	1.976 (± 0.099)	< LOD	0.022 (± 0.001)	1.853 (± 0.006)	0.136 (± 0.004)	1.302 (± 0.005)	0.021 (± 0.001)	0.0030 (± 0.0000)	
TSB medium + subMIC of TEO	P. psychrophila KM02	< LOD	< LOD	0.012 (± 0.000)	< LOD	< LOD	< LOD	< LOD	0.0003 (± 0.0000)	
	P. orientalis KM249	0.001 (± 0.000)	< LOD	< LOD	< LOD	< LOD	< LOD	< LOD	ND	
	P. fluorescens KM148	< LOD	< LOD	0.011 (± 0.001)	< LOD	< LOD	< LOD	< LOD	ND	
TSB medium + subMIC of ME	P. psychrophila KM02	< LOD	< LOD	0.013 (± 0.005)	< LOD	< LOD	< LOD	< LOD	0.0003 (± 0.0000)	
	P. orientalis KM249	< LOD	< LOD	< LOD	< LOD	< LOD	< LOD	< LOD	ND	
	P. fluorescens KM148	< LOD	< LOD	0.011 (± 0.001)	0.004 (± 0.002)	< LOD	< LOD	< LOD	ND	
TSB medium + subMIC of β-PH	P. psychrophila KM02	< LOD	< LOD	0.016 (± 0.001)	< LOD	0.051 (± 0.004)	< LOD	< LOD	ND	
	P. orientalis KM249	< LOD	< LOD	< LOD	< LOD	< LOD	< LOD	< LOD	ND	
	P. fluorescens KM148	< LOD	< LOD	0.007 (± 0.000)	0.004 (± 0.002)	< LOD	< LOD	< LOD	ND	

Concentration [μg/mL] (± SD) was calculated from calibration matrix with known concentration of each AHLs and alkyl quinolone molecule; < LOD – less than limit of detection; ND – not detected.

Table 5
Molecular docking parameters of autoinducers, ME and β-PH docked into *Pseudomonas* QS receptor proteins.

Compound	Molecular docking parameters [kcal/mol]			
	XP Glide GScore	Glide energy	Glide Van der Waals energy	Glide Coulomb energy
LasR protein				
3-oxo-C12-HSL	−9.750	−60.513	−44.667	−15.846
Methyl eugenol	−6.145	−31.765	−25.390	−6.375
β-Phellandrene	−5.750	−22.240	−22.418	0.178
RhlR protein				
C4-HSL	−5.990	−25.471	−21.963	−3.508
Methyl eugenol	−5.589	−26.819	−23.639	−3.180
β-Phellandrene	−6.566	−18.968	−19.107	0.139
PqsR protein				
PQS	−7.772	−36.455	−30.978	−5.477
Methyl eugenol	−4.921	−27.292	−26.874	−0.418
β-Phellandrene	−5.263	−14.894	−14.904	0.009

XP Glide GScore – docking score of ligand-protein interaction.
Glide energy – modified Coulomb + van der Waals interaction energy.

Table 6
The major interactions of ME, β-PHE and autoinducers with QS receptor proteins.

Ligand	Residues/atoms involved in interaction	Distance [Å]	Type of interaction
LasR			
3-Oxo-C12-HSL	ASP73/O^- ← H	2.30	H-bond
	TRP60/NH → O	2.13	H-bond
	TYR56 OH → O	1.80	H-bond
	TYR56/CH → O	2.73	Aromatic H-bond
	TYR56/CH → O	2.52	Aromatic H-bond
	ARG61/NH → H_2O → O	2.03, 1.99	2H-bond
	ARG61/N^+H_2 → H_2O	2.35	H-bond
	TYR56/CH → H_2O	2.72	Aromatic H-bond
	PHE101/CH → O	2.65	Aromatic H-bond
ME	TYR56/⏣ – ⏣	5.45	π-π
	SER129/OH → O	1.80	H-bond
	THR75/OH ← CH	2.74	Aromatic H-bond
	ARG61/NH → H_2O → O	2.03, 1.91	2H-bond
	ARG61/N^+H → H_2O	2.35	H-bond
	TYR56/C → H_2O	3.65	Aromatic H-bond
β-PH	ARG61, ASP65, TYR64, LEU36, LEU39, LEU40, VAL76, ALA127	–	Hydrophobic
RhlR			
C4-HSL	TRP68/NH → O	2.62	H-bond
	TRP68/NH → O	1.99	H-bond
	TYR42/CH → O	2.61	Aromatic H-bond
ME	TRP68/⏣ – ⏣	4.82	π-π
	TRP68/NH → O	1.85	H-bond
β-PH	VAL60, LEU69, TYR72, TYR77	–	Hydrophobic
PqsR			
PQS	LEU207 O ← OH	1.73	H-bond
ME	LEU208, ILE236, ALA237, PRO238	–	Hydrophobic
β-PH	ILE263, ILE236, TRP234, TYR258	–	Hydrophobic

the supplementation of TSB medium with subMIC of TEO resulted in the highest downregulation of M16_2 gene (66%), but in fish juice medium this activity was considerably lower. Only the M3_2 gene was downregulated at a similar level. The overall gene expression after treatment with ME was inhibited by averages of 47% in TSB, and 22%

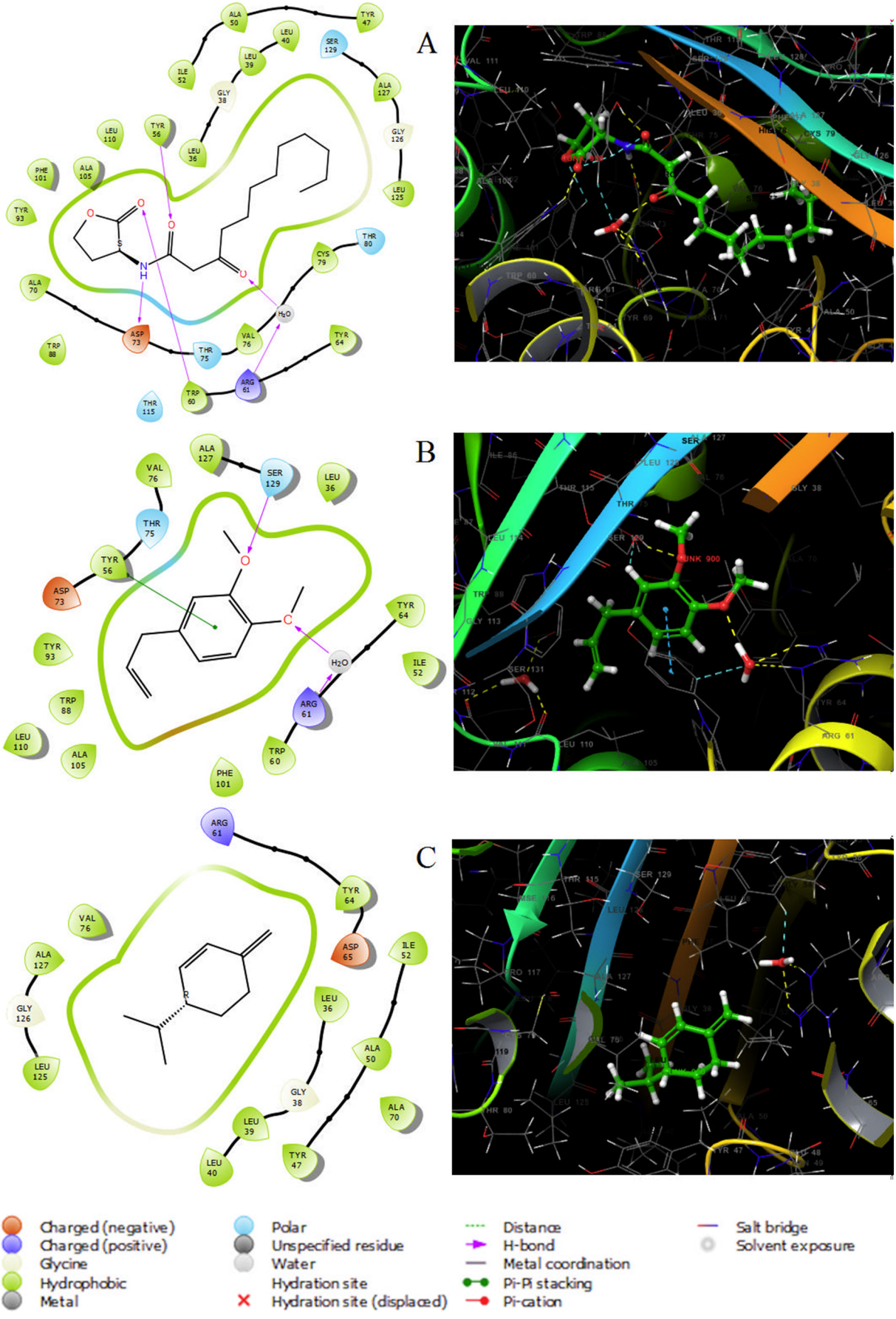

Fig. 2. Interaction of 3-oxo-C12-HSL (A), ME (B), and β-PH (C) with LasR protein.

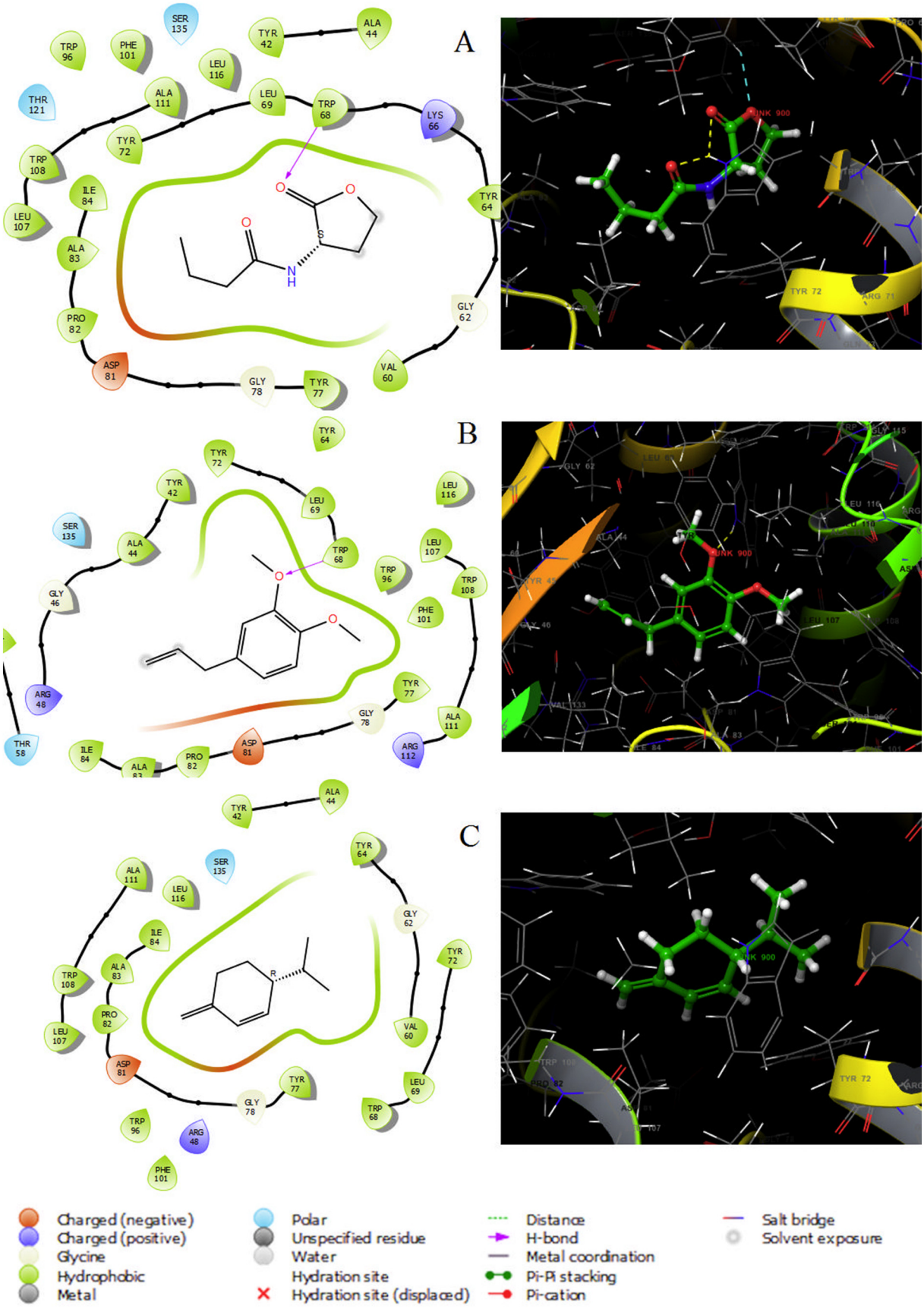

Fig. 3. Interaction of C4-HSL (A), ME (B), and β-PH (C) with RhlR protein.

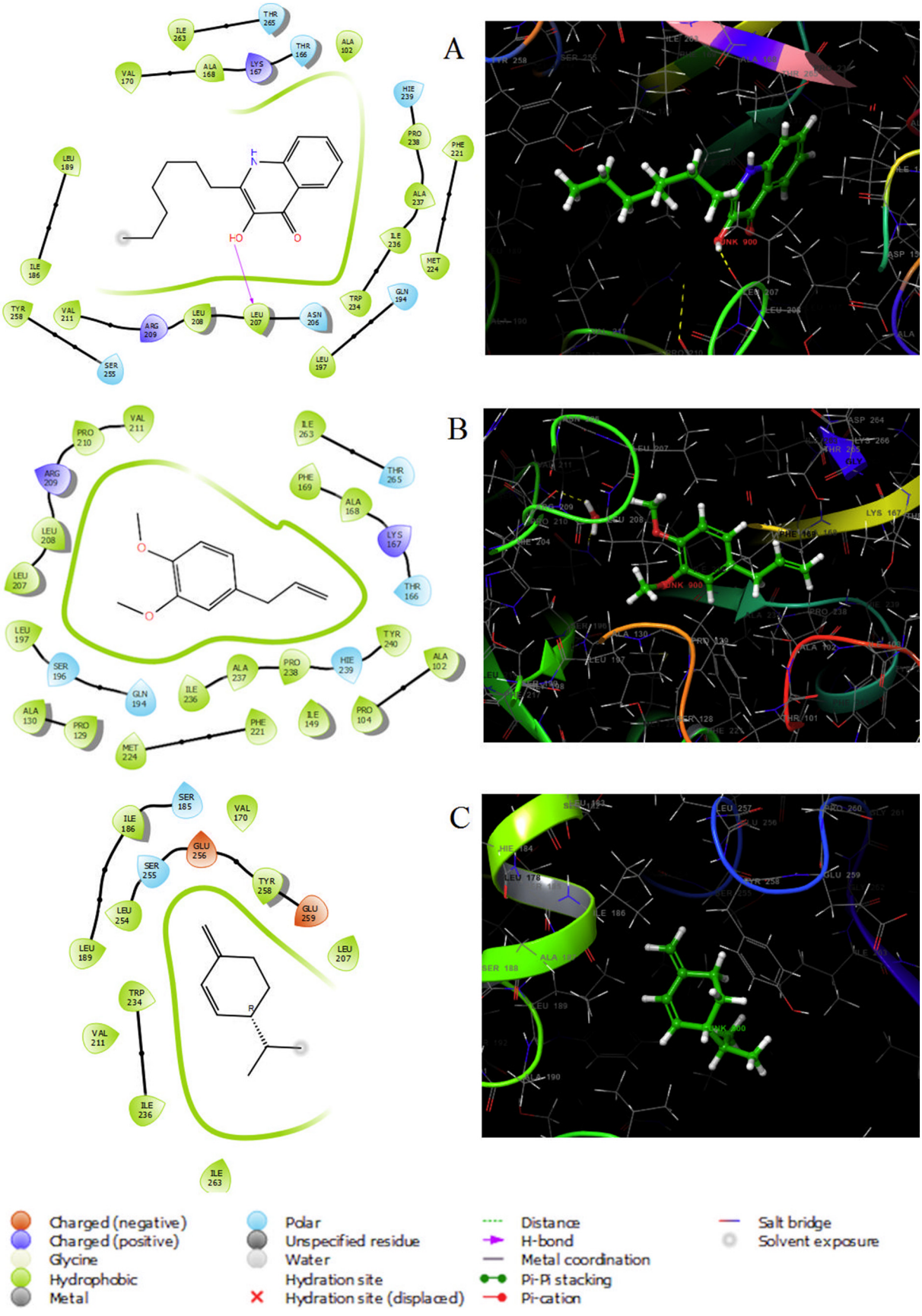

Fig. 4. Interaction of PQS (A), ME (B), and β-PH (C) with PqsR protein.

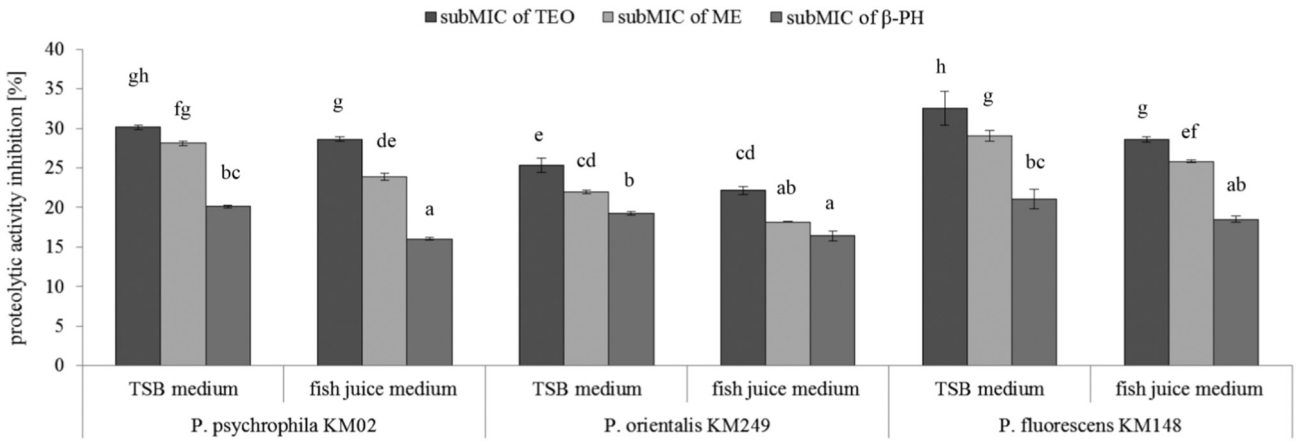

Fig. 5. Inhibition of proteolytic activity of *Pseudomonas* spp. cells after treatment with subMICs of selected compounds supplemented to TSB medium (*in vitro*) and to fish juice medium (*in situ*). The significance differences between experiments was determined by Two-Way ANOVA (treatment: F = 204.934 $p < 0.000$***; medium: F = 191.653 5.p < 0.000***; treatment:medium: F = 1.769, $p = 0.116$). Means with the same letters indicates no significantly differences ($p < 0.05$). Bars indicate standard deviation from three experiments.

in fish juice medium. The effectiveness of the last analyzed compound, β-PH, was also affected by experimental conditions: *in vitro*, the transcription of M16_3 gene was the most decreased (61%), while *in situ*, M22_1 was the most decreased (62%).

4. Discussion

Seafood is considered one of the most valuable food commodities because it is a source of omega-3 fatty acids, easily assimilated proteins and microelements. Although the health benefits from diets rich in seafoods are indisputable, the microbiological quality and safety are still unresolved, and large amount of those commodities are lost due to premature spoilage, mostly caused by the genus *Pseudomonas* (Sterniša et al., 2019). Fish spoilage is strictly related to the physiological activities of microflora, inherently occurring in a given milieu (Caldera et al., 2016). Because QS in pseudomonads is one of the major mechanisms for physiological activity regulation, blocking or disrupting QS by natural phytochemicals is a promising novel method for preventing fish spoilage (Calo et al., 2015).

The current study aimed to evaluate the anti-QS potential and anti-proteolytic activity of TEO and its major compounds towards *P. psychrophila* KM02, *P. orientalis* KM249, and *P. fluorescens* KM148 isolated from salmon *(Salmo salar)*. The effect on QS was established by the analysis of QS autoinducer reduction and molecular docking of TEO bioactive components to QS transcriptional receptor proteins. The impact on proteolytic activity was evaluated by the spectrophotometric method with TNBS reagent and by RT-qPCR analysis of the changes in mRNA expression of genes encoding proteases in analyzed *Pseudomonas* spp. cells.

In the initial step of the work, the chemical composition of TEO by GC–MS analysis was established. Our results indicated that methyl eugenol (24.5%) and β-phellandrene (19.3%) were the major compounds. These results are in agreement with the work of Szczepanik et al. (2018) in which methyl eugenol was also dominant in TEO. To date, only Verma et al. (2010) evaluated methyl eugenol in TEO at a level of 0.7%. This indicates that the composition of the TEO can be influenced by the conditions of growth, time of harvesting, part of the plant or method of extraction.

The biological effect of TEO is strictly related to its concentration. The sufficient concentrations of EOs to kill microorganisms in foods are often higher than the concentrations that are organoleptically acceptable. Thus, the use of sublethal concentrations has been proposed to provide a balance between sensory acceptability and antimicrobial efficacy (Leite de Souza, 2016). Furthermore, the evaluation of anti-QS potential requires determining the sublethal dose of an analyzed substance or compound to microorganisms because this approach does not lead to the death of bacteria cells or significant inhibition of their growth (Truchado et al., 2015).

Although several methods of possible antimicrobial action of essential oils have been proposed, the ability to penetrate through bacterial membranes to the interior of the cell and consequently disturb its integrity is the most probable mechanism (Calo et al., 2015). However, it has been documented that bacterial cells can easily circumvent toxicity effects by modifying the membrane lipid composition, especially if essential oils are present at sublethal concentrations (Di Pasqua et al., 2006; Leite de Souza, 2016). Such modification is fundamental in maintaining both membrane integrity and functionality when bacteria are exposed to external stresses (Siroli et al., 2015). Therefore, we evaluated the changes in *P. psychrophila* KM02, *P. orientalis* KM249 and *P. fluorescens* KM148 cellular FAME profiles by GC/FID analysis. Because the adaptive strategies include alterations, mostly relative to the overall changes in the ratio of saturation to unsaturation, acyl chain length, branching position or cis/trans isomerization (Denich et al., 2003; Leite de Souza, 2016; Siroli et al., 2015), we also compared the differences in the sum of the percentage of fatty acids belonging to different classes.

P. psychrophila KM02 and *P. orientalis* KM249 cells after treatment with the subMIC of TEO showed increased levels of saturated fatty acids with a simultaneous decrease in unsaturated fatty acids. Our results are in contradiction with the work of Di Pasqua et al. (2006) and Siroli et al. (2015), where sublethal concentrations of selected essential oils caused an increase in unsaturated fatty acids, which was perceived as the potential adaptive mechanism. However, neither of these articles evaluated the effect of essential oils on the *P. psychrophila* or *P. orientalis* strain, and as is generally stated, adaptation strategies depend on the bacterial species and type of stress factor to which the cells are exposed (Siroli et al., 2015). Notably, membranes rich in saturated fatty acids and deprived of branched chain fatty acids (as we noticed in terms of *P. psychrophila* KM02) are more resistant to the penetration of biocide compounds to the interior of the cell, since the linear acyl chains can pack tightly side by side (Leite de Souza, 2016). Considering the fact that the biosynthesis pathway by which *Pseudomonas* synthesizes unsaturated fatty acids takes place through the action of the desaturase enzyme and since there is an appreciable decrease in the level of those fatty acids, it is assumed that the action of the desaturase enzyme is disturbed by TEO compounds during cell growth (Di Pasqua et al., 2006). However, such alteration was not established for *P. fluorescens* KM148, which indicates the different strategies in membrane response

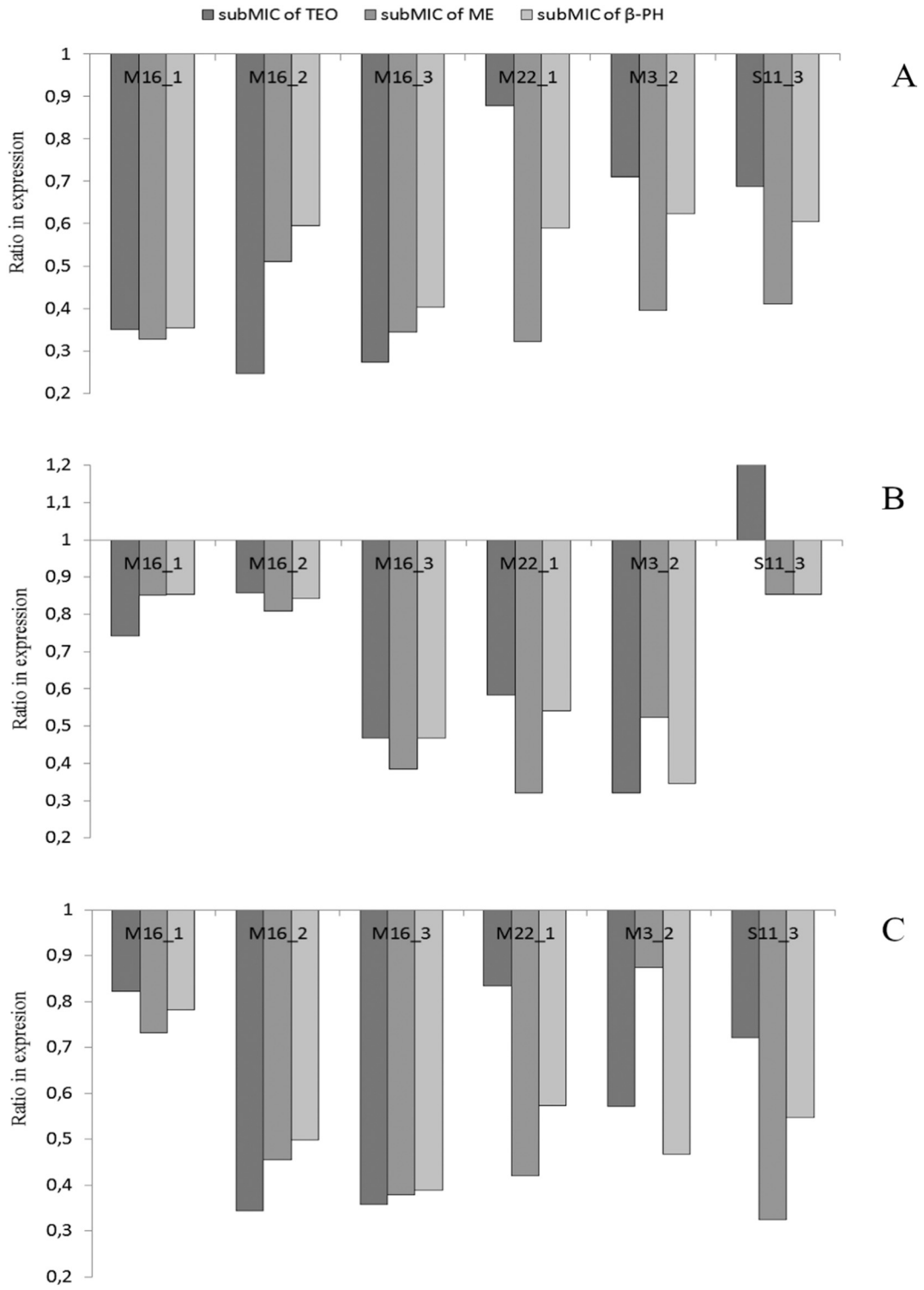

Fig. 6. Comparison of ratio in expression of selected genes encoding proteases in *P. psychrophila* KM02 (A), *P. orientalis* KM249 (B), and *P. fluorescens* KM148 (C) cells after incubation in TSB medium supplemented with subMIC of TEO, subMIC of ME, and subMIC of β-PH. The 16 s rRNA gene was used as reference gene. The transcription level of genes in cells cultured in TSB medium equals 1.

to TEO treatment. Our results are in agreement with the paper of Di Pasqua et al. (2006), who revealed that *P. fluorescens* exhibits high resistance to antimicrobials from essential oils (*e.g.* limonene, eugenol, or carvacrol). The amounts of cyclopropane and hydroxyl fatty acids in the *P. psychrophila* KM02 membranes did not change significantly in response to the subMIC of TEO, in agreement with the paper by Denich et al. (2003). Conversely, *P. orientalis* KM249 and *P. fluorescens* KM148 showed significant decreases in CFA. Because CFA are formed from UFA with high energy demand, as described by Chang and Cronan (1999), it is assumed that treatment with subMIC of TEO induces the ATP depletion or acts against bacterial enzymes, including ATPase (Nazzaro et al., 2013).

The next step of this work concerned the evaluation of changes in the quality and quantity of autoinductors synthesized by the food-

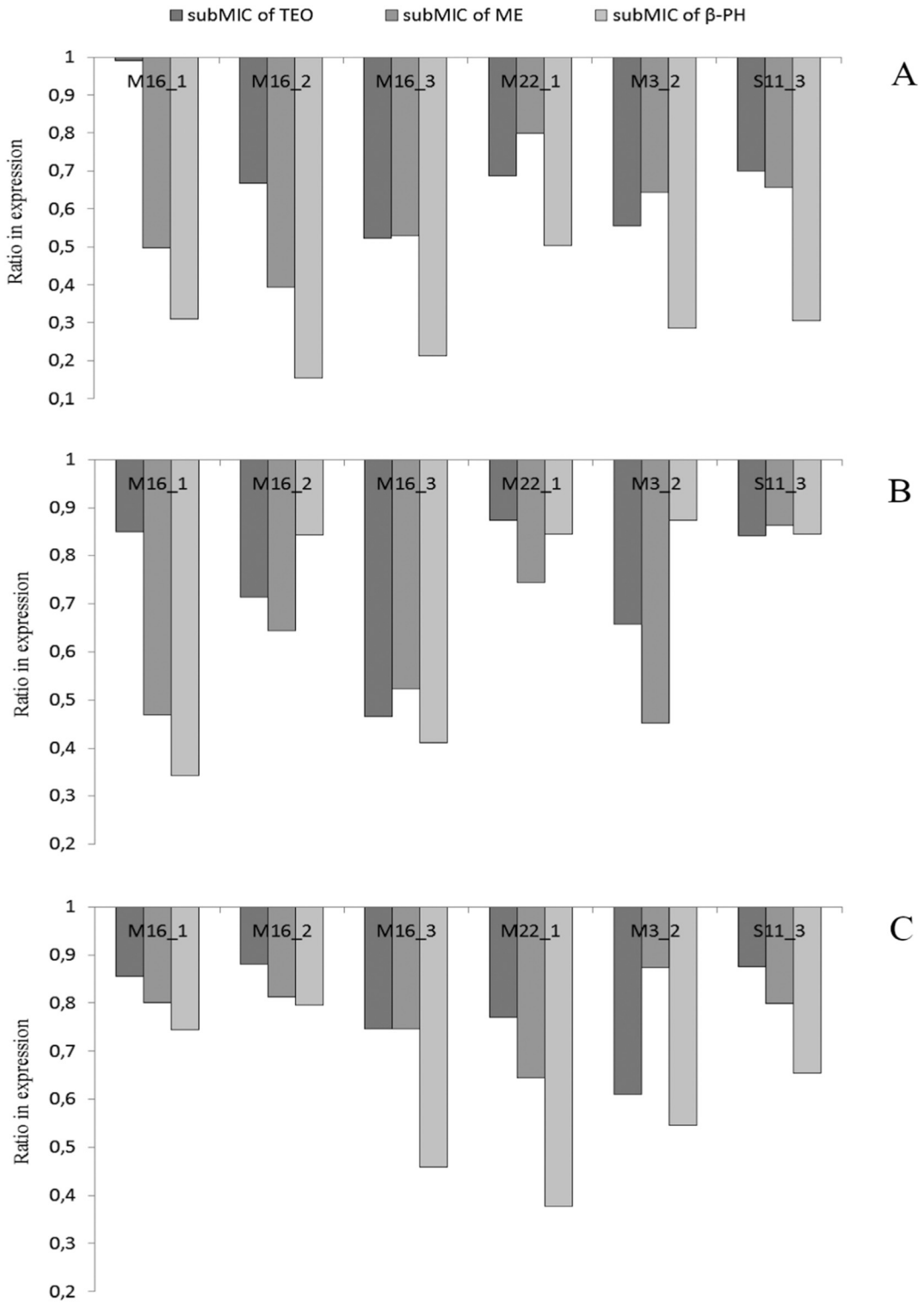

Fig. 7. Comparison of ratio in expression of selected genes encoding proteases in *P. psychrophila* KM02 (A), *P. orientalis* KM249 (B), *P. fluorescens* KM148 (C) cells after incubation in Fish Juice medium supplemented with subMIC of TEO, subMIC of ME, and subMIC of β-PH. The 16 s rRNA gene was used as reference gene. The transcription level of genes in cells cultured in Fish Juice medium equals 1.

associated pseudomonads after incubation with the subMIC of TEO and its major compounds (ME and β-PH) by the RP-UHPLC-ESI-MS system, providing the most accurate evaluation of the AHLs and PQS. AHLs are composed of a homoserine lactone ring and N-acyl chains varying in length, saturation level, or oxidation state and are necessary to regulate bacterial physiological activities (Papenfort and Bassler, 2016). Our results indicated that *P. psychrophila* KM02 synthesized seven different AHLs and PQS autoinducers. The capability of synthesizing AHL by *P. psychrophila* was first reported by Bai and Rai Vittal (2014), who revealed the presence of only N-butryl homoserine lactone (C4-HSL) in supernatants of cells isolated from freshwater fish. In *P. fluorescens* KM148, supernatants six AHLs and PQS molecules were examined, and the *P. orientalis* KM249 strain was able to synthesize only five AHLs with no PQS molecules detected. In our recent study (Myszka et al.,

2020) we examined the other food-associated pseudomonads as effective QS autoinducers producers. In contrast to the *P. orientalis* KM249 strain, the KM149 strain was able to synthesize 3-hydroxy-C4-HSL at 0.64 μg/mL. Moreover, in extracts of *P. fluorescens* KM148, the C12-HSL was present at the level of 0.136 μg/mL, while in KM48 this AHL was present below the limit of detection. Such differences in QS signal molecules are attributed to the phenomenon that bacteria of the same genus or species can produce various AHLs in a strain-dependent manner (Czajkowski and Jafra, 2009). Furthermore, the production of QS autoinductors has to be evaluated within each strain individually because not all pseudomonads possess a QS phenotype or do not produce detectable levels of AHLs, which led to depravation of physiological activities, such as proteolysis. Such a phenomenon was established for *P. putida*-like strains (Caldera et al., 2016; Gopu and Shetty, 2016).

In this work, the greatest values for 3-oxo-C12-HSL and C4-HSL are due to the hierarchy network of the las and rhl QS systems. This means that 3-oxo-C12-HSL is produced first, and as quorum sensing progresses or the population density increases, the dominant AHL synthase becomes RhlI, which synthesizes C4-HSL (Lee and Zhang, 2015). The HPLC analysis revealed that upon treatment with subMICs of TEO, ME and β-PH, almost all of the concentrations were decreased to levels lower than the limit of detection, indicating the effectiveness of the analyzed compounds at inhibiting AHL production. In the *P. psychrophila* KM02 and *P. fluorescens* KM148 supernatants only the 3-oxo-C6-HSL remained unchanged, but the concentration was relatively low and ranged from 0.007 μg/mL to 0.016 μg/mL. A similar finding was obtained for the *P. fluorescens* strain incubated with thyme essential oil for 48 h (Myszka et al., 2016). The lack of C4-HSL after incubation with TEO and its major compounds may be attributed to the fact that the expression of the RhlI enzyme is under the positive control of the LasR transcriptional regulator, which requires 3-oxo-C12-HSL, the product of LasI (Papenfort and Bassler, 2016). To the best of our knowledge, this paper provides for the first time information about PQS synthesis in the *P. psychrophila* strain.

The anti-*quorum sensing* activity of compounds described as quorum sensing inhibitors, apart from disturbing the synthesis of QS autoinductors, may also trigger the QS receptor proteins by competing with native autoinductors synthesized by the given bacteria (Kalia, 2013). Therefore, to elucidate the second possible mechanism of the anti-QS activities of the major bioactive compounds of TEO, molecular docking studies were performed. Since the major signal molecules synthesized by analyzed cells are 3-oxo-C12-HSL, C4-HSL, and PQS, for molecular docking analysis, we used the LasR, RhlR and PqsR molecules. The employment of the receptor proteins native to *P. aeruginosa,* apart from the autoinducers results, was also dictated by the homologous nature of QS-related proteins, which can be proven by the ability of different bacteria to respond to autoinducers produced by others (*e.g.*, *E. coli* possess SdiA receptor, a homolog of LuxR, and thus, it can respond to autoinductors produced by *P. aeruginosa*) (Kalia, 2013).

The comparison of docking scores obtained for native autoinductors, ME and β-PH indicates the potential competition for binding with protein active sites. ME, similarly to 3-oxo-C12-HSL, formed a number of H-bonds with common residues (ARG61 and TYR56) and additional π-π interactions with the aromatic ring of TYR56, which stabilized the whole complex, which is in agreement with Kumar et al. (2013). In the case of β-PH, only hydrophobic interactions were observed, thus resulting in lower docking scores and Glide energy of the complex with LasR. Such differences result from the different chemical structures of the analyzed compounds: ME possesses a highly interactive aromatic ring, which is also considered the major antimicrobial determinant (Calo et al., 2015). The anti-*quorum sensing* activity of ME towards LasR of *P. aeruginosa* has already been reported by Sybiya Vasantha Packiavathy et al. (2012), who also stated that any competitive ligands with higher or closer docking scores would be able to displace the native autoinductors and result in the reduced production of the QS-dependent factors, especially if the common residues are involved in docking. It has been demonstrated that H-bonding is one of the most important features for providing efficient ligand-receptor docking (Sharma et al., 2016). However, H-bonds are not the only ones responsible for good interactions. As shown in Tables 5 and 6, the highest docking score for RhlR protein was with β-PH, which did not create any H-bonds. It is likely the consequence of higher hydrophobic enclosure (XP PhobEn) and lipophilic (XP LipophilicEvdW) terms obtained for docking (data not shown). Similar results were obtained for the PqsR protein, where β-PH was surrounded by more hydrophobic amino acids (tryptophan and tyrosine) than ME (mostly aliphatic amino acids, such as alanine or leucine).

Studies conducted by Zhang et al. (2019) revealed that *P. psychrophila* (next to P. *fragi* and *P. fluorescens*) possess the dominant role in spoilage of food during cold-chain. These microorganisms are adapted to cold and are able to survive at very low temperatures (approximately 0 °C), which results in their predomination in the spoilage of refrigerated foods sorted under aerobic conditions and deprived of any heat treatment. Among proteinaceous foods, *Pseudomonas* species are one of the specific spoilage microflora of chilled stored fish and seafoods and are responsible for the development of sweet, fruity off-odors. This activity is due to the secretion of extracellular proteases that break down food proteins into amino acids and short peptides, which further decompose into aldehydes, ketones, esters, organic acids and various toxic substances. The proteolytic activity of *P. psychrophila* and *P. fluorescens* has already been established by Bai and Rai Vittal (2014) and Xin et al. (2017). Thus, since the secretion of extracellular proteases is regulated by bacterial QS systems (Ding et al., 2019), we hypothesized that decreasing the proteolytic activity of the analyzed strains after incubation with subMICs of TEO, ME and β-PH is the result of QS inhibition by the analyzed compounds.

The proteolytic activity was inhibited both *in vitro* and in fish-based model conditions, but it varied according to the type of medium and applied treatment. The lower effectiveness in fish juice media may result from the more complex composition (mostly higher contents of fats) than that of TSB medium (Burt, 2004). In the present work, proteolytic activity was inhibited to a greater extent in the samples incubated with subMICs of TEO and ME than upon β-PH treatment, regardless of the analyzed strain and medium. This may be related to the AHL results, where β-PH does not reduce the synthesis of 3-oxo-C6-HSL and C12-HSL or 3-oxo-C8-HSL in *P. psychrophila* KM02 and *P. fluorescens* KM148, respectively. Despite the effective decreases in all AHL molecules in *P. orientalis* KM249 by analyzed compounds, the overall inhibition of proteolytic activity was relatively smaller than in the two previous strains. The work of Ding et al. (2019) revealed that decreasing the proteolytic activity of *P. fluorescens* P07 after incubation with catechin was solely the consequence of the reduction in QS autoinducer synthesis. However, the results obtained by Liu et al. (2006) do not indicate any clear correlation between the overall detectable AHLs and the proteolytic activity in the fish samples. Therefore, another explanation for the different impacts of the analyzed compounds on the proteolytic activity of pseudomonads fish isolates can be based on molecular docking results. It should be noted that despite the inseparable network of QS systems, the one that is mostly responsible for the regulation of genes encoding proteases is the *las* system, whereas the *rhl* system is more engaged in the regulation of exopolysaccharide synthesis (Lee and Zhang, 2015). As mentioned above, ME had better potential for competitively binding to LasR, thus effectively inhibiting QS-mediated proteolytic activity as a consequence of downregulating the transcription of genes encoding proteases.

Consequently, to verify whether the decrease in proteolytic activity is regulated at the molecular level, we performed RT-qPCR analysis of changes in the expression of selected genes encoding proteases in the *Pseudomonas* spp. strains after treatment with the analyzed compounds. It is well known that important proteases responsible for spoilage caused by pseudomonads are the extracellular metalloproteases (*e.g.*, for *P. aeruginosa*, alkaline metalloproteases belonging to the AprX

family; Caldera et al., 2016). To date, researchers have mostly been concerned with the effect of QS inhibitors on the expression levels of autoinducers synthases and QS receptors or virulence factors (Truchado et al., 2015), but there are no papers describing their impact on proteolytic activity at the molecular level, especially in food bacterial isolates. The RT-qPCR analysis revealed that M16 family genes encoding metalloproteases were downregulated by all applied treatments, but *in vitro,* the highest inhibition was with the subMIC of TEO, while in the fish-based model, β-PH was the most efficient. In the case of M3_2 gene, the results showed divergent effects. Comparing the changes in gene expression levels depending on the analyzed strain, the smallest inhibition and upregulation of the S11_3 gene were noted for *P. orientalis* KM249 cultures. These observations can represent relevant explanations for the lower effectiveness of the analyzed compounds in the proteolytic activity inhibition of this strain. Based on the overall RT-qPCR results, we provide evidence that subinhibitory concentrations of the analyzed compounds change the expression levels of genes encoding proteases in the *Pseudomonas* spp., and those findings correspond with the outcome from analysis of proteolytic activity inhibition examined by the method with the TNBS reagent.

5. Conclusions

Because the low temperature is insufficient to inhibit *Pseudomonas* spp. growth and because the application of artificial preservatives in fish is limited and there is a growing consumer demand for seafoods on the food market, scientists are facing a great challenge in the development of new/additional preservation techniques, ensuring high quality and safety. Thus, searching for natural phytochemicals (mostly from spices and herbs) that can effectively target the QS system and consequently affect the physiological activities of food-derived bacteria isolates is a promising possibility to meet those demands. The current research for the first time has explored the potential of TEO, ME and β-PH as anti-QS and anti-proteolytic agents against food-associated pseudomonads, both *in vitro* and *in situ*. Given the lower effect obtained in the fish-model product, subsequent studies should focus on the possibility of increasing the effectiveness of the analyzed compounds, taking into account their characteristics, *i.e.*, high volatility and a strong odor. In addition, given the high resistance of analyzed microorganisms to antimicrobials, the possible metabolism of the analyzed compounds during particular food storage must be evaluated, referring to their applicability in the food industry.

Declaration of competing interest

All authors declare no conflict of interest.

Acknowledgements

This work was supported by a grant from the National Science Centre, Poland (no. 2016/23/D/NZ9/00028).

Appendix A. Supplementary data

Supplementary data to this article can be found online at https://doi.org/10.1016/j.ijfoodmicro.2020.108732.

References

Bai, A.J., Rai Vittal, R., 2014. Quorum sensing regulation and inhibition of exoenzyme production and biofilm formation in the food spoilage bacteria *Pseudomonas psychrophila* PSPF19. Food Biotechnol. 28, 293–308. https://doi.org/10.1080/08905436.2014.963601.

Burt, S., 2004. Essential oils: their antibacterial properties and potential applications in foods—a review. Int. J. Food Microbiol. 94, 223–253. https://doi.org/10.1016/j.ijfoodmicro.2004.03.022.

Caldera, L., Franzetti, L., Van Coillie, E., De Vos, P., Stragier, P., De Block, J., Heyndrickx, M., 2016. Identification, enzymatic spoilage characterization and proteolytic activity quantification of Pseudomonas spp. isolated from different foods. Food Microbiol. 54, 142–153. https://doi.org/10.1016/j.fm.2015.10.004.

Calo, J.R., Crandall, P.G., O'Bryan, C.A., Ricke, S.C., 2015. Essential oils as antimicrobials in food systems – a review. Food Control 54, 111–119. https://doi.org/10.1016/j.foodcont.2014.12.040.

Chang, Y.-Y., Cronan, J.E., 1999. Membrane cyclopropane fatty acid content is a major factor in acid resistance of Escherichia coli. Mol. Microbiol. 33, 249–259. https://doi.org/10.1046/j.1365-2958.1999.01456.x.

Clinical and Laboratory Standards Institute, 2012. Methods for Dilution Antimicrobial Susceptibility Tests for Bacteria That Grow Aerobically; Approved Standard, Ninth edition. .

Czajkowski, R., Jafra, S., 2009. Quenching of acyl-homoserine lactone-dependent quorum sensing by enzymatic disruption of signal molecules. Acta Biochim. Pol. 56. https://doi.org/10.18388/abp.2009_2512.

Dalgaard, P., 1995. Qualitative and quantitative characterization of spoilage bacteria from packed fish. Int. J. Food Microbiol. 26, 319–333. https://doi.org/10.1016/0168-1605(94)00137-U.

Denich, T.J., Beaudette, L.A., Lee, H., Trevors, J.T., 2003. Effect of selected environmental and physico-chemical factors on bacterial cytoplasmic membranes. J. Microbiol. Methods 52, 149–182. https://doi.org/10.1016/S0167-7012(02)00155-0.

Di Pasqua, R., Hoskins, N., Betts, G., Mauriello, G., 2006. Changes in membrane fatty acids composition of microbial cells induced by addiction of thymol, carvacrol, limonene, cinnamaldehyde, and eugenol in the growing media. J. Agric. Food Chem. 54, 2745–2749. https://doi.org/10.1021/jf052722l.

Ding, T., Li, T., Li, J., 2019. Virtual screening for quorum sensing inhibitors of *Pseudomonas fluorescens* P07 from a food-derived compound database. J. Appl. Microbiol. https://doi.org/10.1111/jam.14333.

Friesner, R.A., Murphy, R.B., Repasky, M.P., Frye, L.L., Greenwood, J.R., Halgren, T.A., Sanschagrin, P.C., Mainz, D.T., 2006. Extra precision glide: docking and scoring incorporating a model of hydrophobic enclosure for protein − ligand complexes. J. Med. Chem. 49, 6177–6196. https://doi.org/10.1021/jm051256o.

Gopu, V., Shetty, P.H., 2016. Regulation of acylated homoserine lactones (AHLs) in beef by spice marination. J. Food Sci. Technol. 53, 2686–2694. https://doi.org/10.1007/s13197-016-2240-x.

Harder, E., Damm, W., Maple, J., Wu, C., Reboul, M., Xiang, J.Y., Wang, L., Lupyan, D., Dahlgren, M.K., Knight, J.L., Kaus, J.W., Cerutti, D.S., Krilov, G., Jorgensen, W.L., Abel, R., Friesner, R.A., 2016. OPLS3: a force field providing broad coverage of drug-like small molecules and proteins. J. Chem. Theory Comput. 12, 281–296. https://doi.org/10.1021/acs.jctc.5b00864.

Kalia, V.C., 2013. Quorum sensing inhibitors: an overview. Biotechnol. Adv. 31, 224–245. https://doi.org/10.1016/j.biotechadv.2012.10.004.

Kumar, L., Chhibber, S., Harjai, K., 2013. Zingerone inhibit biofilm formation and improve antibiofilm efficacy of ciprofloxacin against Pseudomonas aeruginosa PAO1. Fitoterapia 90, 73–78. https://doi.org/10.1016/j.fitote.2013.06.017.

Lee, J., Zhang, L., 2015. The hierarchy quorum sensing network in Pseudomonas aeruginosa. Protein Cell 6, 26–41. https://doi.org/10.1007/s13238-014-0100-x.

Leite de Souza, E., 2016. The effects of sublethal doses of essential oils and their constituents on antimicrobial susceptibility and antibiotic resistance among food-related bacteria: a review. Trends Food Sci. Technol. 56, 1–12. https://doi.org/10.1016/j.tifs.2016.07.012.

Liu, M., Gray, J.M., Griffiths, M.W., 2006. Occurrence of proteolytic activity and *N* -acyl-homoserine lactone signals in the spoilage of aerobically chill-stored proteinaceous raw foods. J. Food Prot. 69, 2729–2737. https://doi.org/10.4315/0362-028X-69.11.2729.

Lopes-Lutz, D., Alviano, D.S., Alviano, C.S., Kolodziejczyk, P.P., 2008. Screening of chemical composition, antimicrobial and antioxidant activities of Artemisia essential oils. Phytochemistry 69, 1732–1738. https://doi.org/10.1016/j.phytochem.2008.02.014.

Mokhetho, K.C., Sandasi, M., Ahmad, A., Kamatou, G.P., Viljoen, A.M., 2018. Identification of potential anti-quorum sensing compounds in essential oils: a gas chromatography-based metabolomics approach. J. Essent. Oil Res. 30, 399–408. https://doi.org/10.1080/10412905.2018.1503100.

Myszka, K., Schmidt, M.T., Majcher, M., Juzwa, W., Olkowicz, M., Czaczyk, K., 2016. Inhibition of quorum sensing-related biofilm of Pseudomonas fluorescens KM121 by Thymus vulgare essential oil and its major bioactive compounds. Int. Biodeterior. Biodegrad. 114, 252–259. https://doi.org/10.1016/j.ibiod.2016.07.006.

Myszka, K., Olejnik, A., Majcher, M., Sobieszczańska, N., Grygier, A., Powierska-Czarny, J., Rudzińska, M., 2019. Green pepper essential oil as a biopreservative agent for fish-based products: antimicrobial and antivirulence activities against Pseudomonas aeruginosa KM01. LWT - Food Sci. Technol. 6–13. https://doi.org/10.1016/j.lwt.2019.03.047.

Myszka, K., Sobieszczańska, N., Olejnik, A., Majcher, M., Szwengiel, A., Wolko, Ł., Juzwa, W., 2020. Studies on the anti-proliferative and anti-quorum sensing potentials of Myrtus communis L. essential oil for the improved microbial stability of salmon-based products. LWT 127, 109380. https://doi.org/10.1016/j.lwt.2020.109380.

Nazzaro, F., Fratianni, F., De Martino, L., Coppola, R., De Feo, V., 2013. Effect of Essential Oils on Pathogenic Bacteria. Pharmaceuticals 6, 1451–1474. https://doi.org/10.3390/ph6121451.

Papenfort, K., Bassler, B., 2016. Quorum-sensing signal-response systems in Gram-negative bacteria. Nat. Rev. Microbiol. 14, 576–588. https://doi.org/10.1038/nrmicro.2016.89.

Pfaffl, M.W., 2001. A new mathematical model for relative quantification in real-time RT-PCR. Nucleic Acids Res. 29, 45e–445. https://doi.org/10.1093/nar/29.9.e45.

Polychroniadou, A., 1988. A simple procedure using trinitrobenzenesulphonic acid for monitoring proteolysis in cheese. J. Dairy Res. 55, 585–596. https://doi.org/10.

1017/S0022029900033379.
R Core Team, 2015. R: A Language and Environment for Statistical Computing. R Foundation for Statistical Computing, Vienna, Austria.
Ravn, L., Christensen, A.B., Molin, S., Givskov, M., Gram, L., 2001. Methods for detecting acylated homoserine lactones produced by Gram-negative bacteria and their application in studies of AHL-production kinetics. J. Microbiol. Methods 44, 239–251. https://doi.org/10.1016/S0167-7012(01)00217-2.
Roy, A., Kucukural, A., Zhang, Y., 2010. I-TASSER: a unified platform for automated protein structure and function prediction. Nat. Protoc. 5, 725–738. https://doi.org/10.1038/nprot.2010.5.
Ruijter, J.M., Ramakers, C., Hoogaars, W.M.H., Karlen, Y., Bakker, O., van den Hoff, M.J.B., Moorman, A.F.M., 2009. Amplification efficiency: linking baseline and bias in the analysis of quantitative PCR data. Nucleic Acids Res. 37, e45. https://doi.org/10.1093/nar/gkp045.
Ruttkies, C., Schymanski, E.L., Wolf, S., Hollender, J., Neumann, S., 2016. MetFrag relaunched: incorporating strategies beyond in silico fragmentation. J. Cheminformatics 8. https://doi.org/10.1186/s13321-016-0115-9.
Sastry, G.M., Adzhigirey, M., Day, T., Annabhimoju, R., Sherman, W., 2013. Protein and ligand preparation: parameters, protocols, and influence on virtual screening enrichments. J. Comput. Aided Mol. Des. 27, 221–234. https://doi.org/10.1007/s10822-013-9644-8.
Sharma, V., Sharma, P.C., Kumar, V., 2016. In Silico molecular docking analysis of natural pyridoacridines as anticancer agents. Adv. Chem. 2016, 1–9. https://doi.org/10.1155/2016/5409387.
Shen, H., Dührkop, K., Böcker, S., Rousu, J., 2014. Metabolite identification through multiple kernel learning on fragmentation trees. Bioinformatics 30, i157–i164. https://doi.org/10.1093/bioinformatics/btu275.
Siroli, L., Patrignani, F., Gardini, F., Lanciotti, R., 2015. Effects of sub-lethal concentrations of thyme and oregano essential oils, carvacrol, thymol, citral and trans-2-hexenal on membrane fatty acid composition and volatile molecule profile of Listeria monocytogenes, Escherichia coli and Salmonella enteritidis. Food Chem. 182, 185–192. https://doi.org/10.1016/j.foodchem.2015.02.136.
Skandamis, P.N., Nychas, G.-J.E., 2012. Quorum sensing in the context of food microbiology. Appl. Environ. Microbiol. 78, 5473–5482. https://doi.org/10.1128/AEM.00468-12.
Sterniša, M., Klančnik, A., Smole Možina, S., 2019. Spoilage *Pseudomonas* biofilm with *Escherichia coli* protection in fish meat at 5 °C. J. Sci. Food Agric. https://doi.org/10.1002/jsfa.9703.
Sybiya Vasantha Packiavathy, I.A., Agilandeswari, P., Musthafa, K.S., Karutha Pandian, S., Veera Ravi, A., 2012. Antibiofilm and quorum sensing inhibitory potential of Cuminum cyminum and its secondary metabolite methyl eugenol against Gram negative bacterial pathogens. Food Res. Int. 45, 85–92. https://doi.org/10.1016/j.foodres.2011.10.022.
Szczepanik, M., Walczak, M., Zawitowska, B., Michalska-Sionkowska, M., Szumny, A., Wawrzeńczyk, C., Brzezinska, M.S., 2018. Chemical composition, antimicromicrobial activity and insecticidal activity against the lesser mealworm *Alphitobius diaperinus* (Panzer) (Coleoptera: Tenebrionidae) of *Origanum vulgare* L. ssp. *hirtum* (link) and *Artemisia dracunculus* L. essential oils. J. Sci. Food Agric. 98, 767–774. https://doi.org/10.1002/jsfa.8524.
Truchado, P., Larrosa, M., Castro-Ibáñez, I., Allende, A., 2015. Plant food extracts and phytochemicals: their role as quorum sensing inhibitors. Trends Food Sci. Technol. 43, 189–204. https://doi.org/10.1016/j.tifs.2015.02.009.
Verma, M.K., Anand, R., Chisti, A.M., Kitchlu, S., Chandra, S., Shawl, A.S., Khajuria, R.K., 2010. Essential oil composition of *Artemisia dracunculus* L. (tarragon) growing in Kashmir -India. J. Essent. Oil Bear. Plants 13, 331–335. https://doi.org/10.1080/0972060X.2010.10643830.
Xin, L., Meng, Z., Zhang, L., Cui, Y., Han, X., Yi, H., 2017. The diversity and proteolytic properties of psychrotrophic bacteria in raw cows' milk from North China. Int. Dairy J. 66, 34–41. https://doi.org/10.1016/j.idairyj.2016.10.014.
Zhang, Y., Wei, J., Yuan, Y., Yue, T., 2019. Diversity and characterization of spoilage-associated psychrotrophs in food in cold chain. Int. J. Food Microbiol. 290, 86–95. https://doi.org/10.1016/j.ijfoodmicro.2018.09.026.

Table S1. GC/MS characteristic of TEO compounds.

Compound	Formula	RI - Wax	RI - DB-5
Alpha-pinene	C10H16	1035	939
Alpha-terpinene	C10H16	1184	1015
Limonene	C10H16	1208	1030
1,8-Cineole (eucalyptol)	C10H18O	1222	1031
Beta ocimene E	C10H16	1235	1041
Beta-phellandrene	C10H16	1245	1042
Gama-terpinene	C10H16	1249	1072
Beta ocimene Z	C10H16	1250	1051
Beta-caryophyllene	C15H24	1594	1414
Terpinen-4-ol	C10H18O	1606	1180
Methyl chavicol	C10H12O	1657	1199
Germacrene	C15H24	1705	1487
Geranyl acetate	C12H20O2	1761	1384
Elemicin	C12H16O3	1862	1514
Isoelemicin	C12H16O3	1944	1596
Methyl eugenol	C11H14O2	2001	1404
Spathulenol	C15H24O	2108	1578
Thymol	C10H14O	2179	1283
Methyl isoeugenol	C11H14O2	2188	1491

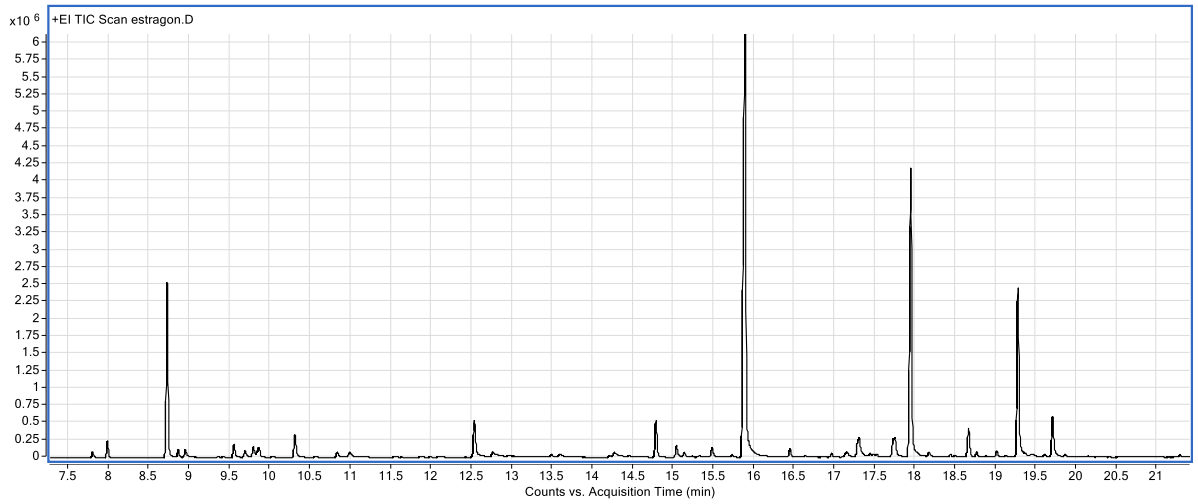

Fig.S1. TIC chromatogram of tarragon essential oil obtained on DB-5 column

Table.S2. HPLC characteristic of QS autoinductors.

Compound	Formula	Abbreviation	$[M+H]^+$	Retention time (min)
N-Butyryl-DL-homoserine lactone	C8H13NO3	C4-HSL	172.097	2.9
N-(3-Oxohexanoyl)homoserine lactone	C10H15NO4	3-oxo-C6-HSL	214.107	8.2
N-Hexanoyl-DL-homoserine lactone	C10H17NO3	C6-HSL	200.128	11.8
N-(3-Oxooctanoyl)-L-homoserine lactone	C12H19NO4	3-oxo-C8-HSL	242.139	11.9
N-(3-Oxododecanoyl)-L-homoserine lactone	C16H27NO4	3-oxo-C12-HSL	298.201	20.5
N-Dodecanoyl-DL-homoserine lactone	C16H29NO3	C12-HSL	284.222	21.3
N-(3-Oxotetradecanoyl)-L-homoserine lactone	C18H31NO4	3-oxo-C14-HSL	326.233	22.9
2-Heptyl-3-hydroxy-4-quinolone	C16H21NO2	PQS	260.165	12.8

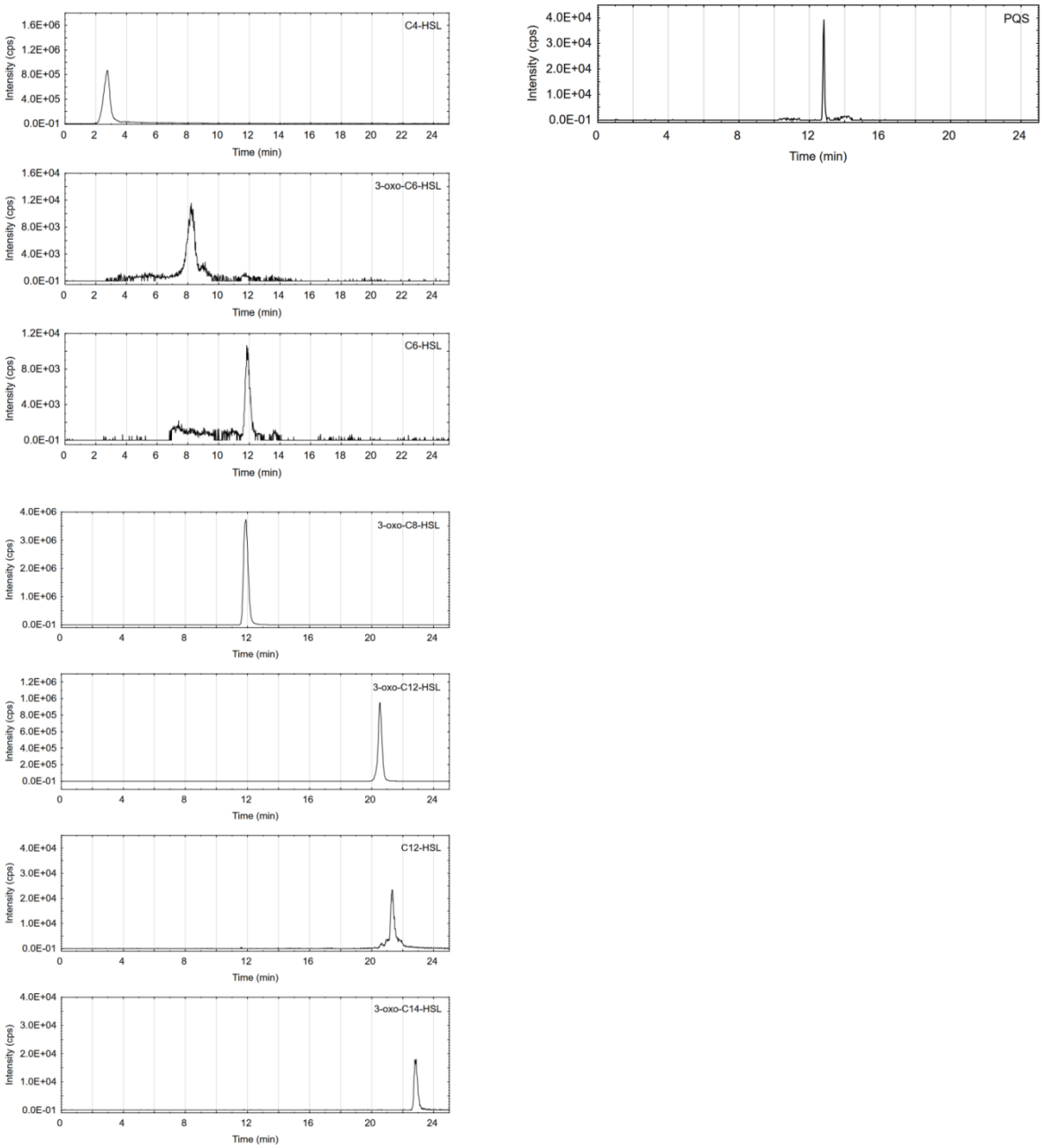

Fig.S2. Chromatograms of QS autoinductors

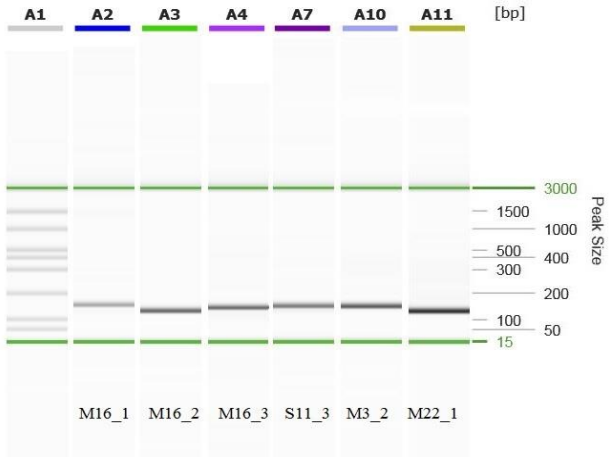

Fig.S3. Capillary electrophoresis gel image of analyzed genes' amplicons.

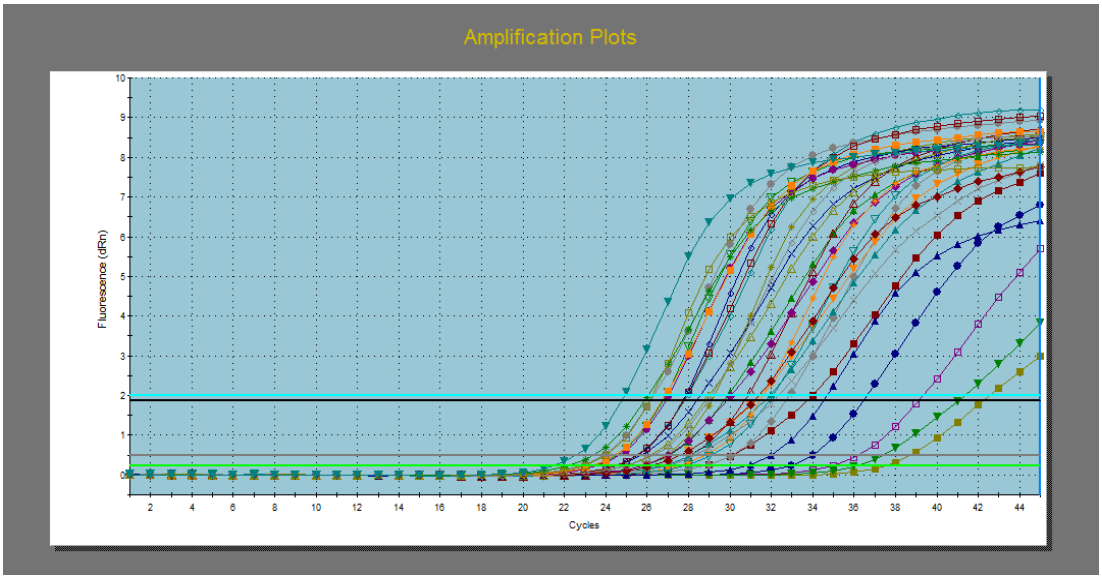

Fig.S4. Amplification Plots of analyzed genes for TSB medium.

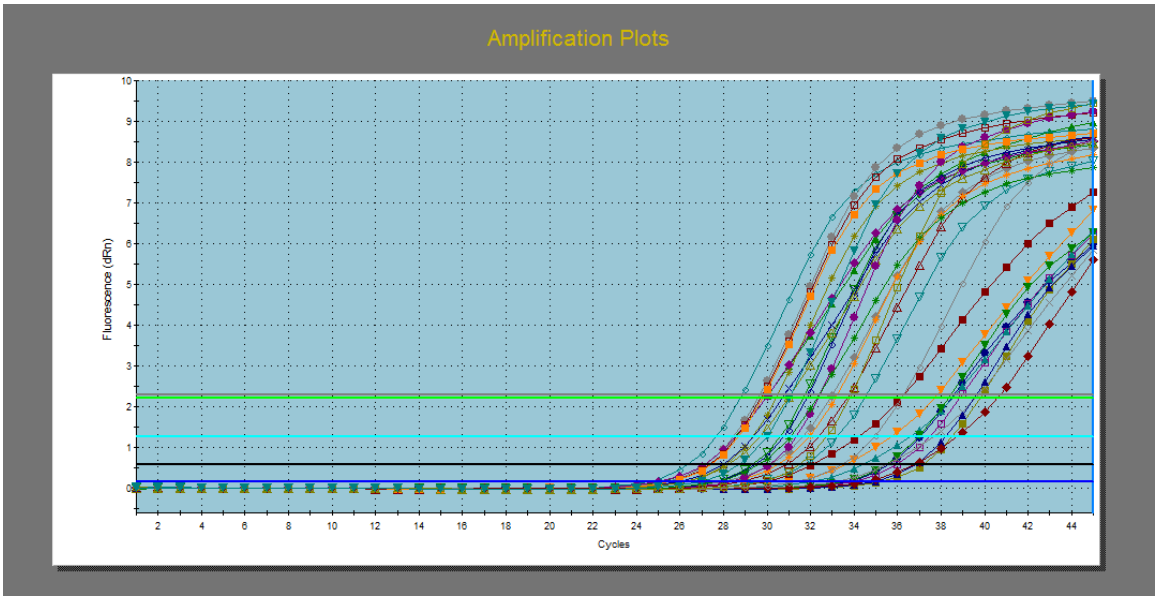

Fig.S5. Amplification Plots of analyzed genes for Fish Juice medium.

Food Control 130 (2021) 108284

Contents lists available at ScienceDirect

Food Control

journal homepage: www.elsevier.com/locate/foodcont

Effect of black pepper essential oil on quorum sensing and efflux pump systems in the fish-borne spoiler *Pseudomonas psychrophila* KM02 identified by RNA-seq, RT-qPCR and molecular docking analyses

Natalia Tomaś [a,*], Kamila Myszka [a], Łukasz Wolko [b], Katarzyna Nuc [b], Artur Szwengiel [c], Anna Grygier [c], Małgorzata Majcher [c]

[a] Department of Biotechnology and Food Microbiology, Poznan University of Life Sciences, Wojska Polskiego 48, 60-637, Poznań, Poland
[b] Department of Biochemistry and Biotechnology, Poznan University of Life Sciences, Dojazd 11, 60-632, Poznań, Poland
[c] Institute of Food Technology of Plant Origin, Faculty of Food Science and Nutrition, Poznań University of Life Sciences, Wojska Polskiego 31, 60-624, Poznań, Poland

ARTICLE INFO

Keywords:
Antimicrobial resistance
Transcriptomic
Proteolytic activity
Exopolysaccharide synthesis
Fish spoilage

ABSTRACT

Given the increasing consumption of aquatic foods and green consumerism, efficient methods for extending the shelf-life and maintaining the safety of seafood are urgently required. The present study aimed to evaluate the effect of black pepper essential oil (BPEO) and its major compounds – limonene (LIM) and beta-caryophyllene (CAR) on quorum sensing (QS) and efflux pump (EP) systems in *Pseudomonas psychrophila* KM02. Transcriptomic analysis was performed to select antimicrobial resistance genes that were only truly expressed within the system mimicking the food matrices. Compounds analyzed at subinhibitory concentrations (subMICs) (135, 65 and 35 μL/mL) reduced QS autoinducer synthesis to levels lower than the limit of detection and decreased proteolytic activity and exopolysaccharide synthesis by 35, 29 and 28%, and by 58, 32 and 41%, respectively. These phenotypic results were confirmed by changes in the ratio of expression of selected genes. Furthermore, the anti-QS activity and anti-EP of LIM and CAR were evaluated by molecular docking analyses with QS receptor proteins (LasR, RhlR, TraR, and PqsR) and inner membrane EP proteins (MuxB, MexB, and Mfs). The mRNA transcript levels of membrane fusion and outer membrane proteins, and transcription of repressor regulators MarR and TetR were considerable decreased. Our work showed that BPEO major compounds affected the functioning of the QS and EP system in KM02 and consequently reduced the spoilage potential.

1. Introduction

The importance of research regarding fish microbiota is related to increases in aquatic food production and consumption (Elbashir et al., 2018). Among specific fish-borne spoiler organisms, *Pseudomonas* species dominate (Sterniša et al., 2020). Recent findings identified *Pseudomonas psychrophila* as metabolically active cold-tolerant fish spoiler (Jia et al., 2020; Sobieszczańska et al., 2020; Sterniša et al., 2019; Zhuang et al., 2020). *P. psychrophila* produces extracellular enzymes (mostly proteinases) and exopolysaccharides that affect the quality of fish-based food products (Zhuang et al., 2020). The metabolic activities of *P. psychrophila* are regulated by the quorum sensing (QS) system (Bai & Vittal, 2014) which allows the bacteria to thrive under unfavorable conditions by regulating the transcription of specific genes (Schuster et al., 2003).

Due to the indiscriminative usage of antimicrobials in aquatic farming and preservatives in food chains, sensitivity to these substances is reduced in pseudomonads (Sterniša et al., 2020), which have developed an antimicrobial resistance (AMR) phenotype that is related to the efflux pump systems (EP) (Kabra et al., 2019). EPs effectively reduce the intracellular concentrations of antimicrobials (i.e., wide range of substrates that include, antibiotics, heavy metals, organic pollutants, plant-produced compounds, and sanitizers) by extrusion using energy derived from ionic gradients across the cell membrane or from ATP hydrolysis by ATPase (Rampioni et al., 2017). Additionally, the active efflux mechanism is engaged in QS (Seukep et al., 2019) and bacteria with deactivated or deleted EP are deficient in the secretion of QS signals that cannot diffuse through the bacterial membranes.

QS and EP functions can be blocked by phytochemicals (Yu et al., 2020) such as essential oils (EOs), which are excellent alternative

* Corresponding author.
E-mail address: natalia.tomas@up.poznan.pl (N. Tomaś).

https://doi.org/10.1016/j.foodcont.2021.108284
Received 18 March 2021; Received in revised form 25 May 2021; Accepted 26 May 2021
Available online 8 June 2021

resistance-modifying agents due to the presence of secondary metabolites, which include terpenes and phenylpropanoids. EOs can disturb cellular membranes and change their permeability and fluidity (Yu et al., 2020), which lead the bacteria to lose the ability to maintain the inherent properties necessary for EP activity (Blanco et al., 2016). Black pepper is one of the oldest and most extensively used spices in the world and possesses a wide spectrum of antimicrobial, antioxidative and medicinal properties. The potential application of black pepper essential oil (BPEO) as a biopreservative agent in the food industry was comprehensively reviewed by Myszka, Leja, and Majcher (2019).

EP and QS inhibition are mostly analyzed in clinical isolates, although recently, more studies have revealed AMR genes and EP and QS systems amidst foodborne pseudomonads (Quintieri et al., 2019). The combination of multidirectional analyses that consider phenotypic, genotypic, transcriptomic and computational analyses of strains isolated from foods provides a completely new approach in food microbiology (Lamas, 2019), and it is needed for efficient food preservation and to ensure safety, especially when green consumerism is in high demand.

In this work the *Pseudomonas psychrophila* KM02 strain isolated from commercially available raw salmon fillets was screened for genes involved in QS and EP systems based on genomic and transcriptomic analyses. BPEO was acquired, its chemical composition was characterized, and then a subinhibitory concentration (subMIC) evaluation against the KM02 strain was performed. The changes in membrane fatty acid (FA) composition, QS autoinducer profile, proteolytic activity, exopolysaccharides synthesis and expression of selected metabolic activity-related and QS and EP-system related genes was also evaluated. Finally, an *in silico* docking analysis was performed to provide a molecular explanation of BPEO's potential for QS and EP inhibition.

2. Materials and methods

2.1. Microorganism and culture conditions

The KM02 strain was revived as needed and cultured in TSB medium (BD Biosciences, San Jose, CA, USA). The culture was carried out in fish juice medium (FJM) prepared from fresh salmon fillets as described in our previous study (Sobieszczańska et al., 2020) and supplemented with subMICs of BPEO and its major compounds. Incubation was carried out at 4 ± 2 °C for 72 h to obtain approx. 10^8 CFU/mL. These culture conditions were used in the following experiments with two exceptions. In the RNA-seq analysis, KM02 cells were cultured in modified TSB medium with fish peptone (HiMedia Laboratories, Mumbai, India). In the RT-qPCR analysis of AMR genes expression, the cultures were supplemented with nalidixic acid (NA) (BioMaxima, Lublin, Poland) at a concentration of 30 μg/mL for 24 h and then, subMICs of BPEO, LIM and CAR (Sigma-Aldrich, Saint Louis, MO, USA) were added for the following 48 h.

2.2. BPEO extraction and identification of compounds

BPEO was obtained by hydrodistillation in a Clevenger-type apparatus from dried fruits of *Piper nigrum* L. cultivated in Vietnam. The compounds were further identified using a Hewlett-Packard HP 7890A gas chromatograph coupled to a 5975C mass spectrometer (Agilent Technologies, Santa Clara, CA, USA) as described in our previous study (Sobieszczańska et al., 2020).

2.3. SubMIC determination

SubMICs of BPEO, LIM and CAR in KM02 were determined by the broth macrodilution method according to CLSI (2012). Dimethyl sulfoxide (DMSO) (Sigma-Aldrich) was used to dissolve the analyzed substances and obtain a range of different concentrations. The maximum concentration of DMSO was 1%. After 72-h of incubation at 4 °C, the samples were tested visually and the first concentration that resulted in no significant growth inhibition (just below the MIC) was selected as subMIC for the experiments.

2.4. Microorganism and whole transcriptomic analysis (RNA-seq) of KM02

RNA-seq analysis was performed to identify antimicrobial resistance genes that were only truly expressed in KM02 cells within the system that mimicked the food matrices. The KM02 fish isolate was grown for 72 h at 4 °C in modified tryptic soy broth (TSB) medium with fish peptone (g/1000 mL of distilled water: 20.0 g of fish peptone; 2.5 g of glucose; 5.0 g of sodium chloride; and 2.5 g dipotassium phosphate) at 4 °C for 72 h to reach approx. 10^8 CFU/mL. The RNAqueous Kit (Thermo Fisher Scientific, Waltham, MA, USA) was used for total bacterial RNA isolation according to the manufacturer's instructions. Ribosomal RNA was removed using a Ribominus Transcriptome Isolation Kit (Invitrogen, Carlsbad, CA, USA). The libraries were constructed using the Collibri™ Stranded RNA Library Prep Kit for Illumina™ and the Collibri™ H/M/R rRNA Depletion Kit (Invitrogen), and they were quantitatively and qualitatively assessed using a Qubit fluorimeter (Thermo Fisher Scientific) and Bioanalyzer DNA electrophoregram (Agilent Technologies). Sequencing was carried out on a MiSeq Illumina sequencer by using a MiSeq Reagent Kit v3 (150 cycles) (Ilumina, Hayward, CA, USA). Reads were mapped to the corresponding genome assembly of KM02 (NZ_CP049044.1) and normalized by the RPKM (reads per kilobase per million mapped reads) calculated in CLC (version 20). The RPKM value represents a probabilistic estimate of the abundance of gene transcripts across sample. RNA-Seq data were deposited in the SRA NCBI data repository (Bioproject: PRJNA509367, Biosample: SRX9799402; SRA: SRR13376050).

2.5. Identification of AMR and selection of genes of interest

AMR genes were identified in the KM02 genome using the Resistance Gene Identifier (RGI) analysis tool (Alcock et al., 2019) which utilizes the Comprehensive Antibiotic Resistance Database (CARD) (Fanelli et al., 2020). Additionally, the Rapid Annotations using Subsystems Technologies (RAST) online bioinformatics tool was used for functional subgrouping of CDS involved in efflux and multidrug resistance. Subsequently, the BLASTP algorithm of the NCBI site (https://blast.ncbi.nlm.nih.gov/Blast.cgi) where amino acid sequences of selected proteins in FASTA format were submitted as a query against nonredundant protein sequences of *P. aeruginosa* (taxid: 287), *P. psychrophila* (taxid: 122355) or *E. coli* (taxid: 562) was used for homology prediction by pairwise alignment. From the set of whole–genome annotated CDSs, only those expressed in experimental conditions as indicated by RNA-seq were selected for further analysis.

2.6. Composition of fatty acid methyl esters (FAME)

The profile of the membrane fatty acid (FA) composition was evaluated by the method described in our previous study (Myszka, Olejnik, et al., 2019) using a GC-FID analysis performed on a Trace 1300 system (Thermo Fisher Scientific). FA was identified according to the retention times obtained for standard Bacterial Acid Methyl Esters (BAME) (Sigma-Aldrich) under equal chromatographic conditions. For each identified FA, the relative percentage abundance was determined based on the peak area in relation to the sum of the peak areas of the total detected FAs.

2.7. QS autoinducers estimation

The cell-free supernatants of KM02 cultures after incubation with subMICs of BPEO and its major compounds were extracted twice by ethyl acetate (with 0.1% formic acid) (Sigma Aldrich) and concentrated by rotary evaporation (Ravn et al., 2001). The extract was dissolved in

Table 1
List of genes evaluated in RT-qPCR analyses.

Gene name	Gene definition and role	Sequence of Fwd primer (5′-3′) Sequence of Rev primer (5′-3′)	Tm (°C)	Size (bp)
16S rRNA	the small subunit ribosomal RNA, internal reference gene	GGAGACTGCCGGTGACAAACT TGTAGCCCAGGCCGTAAGG	56	75
muxA	the RND efflux membrane fusion protein, part of the MuxABC-OpmB multidrug efflux complex	GTGTACTTCAAGGCGCTG TTGACCATCTGCCCTTCC	57	110
opmB	the outer membrane efflux protein that shows functional cooperation with MuxABC	GGCAGAGGTGGATCGTAA CACCTTCAATTGCACCAT	54	112
mexA	the RND efflux membrane fusion protein, part of the MexAB-OprM multidrug efflux complex	CCTTTTACCTTGACCACC TTTTACATCGCTGCCTTC	53	120
oprM	the outer membrane efflux protein that shows functional cooperation with MexAB	AGAACTACTTTGCAACCGA GTTTCAGCAGCTCTTTGT	55	108
tetR	the transcriptional local repressor that regulates the function of efflux pumps, osmotic stress etc.	TGTGTTTTCGCGCTTTCT GTAACTCTTCAAGGCTGGG	57	101
marR	the transcriptional global repressor that regulates the multiple antibiotic resistance	AAGGTGCTGATTATCATGG AGCTTTTTTTGCTCGAGG	54	119
hdts_1	1-acyl-sn-glycerol-3-phosphate acyltransferase; QS autoinducer probable synthase	GACGCGAGTGTTTTTGAA TAGGCCGAGAGGAAGAAG	54	120
hdts_2	1-acyl-sn-glycerol-3-phosphate acyltransferase; QS autoinducer probable synthase	CCCGCTTTCATTCCTGTC AATCAACTGGCTGTCACC	57	115
hdts_3	1-acylglycerol-3-phosphate O-acyltransferase; QS autoinducer probable synthase	CAGATGGATCCTGGGCTA AGTTGGATTGATGGTTGG	54	95
hdts_4	1-acyl-sn-glycerol-3-phosphate acyltransferase; QS autoinducer probable synthase	GACGTACAAGGTGCCGAA GCAATTGGCATTCCTCAC	55	111
hdts_5	1-acyl-sn-glycerol-3-phosphate acyltransferase; QS autoinducer probable synthase	CATCGTCTGCGTAAAGAGT ACGCCGGTATAGGTCACA	57	119
desA	the fatty acid desaturase responsible for converting SFA into UFA in bacterial membranes	CATCCACCGCAAACACCA TGAGCTTCTTCGCGATAC	56	117
algA	alginate lyase; mannose-1-P-guanylyltransferase/mannose-6-P-isomerase	TGGTGACCTTTGGCATTT CAAACCGCTCGACCTTAAA	55	102
algU	sigma factor σ; activator of the alginate synthesis operon	GTTGATCGTGCGTTTTGT CATGTGTAAAAGGCGCTG	56	117
mucA	anti-sigma factor σ; negative regulator of a*lgU*	GAAGCGGACGAACTGGAA GGAATCAACAGGTCCTTG	54	119
M22_1	metallopeptidase involved in peptide degradation	CGTGCCTACCGAGATTGA CGGAATACCCCAGGCAAA	56	112
M3_2	metallopeptidase involved in peptide degradation	GCTTTGCCCTTGATCGTA AAAAGTCATCCAGCCCCA	55	132
S11_3	serine peptidase with a wide range of peptidase activity	TATCGTCATCGACTCAGG GGTTCATAAAGTGGGTGT	51	134

100 mL methanol (Sigma Aldrich), and 5 μL of solution was injected for reverse phase-high performance liquid chromatography (RP-UHPLC) (Dionex UltiMate 3000 UHPLC, Thermo Fisher Scientific, Sunnyvale, CA, USA) with an ultrahigh-resolution orthogonal quadrupole time of flight (qTOF) mass spectrometer (maXis impact, Bruker Daltonik, Bremen, Germany) with an ESI source (ESI-MS). Analyses were performed as described in detail in our previous study (Sobieszczańska et al., 2020).

2.8. Evaluation of proteolytic activity inhibition

The changes in proteolytic activity were examined according to a spectrophotometric method originally described by Polychroniadou (1988) with some modifications as presented in our previous study (Sobieszczańska et al., 2020). The principle of the analysis is based on the measurement of the intensity of the yellow-orange color product (A420 nm) generated by the reaction between the released α-amino groups and the TNBS reagent (Sigma-Aldrich). The percent inhibition of proteolytic activity after treatment with subMICs of BPEO and its major compounds was calculated based on the following equations:

$$\% PI = 100 - \left(\frac{AP_t}{AP_c} \times 100\right)$$

where:

AP_t – absorbance value obtained for the sample with the given treatment;

AP_c – absorbance value obtained for the control sample (cells cultivated in fish juice medium)

2.9. Exopolysaccharides extraction and quantification

The procedure employed for analyzing exopolysaccharides in the KM02 cultures was described in detail in our previous study (Myszka et al., 2020). Briefly, after incubation, cells were harvested and subjected to an extraction procedure according to Forde and Fitzgerald (1999). The amounts of exopolysaccharides were quantified by colorimetry (A500 nm), by measuring the condensation of furan (corresponding to exopolysaccharides) with added tryptophan (Sigma-Aldrich) (Parkar et al., 2001). A standard curve using sodium alginate (Sigma-Aldrich) solution was prepared. The percent inhibition of exopolysaccharide synthesis in KM02 after treatment with subMICs of BPEO and its major compounds was calculated using the following formula:

$$\% EI = 100 - \left(\frac{EPS_t}{EPS_c} \times 100\right)$$

where:

EPS_t – μg/10^8 CFU of exopolysaccharides obtained for the sample with the given treatment;

EPS_c – μg/10^8 CFU of exopolysaccharides obtained for the control sample.

2.10. RNA isolation and cDNA synthesis

KM02 cultures were treated with RNAprotect® Bacteria Reagent (Qiagen, Valencia, CA, USA). Total RNA was isolated on a PureLink™ RNA Mini Kit (Thermo Fisher Scientific) and purified using the

PureLink™ DNase Set (Invitrogen) according to the manufacturer's protocols. The quantity and quality of isolated RNA were analyzed by fluorescence-based Qubit™ XR RNA and Qubit™ IQ RNA Assay Kits (Thermo Fisher Scientific) on a Qubit Fluorometer 4 (Thermo Fisher Scientific). The first strand of + cDNA was synthesized from 1.0 μg of total RNA with the High Capacity RNA-to-cDNA Kit (Life Technologies, Carlsbad, USA).

2.11. Quantitative real-time PCR experiment

RT-qPCR analyses were performed in a CFX96 system (BioRad, Hercules, CA) using GoTaq® Master Mix (Promega, Walldorf, Germany). The primers (Table 1) were designed using the CLC Genomics Workbench (Qiagen) based on the genome sequence of KM02 (GenBank accession no: CP049044). The cycling conditions were as follows: initial denaturation at 95 °C for 2 min; 40 cycles of denaturation at 95 °C for 15 s, annealing at 52 °C and extension at 72 °C for 15 s; followed by a melting curve. The amplification efficiency (E) was estimated using LinRegPCR software (Ruijter et al., 2009). The Pfaffl method (Pfaffl, 2001) was used to calculate the changes in gene expression. The results are presented as the ratio of gene expression in the treated samples compared with control samples (with expression equal to 1), with the expression normalized to the internal reference gene (16s rRNA):

$$ratio = \frac{E_{GOI}^{\Delta Ct_{target}(control-sample)}}{E_{ref}^{\Delta Ct_{ref}(control-sample)}}$$

where:

GOI – gene of interest, which changes in expression are calculated;
ref – reference gene, which expression is used for normalization.

2.12. Inhibition of EP activity and QS by in silico analysis

The QS receptor proteins were prepared for the molecular docking analysis as described in detail in our previous study (Sobieszczańska et al., 2020). The crystallographic structures of the identified EP proteins were modeled using the I-Tasser webserver (Roy et al., 2010). All protein structures were prepared for docking in Protein Preparation Wizard (Sastry et al., 2013) in the Schrodinger software suite, release 2020-4 (Schrödinger LLC, New York, NY). The docking grids were generated by selecting the residues involved in ligand binding sites. The three-dimensional structures of docked ligands were retrieved in SD format from the PubChem database and processed in the Ligand Preparation Panel. The molecular docking analyses were performed in the Glide Ligand Docking Panel, version 12.6 in the Schrödinger Maestro suite using Extra Precision mode (XP) (Friesner et al., 2006). Each generated protein-ligand complex was analyzed based on its docking score value (XP Glide GScore), which is used to show the estimated free energy of binding and the modified Coulomb-van der Waals interaction energy score. The docking results are also presented as 2D and 3D figures, which indicate the binding pose of a given ligand (conformation and orientation towards the protein). From the obtained figures, the major protein residues involved in docking, the length of the created bonds and the hydrophobic contacts were listed.

2.13. Statistical analysis

The experiments were performed in triplicate, and the results are expressed as the mean ± standard deviation. Significant differences ($p < 0.05$) were established by Student's t-test or analysis of variance (ANOVA) followed by Tukey's post hoc test performed in R (RStudio Team, 2015).

3. Results and discussion

Seafood products are prone to microbial deterioration because of the high water content and *postmortem* pH value (usually >6) of muscle (Hassoun & Çoban, 2017). These features contribute to a reduction in shelf life and economic losses in the fish industry (Jia et al., 2020). Bacteria from aquatic production ecosystems are subjected to enhanced selective pressure because of antibiotic overuse, which results in the overexpression of EP and QS systems (Quintieri et al., 2019). Given the increasing aquatic food consumption, efficient methods of extending the shelf-life and maintaining the safety of seafood are urgently required (Zhuang et al., 2020). In this work, we performed genomic and transcriptomic analyses to evaluate the potential of the alternative antimicrobial BPEO to inhibit QS and EP in KM02.

Table 2
GC/MS results of TEO composition with relative percentage values of individual compounds.

Compound name	RI - Wax	RI - DB-5	% Composition
α-pinene	939	1035	8.7
camphene	953	1080	0.8
β-pinene	980	1118	8.4
y-carene		1148	2.3
β-myrcene	990	1158	11.4
α-phellandrene	1006	1170	8.2
limonene	**1030**	**1208**	**19.1**
y-terpinene	1072	1249	0.8
p-cymene	1026	1274	2.9
α terpinolene	1083	1279	2.5
elemene		1456	1.9
α-cubebene	1348	1472	3.3
linalool	1100	1544	1.1
β-caryophyllene	**1414**	**1594**	**19.6**
α humulene	1449	1668	2.7
β-bisabolene		1736	1.5
β-edusmene		1741	1.3
delta-cadinene		1748	1.7
caryophyllene oxide	1573	1962	1.8

[%] Composition of individual compound was calculated from the chromatogram obtained in triplicate (normalized peak area %). Values in bold indicate the most abundant compounds. RI – Wax – retention index on Suplecowax 10 column. RI – DB-5 – retention index on DB-5 column.

3.1. Chemical composition of BPEO and subMICs

Recently, a growing trend has been observed for minimally processed food, in which consumers demand a lack of synthetic additives (Calo et al., 2015). Therefore, modern food technology is facing a great challenge of ensuring the microbiological safety of food, which can be accomplished by using natural antimicrobials to inhibit the growth and/or metabolic activities of bacteria (Hassoun & Çoban, 2017). The resistance mediated by EP could be successfully overcome by specific small-molecule inhibitors (Aparna et al., 2014). EOs are widely observed secondary metabolites of plants that are effective at subinhibitory concentrations, and they have great potential for utilization in the food industry to combat foodborne pathogens and spoilage organisms (Rao et al., 2019). The composition of EOs determines the range and type of antimicrobial activity (Yu et al., 2020); thus, to characterize the chemical composition of the obtained BPEO, a GC/MS analysis was performed.

As presented in Table 2, a total of 19 individual compounds were identified, and the most abundant compounds were monoterpene limonene (LIM) (19.1%) and sesquiterpene beta-caryophyllene (CAR) (19.6%). Our results are consistent with the average chemical composition of BPEO obtained from different geographical regions, as described in the work of Dosoky et al. (2019). The subMICs of BPEO, LIM and CAR towards the KM02 fish isolate were evaluated by the broth macrodilution method, and the following values were obtained: 135, 65 and 35 μL/mL (117.9, 54.7 and 31.6 mg/mL), respectively. These subMICs did not show any signs of significant growth inhibition, which was confirmed by the growth curve analysis (data not shown). However,

Table 3
AMR genes in *P. psychrophila* KM02 genome according to RGI analysis tool and corresponding protein products.

Genome location	% Identity of Matching Region	Detection criteria	Drug Class	Resistance Mechanism	AMR Gene Family	Protein product
1804483..1807638	41.86	protein homolog model	fluoroquinolone antibiotic; tetracycline antibiotic	antibiotic efflux	resistance-nodulation-cell division (RND) antibiotic efflux pump	WP_048351074.1
3137702..3140881	66.25	protein homolog model	fluoroquinolone antibiotic; tetracycline antibiotic	antibiotic efflux	resistance-nodulation-cell division (RND) antibiotic efflux pump	WP_019827266.1
3297653..3300754	43.37	protein homolog model	fluoroquinolone antibiotic; tetracycline antibiotic	antibiotic efflux	resistance-nodulation-cell division (RND) antibiotic efflux pump	WP_048351922.1
3402303..3403625	72.58	protein homolog model	fluoroquinolone antibiotic	antibiotic efflux	major facilitator superfamily (MFS) antibiotic efflux pump	WP_048352147.1

Table 4
RNA-seq results of proteins designated as AMR in the genome of *P. psychrophila* KM02 cultivated in modified TSB medium.

Protein product	Gene name	EP complex	Locus tag	RPKM value	Genome location
WP_019827863.1	MexA	MexAB-OprM	G5J76_RS08190	16.23	1807642..1808793
WP_048351074.1	MexB		G5J76_RS08185	31.11	1804483..1807638
WP_019827865.1	OprM		G5J76_RS08180	51.52	1803035..1804486
WP_019827265.1	MexE	MexEF-OprN	G5J76_RS14170	3.76	3140897..3142141
WP_019827266.1	MexF		G5J76_RS14165	0	3137702..3140881
WP_046810712.1	OprN		G5J76_RS14160	0	3136296..3137705
WP_019827131.1	MexC	MexCD-OprJ	G5J76_RS14800	0	3300757..3301953
WP_070334534.1	MexD		G5J76_RS14795	12.06	3297653..3300754
WP_019827133.1	OprJ		G5J76_RS14790	0	3296965..3297600
WP_048352147.1	Mfs	-	G5J76_RS15280	3.53	3402303..3403625
WP_019828288.1	TriA	TriABC-OpmH	G5J76_RS03425	0	798814..799905
WP_019828289.1	TriB		G5J76_RS03420	4.38	797750..798817
WP_019828290.1	TriC		G5J76_RS03415	3.05	794691..797753
WP_048352378.1	OpmH		G5J76_RS00940	13.01	218673..220109
WP_048351981.1	MuxA	MuxABC-OmpB	G5J76_RS12585	7.15	2756904..2758211
WP_019828952.1	MuxB		G5J76_RS12590	7.54	2758208..2761309
WP_019828953.1	MuxC		G5J76_RS12595	1.50	2761306..2764413
WP_019828954.1	OmpB		G5J76_RS12600	6.25	2764410..2765906
WP_048351711.1	EmrA	EmrAB-TolC	G5J76_RS20105	0	4440471..4441676
WP_019823174.1	EmrB		G5J76_RS20100	6.11	4438878..4440407
WP_046809716.1	TolC		G5J76_RS20110	0	4441686..4443161

RPKM – reads per kilo base per million mapped reads was calculated according to following equation: RPKM=(number of reads mapped to a gene x gene length x 10^6)/(total number of reads from given library x gene length in bp).

they are known to affect the viability of food spoilage bacteria (Myszka et al., 2017).

3.2. Identification and selection of AMR genes

Bioinformatic tools, such as CARD or RAST, provide convenient and quick answers about AMR potential and the results have been correlated with actual resistance traits of bacteria by many researchers (Camiade et al., 2020; Hendriksen et al., 2019; Thomas et al., 2017).

In this study, according to the CARD analysis tool, 4 strict hits of genes were observed in the genome of KM02 (Table 3) that contribute to AMR through an efflux mechanism classified into the major facilitator superfamily (MFS) (1 hit) and resistance-nodulation-cell division (RND) (3 hits). The pairwise alignment of the obtained proteins revealed homology with AbaQ and well-established triparty complexes of EP, such as MexAB-OprM, MexEF-OprN and MexCD-OprJ. Additionally, the TriABC-OpmH, MuxABC-OpmB and EmrAB-TolC complexes were also recognized using the RAST analysis tool. These EPs are cellular systems that confer bacterial resistance through detoxification by exporting a wide range of toxic compounds outside of the cell (Du et al., 2018), and promoting adaptation to cold temperature (Quintieri et al., 2019) or other stress factors (Blanco et al., 2016). Although bioinformatic analyses of genomes offer more comprehensive information on the genotypic characteristics of foodborne bacteria including identification of AMR compared to conventional antimicrobial tests (Thomas et al., 2017), recent findings have indicated that using only genomic data in the surveillance of AMR in food isolates might severely underestimate true resistance rates (Zwe et al., 2020). Furthermore, the presence of structurally homologous proteins in the genome of a given strain does not indicate whether they are active and expressed in cells (Camiade et al., 2020). Therefore, we performed a RNA-seq analysis of the KM02 strain cultivated in modified TSB medium with fish peptone to simulate the inherent conditions of life and select those AMR genes that are truly expressed. The RPKM calculation removed effects caused by sequencing depth and gene length when calculating gene expression (Liu et al., 2019).

The RNA-seq results for genes selected from the genome of KM02 are presented in Table 4. Among all of the recognized EP complexes, MexF with OprN from MexEF-OprN and EmrA with TolC from EmrAB-TolC were not expressed (FPKM value = 0) in KM02 cells and thus were not considered for further analyses. Pseudomonads are characterized by a cell envelope that consists of two membranes that function as a barrier to antimicrobials. Therefore, to effectively drive the efflux of compounds across the outer membrane, the assemblies of at least three proteins must be involved (Du et al., 2018). MexC represents a membrane fusion protein, and it likely assembles the RND-transporter (MexD) and the outer membrane channel protein (OprJ) into a functional pump unit (Mokhonov et al., 2004). When MexCD-OprJ is truly overexpressed (similar to MexEF-OprN) the transcription rates were high (>20), suggesting the RPKM value for MexE and MexD was probably not significant. Similarly, although the inner and outer membrane proteins from TriABC-OpmH complexes are expressed, Mima et al. (2007) indicated that this pump requires two membrane fusion proteins for function. Nevertheless, according to the results of experiments conducted by Yoneyama et al. (1997), the efflux machinery may be constructed such that the inner and outer membrane proteins loosely interact with each

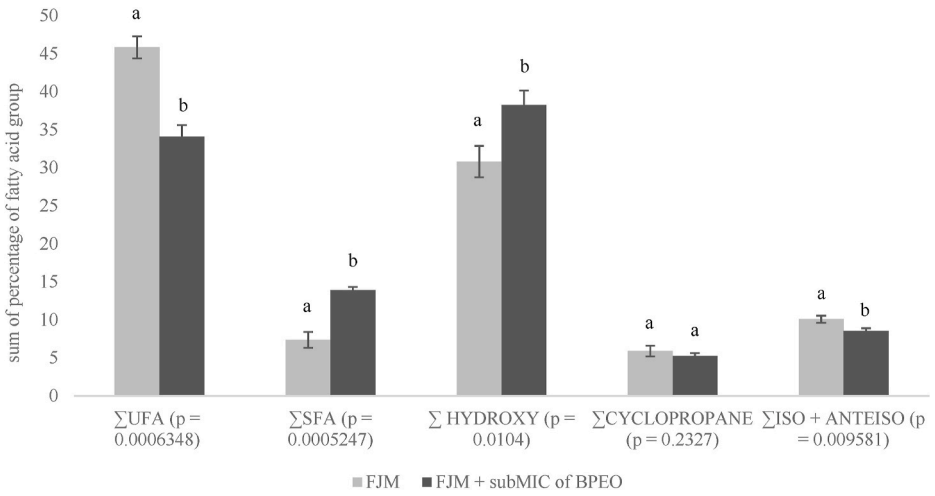

Fig. 1. The relative percentage of cellular fatty acid groups in *P. psychrophila* KM02 upon treatment with suMIC of BPEO

Values are expressed as mean ± sd, and are calculated from three independent biological replicates. The same letters indicates not statistically differences in sum of percentage of fatty acid group as provided by student's T test ($p < 0.05$).

∑UFA – sum of unsaturated fatty acids; ∑SFA – sum of saturated fatty acids; ∑HYDROXY – sum of fatty acids with hydroxyl group; ∑CYCLOPROPANE – sum of fatty acids with cyclopropane group; ∑ISO + ANTEISO – sum of fatty acids with branched chain.

other and still extrude antimicrobials, even in strains lacking membrane fusion proteins. However, the presence of all three RND components is required to function fully at maximum efficiency. The highest expression (RPKM = 51.21) of the outer membrane protein OprM indicated its probable involvement with other EP complexes (e.g. MexXY). Furthermore, OprM can replace the OprJ protein in MexCD-OprJ pump, but it is not able to induce antimicrobial resistance alone.

3.3. Effect of subMICs of BPEO on the KM02 cellular FA profile

The resistance of KM02 is not only determined by multidrug EP, but also results from a low permeability of the outer membrane. Moreover, EP proteins are embedded in these membranes; thus theirs dynamics, conformation and functionality in substrate extrusion are strictly dependent on their unique interactions with lipids. Consequently, changes in the FA composition may affect membrane-specific fluidity and disrupt efflux, which is called indirect inhibition. An example of indirect inhibition by influencing the bacterial membrane properties has been described for the MexAB-OprM inhibitor carbonyl cyanide m-chlorophenylhydrazon, which disrupts the proton gradient across the membrane (Mangiaterra et al., 2017). The exposure of bacterial cells to subMICs of EOs results in changes in the structure, composition and properties (mostly fluidity) of the cell membrane, which is the first target in the antimicrobial action of EOs (Rao et al., 2019). Therefore, a GC/FID analysis of the FA composition upon treatment with BPEO was performed and the relative percentage of each FA group was calculated.

As presented in Fig. 1, significant effect of the treatment was the decrease in unsaturated and branched FAs with increasing saturated and hydroxy FA levels. There was no significant change in cyclopropane FA, which are known to confer bacterial resistance to acid shock (Chang & Cronan, 1999) or freeze-drying (Muñoz-Rojas et al., 2006). According to Chao et al. (2010) branched-chain FAs affect membrane physiology in the manner that is similar to monounsaturated FAs, and their presence affects bacterial biofilm development. FAs with hydroxyl groups are mostly related to the lipopolysaccharides of the bacterial membrane, and their abundance after treatment with aromatic hydrocarbons is strain-dependent (Mrozik et al., 2004). The major effect of a given treatment on cellular membranes is demonstrated by the saturated/unsaturated FA ratio (Lyu et al., 2017), as an increasing degree of membrane lipid saturation appears to be one of the major mechanisms by which bacterial cells adapt to the presence of aromatic compounds (Mrozik et al., 2004). According to the reviewed literature in the work of Leite de Souza (2016), when EO components enter bacterial cells, they induce changes in the physical properties of the cell membranes and/or inhibit certain FA metabolizing enzymes. In *Pseudomonas* spp., the biosynthesis of unsaturated FAs occurs through the action of desaturase on primarily synthesized saturated FAs (Di Pasqua et al., 2006). Based on the obtained results, the expression of the gene encoding the enzyme responsible for SFA desaturation (*desa*) was hypothesized to be altered by the applied treatment. The comparative quantitation RT-qPCR analysis showed that the ratio of *desa* gene expression to the control culture (expression 1.0) was 0.0181 (±0.0016), 0.0668 (±0.0109) and 0.0504 (±0.0091) upon 72-h incubation at 4 °C with subMICs of BPEO, LIM, and CAR, which indicated a reduction in the presence of *desa* transcripts of 98.2%, 93.3% and 95.0%, respectively.

Table 5
RP-UHPLC-ESI-MS results of quality and quantity of autoinducers synthesized by *P. psychrophila* KM02 under different conditions.

Experiment variant	Concentration [μg mL^{-1}] (±SD) of signal molecules under different growth conditions								
	acyl homoserine lactones							alkyl quinolone molecules	
	3-oxo-C12-HSL	3-oxo-C14-HSL	3-oxo-C6-HSL	**3-oxo-C8-HSL**	C12-HSL	**C4-HSL**	C6-HSL	**PQS**	HHQ
FJM	**1.908 (±0.031)**	0.007 (±0.000)	0.015 (±0.000)	**1.119 (±0.063)**	0.136 (±0.004)	**1.217 (±0.010)**	0.017 (±0.000)	**0.007625** (±3.5E-05)	N/D
FJM + subMIC of BPEO	**<LOD**	<LOD	0.008 (±0.000)	**<LOD**	<LOD	**<LOD**	<LOD	**0.006713** (±0.000193)	N/D
FJM + subMIC of LIM	**<LOD**	<LOD	0.011 (±0.001)	**<LOD**	<LOD	**<LOD**	<LOD	**<LOD**	N/D
FJM + subMIC of CAR	**<LOD**	<LOD	0.008 (±0.000)	**<LOD**	<LOD	**<LOD**	<LOD	**<LOD**	N/D

Concentration [μg mL-1] (±SD) was calculated from calibration matrix with known concentration of each AHLs and alkyl quinolone molecules.
<LOD – less than limit of detection; LOD for 3-oxo-C12-HSL, 3-oxo-C14-HSL, 3-oxo-C6-HSL it was 0.005 μg/mL, for 3-oxo-C8-HSL, C12-HSL, C4-HSL and C6-HSL was 0.004 μg/mL; for HHQ and PQS were 0.0002 and 0.0001 μg/mL, respectively ND – not detected.

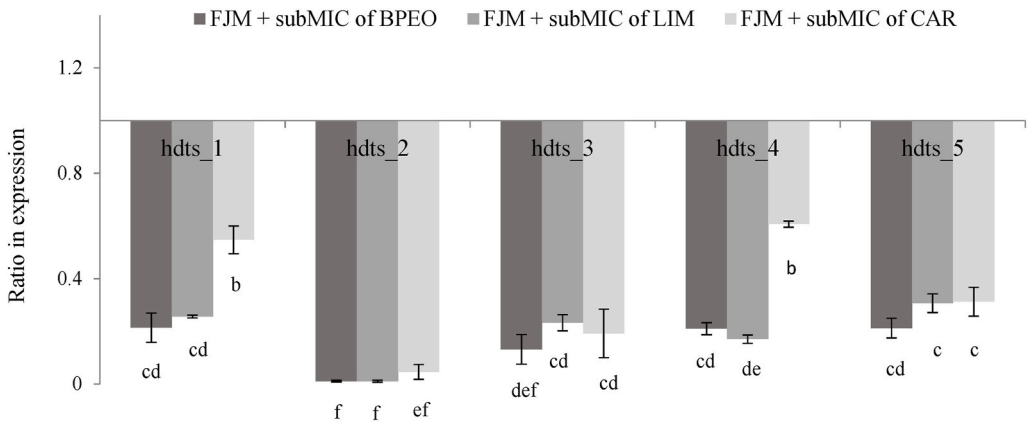

Fig. 2. The ratio in hdts genes expression upon treatment with subMIC of BPEO, LIM and CAR.
Values are expressed as mean ± sd ratio to control expression designated as 1, and are calculated from three independent biological replicates. The same letters indicates not statistically differences in expression as provided by Tukey's test after ANOVA analysis ($p < 0.001$).

Table 6
The percentage inhibition of proteolytic activity in *P. psychrophila* KM02 and ratio in gene expression after 72-h at 4 °C treatment with subMIC of BPEO, LIM and CAR.

Growth medium	Proteolytic activity inhibition relative to control culture (FJM growth medium)			
	% change obtained in spectrophotometric analyses (F = 1324, p = 4.01e-11***)	Ratio in expression of genes encoding proteases (F = 87.21, p < 2e-16***)		
		M22_1	*M3_2*	*S11_3*
FJM + subMIC of BPEO	−34.9 (±0.69)[a]	0.24 (±0.08)[c]	0.13 (±0.01)[c]	0.17 (±0.01)[c]
FJM + subMIC of LIM	−29.2 (±0.51)[b]	0.16 (±0.05)[c]	0.58 (±0.08)[b]	0.18 (±0.07)[c]
FJM + subMIC of CAR	−27.7 (±0.86)[b]	0.80 (±0.03)[a]	0.28 (±0.06)[c]	0.28 (±0.10)[c]

Values are expressed as mean ± sd from three independent biological replicates. The same letters indicates not statistically differences in expression as provided by Tukey's test after ANOVA analysis ($p < 0.001$).

3.4. Effect of subMICs of BPEO, LIM and CAR on KM02 autoinducer synthesis

The QS mechanism consists of three basic elements, namely, signal synthase, signal receptors and signal molecules, used by bacteria to coordinate the activities of cells (Chan et al., 2015). The search for QS inhibitors is mostly based on a compound's ability to inhibit the synthesis of QS signal molecules. In our previous work (Sobieszczańska et al., 2020) we demonstrated that KM02 produces the signaling molecules belonging to AHL and alkyl quinolones, and that the QS system is involved in its metabolic activity. Moreover, in the recent paper of Machado et al. (2020) the significance of QS systems among food-related bacteria is comprehensively described.

In this study, treatment with subMICs of BPEO, LIM and CAR resulted in lowering the autoinducer concentrations to values lower than the limit of detection from control values of 1.908, 1.217, 1.119, and 0.007625 μg/mL for 3-oxo-C12-HSL, C4-HSL, 3-oxo-C8-HSL and PQS molecules, respectively (Table 5). The concentrations of signal molecules produced by a single strain are consistent with the work of Li et al. (2018), who found that *P. fluorescens* produced 1.5 μg/ml C8-HSL. Because no *luxI* homologs were found in the genome of KM02 (data not shown), we hypothesized that signaling molecules are synthesized by hdts family proteins (Laue et al., 2000). Therefore, to investigate the molecular mechanism of synthesis inhibition, the changes in the expression of genes encoding probable autoinducer synthases (*hdts_1, hdts_2, hdts_3, hdts_4* and *hdts_5*) in KM02 were evaluated. As presented in Fig. 2, the highest reduction in *hdts* expression was obtained for BPEO (range from 79 to 99%), and the lowest was obtained for CAR (range from 39 to 95%). Interestingly, equal efficiency in the reduction of the *hdts_2* gene was observed regardless of the applied treatment. The inhibition of QS signaling molecules is considered a mechanism underlying the anti-QS activity of a given compound (Chan et al., 2015).

3.5. Effect of subMICs of BPEO, LIM and CAR on KM02 proteolytic activity

Aquatic food spoilage is mostly related to protein degradation processes, which manifest in changes in the physicochemical properties of fish flesh and the production of off-odors. The spoilage process has proteolytic enzymes whose synthesis is regulated by the QS system (Zhuang et al., 2020); thus, their inhibition can efficiently delay fish spoilage and extend shelf life. To evaluate the percent inhibition of KM02 proteolysis after treatment with subMICs of the analyzed compounds, a spectrophotometric method with TNBS reagent was used.

The results (Table 6) showed that the proteolytic activity was lowered by approx. 30% by the applied treatments, with the highest reduction in FJM supplemented with the subMIC of BPEO (−34.9%) and the lowest (−27.7%) in culture treated with the subMIC of CAR. This finding is consistent with RT-qPCR experimental results, thus confirming that the most efficient treatment for downregulation the expression of genes encoding metalloproteases was BPEO, with 76, 87 and 83% relative mRNA transcripts of *M22, M3* and *S11*, respectively. In our previous study (Sobieszczańska et al., 2020) these genes were analyzed in other *Pseudomonas* species (*P. orientalis* and *P. fluorescens*), and their expression was also downregulated by tarragon essential oil, methyl eugenol and beta-phellandrene administered at subMIC concentrations. The inhibition of bacterial proteolysis as a consequence of disturbing the QS system was found by other researchers with other bacteria (Li et al., 2018; Pattnaik et al., 2018; Zhao et al., 2018), and the usefulness of EO in the inhibition of this process was described in the work of Machado et al. (2020).

3.6. Effect of subMICs of BPEO, LIM and CAR on KM02 exopolysaccharide synthesis

Another factor that affects the predominance and persistence of pseudomonads in food matrices and is controlled by the QS system is related to the ability to synthesize exopolysaccharides, which enhance bacterial resistance to adverse conditions (Goltermann &

Table 7
The percentage inhibition of exopolysaccharide synthesis in *P. psychrophila* KM02 and ratio in gene expression after 72-h at 4 °C treatment with subMIC of BPEO, LIM and CAR.

Growth medium	Exopolysaccharide synthesis inhibition relative to control culture (FJM growth medium)			
	% change obtained in spectrophotometric analyses (F = 126.1, p = 4.49e-07***)	Ratio in expression of genes involved in alginate synthesis (F = 49.24, p = 9.7e-14***)		
		algA	*algU*	*mucA*
FJM + subMIC of BPEO	−58.1 (±2.3)[a]	0.18 (±0.06)[c]	0.64 (±0.08)[b]	0.40 (±0.03)[bc]
FJM + subMIC of LIM	−32.0 (±2.2)[b]	0.29 (±0.12)[c]	0.43 (±0.10)[bc]	3.08 (±0.84)[a]
FJM + subMIC of CAR	−40.5 (±5.2)[b]	0.26 (0.05)[c]	0.21 (±0.08)[c]	0.72 (±0.08)[b]

Values are expressed as mean ± sd from three independent biological replicates. The same letters indicate not statistically differences in expression as provided by Tukey's test after ANOVA analysis ($p < 0.001$).

Tolker-Nielsen, 2017). In this work, the ability of KM02 to produce exopolysaccharides and the inhibition of this activity by the subMICs of BPEO, LIM and CAR were evaluated. Upon reference conditions, KM02 produced 30.6 μg/10^7 CFUs of exopolysaccharides. As presented in Table 7, the highest percentage inhibition was observed in growth medium supplemented with BPEO (−58.1%), while the single compounds were less effective (−32.0% LIM, and −40.5% CAR). This tendency was consistent with the RT-qPCR results of the ratio of the expression of genes responsible for alginate synthesis, i.e., *algA* (alginate lyase), and alginate switching genes, which mediate the conversion to constitutive Alg + phenotype: *algU* (sigma factor α) and *mucA* (anti-sigma factor α) (Muhammadi & Ahmed, 2007). BPEO, LIM and CAR reduced the mRNA level of the *algA* gene by 82, 71 and 74%, with simultaneous reduction of transcription of the *algU* gene by 36, 57 and 79%, respectively. Interestingly, the lowest exopolysaccharide synthesis inhibition was observed when KM02 cells were exposed to subMIC of LIM, which was the only compound that upregulated *mucA* gene expression (ratio 3.08). Similar results were obtained in *Pseudomonas fluorescens* KM48 and *Pseudomonas orientalis* KM149 cells treated with *Myrtus communis* L. EO, which significantly upregulated *mucA* gene expression (Myszka et al., 2020). This result could have occurred due to similar action of a monoterpene – LIM and myrtle EO in which the major compounds were eucalyptol, alpha-pinene and myrtenyl acetate. According to Muhammadi and Ahmed (2007), the inhibition of *algU* activity by *muc* genes results in a nonmucoid phenotype; therefore it can be deduced that increased *mucA* expression is involved in increased regulatory action of *algU* genes and decreased alginate synthesis. Our results indicate that BPEO can be a promising source of compounds that alter bacterial polysaccharide production and delay fish spoilage.

3.7. Effect of subMICs of BPEO, LIM and CAR on KM02 on AMR gene expression

The development of AMR in bacteria is strictly related to the presence and functionality of EP systems, which are crucial for stress-adaptations, pathogenicity and resistance to antimicrobials (Yu et al., 2020). The level of bacterial resistance can be regulated according to different external factors or stresses, resulting in alleviated EP expression (Camiade et al., 2020). Compounds that are perceived as potential EP inhibitors are able to stop this process or even decrease EP

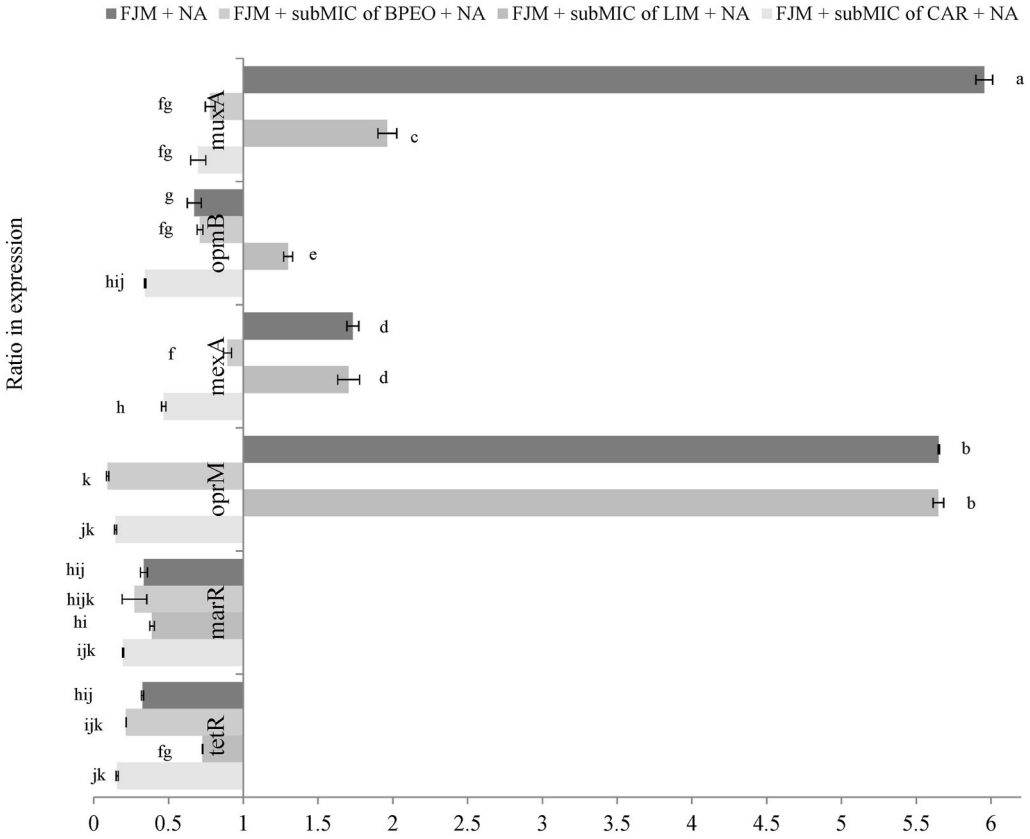

Fig. 3. The ratio in expression of genes encoding AMR genes upon treatment with subMIC of BPEO, LIM and CAR
Values are expressed as mean ± sd ratio to control expression designated as 1, and are calculated from three independent biological replicates. The same letters indicates not statistically differences in expression as provided by Tukey's test after ANOVA analysis ($p < 0.001$).

Table 8
The molecular docking analysis results of LIM, CAR, and inhibitors against *P. psychrophila* KM02 QS systems.

Molecular docking variant	XP Glide GScore [kcal/mol]	Glide Van der Waals energy [kcal/mol]	Glide Coulomb energy [kcal/mol]	Residues involved in interaction	Bond length [Å]	Type of interaction
LasR – LIM	−5.113	−18.908	−0.406	TYR64, ILE52, ALA50, TYR47	-	hydrophobic
LasR – CAR	−5.831	−0.974	0.147	LEU40, ILE52, ALA50, TYR47	-	hydrophobic
LasR-C30 Furanone	−4.563	−15.674	−5.374	SER129	1.88	halogen bond
				TRP60	1.73	H-bond
				TRP60	3.32	aromatic H-bond
LasR– 3-oxo-C12-HSL	−9.750	−44.667	−15.846	ASP73	2.30	H-bond
				TRP60	2.13	H-bond
				TYR56	1.80	H-bond
				TYR56	2.73, 2.52	aromatic H-bond
				ARG61	2.03, 1.99	2H-bond
				ARG61	2.35	H-bond
				TYR56	2.72	aromatic H-bond
				PHE101	2.65	aromatic H-bond
RhlR – LIM	−5.919	−17.245	−0.672	TRP68, LEU69, TYR72, PRO82	-	hydrophobic
RhlR – CAR	−7.285	−22.837	−0.778	TRP68, LEU69, TYR72, TYR42	-	hydrophobic
RHLR-C30 Furanone	−5.518	−17.191	−1.094	TRP68	2.04	aromatic H-bond
				TYR42, TYR64	-	hydrophobic
RhlR – C4HSL	−5.990	−21.963	−3.508	TRP68	2.62, 1.99	H-bond
				TYR42	2.61	aromatic H-bond
				ASP81	-	charged negative
TraR – LIM	−5.236	−17.294	0.369	TYR102,ALA38, LEU40, ALA105	-	hydrophobic
TraR – CAR	−6.811	−10.881	−0.011	TYR39, ALA38, TYR53, ALA76	-	hydrophobic hydrophobic
				THR115		polar
TraR – C30 Furanone	−4.978	−19.551	−2.022	TRP57	2.12	aromatic H-bond
				TYR61, VAL73	-	hydrophobic
TraR – 3-oxo-C8-HSL	−7.272	−37.530	−5.992	TRP57, ASP70	2.13, 1.77	aromatic H-bond
				TRP85	3.27	H-bond
PqsR – LIM	−5.138	−13.522	−0.192	TYR258, TRP234, LEU257, ILE236	-	hydrophobic
PqsR – CAR	−4.626	−15.761	−0.344	TYR258, ILE186, ALA187	-	hydrophobic
PqsR - QZN	−8.552	−36.205	−5.018	LEU207	1.70	aromatic H-bond
				TYR258, TRP234, PRO238,	-	hydrophobic
				ILE236	-	hydrophobic
PqsR – PQS	−7.772	−30.978	−5.477	LEU207	1.73	H-bond
				TRP234, ILE236, LEU208, ALA237	-	hydrophobic

expression. Therefore, to determine the effect of BPEO and its major compounds on EP systems identified in KM02, a RT-qPCR analysis of genes encoding membrane fusion proteins (*mexA* and *muxA*), and corresponding outer membrane proteins (*oprM* and *opmB*) was performed. Additionally, the genes belonging to transcriptional regulators of RND EP systems (*marR* and *tetR*) identified in the KM02 genome were also evaluated. The inactivation of MarR family proteins that act as transcriptional repressors results in reduced antibiotic accumulation by modulating efflux pump and porin expression (Alekshun & Levy, 1999). Similarly, TetR belongs to the transcriptional repressor family that regulates the expression of genes that encode proteins involved in multidrug resistance, antibiotic biosynthesis, osmotic stress, and pathogenicity, as well as enzymes implicated in different catabolic pathways (Ramos et al., 2005).

To determine the real impact of the analyzed compounds on AMR genes, first, the KM02 cultures were treated for 24 h at 4 °C with NA, a quinolone antibiotic (to which KM02 cells showed no susceptibility), and then, the subMICs were added and incubated for the following 48 h. The ratio of gene expression is shown in Fig. 3. The mRNA levels of the *muxA, mexA,* and *oprM* genes were significantly increased by NA treatment, explaining their probable involvement in conferring resistance. Our results are in agreement with Takrami et al. (2017), who demonstrated the resistance of *P. aeruginosa* to NA. In contrast, when cultures were supplemented with both NA and subMICs of BPEO and CAR, downregulated expression was observed. According to Yang et al. (2011), inactivation of *muxA* in MuxABC-OpmB resulted in increased resistance to antibiotics and attenuated virulence of *P. aeruginosa.* Similarly, the expression of the *opmB* gene was also downregulated, which indicates an alteration of the function of the whole complex. Interestingly, there was no significant change in the expression of the *mexA* and *oprM* genes in the cultures treated with NA and with NA and LIM, showing no inhibitory effect of LIM on MexAB-OprM EP. This finding is different from those in the work by de Araújo et al. (2021), where LIM, in association with ethidium bromide and antibiotics, demonstrated enhanced antibacterial activity and inhibited the MrsA and TetK pumps in *Staphylococcus aureus.* All the treatments led to equal inhibition of the expression of *marR*, which acts as a repressors and regulates multiple antibiotic resistance, EPs, osmotic stress, etc. (Ramos et al., 2005). This result probably occurred because this protein is overexpressed only when cells are not engaged in the efflux of toxic compounds. Similarly, the mRNA transcripts of the *tetR* gene (the local regulatory factor of multidrug resistance) were decreased. According to Du et al. (2018), efflux regulation can differ between species and depends on the cellular physiological status of cells.

3.8. Inhibition of QS by in silico analysis

The QS system is essential for triggering collective behavior in

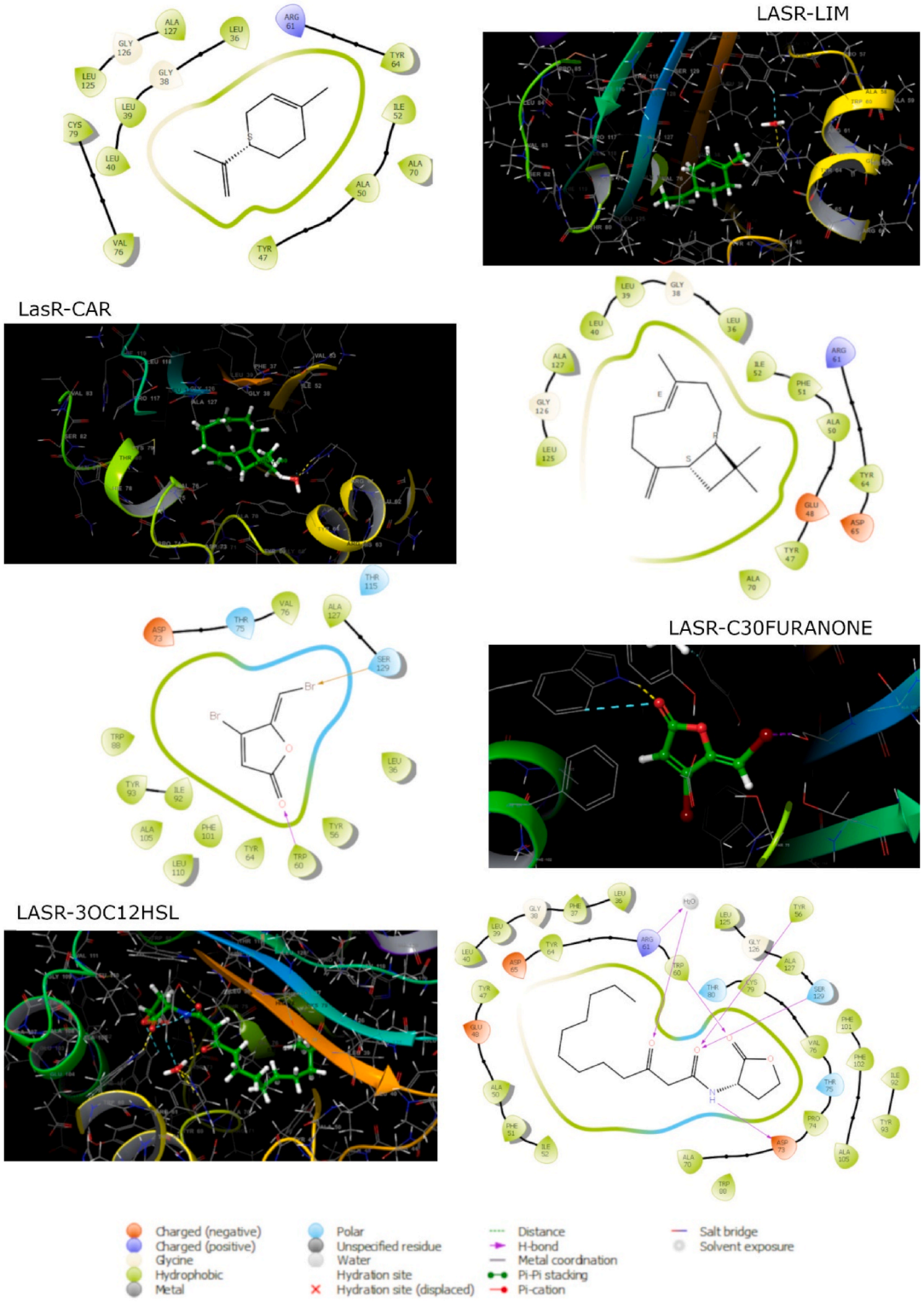

Fig. 4. The presentation of molecular docking of LasR protein with limonene (LASR-LIM), beta-caryophyllene (LASR-CAR), inhibitor C30-furanone (LASR-C30FURANONE), and cognate AHL molecule 3-oxo-C12-HSL (LASR-3OC12HSL).

bacteria, either pathogenicity or metabolic activity, and it depends on specific interactions between autoinducers synthesized or occurring in the surroundings of cells and cognate receptor proteins that act as transcriptional regulators of specific genes (Machado et al., 2020). Therefore, to investigate the potential inhibitory effect on the QS system of BPEO major compounds, we performed a molecular docking analysis, which is widely used by researchers to explore the interaction of ligand molecules with the specific active site of the protein, and calculate docking score of the ligand-receptor complex (Annapoorani et al., 2012). Based on the QS autoinducer results and our previous study (Sobieszczańska et al., 2020), we selected the LasR, RhlR, TraR and PqsR proteins for molecular docking analyses with LIM, CAR, and the respective signal molecules: 3-oxo-C12-HSL, C4-HSL, 3-oxo-C8-HSL, and PQS. Additionally, docking experiments with known QS inhibitors,

Table 9
The molecular docking analysis results of LIM, CAR, and inhibitors against *P. psychrophila* KM02 EP systems.

Molecular docking variant	XP Glide GScore [kcal/mol]	Glide Van der Waals energy [kcal/mol]	Glide Coulomb energy [kcal/mol]	Residues involved in interaction	Bond length [Å]	Type of interaction
MFS – LIM	−2.332	−12.940	0.251	ARG30	-	hydrophobic
				ALA347		
				TYR248		
MFS – CAR	−4.092	−17.646	−0.257	PHE120	-	polar
				ARG30		hydrophobic
				ALA347		hydrophobic
MFS – kaempferol	−8.011	−30.496	−8.505	PHE120	4.75	π – π
				ARG30	1.95	aromatic H-bond
				ALA347	1.98	aromatic H-bond
				ASN374	2.36	aromatic H-bond
				TYR248	2.73	H-bond
MEXB – LIM	−3.034	−17.740	−0.073	ASN33	-	hydrophobic
				PRO36		hydrophobic
				GLU672		polar
MEXB – CAR	−4.434	−26.185	−0.531	ASN33	-	polar
				PRO36		polar
				ALA39		hydrophobic
MEXB – PaβN	−6.414	−36.114	−7.131	PHE388	4.52	π – π
				GLN469	2.70	H-bond
				GLY296	2.77	H-bond
				GLY296	2.20	aromatic H-bond
				ASN33	2.16	aromatic H-bond
				PRO36	2.27	aromatic H-bond
				GLU672	2.28	aromatic H-bond
				GLU672	2.05	aromatic H-bond
				GLU672	4.40	salt bridge
MUXB – LIM	−3.311	−14.913	1.286	ARG323	-	charged positive
				THR657		charged positive
				ASP660		hydrophobic
MUXB – CAR	−2.826	−10.653	−0.012	GLN654	-	hydrophobic
				ALA135		
MUXB – theobromine	−4.365	−20.759	−6.496	GLN654	1.68	aromatic H-bond
				GLN563	2.06	aromatic H-bond
				ARG323	-	charged positive
				THR657	-	charged positive

C30-furanone (Li et al., 2018), quinazolinone analogs (Ilangovan et al., 2013), Phe-Arg-β-naphthylamide (Rampioni et al., 2017), kaempferol and theobromine (Ghosh et al., 2020) were performed. For each analyzed complex, apart from the XP Glide GScore, which approximates the ligand binding free energy, the major interactions regarding residues involved in docking, distances and types of interactions are presented in Table 8.

The interactions between the LasR protein and 3-oxo-C12-HSL had the highest docking score value (−9.750 kcal/mol) due to the range of H-bonds created with the ASP73, TRP60, TYR56, ARG61, TYR56 and PHE101 residues (Fig. 4). According to Klebe (2013), hydrogen bonds provide the stability of complex molecules and play a key role in molecular recognition. The known inhibitor of the LasR protein C30 furanone also formed an H-bond with the TRP60 residue with an additional halogen bond between the Br atom and SER129. Interestingly, LIM and CAR had higher XP Glide GScore values (−5.113 and −5.831 kcal/mol respectively) than the inhibitor molecule, which may be due to the high number of hydrophobic bonds in the surrounding of the common residues LEU36, ARG61, TYR64, and ALA127 are the key amino acid residues taking part in the interaction with the LasR receptor. Our results are in agreement with the work of Annapoorani et al. (2012), where the virtual screening of QS inhibitors among 1,920 natural compounds included a docking analysis against LasR and identified the same active binding site.

Second, in the QS hierarchy, the RhlR protein exhibited the highest binding affinity with the CAR molecule (−7.285 kcal/mol), which had tight hydrophobic enclosure of TRP68, LEU69, TYR72, and TYR42 residues. The other docked compounds had almost equal docking score values and occupied the same active site of the RhlR protein (Supplement_Fig. 6). H-bonds were only observed in the complex with cognate AHL and C30 furanone inhibitor. The common residue involved in docking was TRP68, indicating its role in the active binding site of the RhlR protein (Pattnaik et al., 2018). In contrast, in the work of Kumar et al. (2015), the major residues that formed H-bonds with the C4-HSL molecule were TYR68 and ASP81. Such minor differences may be attributed to the protein preparation procedure, which in our work involved the application of the OPLS3e (Optimized Potentials for Liquid Simulations) force field for restrained minimization, while others used OPLS 2005. OPLS3e leads to greater accuracy because it lowers the relative binding free energy error in docking procedures (Roos et al., 2019).

The cognate receptor protein for the 3-oxo-C8-HSL signaling molecule is TraR, which interacts via H-bonds with TRP57, ASP70 and TRP85 residues (Supplement_Fig. 7). The total docking score of LIM and CAR was higher (−5.236 and −6.811 kcal/mol) than the score of the inhibitor – C30 furanone (−4.978 kcal/mol); however, not the same residues of the TraR protein were involved in the complex interactions. Nevertheless, the effective binding of a given compound results in conformational changes in the protein, which consequently disturb its transcriptional activity in the activation of QS-dependent gene expression (Kumar et al., 2015).

The last analyzed protein (PqsR) is chemically distinct from previously described QS systems, also known as MvfR. PqsR formed a stable complex via H-bonds with its cognate signaling molecule, 2-alkyl-4-quinolone (Supplement_Fig. 8), and the docking score value was −7.772 kcal/mol. Interestingly, the PqsR protein had a higher affinity for the inhibitor 3-NH2-7Cl–C9-quinazolinone (QZN), whose structure is similar for the natural ligands (Soheili et al., 2019). This phenomenon can result from high hydrophobic interactions in addition to the formation of the same H-bond with the LEU207 residue as in the case of the

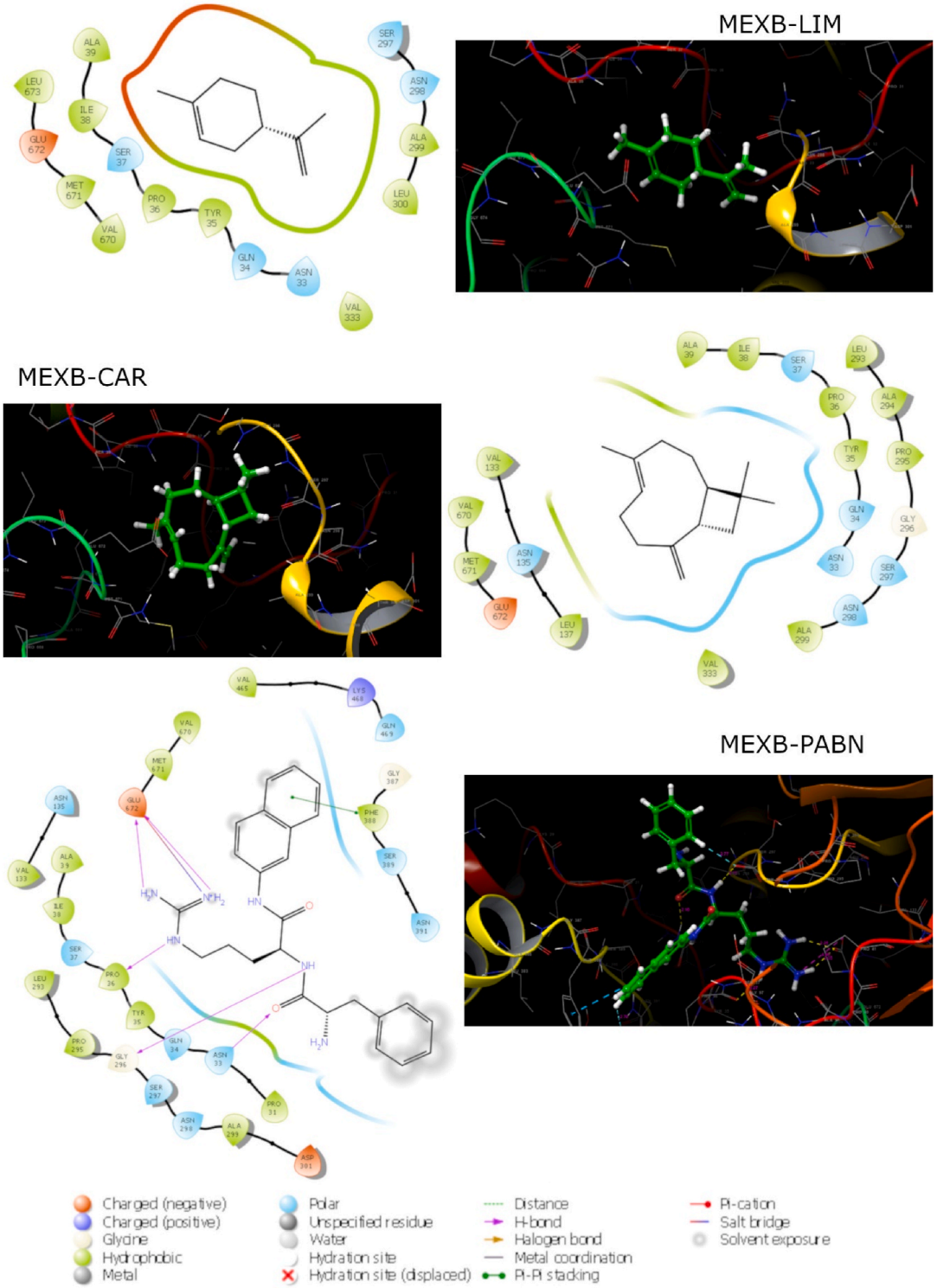

Fig. 5. The presentation of molecular docking of MexB protein with limonene (MEXB-LIM), beta-caryophyllene (MEXB-CAR) and inhibitor kaempferol (MEXB- PaβN).

PQS molecule. Because LIM and CAR molecules are considerably smaller molecules than PQS or QZN, they occupy only a small part of the binding site of the PqsR protein.

These results indicated that LIM and CAR might efficiently bind to the transcriptional regulators of the QS system in KM02, which would lead to inhibition of QS-dependent metabolic activity of cells, resulting in lower spoilage potential and pathogenic phenotype (Ding et al., 2019).

3.9. Inhibition of EP systems by in silico analysis

In addition to altering EP related gene expression, an effective way to target AMR is to directly bind and block EP via specific substrates/drugs, either in a competitive or a non-competitive manner (Kabra et al., 2019).

Considering previous evidence that natural products may act as EPIs in bacteria (Aparna et al., 2014), this work aimed to evaluate the ability of BPEO major compounds to inhibit MexAB-OprM and MuxABC-OpmB efflux systems identified in KM02 by *in silico* molecular docking analysis. To date, studies of hybrid transporters demonstrated that outer membrane factor proteins do not possess any substrate specificity, and their involvement in transport reactions is determined only by their ability to bind an inner membrane complex. However, recent findings (Marshall & Bavro, 2020) have shown that some specificity resides at least in part with the outer membrane channel of the ArcAB-TolC complex. In general, the substrate specificity of the complex appears to be determined by the inner membrane component of a given EP (Li et al., 2016); thus molecular docking analyses were conducted with the MexB, MuxB, and Mfs proteins that are responsible for drug binding and transport and interaction with partner proteins. From experiments, the same molecular docking parameters used in the QS analyses were extracted and analyzed.

The overall docking results are presented in Table 9. Although the highest docking score values were obtained for known inhibitors of the analyzed proteins (from −4.365 to −8.011 kcal/mol), the molecular docking results provided evidence that BPEO major compounds target the same EP binding pockets and thus can successfully alter the EP systems. The Mfs protein interacted with the highest affinity with kaempferol inhibitor (−8.011 kcal/mol) via pi-pi bond with PHE120 residue and H bonds with ARG30, ALA347, ASN374, and TYR248 residues. ARG30 and ALA347 were also involved in LIM and CAR docking, although they only interacted hydrophobically (Supplement_Fig. 9), which resulted in lower docking score values (−2.332 and −4.092 kcal/mol, respectively).

The Phe-Arg-β-naphthylamide (PaβN) inhibitor (Rampioni et al., 2017) had high interactions (−6.414 kcal/mol) with the MexB protein by PHE388, GLU672, PRO36, GLY296 and ASN33 residues (Fig. 5). Our results are in agreement with that of Aparna et al. (2014), who also evaluated that whether the binding site is formed by residues PRO36, PHE388 and GLN469 in the *P. aeruginosa* MexB protein. Among the BPEO major compounds, the CAR molecules had a higher affinity and van der Waals energy with MexB, which can be due to electrostatic interactions with ASN33 and PRO36 residues. Electrostatic interactions are the dominant energetic factor in protein-ligand binding (Klebe, 2013).

A direct MuxB protein inhibitor has not been previously reported; thus, we conducted a series of molecular docking experiments with known RND EP inhibitors (data not shown); and selected theobromine (Ghosh et al., 2020), that was successfully docked in the binding pocket with an XP Glide GScore value of −4.365 kcal/mol. The major interactions concerned aromatic H-bonds with GLN654 and GLN563 and electrostatic interactions with positively charged ARG323 and THR657 residues (Supplement_Fig. 10). Compared with the previous two EP proteins, LIM has a higher docking score value (−3.311 kcal/mol) than CAR (−2.826 kcal/mol), which can be explained by the same electrostatic interactions between the ARG323 and THR657 residues as in the inhibitor docking variant.

4. Conclusions

In conclusion, the QS system, which regulates bacterial gene expression and the EP system, which provides for the extrusion of toxic compounds outside the cell, are both essential for microorganisms to circumvent stress and negative environmental conditions (Seukep et al., 2019). Throughout the whole aquatic food production chain, bacteria from fish habitats are exposed to different stressors that trigger a specific reaction in the cells (Zhuang et al., 2020). Because the major function of the QS and EP systems is bacterial adjustment and survival under given conditions, research concerning the effective inhibition or alteration of those systems is needed to ensure food quality and safety, especially fish and aquatic food products, which are considered beneficial for health (Elbashir et al., 2018). In this work, we performed a series of analyses to evaluate the phenotypic and molecular responses of *P. psychrophila* fish isolates, grown in fish juice medium as a food-mimicking system to investigate the effectiveness and mode of action of BPEO towards QS and EP systems. EOs are green antimicrobials in food that are low-cost, biocompatible, and non-toxic (or less toxic) to eukaryotic cells and the environment (Yu et al., 2020). Although many studies have provided strong evidence of EO antimicrobial activity in *in vitro* and *in situ* conditions that results in decreased food spoilage activity (Calo et al., 2015), more investigations regarding the control the spread of AMR dispersal in food-related microbiota are needed.

CRediT authorship contribution statement

Natalia Tomaś: Conceptualization, Investigation, Formal analysis, Visualization, Writing – original draft, Writing – review & editing. **Kamila Myszka:** Conceptualization, Methodology, Investigation, Resources, Project administration, Funding acquisition, Supervision. **Łukasz Wolko:** Methodology, Investigation, Visualization. **Katarzyna Nuc:** Methodology, Investigation, Visualization. **Artur Szwengiel:** Methodology, Investigation, Visualization. **Anna Grygier:** Methodology, Investigation, Visualization. **Małgorzata Majcher:** Methodology, Investigation, Visualization.

Declaration of competing interest

The authors declare that there are no conflicts of interest associated with this publication.

Acknowledgements

This study was supported by a grant from the National Science Centre, Poland (no. 2016/23/D/NZ9/00028).

Appendix A. Supplementary data

Supplementary data to this article can be found online at https://doi.org/10.1016/j.foodcont.2021.108284.

References

Alcock, B. P., Raphenya, A. R., Lau, T. T. Y., Tsang, K. K., Bouchard, M., Edalatmand, A., Huynh, W., Nguyen, A.-L. V., Cheng, A. A., Liu, S., Min, S. Y., Miroshnichenko, A., Tran, H.-K., Werfalli, R. E., Nasir, J. A., Oloni, M., Speicher, D. J., Florescu, A., Singh, B., … McArthur, A. G. (2019). CARD 2020: Antibiotic resistome surveillance with the comprehensive antibiotic resistance database. *Nucleic Acids Research, 8*(48), 517–525. https://doi.org/10.1093/nar/gkz935

Alekshun, M. N., & Levy, S. B. (1999). The mar regulon: Multiple resistance to antibiotics and other toxic chemicals. *Trends in Microbiology, 7*, 410–413. https://doi.org/10.1016/S0966-842X(99)01589-9

Annapoorani, A., Umamageswaran, V., Parameswari, R., Pandian, S. K., & Ravi, A. V. (2012). Computational discovery of putative quorum sensing inhibitors against LasR and RhlR receptor proteins of *Pseudomonas aeruginosa*. *Journal of Computer-Aided Molecular Design, 26*, 1067–1077. https://doi.org/10.1007/s10822-012-9599-1

Aparna, V., Dineshkumar, K., Mohanalakshmi, N., Velmurugan, D., & Hopper, W. (2014). Identification of natural compound inhibitors for multidrug efflux pumps of *Escherichia coli* and *Pseudomonas aeruginosa* using in silico high-throughput virtual screening and in vitro validation. *PLoS One, 9*, Article e101840. https://doi.org/10.1371/journal.pone.0101840

de Araújo, A. C. J., Freitas, P. R., Dos Santos Barbosa, C. R., Muniz, D. F., Ribeiro-Filho, J., Tintino, S. R., Júnior, J. P. S., Filho, J. M. B., de Sousa, G. R., & Coutinho, H. D. M. (2021). Modulation of drug resistance by limonene: Inhibition of efflux pumps in *Staphylococcus aureus* strains RN-4220 and IS-58. *Current Drug Metabolism, 22*(2), 110–113. https://doi.org/10.2174/1389200221999210104204718

Bai, A. J., & Vittal, R. (2014). Quorum sensing regulation and inhibition of exoenzyme production and biofilm formation in the food spoilage bacteria *Pseudomonas psychrophila* PSPF19. *Food Biotechnology, 28*, 293–308. https://doi.org/10.1080/08905436.2014.963601

Blanco, P., Hernando-Amado, S., Reales-Calderon, J., Corona, F., Lira, F., Alcalde-Rico, M., Bernardini, A., Sanchez, M., & Martinez, J. (2016). Bacterial multidrug efflux pumps: Much more than antibiotic resistance determinants. *Microorganisms, 4*(1), 14. https://doi.org/10.3390/microorganisms4010014

Calo, J. R., Crandall, P. G., O'Bryan, C. A., & Ricke, S. C. (2015). Essential oils as antimicrobials in food systems – a review. *Food Control, 54*, 111–119. https://doi.org/10.1016/j.foodcont.2014.12.040

Camiade, M., Bodilis, J., Chaftar, N., Riah-Anglet, W., Gardères, J., Buquet, S., Ribeiro, A. F., & Pawlak, B. (2020). Antibiotic resistance patterns of *Pseudomonas* spp. isolated from faecal wastes in the environment and contaminated surface water. *FEMS Microbiology Ecology, 96*(2). https://doi.org/10.1093/femsec/fiaa008. fiaa008.

Chang, Y.-Y., & Cronan, J. E. (1999). Membrane cyclopropane fatty acid content is a major factor in acid resistance of *Escherichia coli*. *Molecular Microbiology, 33*(2), 249–259. https://doi.org/10.1046/j.1365-2958.1999.01456.x

Chan, K.-G., Liu, Y.-C., & Chang, C.-Y. (2015). Inhibiting N-acyl-homoserine lactone synthesis and quenching *Pseudomonas* quinolone quorum sensing to attenuate virulence. *Frontiers in Microbiology, 6*, 1173. https://doi.org/10.3389/fmicb.2015.01173

Chao, J., Wolfaardt, G. M., & Arts, M. T. (2010). Characterization of *Pseudomonas aeruginosa* fatty acid profiles in biofilms and batch planktonic cultures. *Canadian Journal of Microbiology, 56*(12), 1028–1039. https://doi.org/10.1139/W10-093

Clinical and Laboratory Standards Institute. (2012). *Methods for dilution antimicrobial susceptibility tests for bacteria that grow aerobically*. Approved Standard—Ninth Edition, ISBN 1-56238-784-7.

Di Pasqua, R., Hoskins, N., Betts, G., & Mauriello, G. (2006). Changes in membrane fatty acids composition of microbial cells induced by addiction of thymol, carvacrol, limonene, cinnamaldehyde, and eugenol in the growing media. *Journal of Agricultural and Food Chemistry, 54*(7), 2745–2749. https://doi.org/10.1021/jf0527221

Ding, T., Li, T., & Li, J. (2019). Virtual screening for quorum sensing inhibitors of *Pseudomonas fluorescens* P07 from a food-derived compound database. *Journal of Applied Microbiology, 127*(3), 763–777. https://doi.org/10.1111/jam.14333

Dosoky, N. S., Satyal, P., Barata, L. M., da Silva, J. K. R., & Setzer, W. N. (2019). Volatiles of black pepper fruits (*Piper nigrum* L.). *Molecules, 24*(23), 4244. https://doi.org/10.3390/molecules24234244

Du, D., Wang-Kan, X., Neuberger, A., van Veen, H. W., Pos, K. M., Piddock, L. J. V., & Luisi, B. F. (2018). Multidrug efflux pumps: Structure, function and regulation. *Nature Reviews Microbiology, 16*, 523–539. https://doi.org/10.1038/s41579-018-0048-6

Elbashir, S., Parveen, S., Schwarz, J., Rippen, T., Jahncke, M., & DePaola, A. (2018). Seafood pathogens and information on antimicrobial resistance: A review. *Food Microbiology, 70*, 85–93. https://doi.org/10.1016/j.fm.2017.09.011

Fanelli, F., Chieffi, D., Di Pinto, A., Mottola, A., Baruzzi, F., & Fusco, V. (2020). Phenotype and genomic background of *Arcobacter butzleri* strains and taxogenomic assessment of the species. *Food Microbiology, 89*, 103416. https://doi.org/10.1016/j.fm.2020.103416

Forde, A., & Fitzgerald, G. F. (1999). Analysis of exopolysaccharide (EPS) production mediated by the bacteriophage adsorption blocking plasmid, pCI658, isolated from *Lactococcus lactis* ssp. *cremoris* HO2. *International Dairy Journal, 9*(7), 465–472. https://doi.org/10.1016/S0958-6946(99)00115-6

Friesner, R. A., Murphy, R. B., Repasky, M. P., Frye, L. L., Greenwood, J. R., Halgren, T. A., Sanschagrin, P. C., & Mainz, D. T. (2006). Extra precision Glide: Docking and scoring incorporating a model of hydrophobic enclosure for Protein−Ligand complexes. *Journal of Medicinal Chemistry, 49*(21), 6177–6196. https://doi.org/10.1021/jm051256o

Ghosh, A., Roymahapatra, G., Paul, D., & Mandal, S. M. (2020). Theoretical analysis of bacterial efflux pumps inhibitors: Strategies in-search of competent molecules and develop next. *Computational Biology and Chemistry, 87*, 107275. https://doi.org/10.1016/j.compbiolchem.2020.107275

Goltermann, L., & Tolker-Niefordelsen, T. (2017). Importance of the exopolysaccharide matrix in antimicrobial tolerance of *Pseudomonas aeruginosa* aggregates. *Journal of Medicinal Chemistry, 61*, Article e02696-16. https://doi.org/10.1128/AAC.02696-16

Hassoun, A., & Emir Çoban, Ö. (2017). Essential oils for antimicrobial and antioxidant applications in fish and other seafood products. *Trends in Food Science & Technology, 68*, 26–36. https://doi.org/10.1016/j.tifs.2017.07.016

Hendriksen, R. S., Bortolaia, V., Tate, H., Tyson, G. H., Aarestrup, F. M., & McDermott, P. F. (2019). Using genomics to track global antimicrobial resistance. *Frontiers in Public Health, 7*, 242. https://doi.org/10.3389/fpubh.2019.00242

Ilangovan, A., Fletcher, M., Rampioni, G., Pustelny, C., Rumbaugh, K., Heeb, S., Cámara, M., Truman, A., Chhabra, S. R., Emsley, J., & Williams, P. (2013). Structural basis for native agonist and synthetic inhibitor recognition by the *Pseudomonas aeruginosa* quorum sensing regulator PqsR (MvfR). *PLoS Pathogens, 9*(7), Article e1003508. https://doi.org/10.1371/journal.ppat.1003508

Jia, S., Hong, H., Yang, Q., Liu, X., Zhuang, S., Li, Y., Liu, J., & Luo, Y. (2020). TMT-based proteomic analysis of the fish-borne spoiler *Pseudomonas psychrophila* subjected to chitosan oligosaccharides in fish juice system. *Food Microbiology, 90*, 103494. https://doi.org/10.1016/j.fm.2020.103494

Kabra, R., Chauhan, N., Kumar, A., Ingale, P., & Singh, S. (2019). Efflux pumps and antimicrobial resistance: Paradoxical components in systems genomics. *Progress in Biophysics and Molecular Biology, 141*, 15–24. https://doi.org/10.1016/j.pbiomolbio.2018.07.008

Klebe, G. (2013). *Drug design: Methodology, concepts, and mode-of-action*. Springer Berlin Heidelberg. https://doi.org/10.1007/978-3-642-17907-5

Kumar, L., Chhibber, S., Kumar, R., Kumar, M., & Harjai, K. (2015). Zingerone silences quorum sensing and attenuates virulence of *Pseudomonas aeruginosa*. *Fitoterapia, 102*, 84–95. https://doi.org/10.1016/j.fitote.2015.02.002

Lamas, A., Regal, P., Vázquez, B., Miranda, J. M., Franco, C. M., & Cepeda, A. (2019). Transcriptomics: A powerful tool to evaluate the behavior of foodborne pathogens in the food production chain. *Food Research International, 125*, 108543. https://doi.org/10.1016/j.foodres.2019.108543

Laue, B. E., Jiang, Y., Chhabra, S. R., Jacob, S., Stewart, G. S. A. B., Hardman, A., Downie, J. A., O'Gara, F., & Williams, P. (2000). The biocontrol strain *Pseudomonas fluorescens* F113 produces the Rhizobium small bacteriocin, N-(3-hydroxy-7-cis-tetradecenoyl)homoserine lactone, via HdtS, a putative novel N-acylhomoserine lactone synthase. *Microbiology, 146*, 2469–2480. https://doi.org/10.1099/00221287-146-10-2469

Leite de Souza, E. (2016). The effects of sublethal doses of essential oils and their constituents on antimicrobial susceptibility and antibiotic resistance among food-related bacteria: A review. *Trends in Food Science & Technology, 56*, 1–12. https://doi.org/10.1016/j.tifs.2016.07.012

Li, X.-Z., Elkins, C. A., & Zgurskaya, H. I. (2016). Efflux-mediated antimicrobial resistance in bacteria. *Efflux-mediated antimicrobial resistance in bacteria mechanisms, regulation and clinical implications*. Springer International Publishing. https://doi.org/10.1007/978-3-319-39658-3

Liu, X., Xu, J., Zhu, J., Du, P., & Sun, A. (2019). Combined transcriptome and proteome analysis of RpoS regulon reveals its role in spoilage potential of *Pseudomonas fluorescens*. *Frontiers in Microbiology, 10*, 94. https://doi.org/10.3389/fmicb.2019.00094

Li, T., Wang, D., Liu, N., Ma, Y., Ding, T., Mei, Y., & Li, J. (2018). Inhibition of quorum sensing-controlled virulence factors and biofilm formation in *Pseudomonas fluorescens* by cinnamaldehyde. *International Journal of Food Microbiology, 269*, 98–106. https://doi.org/10.1016/j.ijfoodmicro.2018.01.023

Lyu, F., Gao, F., Wei, Q., & Liu, L. (2017). Changes of membrane fatty acids and proteins of *Shewanella putrefaciens* treated with cinnamon oil and gamma irradiation. *Bioresources and Bioprocessing, 4*(10). https://doi.org/10.1186/s40643-017-0140-1

Machado, I., Silva, L. R., Giaouris, E. D., Melo, L. F., & Simões, M. (2020). Quorum sensing in food spoilage and natural-based strategies for its inhibition. *Food Research International, 127*, 108754. https://doi.org/10.1016/j.foodres.2019.108754

Mangiaterra, G., Laudadio, E., Cometti, M., Mobbili, G., Minnelli, C., Massaccesi, L., Citterio, B., Biavasco, F., & Galeazzi, R. (2017). Inhibitors of multidrug efflux pumps of *Pseudomonas aeruginosa* from natural sources: An in silico high-throughput virtual screening and in vitro validation. *Medicinal Chemistry Research, 26*, 414–430. https://doi.org/10.1007/s00044-016-1761-1

Marshall, R. L., & Bavro, V. N. (2020). Mutations in the TolC periplasmic domain affect substrate specificity of the AcrAB-TolC pump. *Frontiers in Molecular Bioscience, 7*, 166. https://doi.org/10.3389/fmolb.2020.00166

Mima, T., Joshi, S., Gomez-Escalada, M., & Schweizer, H. P. (2007). Identification and characterization of TriABC-OpmH, a triclosan efflux pump of *Pseudomonas aeruginosa* requiring two membrane fusion proteins. *Journal of Bacteriology, 189*, 7600–7609. https://doi.org/10.1128/JB.00850-07

Mokhonov, V. V., Mokhonova, E. I., Akama, H., & Nakae, T. (2004). Role of the membrane fusion protein in the assembly of resistance-nodulation-cell division multidrug efflux pump in *Pseudomonas aeruginosa*. *Biochemical and Biophysical Research Communications, 322*, 483–489. https://doi.org/10.1016/j.bbrc.2004.07.140

Mrozik, A., Piotrowska-Seget, Z., & Łabużek, S. (2004). Changes in whole cell-derived fatty acids induced by naphthalene in bacteria from genus *Pseudomonas*. *Microbiological Research, 159*, 87–95. https://doi.org/10.1016/j.micres.2004.02.001

Muhammadi, & Ahmed, N. (2007). Genetics of bacterial alginate: Alginate genes distribution, organization and biosynthesis in bacteria. *Current Genomics, 8*(3), 191–202. https://doi.org/10.2174/138920207780833810

Muñoz-Rojas, J., Bernal, P., Duque, E., Godoy, P., Segura, A., & Ramos, J.-L. (2006). Involvement of cyclopropane fatty acids in the response of *Pseudomonas putida* KT2440 to freeze-drying. *Applied and Environmental Microbiology, 72*, 472–477. https://doi.org/10.1128/AEM.72.1.472-477.2006

Myszka, K., Leja, K., & Majcher, M. (2019a). A current opinion on the antimicrobial importance of popular pepper essential oil and its application in food industry. *Journal of Essential Oil Research, 31*(1), 1–18. https://doi.org/10.1080/10412905.2018.1511482

Myszka, K., Olejnik, A., Majcher, M., Sobieszczańska, N., Grygier, A., Powierska-Czarny, J., & Rudzińska, M. (2019). Green pepper essential oil as a biopreservative agent for fish-based products: Antimicrobial and antivirulence activities against *Pseudomonas aeruginosa* KM01. *LWT – Food Science and Technology, 108*, 6–13. https://doi.org/10.1016/j.lwt.2019.03.047

Myszka, K., Schmidt, M. T., Majcher, M., Juzwa, W., & Czaczyk, K. (2017). β-Caryophyllene-rich pepper essential oils suppress spoilage activity of *Pseudomonas fluorescens* KM06 in fresh-cut lettuce. *LWT – Food Science and Technology, 83*, 118–126. https://doi.org/10.1016/j.lwt.2017.05.012

Myszka, K., Sobieszczańska, N., Olejnik, A., Majcher, M., Szwengiel, A., Wolko, Ł., & Juzwa, W. (2020). Studies on the anti-proliferative and anti-quorum sensing potentials of *Myrtus communis* L. essential oil for the improved microbial stability of salmon-based products. *LWT – Food Science and Technology, 127*, 109380. https://doi.org/10.1016/j.lwt.2020.109380

Parkar, S. G., Flint, S. H., Palmer, J. S., & Brooks, J. D. (2001). Factors influencing attachment of thermophilic bacilli to stainless steel: Thermophilic bacilli on steel. *Journal of Applied Microbiology, 90*(6), 901–908. https://doi.org/10.1046/j.1365-2672.2001.01323.x

Pattnaik, S. S., Ranganathan, S., Ampasala, D. R., Syed, A., Ameen, F., & Busi, S. (2018). Attenuation of quorum sensing regulated virulence and biofilm development in *Pseudomonas aeruginosa* PAO1 by *Diaporthe phaseolorum* SSP12. *Microbial Pathogenesis, 118*, 177–189. https://doi.org/10.1016/j.micpath.2018.03.031

Pfaffl, M. W. (2001). A new mathematical model for relative quantification in real-time RT-PCR. *Nucleic Acids Research, 29*(9), 45e–445. https://doi.org/10.1093/nar/29.9.e45

Polychroniadou, A. (1988). A simple procedure using trinitrobenzenesulphonic acid for monitoring proteolysis in cheese. *Journal of Dairy Research, 55*(4), 585–596. https://doi.org/10.1017/S0022029900033379

Quintieri, L., Fanelli, F., & Caputo, L. (2019). Antibiotic resistant *Pseudomonas* spp. Spoilers in fresh dairy products: An underestimated risk and the control strategies. *Foods, 8*(9), 372. https://doi.org/10.3390/foods8090372

Ramos, J. L., Martínez-Bueno, M., Molina-Henares, A. J., Terán, W., Watanabe, K., Zhang, X., Gallegos, M. T., Brennan, R., & Tobes, R. (2005). The TetR family of transcriptional repressors. *Microbiology and Molecular Biology Reviews, 69*(2), 326–356. https://doi.org/10.1128/MMBR.69.2.326-356.2005

Rampioni, G., Pillai, C. R., Longo, F., Bondì, R., Baldelli, V., Messina, M., Imperi, F., Visca, P., & Leoni, L. (2017). Effect of efflux pump inhibition on *Pseudomonas aeruginosa* transcriptome and virulence. *Scientific Reports, 7*. https://doi.org/10.1038/s41598-017-11892-9

Rao, J., Chen, B., & McClements, D. J. (2019). Improving the efficacy of essential oils as antimicrobials in foods: Mechanisms of action. *Annual Review of Food Science and Technology, 10*, 365–387. https://doi.org/10.1146/annurev-food-032818-121727

Ravn, L., Christensen, A. B., Molin, S., Givskov, M., & Gram, L. (2001). Methods for detecting acylated homoserine lactones produced by Gram-negative bacteria and their application in studies of AHL-production kinetics. *Journal of Microbiological Methods, 44*(3), 239–251. https://doi.org/10.1016/S0167-7012(01)00217-2

Roos, K., Wu, C., Damm, W., Reboul, M., Stevenson, J. M., Lu, C., Dahlgren, M. K., Mondal, S., Chen, W., Wang, L., Abel, R., Friesner, R. A., & Harder, E. D. (2019). OPLS3e: Extending Force Field Coverage for Drug-Like Small Molecules. *Journal of Chemical Theory and Computation, 15*, 1863–1874. https://doi.org/10.1021/acs.jctc.8b01026

Roy, A., Kucukural, A., & Zhang, Y. (2010). I-TASSER: a unified platform for automated protein structure and function prediction. *Nature Protocols, 5*, 725–738. https://doi.org/10.1038/nprot.2010.5

RStudio Team. (2015). *RStudio*. Boston, MA: Integrated Development Environment for R. Available at: http://www.rstudio.com/.

Ruijter, J. M., Ramakers, C., Hoogaars, W. M. H., Karlen, Y., Bakker, O., van den Hoff, M. J. B., & Moorman, A. F. M. (2009). Amplification efficiency: Linking baseline and bias in the analysis of quantitative PCR data. *Nucleic Acids Research, 37*(6), e45. https://doi.org/10.1093/nar/gkp045

Sastry, G. M., Adzhigirey, M., Day, T., Annabhimoju, R., & Sherman, W. (2013). Protein and ligand preparation: Parameters, protocols, and influence on virtual screening enrichments. *Journal of Computer-Aided Molecular Design, 27*(3), 221–234. https://doi.org/10.1007/s10822-013-9644-8

Schuster, M., Lostroh, C. P., Ogi, T., & Greenberg, E. P. (2003). Identification, timing, and signal specificity of Pseudomonas aeruginosa quorum-controlled genes: A transcriptome analysis. *Journal of Bacteriology, 185*(7), 2066–2079. https://doi.org/10.1128/JB.185.7.2066-2079.2003

Seukep, A. J., Kuete, V., Nahar, L., Sarker, S. D., & Guo, M. (2019). Plant-derived secondary metabolites as the main source of efflux pump inhibitors and methods for identification. *Journal of Pharmaceutical Analysis, 10*(4), 277–290. https://doi.org/10.1016/j.jpha.2019.11.002

Sobieszczańska, N., Myszka, K., Szwengiel, A., Majcher, M., Grygier, A., & Wolko, Ł. (2020). Tarragon essential oil as a source of bioactive compounds with anti-quorum sensing and anti-proteolytic activity against *Pseudomonas* spp. isolated from fish – *in vitro, in silico* and *in situ* approaches. *International Journal of Food Microbiology, 331*, 108732. https://doi.org/10.1016/j.ijfoodmicro.2020.108732

Soheili, V., Tajani, A. S., Ghodsi, R., & Bazzaz, B. S. F. (2019). Anti-PqsR compounds as next-generation antibacterial agents against *Pseudomonas aeruginosa*: A review. *European Journal of Medicinal Chemistry, 172*, 26–35. https://doi.org/10.1016/j.ejmech.2019.03.049

Sterniša, M., Bucar, F., Kunert, O., & Smole Možina, S. (2020). Targeting fish spoilers *Pseudomonas* and *Shewanella* with oregano and nettle extracts. *International Journal of Food Microbiology, 328*, 108664. https://doi.org/10.1016/j.ijfoodmicro.2020.108664

Sterniša, M., Klančnik, A., & Smole Možina, S. (2019). Spoilage *Pseudomonas* biofilm with *Escherichia coli* protection in fish meat at 5 °C. *Journal of the Science of Food and Agriculture, 99*(10). https://doi.org/10.1002/jsfa.9703

Takrami, S. R., Ranji, N., & Hakimi, F. (2017). New mutations in ciprofloxacin resistant strains of *Pseudomonas aeruginosa* isolated from Guilan Province, Northern Iran. *Molecular Genetics, Microbiology and Virology, 32*, 218–223. https://doi.org/10.3103/S089141681704005X

Thomas, M., Fenske, G. J., Antony, L., Ghimire, S., Welsh, R., Ramachandran, A., & Scaria, J. (2017). Whole genome sequencing-based detection of antimicrobial resistance and virulence in non-typhoidal *Salmonella enterica* isolated from wildlife. *Gut Pathogens, 9*. https://doi.org/10.1186/s13099-017-0213-x

Yang, L., Chen, L., Shen, L., Surette, M., & Duan, K. (2011). Inactivation of MuxABC-OpmB transporter system in *Pseudomonas aeruginosa* leads to increased ampicillin and carbenicillin resistance and decreased virulence. *Journal of Microbiology, 49*, 107–114. https://doi.org/10.1007/s12275-011-0186-2

Yoneyama, H., Ocaktan, A., Tsuda, M., & Nakae, T. (1997). The role ofmex-gene products in antibiotic extrusion in *Pseudomonas aeruginosa*. *Biochemical and Biophysical Research Communications, 233*(3), 611–618. https://doi.org/10.1006/bbrc.1997.6506

Yu, Z., Tang, J., Khare, T., & Kumar, V. (2020). The alarming antimicrobial resistance in ESKAPEE pathogens: Can essential oils come to the rescue? *Fitoterapia, 140*, 104433. https://doi.org/10.1016/j.fitote.2019.104433

Zhao, D., Lyu, F., Liu, S., Zhang, J., Ding, Y., Chen, W., & Zhou, X. (2018). Involvement of bacterial quorum sensing signals in spoilage potential of *Aeromonas veronii* bv. *veronii* isolated from fermented surimi. *Journal of Food Biochemistry, 42*(2), Article e12487. https://doi.org/10.1111/jfbc.12487

Zhuang, S., Hong, H., Zhang, L., & Luo, Y. (2020). Spoilage-related microbiota in fish and crustaceans during storage: Research progress and future trends. *Comprehensive Reviews in Food Science and Food Safety, 20*(1). https://doi.org/10.1111/1541-4337.12659

Zwe, Y. H., Chin, S. F., Kohli, G. S., Aung, K. T., Yang, L., & Yuk, H. G. (2020). Whole genome sequencing (WGS) fails to detect antimicrobial resistance (AMR) from heteroresistant subpopulation of *Salmonella enterica*. *Food Microbiology, 91*, 103530. https://doi.org/10.1016/j.fm.2020.103530

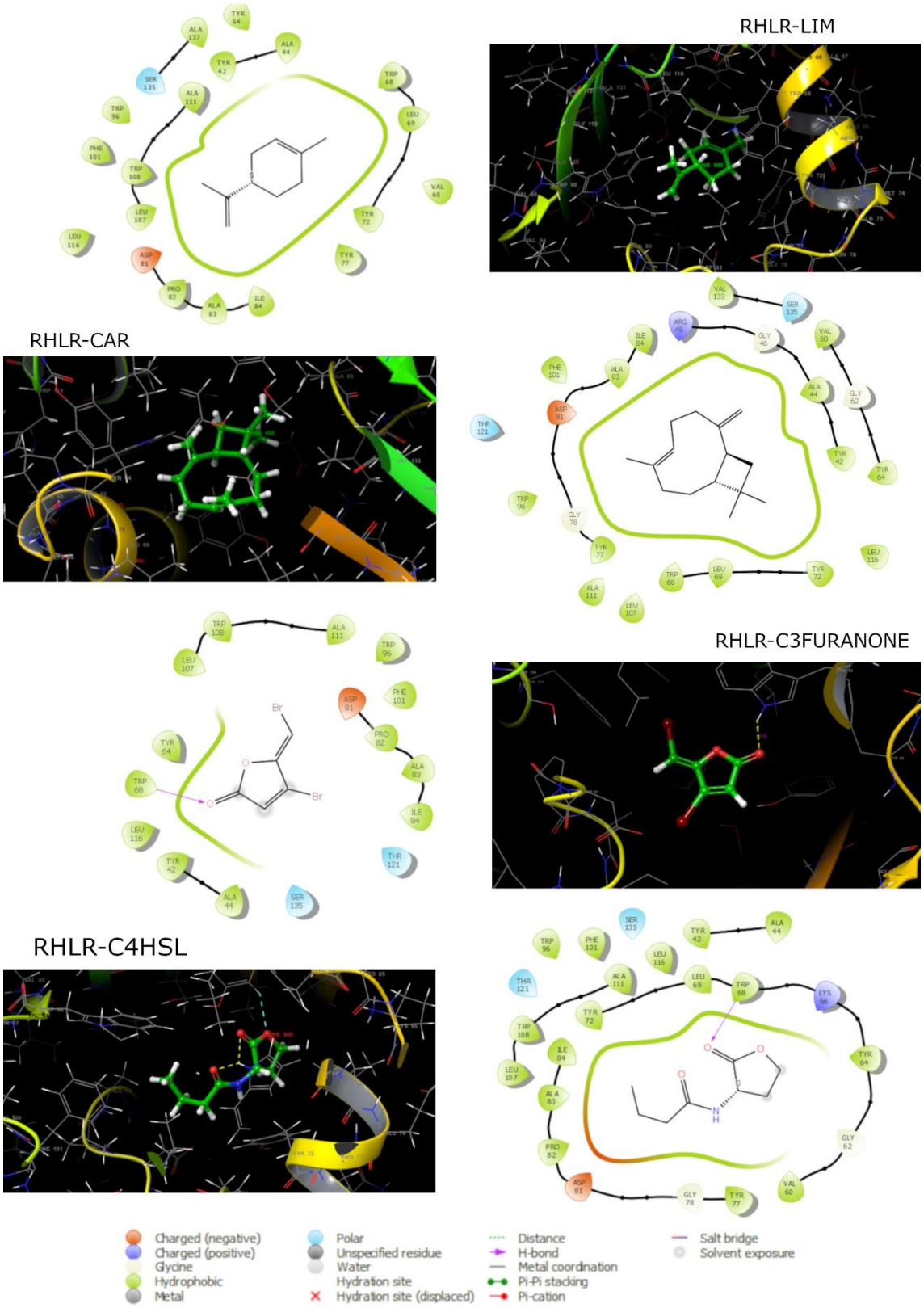

Supplement_Fig. 6. The presentation of molecular docking of RhlR protein with limonene (RHLR-LIM), beta-caryophyllene (RHLR-CAR), inhibitor C30-furanone (RHLR-C30FURANONE) and cognate AHL molecule C4-HSL (RHLR-C4HSL)

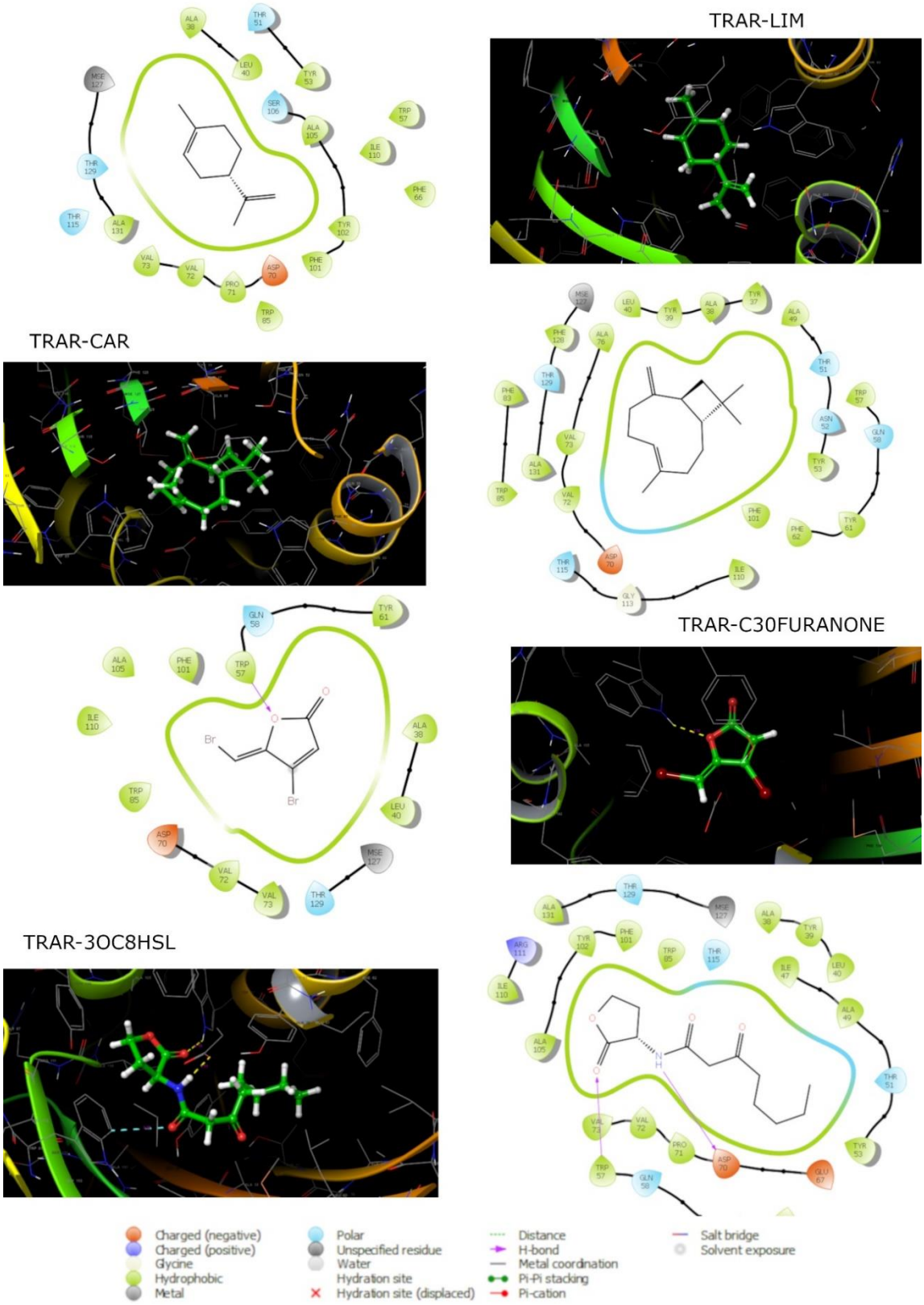

Supplement_Fig.7. The presentation of molecular docking of TraR protein with limonene (TRAR-LIM), beta-caryophyllene (TRAR-CAR), inhibitor C30-furanone (TRAR-C30FURANONE), and cognate AHL molecule 3-oxo-C8-HSL (TRAR-3OC8HSL)

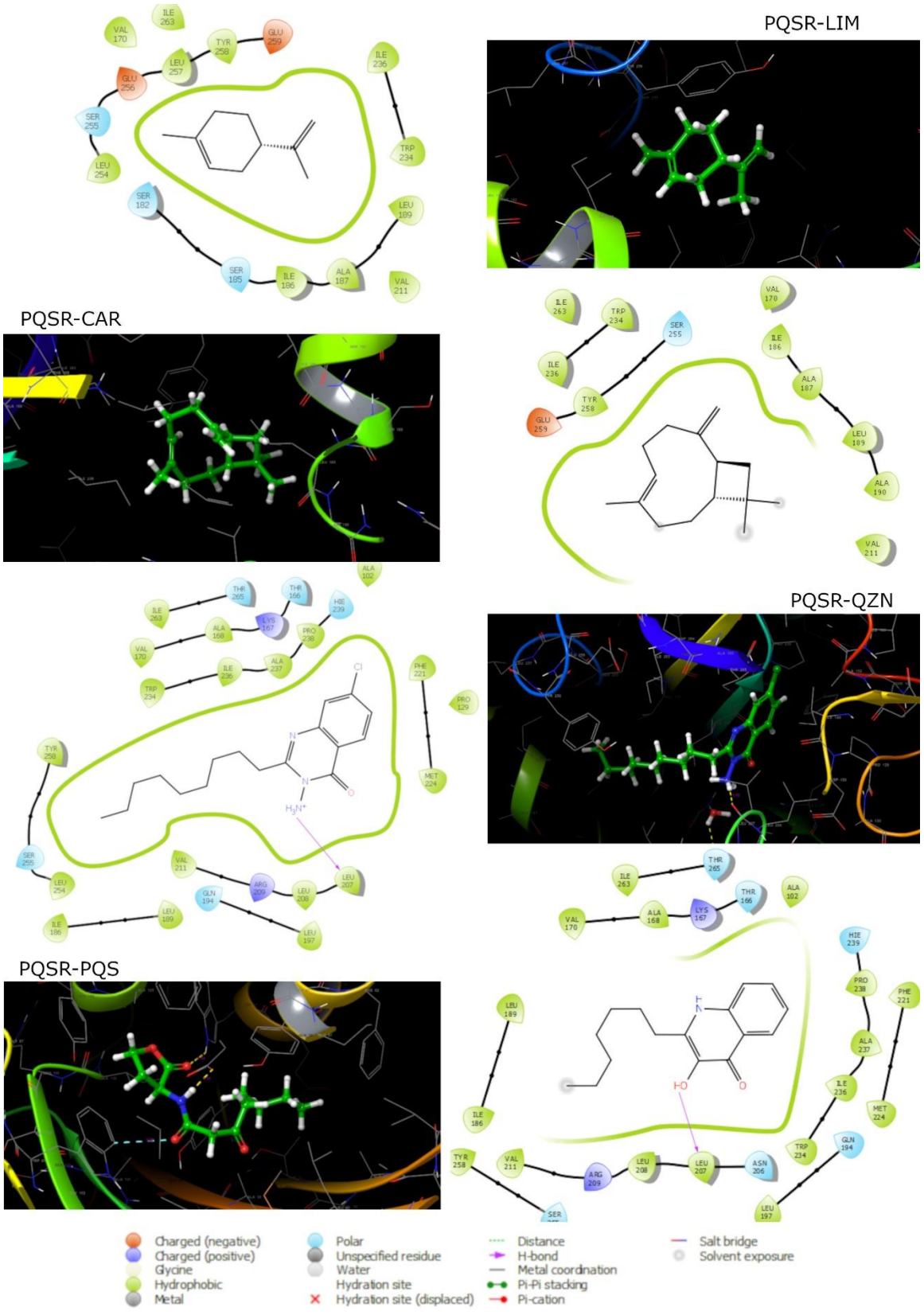

Supplement_Fig.8. The presentation of molecular docking of PqsR protein with limonene (PQSR-LIM), beta-caryophyllene (PQSR-CAR), inhibitor QZN (PQSR-QZN) and cognate PQS molecule (PQSR-PQS)

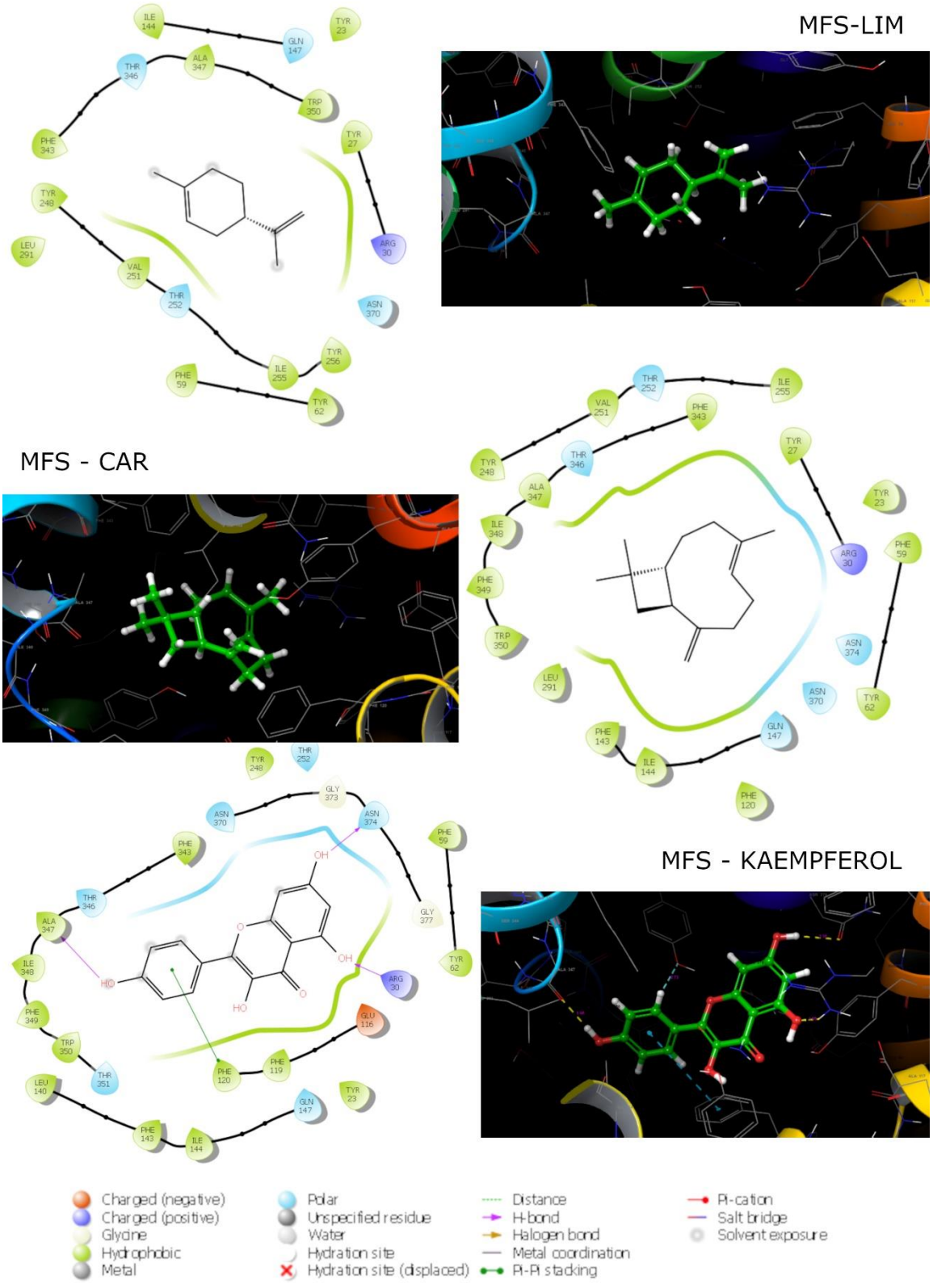

Supplement_Fig.9. The presentation of molecular docking of Mfs protein with limonene (MFS-LIM), beta-caryophyllene (MFS-CAR) and inhibitor kaempferol (MFS-KAEMPFEROL)

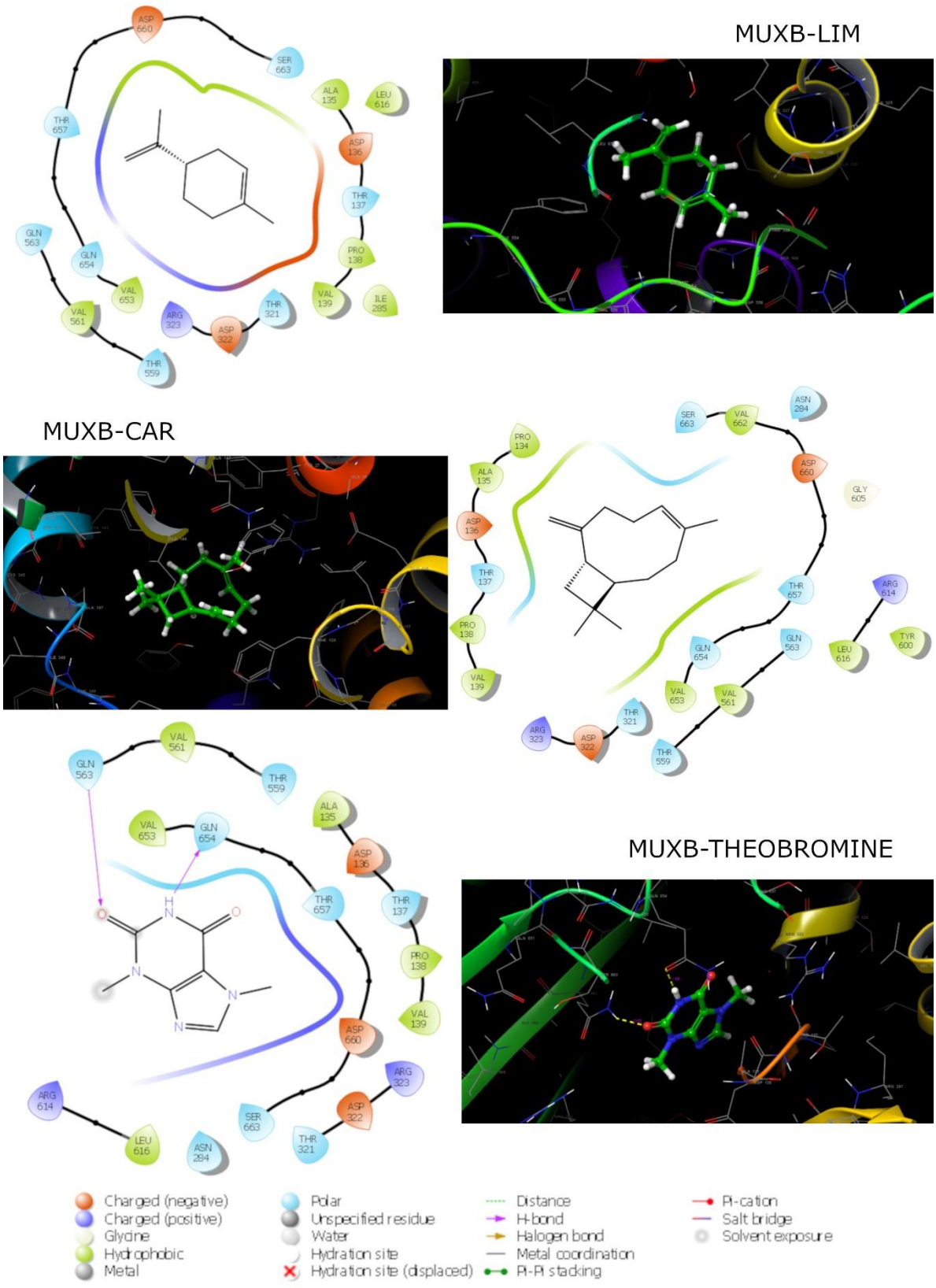

Supplement_Fig.10. The presentation of molecular docking of MuxB protein with limonene (MUXB-LIM), beta-caryophyllene (MUXB-CAR) and inhibitor (MEXB- PaβN)

scientific reports

Check for updates

OPEN

Black pepper and tarragon essential oils suppress the lipolytic potential and the type II secretion system of *P. psychrophila* KM02

Natalia Tomaś[1]✉, Kamila Myszka[1] & Łukasz Wolko[2]

Given the increasing consumer demand for raw, nonprocessed, safe, and long shelf-life fish and seafood products, research concerning the application of natural antimicrobials as alternatives to preservatives is of great interest. The aim of the following paper was to evaluate the effect of essential oils (EOs) from black pepper (BPEO) and tarragon (TEO), and their bioactive compounds: limonene (LIM), β-caryophyllene (CAR), methyl eugenol (ME), and β-phellandrene (PHE) on the lipolytic activity and type II secretion system (T2SS) of *Pseudomonas psychrophila* KM02 (KM02) fish isolates grown in vitro and in fish model conditions. Spectrophotometric analysis with the p-NPP reagent showed inhibition of lipolysis from 11 to 46%. These results were confirmed by RT-qPCR, as the expression levels of *lipA*, *lipB*, and genes encoding T2SS were also considerably decreased. The supplementation of marinade with BPEO and TEO contributed to KM02 growth inhibition during vacuum packaging of salmon fillets relative to control samples. Whole-genome sequencing (WGS) provided insight into the spoilage potential of KM02, proving its importance as a spoilage microorganism whose metabolic activity should be inhibited to maintain the quality and safety of fresh fish in the food market.

Fresh fish and minimally processed fish-based products are susceptible to spoilage caused by microbiological reactions, which results in large economic losses for the fish industry and leads to sensory impairment[1,2]. It was stated that one-fourth of the world's food supplies and 30% of landed fish/fish-based products are lost through microbial activity alone[3]. Lipid deterioration can easily take place limiting the shelf-life of aerobically stored fishery products[4].

Pseudomonas spp. contribute to seafood spoilage by synthesizing extracellular lipases that hydrolyze triglycerides into free fatty acids, mono- and diacylglycerols, and glycerol, which undergo further degradation to create off-flavor low-molecular weight compounds. Lipases are usually very heat stable[5]. Even a small degree of lipolysis (1–2%) of fat can change the taste of products[6]. *Pseudomonas psychrophila* has emerged as the dominant fish-associated pseudomonads and possess the strongest potential to synthesize lipases secreted via the type II secretory pathway (T2SS)[1,7,8]. Regulation of this bacterial activity involves not only the level of lipase gene transcription and the translation of a particular mRNA but also subsequent translocation through the cell wall[9]. Because treatment that inactivate the T2SS results in loss of secretion of enzymes, combining that treatment with one that downregulate the expression of genes encoding lipases is considered a target for food quality improvement interventions[10]. However this concept requires further analysis involving integrated molecular and phenotype-based approaches. Supplementing studies with a whole genome sequencing (WGS) and de novo assembly data can provide insight into the functional profile/food spoilage features of *P. psychrophila*. WGS data can allow for characterization of potential hazards to the quality and safety of foods associated with microorganisms[11]. Importantly, complete genome assembly which is superior to the study of genome fragments and provides the only accurate reference for interpreting the meta-genomes and -transcriptomes[12] of this species has not been performed to date.

The work of Steniša et al.[13] indicates that the presence and metabolic activity of *P. psychrophila* in seafoods must be controlled. In general, growing concerns regarding the use of synthetic preservatives associated with the selection of resistant strains and the triggering of allergic reactions in consumers has prompted research into the development of new solutions to reduce microbial load and microbe activities in fishery products. Recently,

[1]Department of Biotechnology and Food Microbiology, Poznan University of Life Sciences, Wojska Polskiego 48, 60-637 Poznań, Poland. [2]Department of Biochemistry and Biotechnology, Poznan University of Life Sciences, Dojazd 11, 60-632 Poznań, Poland. ✉email: natalia.tomas@up.poznan.pl

interest into the use of essential oils (EOs) in seafoods has been growing. Black pepper EO (BPEO) and tarragon EO (TEO) are EOs that may prolong shelf life while maintaining the fresh characteristics of fish[8,14]. In the current study, we used limonene (LIM) (19.1%) and β-caryophyllene (CAR) (19.6%)-rich BPEO and TEO where methyl eugenol (ME) (24.5%) and β-phellandrene (PHE) (19.3%) were the most abundant compounds. The chemical profiles of BPEO and TEO determined by gas chromatography coupled to mass spectrometry were presented in our previous works[8,14]. The contents of the oils correspond with the international standard regulations that set minimum and maximum concentrations of LIM and CAR for BPEO and ME and PHE for TEO[15,16].

BPEO and TEO extended the shelf life of chill stored carp[17], talang gueenfish[18], and brook trout[19]. The mode of activity of the oils affects bacterial membrane structures, which changes the permeability of the bacterial cell wall. This can be accompanied by disruption in membrane function, such as electron transfer and enzyme activities[20]. The interference of the bioactive compounds of the oils with nucleic acids was also recognized as a possible antimicrobial activity of EOs[21]. However, the influence of BPEO and TEO on the expression of genes involved in lipase synthesis and secretion in the presence of the food spoiler *P. psychrophila* has not been evaluated. The above information can support the development of new technologies to prevent lipids deterioration in seafoods.

In this work, the inhibition of lipolysis of *P. psychrophila* KM02 (KM02) by BPEO, and TEO was investigated. KM02 cells were incubated with subinhibitory concentrations (subMICs) of the analyzed agents in vitro and in fish juice medium and the following aspects were examined: (i) the changes in lipolytic activity by a spectrophotometric method with p-NPP reagent, (ii) the expression of genes encoding lipases and T2SS by RT-qPCR analyses, and (iii) the growth inhibitory activity during vacuum packaging of marinated salmon fillets supplemented with BPEO and TEO. Additionally, to better understand and investigate the metabolic potential of the KM02 isolate, this work was introduced with a characterization of the whole genome, sequenced by Illumina and Nanopore techniques and de novo assembly.

Materials and methods

Microorganism and culture conditions. The KM02 strain isolated from commercial chill-stored fresh salmon was used in this study. Identification of restriction length polymorphisms of 16S rRNA gene amplicons and sequencing were carried out for bacterial identification. Cryovials (MWE, UK) were used for the preservation the strain.

The cells were cultured in tryptic soy broth medium (TSB) (BD Biosciences, USA) and fish juice medium prepared from fresh salmon fillets for a total of 72 h at 4 °C as described in the work of Sobieszczańska et al.[8] The media were supplemented with previously selected[8,14] subMICs of BPEO (135.0 µl/ml), LIM (Sigma–Aldrich, Merck KGaA, USA) (65.0 µl/ml) CAR (Sigma–Aldrich, Merck KGaA, USA) (35.0 µl/ml), TEO (75.0 µl/ml), ME (Sigma–Aldrich, Merck KGaA, USA) (10.0 µl/ml), and PHE (Sigma–Aldrich, Merck KGaA, USA) (8.0 µ/ml). The subMICs of the examined agents were determined by the macrodilution method, following the standard protocol M07 from the Clinical and Laboratory Standard Institute[22].

Whole genome analysis of *P. psychrophila* KM02. KM02, grown on TSB (Becton Dickinson, USA) medium, was subjected to whole genome sequencing analysis at a commercial laboratory (Genomed S.A., Poland). The bacterial genomic DNA was extracted with a Qiagen DNeasy Blood and Tissue kit (Qiagen, Germany) according to the manufacturer's instructions, followed by fragmentation by sonication. Genome sequence and library preparations were constructed by two methods: the Illumina MiSeq Platform (Illumina, USA) and MinION sequencer (Oxford Nanopore Technologies, UK) by using the Nextera XT DNA library 300-bp paired-end preparation kit and the SQK-NSK007 Rapid Sequencing kit, respectively.

Raw sequencing data were processed with the CLC Genomics Workbench v. 20.0 and CLC Microbial Genomics Module v 20 plugin (Qiagen, USA). The sequence reads from the MiSeq Illumina platform were demultiplexed to the probes, and the overlapping paired-end reads were merged. Only fragments that passed the merging (~ 90%) were retained for downstream processing. Then, the reads from both the MiSeq and MinION sequencing platforms were combined together and used for de novo assembly. Sequence assembly was conducted using an increasing word size (k = 21, 41, 61), where the contigs from the previous iteration were used as input in the next iteration together with the input reads. The complete sequence of the bacterial chromosome was deposited in the NCBI GenBank database under accession number NZ_CP049044.1. Whole genome alignments were performed using Mauve 2.4.0[23]. Genome visualization was created with the GView Server (https://server.gview.ca)[24]. Pangenome analysis with KEGG and COG distributions was calculated using BPGA 1.3[25–28]. The phylogenetic tree was constructed based on genome assembly sequences by the K-mer method, with the following parameters: K-mer length = 16, index k-mers with prefix ATGAC, and method FFP.

Protein coding sequences (CDSs) were assigned to the KM02 whole genome sequence using the Find Prokaryotic Genes tool in the CLC Microbial Genomics Module. Thereafter, functional annotations of CDSs were performed using SwissPROT (with Gene Ontology (GO)-term annotations) and the protein family (Pfam) database. In the next step, the original reads were mapped back to the annotated genomes to assess the abundance of the functional annotations and build functional profiles. The COG distributions of KM02 were calculated using the WebMGA internet service (http://weizhong-lab.ucsd.edu/webMGA/server/)[29].

Lipolytic activity determination. The changes in KM02 lipolytic activity after treatment with subMICs of BPEO, TEO, and their major bioactive compounds were estimated by spectrophotometric analysis[30]. Briefly, 10 ml isopropanol containing 30 mg of p-nitrophenyl palmitate (p-NPP) (Sigma–Aldrich, Merck KGaA, USA) was mixed with 90 ml of 0.05 M Sörensen phosphate buffer (Sigma–Aldrich, Merck KGaA, USA). First, 2.4 mL was prewarmed at 37 °C and then mixed with the supernatant of the KM02 culture (0.1 mL). The samples were then incubated at 37 °C for 15 min. The absorbance was read at 420 nm on a SPECORD®UV–VIS spectropho-

tometer (Analytic Jena, Germany). Samples mixed with 0.1 mL of water served as reference probes. The percentage of lipolytic activity inhibition was calculated according to the following formula:

$$\%\ \mathrm{LI}\ = 100 - (\mathrm{A_t}/\mathrm{A_c} * 100)$$

where A_t—absorbance value obtained for KM02 incubated on medium supplemented with subMICs. A_c—absorbance value obtained for the control probe (KM02 cells without any treatment).

RNA isolation and RT-qPCR analyses. The comparative quantitation method for evaluating the changes in the expression of the selected genes (Supplementary Table S1) was performed as described in our previous study with some modifications[14]. Briefly, total RNA was stabilized by RNAprotect® Bacteria Reagent (Qiagen, USA) and isolated on a PureLink™ RNA Mini Kit (Thermo Fisher Scientific, USA) followed by purification with PureLink™ DNase Set (Invitrogen, USA) according to the manufacturer's protocols. The quality and quantity of RNA were examined on a Qubit Fluorometer 4 (Invitrogen, USA) using Qubit™ XR RNA and Qubit™ IQ RNA Assay Kits (Thermo Fisher Scientific, USA). Subsequently, 1 µg of RNA was reverse-transcribed with the High Capacity RNA-to-cDNA Kit (Life Technologies, USA).

RT-qPCR analyses were performed in a CFX96 system (BioRad, Hercules, USA) using GoTaq® Master Mix (Promega, Germany). In the RT-qPCR analyses, 16S rRNA served as the reference gene. For the selected genes of interest (GOIs) the primers were designed with the Primer-BLAST tool[31] in the NCBI database. The cycling conditions were as follows: initial denaturation at 95 °C for 2 min and 40 cycles of denaturation at 95 °C for 15 s and annealing and extension at 60 °C for 1 min. The melting curve was also applied. To estimate the amplification efficiency (E_{GOI}/E_{ref}), LinRegPCR software[32] was used. The results are presented as the ratio of gene expression in the treated samples relative to the control samples (with expression equal to 1), normalized to the internal reference gene, according to the following equation[33]:

$$ratio = \frac{E_{GOI}{}^{\Delta C_{ttarget}(control-sample)}}{E_{ref.}{}^{\Delta C_{tref}(control-sample)}}$$

where GOI—gene of interest for which the changes in expression were calculated; ref—reference gene, whose expression was used for normalization.

In situ determination of the antimicrobial properties of BPEO and TEO toward *P. psychrophila* KM02. Ten grams of commercial raw salmon fillet samples were inoculated with 1 mL of KM02 culture standardized to an initial level of approximately 10^4 CFU/g. The samples were air-dried at room temperature for 20 min in a biosafety laminar box (Thermo Fisher Scientific, USA). The marinade of the salmon consisted of 95% olive oil and 5% vinegar. All ingredients were purchase from local manufacturers. Next, 5 mL of marinade was supplemented with subMICs of BPEO/TEO. Marinade without essential oils served as reference samples. The marinades were poured into the salmon samples. The fish were packed into sterile polyvinyl chloride bags (Kraina Foils Packaging, Poland). Vacuum conditions were obtained with a Multivac T200 packaging machine (Wolfertschwenden, Germany). All samples were prepared under sterile conditions and stored at 4 °C ± 1 °C for 5 days.

Verification of KM02 growth on the cold-stored products was carried out at 1, 3 and 5 days of storage. The products were aseptically opened and placed in a sterile polyethylene bag (Sigma-Aldrich, Merck, KGaA, USA). A volume of 90 mL of 0.1% sterile peptone water (Oxoid, UK) was added to achieve a 1:10 dilution. The samples were homogenized for 2 min with a Pulsifier (Microgen Bioproducts, UK). Next tenfold serial dilutions were prepared, and 0.1 mL aliquots were surface-spread on cephalordine fucidin cetrimide agar (Oxoid, UK). Counts of KM02 are presented as the log CFU/g value.

Statistical analysis. The experiments were performed in triplicate, and the results are expressed as the mean ± standard deviation. Significant differences ($p < 0.05$) were established by analysis of variance (ANOVA) followed by post hoc tests performed in R (R Core Team 2020).

Results and discussion

Characteristics of the *P. psychrophila* KM02 genome and pangenome. The growth and metabolic activities of microorganisms are considered the main causes of fish-based product spoilage. Our previous work identified *P. psychrophila* as a specific spoilage organism in the salmon microbiome[8]. At temperatures that can occur during the processing and storage of fish, the enzymatic activity of pseudomonads can result in off-odors[34]. However, determination of the physiological characteristics of *P. psychrophila* in in vitro and in situ conditions requires detailed investigation. WGS and de novo assembly provide complete information about bacterial strains isolated from various sources and increase the value of biological studies[12]. These are important because foodborne microorganisms are subjected to harsh conditions in the food chain[35]. Therefore, in this study, WGS technology was applied to understand the spoilage potential of the KM02 strain.

Initially, KM02 was isolated from salmon fillets kept in a cold environment, and the complete genome sequence was obtained by combining the Ilumina and MinION platforms. Reads were de novo assembled, resulting in one scaffold with 20 × coverage. A complete genome sequence of KM02 comprised 5,313,922 base pairs of a circular chromosome with a 57.4% G + C content (Fig. 1), coding 4,813 total genes, out of which 4,713 were protein coding DNA sequences (CDSs) and 54 were pseudogenes. No plasmids were found. Other chromosome features of KM02 are presented in Supplementary Table S2. In comparison to KM02, a previously sequenced

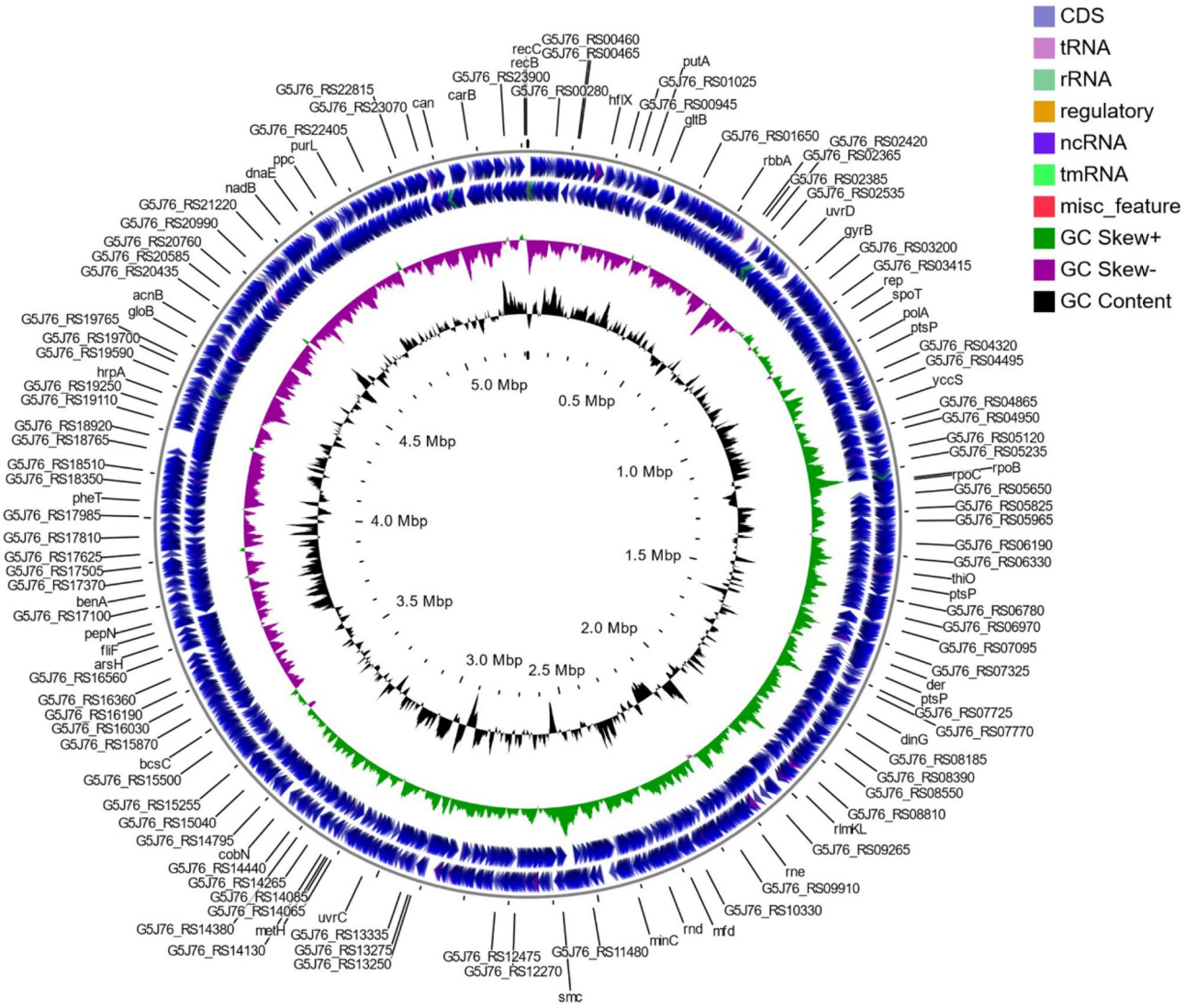

Figure 1. Circular representation of the *P. psychrophila* KM02 genome.

genome of the *P. psychrophila* HA-4 strain also isolated from a cold environment, consisted of 5,235,696 bases with a mean G + C percentage of 56.4% and 4,721 predicted coding sequences[36]. Similarly, the draft genome of *P. psychrophila* MTCC 12,324 isolated from the Arctic was composed of 5,269,174 bases, with a mean G + C content of 57.52%[37]. Given the above, it can be concluded that *P. psychrophila* species genome characteristics are rather equal between strains, in contrast to other species, such as *Escherichia coli*[38]. However, only small variations in *P. psychrophila* genome features were able to be identified by analyzing the small number of available sequenced strains; many more sequences strains are available for *E. coli* species, and identification of genome variations is dependent on the number of genomes available for analysis[38]. Nevertheless, according to the work of Wessels et al.[39], who sequenced 35 various *Pseudomonas* spp. fish- isolates, the genome sizes and number of genes ranged from 4,505,98 bp to 6,279,60 bp and 4,123 to 5,874, respectively[39]. Similar values were also obtained for genomes of *Pseudomonas fragi* and *Pseudomonas lundensis* isolated from spoiled meat and milk samples[40]. Based on the summary of the available sequenced bacterial genomes, such values are considered average, characteristic for bacteria isolated from environmental sources[38].

To assess the essential genomic elements of *P. psychrophila* species, pangenome analysis was performed. There were 8 *P. psychrophila* genome assemblies in the GenBank NCBI database. Due to problems with gbff file validation HA-4 assembly (GCA_000282975.1) was excluded from the pangenome analysis. Details on the contribution of specific *P. psychrophila* genomes to the pangenome of this species are depicted in Table 1. *P. psychrophila* was characterized by 3914 core genes (shared by all strains), while strain KM02 had 548 accessory genes (shared by two or more strains, but not all), 2 unique and 0 absent genes. In the most distinct strain, MF6762, the number of unique genes reached 574. Interestingly, this strain has also been isolated from food (raw chicken), while other sequenced *P. psychrophila* strains were isolated from cold environments (rooms of food storage or cold water). As presented in the core-pangenome plot (Supplementary Fig. S2), *P. psychrophila* had a small variations among strains and varied only in the range of less than 2 Mb of gene families. This indicates a rather confined and homogeneous group of *P. psychrophila* strains in the context of gene products[38]. According to the outcomes

Strain	Assembly level	Isolation source	Total sequence length	GenBank assembly accession	No. of core genes	No. of accessory genes	No. of unique genes	No. of exclusively absent genes
KM02	Complete Genome	Raw salmon fillets kept in cold	5,313,922	GCA_011040435.1	3,914	548	2	0
BS3667	Chromosome	Unknown	5,322,478	GCA_900106105.1	3,914	554	42	13
DSM 17,535	126 contigs	Cold room for food storage	5,334,010	GCF_001043005.1	3,914	489	41	14
CCUG 53,877	36 contigs	Cold room for food storage	5,269,270	GCA_008801485.1	3,914	537	26	2
MF6762	77 contigs	Raw chicken	5,804,172	GCF_016405605.1	3,914	427	574	27
CF149	50 contigs	Hyporheic zone of the Clark Fork River	5,154,320	GCA_000416155.1	3,914	382	219	48
RGCB 166	150 contigs	Surface water of the Arctic Fjord	5,269,174	GCA_001005765.1	3,914	263	144	133
HA-4	145 contigs	Activated sludge sample	5,235,696	GCA_000282975.1	–	–	–	–

Table 1. *P. psychrophila* pangenome characteristics.

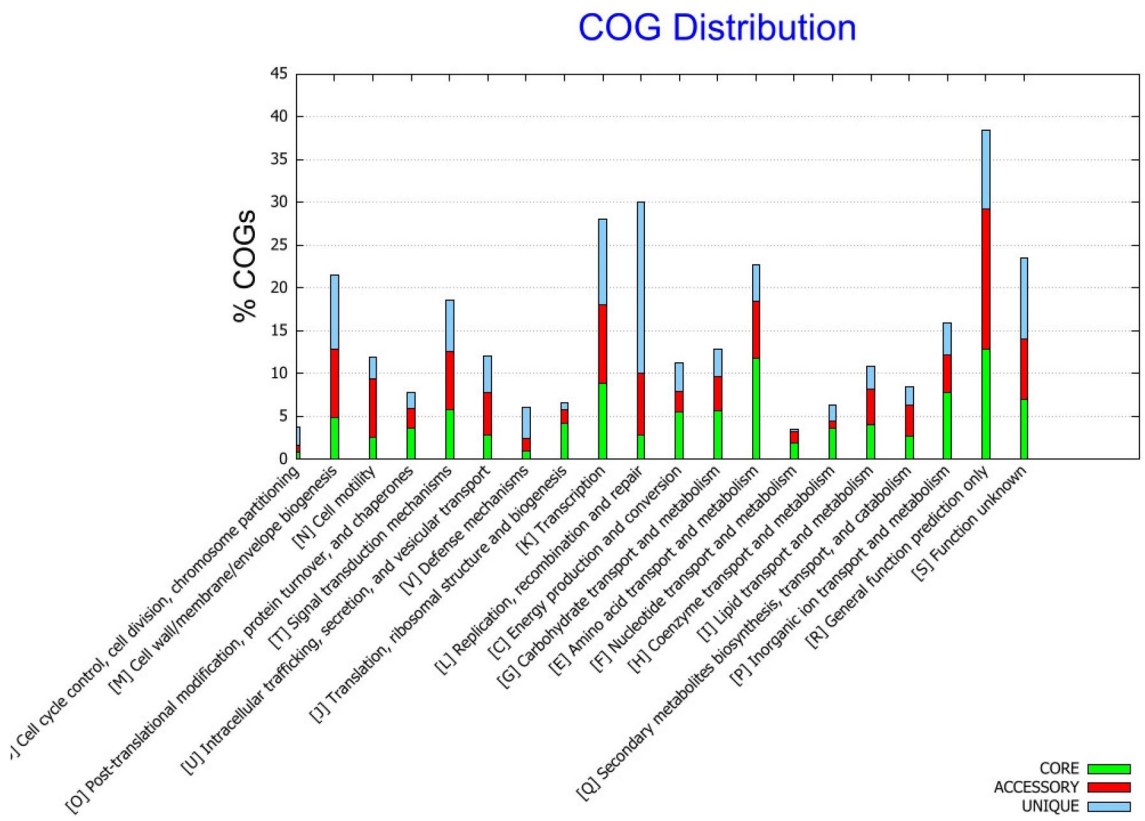

Figure 2. Clusters of orthologous groups distribution of *P. psychrophila* pangenome.

of the attribution of the Clusters of Orthologous Groups (COGs) functional categories to the *P. psychrophila* pangenome (Fig. 2), the highest percentage of unique genes was related to the 'replication, recombination and repair' category. Simultaneously, the fraction of pangenome core, after the 'genes of general function prediction only' category, was the most abundantly represented in 'amino acid transport and metabolism' (above 10%). Similar results were obtained for the pangenome of fish-pathogenic *Aeromonas hydrophila* strains, in which the core genome was represented by 9.61% of genes annotated to the 'amino acid transport and metabolism function' COG category[41]. This functional group was also well represented in the accessory genome of *P. fragi*, which has been recognized as a contributor to the spoilage of fresh meat and fish and pasteurized milk by secreted lipases and proteases[40]. Regarding lipid transport and metabolism, the core, accessory and unique percentages of representatives in *P. psychrophila* pangenome were equally distributed. Furthermore, based on KEGG pangenome analysis (Fig. 3), a high metabolic activity of *P. psychrophila* (almost 70% of the pangenome) was also confirmed. KEGG detailed distribution revealed that the most enriched metabolic functions were 'amino

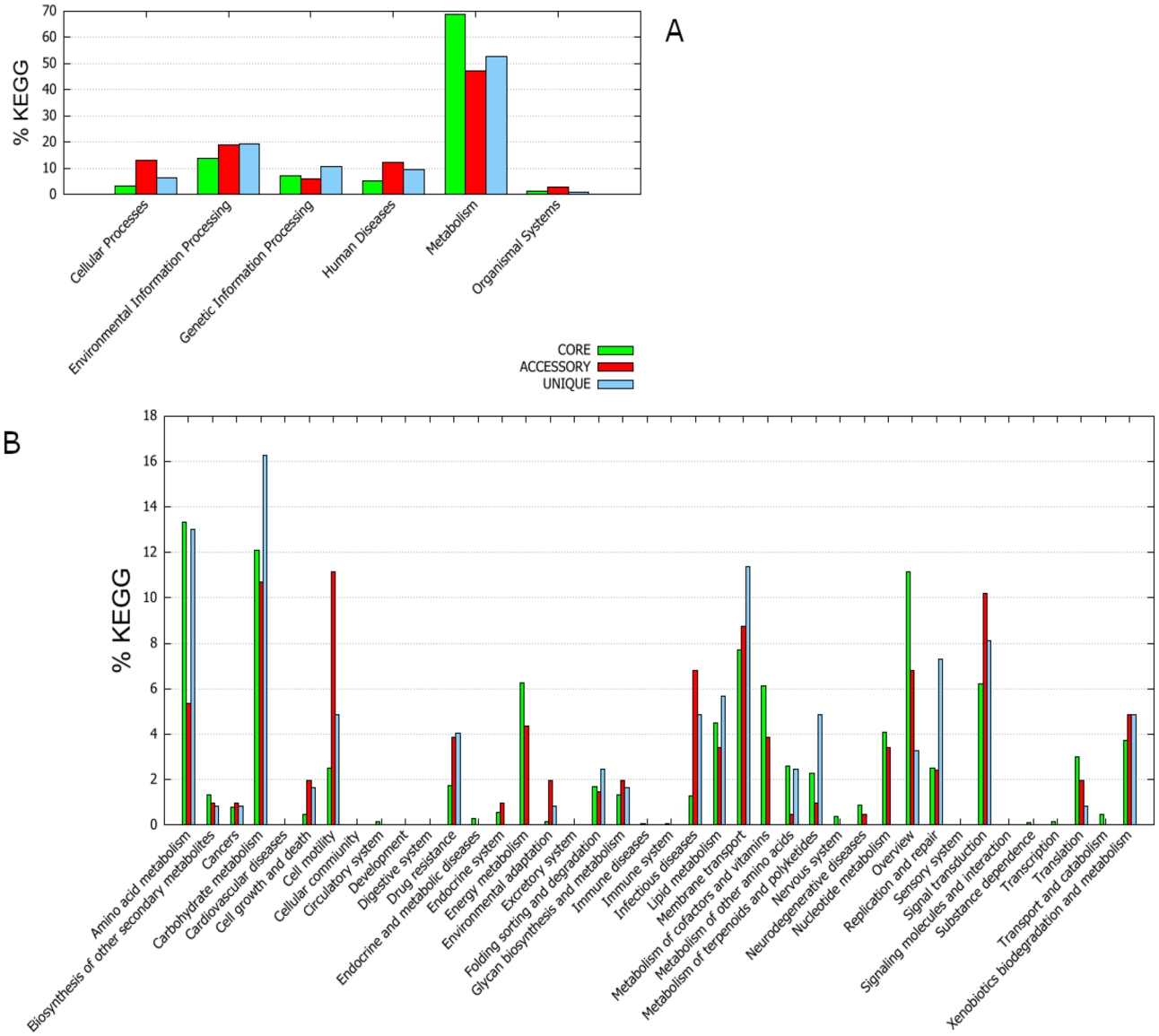

Figure 3. KEGG distribution of *P. psychrophila* pangenome. (**A**) General distribution; (**B**) details distribution.

acid metabolism', 'lipid metabolism' and 'membrane transport' and they accounted for approx. 13%, 4%, and 8% of the core genes, respectively.

A K-mer phylogenetic tree based on the genome assembly sequences showed the closest evolutionary relationship with *P. psychrophila* BS3667 (Fig. 4) with 99.9181% identity; however the sample and isolation source of this strain is not known.

To characterize the KM02 genome, a number of available bioinformatic tools were applied. Similar to pangenome analysis, the distribution of COG of the KM02 strain was also determined. As presented in Fig. 5, gene products with 'unknown function' and with 'general function prediction only' comprised approx. 40% in total. Therefore, to clarify the significance of the remaining known function assigned to the COG, the numbers of those families were subtracted from the percentage calculations. Consequently, 'amino acid and lipid transport and metabolism protein' orthologs accounted for 9 and 3% of all categorized proteins, respectively. COG results for KM02 are in agreement with the genome of other seafood spoilage contributors, such as *Shewanella baltica* isolated from spoiled shrimp[42]. These psychrotrophic bacteria, similar to *Pseudomonas* spp. dominate in spoilage of iced-stored fish meat[43,44] and the COG category of 'amino acid' and 'lipid transport and metabolism' represented 8.66% and 3.8% of the genome, respectively[42]. In regard to the proteins related to those activities, the most dominant annotations involved COG1028 (dehydrogenases with different specificities), COG0834 (ABC-type amino acid transport/signal transduction system), COG0665 (glycine/D-amino acid oxidases), COG1280 (putative threonine efflux protein), COG0612 (predicted Zn-dependent peptidases), COG0006 (Xaa-Pro aminopeptidase), COG1686 (D-alanyl-D-alanine carboxypeptidase), and COG0024 (methionine aminopeptidase) among others. Similarly, in the genome of *Pseudomonas fluorescens* SRM1 isolated from spoiled milk, the operon containing proteases, lipases and the ABC-transporter, which directs enzyme secretion, was identified[45]. High

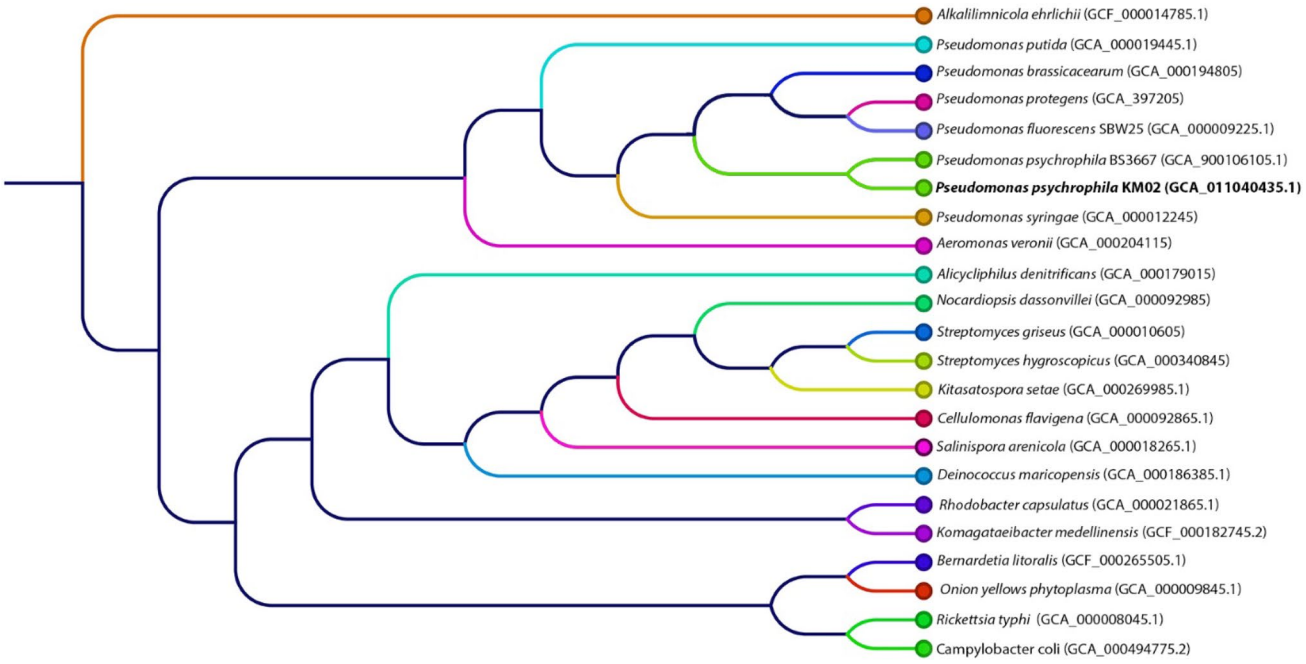

Figure 4. K-mer phylogenic tree of *P. psychrophila* KM02.

enzymatic activity is required for efficient utilization of complex compounds from which bacteria produce energy. Furthermore, Gene Ontology system was used to determine the biological relevance of genes and gene products. In KM02, 870 GO terms were assigned to biological process, 77 GO terms to cellular component and 680 GO terms to molecular function (Supplementary Fig. S1). Among the 'biological process' GO terms, the most abundant were genes involved in 'metabolic process' (GO:0008152) and 'cellular process' (GO:0009987) as they consist of ancestor annotations of predicted genes, which are also annotated to child GO terms representing more specific entities[46]. Among the child terms that confirmed a wide spoilage potential of KM02, those containing: 'catabolic', 'proteolysis', 'protein', 'lipid', and 'fatty acid' phrases were revised and selected. In the 'organic substance catabolic process' GO term, the most abundant genes were genes involved in chemical reactions and pathways of organonitrogen compounds, organic acids, organic cyclic compounds, carbohydrates, organophosphates, macromolecules, proteins and lipids (Fig. 6A). In 'cellular catabolic process' group, which indicates the activity of individual cells, the most abundant pathways were pathways resulting in the degradation of aromatic compounds, nitrogen compounds, drugs, neurotransmitters, macromolecules, peptides, and sulfur compounds (Fig. 6B). As reported in Liu et al.[47], the transcriptome of the *P. fluorescens* strain strongly associated with food spoilage differed from the RpoS-mutant strain in regard biological processes; the greatest differences were seen in GO biological processes such as signaling, protein catabolic process and secretion. Because *RpoS* contributes to the spoilage activities of *P. fluorescens*[48], we can conclude that the abovementioned significantly downregulated genes are strongly involved in the spoilage of foods. Regarding the secretion system, according to the cellular component GO categories, the presence of the T2SS complex and transmembrane transporter activity molecular function was also noted. Among the other molecular function terms, the most abundant were 'catalytic activity', and those important for protein and lipid degradation were 'hydrolase activity', 'catalytic activity, acting on a protein', and 'hydrolase activity, acting on ester bonds' (Table 2). The functions of the assigned genes were also deduced on the basis of the sequence similarity of their presumptive protein products to the protein motifs in the Pfam database[49]. From among a wide range of annotated Pfam protein domains, only those related to hydrolase activity, protein secretion, lipid degradation and other fish spoilage aspects were selected, and their genome abundances are presented in Table 3. These data will significantly complement the current knowledge on the lipolytic activity of pseudomonads. Highly enriched Pfam domains were involved in the hydrolase activity represented by Aminohydro_1 and Abhydrolase_1 with relative abundances of 11,828 and 7768, respectively. Furthermore, most of the Pfam annotations assigned to the KM02 genome were related to peptidase activity, e.g., Peptidase_M20, Peptidase_M24 or Peptidase_M23. Most of these enzymes are classified as metallopeptidases, whose catalytic activity involves metals[50]. Proteins and lipids degraded to smaller molecules such as oligopeptides or single fatty acids are further metabolized by bacteria to form derivatives with undesirable odors. For example, ELFV_dehydrog represents the family of dehydrogenases of amino acids that catalyze the oxidative deamination of an amino acid to its keto acid analogs, known from spoiled fish[51]. In the context of lipid degradation, Pfam results revealed the presence of proteins representing Lipase_3 and Lipase_GDSL domains with abundance values of 2131 and 1246, respectively. Our results are in agreement with the work of Lo et al.[45], who sequenced the *P. fluorescens* SRM1 strain and found that its genome contains heat-stable lipases encoded by *lipA* and *lipB* genes, which are responsible for spoilage of raw milk[45].

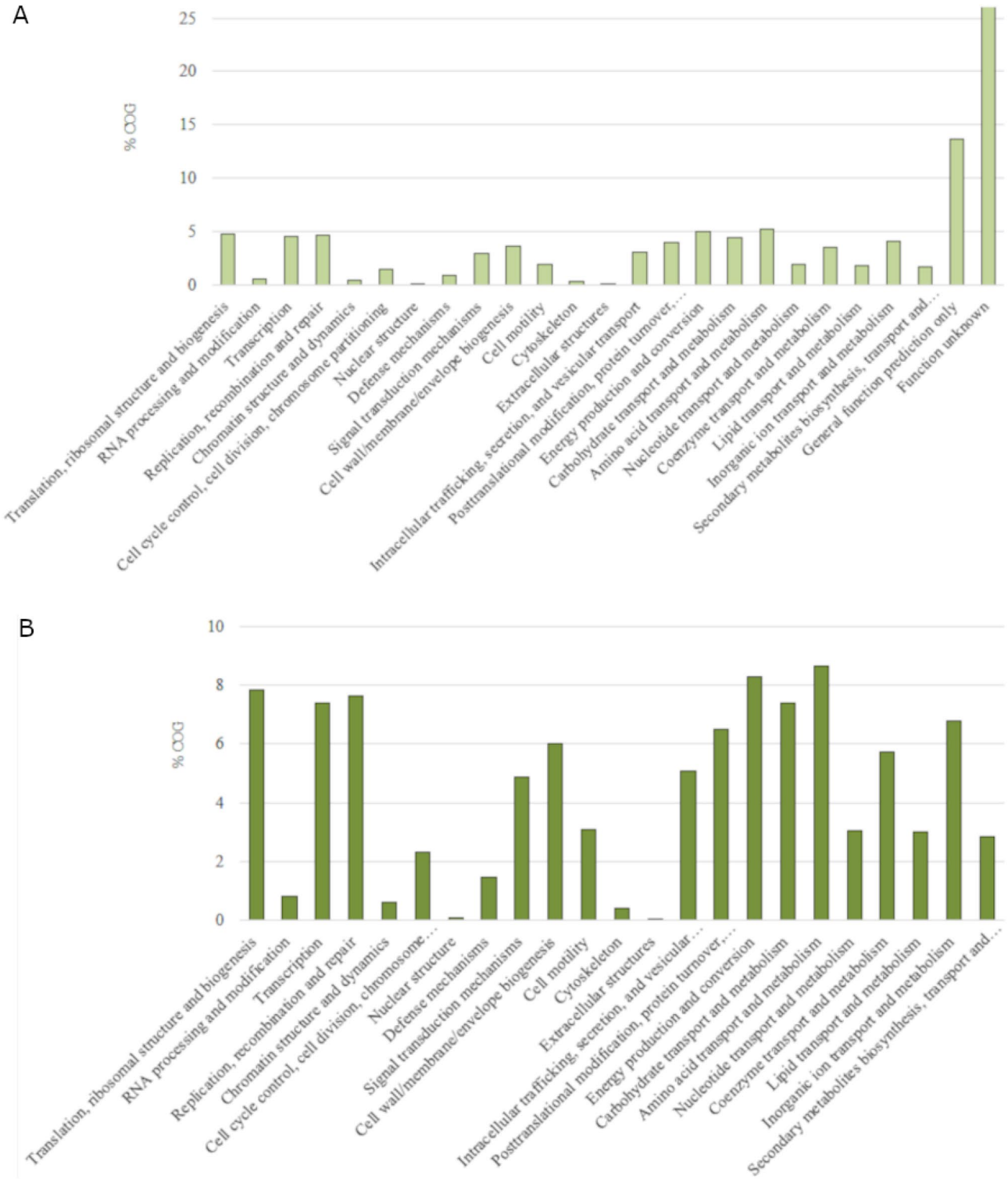

Figure 5. COG distribution of *P. psychrophila* KM02 genome.

Effect of subMICs of BPEO, TEO, and their major compounds on *P. psychrophila* KM02 lipolytic activity. In light of the increasing use of EOs as modern fish biopreservatives, the current study assessed the anti-lipolytic potentials of BPEO and TEO and their major compounds toward KM02. Although the spoilage of fishery products is mainly caused by gram-negative microbes[51] it is advisable to inhibit pseudomonad metabolic activity in seafoods. For this study, the subMIC concentrations of all agents were used; the concentrations of EOs above subMIC levels in foods can be sensorily unacceptable for consumers[52]. Many studies have demonstrated that plant EOs (e.g., oils of cinnamon and glove) can suppress bacterial metabolic activities/production of viru-

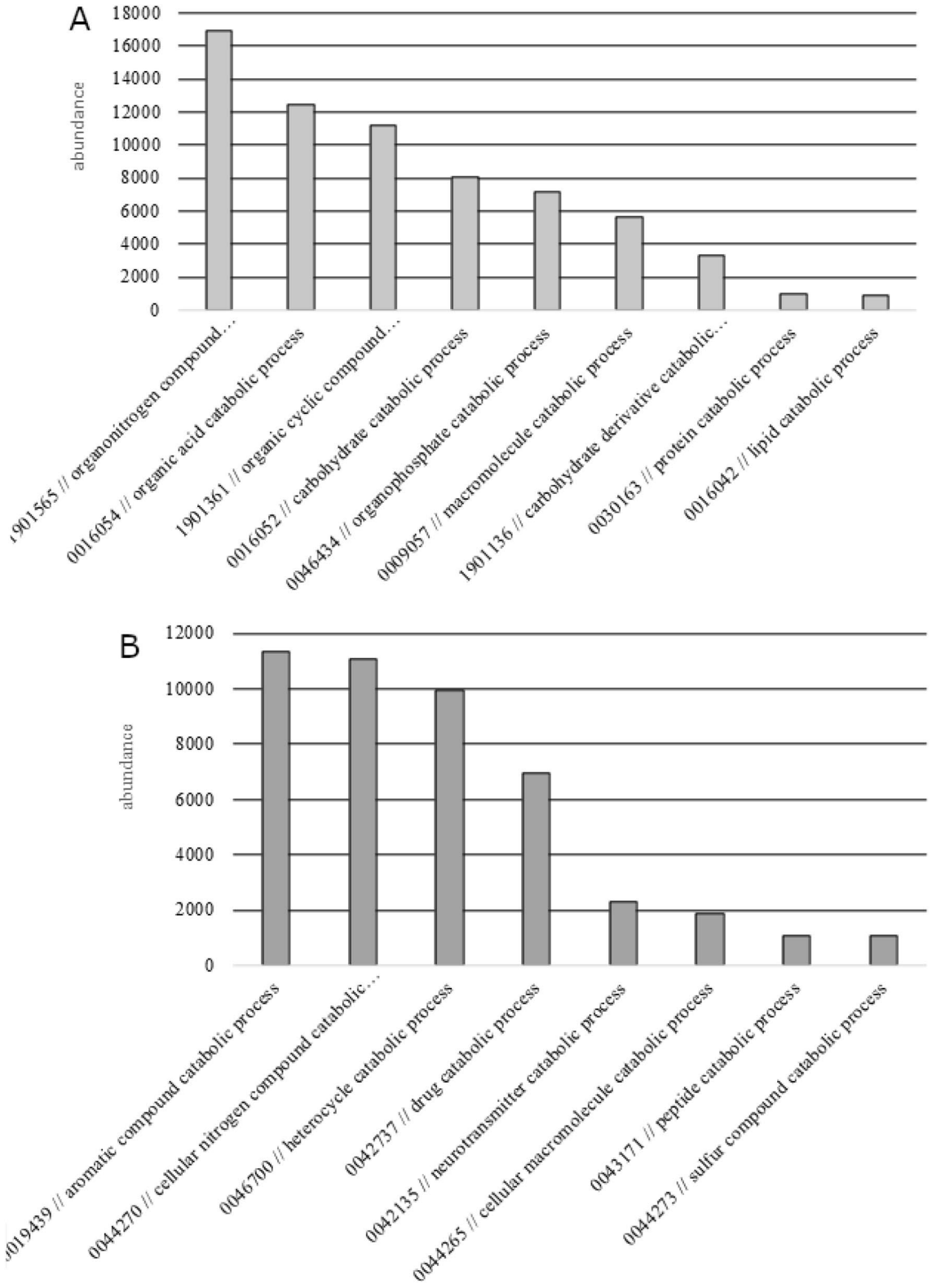

Figure 6. Gene abundance of selected GO terms in *P. psychrophila* KM02 genome. (**A**) Selected child terms of 'organic substance catabolic process' GO term. (**B**) Selected child terms of 'cellular catabolic process' GO term.

lence factors when used at subMIC concentrations[53]. However, to date the inhibition of lipase production by plant- derived antimicrobials has only been shown in *Serratia marcescens* and *P. fluorescens* cultures[54,55].

Biological domain	GO term	Definition according to QuickGO browser (https://www.ebi.ac.uk/QuickGO/)	Genome abundance
GO cellular component	1902494//catalytic complex	A protein complex which is capable of catalytic activity	23,765
	0098796//membrane protein complex	Any protein complex that is part of a membrane	20,030
	1902495//transmembrane transporter complex	A transmembrane protein complex which enables the transfer of a substance from one side of a membrane to the other	15,286
	0015627//type II protein secretion system complex	A large protein complex, containing 12–15 subunits, that spans the cell envelope of Gram-negative bacteria and mediates the movement of proteins into the extracellular environment	767
GO molecular function	0016787//hydrolase activity	Catalysis of the hydrolysis of various bonds, e.g. C–O, C–N, C–C, phosphoric anhydride bonds, etc	284,201
	0008233//peptidase activity	Catalysis of the hydrolysis of a peptide bond	39,142
	0022857//transmembrane transporter activity	Enables the transfer of a substance, usually a specific substance or a group of related substances, from one side of a membrane to the other	207,467
	0140096//catalytic activity, acting on a protein	Catalytic activity that acts to modify a protein	85,264
	0016788//hydrolase activity, acting on ester bonds	Catalysis of the hydrolysis of any ester bond	44,622

Table 2. Selected GO terms of annotated *P. psychrophila* KM02 genome.

Pfam ID/name	Description/putative function	Genome abundance
Amidohydro_1	A large metal dependent hydrolase superfamily	11,828
Abhydrolase_1	A superfamily of hydrolytic enzymes including proteases, lipases, peroxidases, esterases, epoxide hydrolases and dehalogenases	7768
AA_permease_2	Integral membrane proteins involved in the transport of amino acids into the cell	6643
Abhydrolase_6	Family contains alpha/beta hydrolase enzymes of diverse specificity	6099
MMPL	Putative integral membrane proteins from bacteria with probably function of lipid transport	5848
Peptidase_M20	Family includes a range of zinc metallopeptidases belonging to several families in the peptidase classification	5763
CN_hydrolase	Family contains hydrolases that break carbon–nitrogen bonds	5612
Amidase	A large group of hydrolytic enzymes that catalyse the hydrolysis of amide bonds (CO-NH2) of diverged substrates	5466
T2SSE	Family contains components of both the Type II (T2SS) and Type IV (T4SS) protein secretion system from Gram-negative bacteria	5142
Hydrolase_4	Domain found in bacteria and eukaryotes; the majority of the members in this family carry the exopeptidase active-site residues	4896
MotA_ExbB	Family groups together integral membrane proteins that appear to be involved translocation of proteins across a membrane	4393
Peptidase_M24	Family contains metallopeptidases that belong to MEROPS peptidase family M24	3955
M20_dimer	Domain consists of 4 beta strands and two alpha helices which make up the dimerisation surface of members of the M20 family of peptidases	3075
Secretin	Family includes: protein D that is involved in the general (type II) secretion pathway (GSP) within Gram-negative bacteria, a signal sequence-dependent process responsible for protein export	3050
Peptidase_M23	Members of this family are zinc metallopeptidases with a range of specificities	2758
Lon_C	The Lon serine proteases must hydrolyse ATP to degrade protein substrates; classified as family S16 in Merops	2446
Zn_protease	Family annotated as being ATP-dependant zinc proteases	2408
ELFV_dehydrog	Family that catalyze the oxidative deamination of an amino acid to its keto acid derivatives	2372
Peptidase_S11	Include a wide range of peptidase activity, including exopeptidase, endopeptidase, oligopeptidase and omega-peptidase activity	2249
Cys_Met_Meta_PP	Family includes enzymes involved in cysteine and methionine metabolism; acting as a coenzyme in a multitude of reactions, including decarboxylation, deamination and transamination	2191
Autotransporter	Family corresponds to the presumed integral membrane beta-barrel domain that transports the proteins products through the outer membrane	2160
Secretin_N	Domain found in bacterial type II/III secretory system proteins	2132
Lipase_3	A domain with an alpha/beta hydrolase fold that hydrolyse ester linkages of triglycerides	2131
Amidohydro_2	Amidohydrolases related to Amidohydro_1, family includes adenine deaminase that hydrolyses adenine to form hypoxanthine and ammonia	2066
Peptidase_M3	Group of metallopeptidases (oligopeptidases) that cleave medium sized peptides	1757
Ser_hydrolase	Family with serine hydrolase activity	1683
Peptidase_C13	Family of cysteine proteases that hydrolyses a peptide bond using the thiol group of a cysteine residue as a nucleophile	1623
Peptidase_S9	Family of serine-type peptidase activity	1622
Aminopep	Family of bacterial proteins has a conserved HEXXH motif, suggesting that members are putative peptidases of zincin fold	1550
Abhydrolase_2	Family consists of phospholipases and carboxylesterases with broad substrate specificity	1527
Lipase_GDSL	GDSL esterases and lipases are hydrolytic enzymes with multifunctional properties	1246
FA_desaturase	enzymes that catalyse the insertion of a double bond at the delta position of fatty acids	1240

Table 3. Selected Pfam annotated domains in *P. psychrophila* KM02 genome.

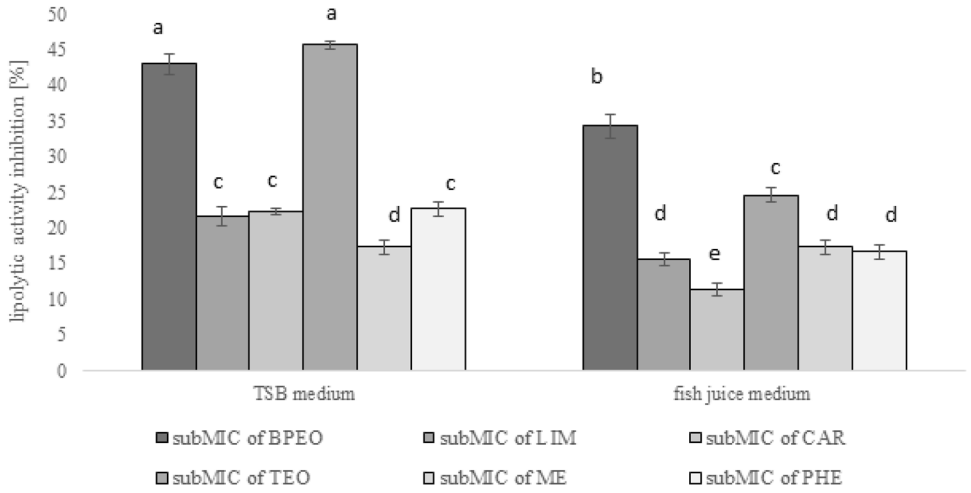

Figure 7. Inhibition of lipolytic activity of P. psychrophila KM02 grown on modified TSB and fish juice medium supplemented with subMICs of black pepper (BPEO) and tarragon essential oils (TEO), limonene (LIM), β-caryophyllene (CAR), methyl eugenol (ME), and β-phellandrene (PHE). Values are calculated from three independent replicates. Error bars represents standard deviation values. The same letter indicates not statistically differences in expression as provided by Tukey's test after ANOVA analysis ($F = 308.6$, $p < 0.05$).

To investigate whether the analyzed compounds changed the lipolytic activity in KM02 cells, first, the spectrophotometric method with p-NPP reagent was used. As presented in Fig. 7, all treatments resulted in a considerable lipolysis decrease depending on the compound and medium, and it ranged from 11 to 46%. The highest inhibition potential was observed for the bulk of BPEO and TEO applied in modified TSB medium, and it was approximately twice that of major compounds used alone. The anti-lipolytic action of EO obtained from juniper toward fish-related *P. fluorescens* was also investigated, where the whole oil inhibited lipase production by 45%, while its major compounds, i.e., α-pinene and sabinene were significantly less effective[55]. A similar outcome was observed in the context of proteolytic enzyme inhibition in KM02, which was reduced to less than 20% by PHE and 28% by CAR, while TEO and BPEO resulted in significantly higher effects[8,14]. The explanation of such findings may be related to the lower antimicrobial effect of single terpenes, which was also seen in in vitro tests[52]. Notably, a combination of two different EO constituents or the presence of minor components in the entire EO volume can cause additive or synergistic antimicrobial effects[56]. For example, the inhibitory effect of LIM on *P. aeruginosa* was enhanced by the addition of on equal volume of eucalyptol[57].

In fish juice medium, the overall anti-lipolytic activity was significantly ($p < 0.05$) lower than that under *in vitro* conditions, with the exception of ME. However, based on the results, this compound inhibited lipolytic activity by only 17%. The decreased antimicrobial effectiveness of EOs and their major constituents is probably due to the more complex composition and physiochemical characteristics of the medium extracted from fish fillets. According to our previous study[55], fish juice medium constituted 1.8 mg/g protein and 0.0635 mg/g lipids, which ideally mimics fish muscle conditions. These food components usually considerably reduce EOs bioactivity and protect bacteria by absorbing some volume of added EOs[58]. Therefore, to maintain equal antimicrobial efficacy in real food matrices where high molecular compounds are present, higher concentrations of antimicrobials are needed[59]. Furthermore, *P. psychrophila* was the least sensitive analyzed fish isolate for rosemary extract applied in a food model of common carp fillets, and its lipolytic potential was arrested by only one day in relative to the control culture[7].

Similarly to *Actinobacter baumannii* and *Vibrio cholerae* strains, the genome of KM02 harbors genes encoding lipases (*lipA, lipB*)[60]. In this work, the anti-lipolytic activity of subMICs among the compounds was verified by RT-qPCR experiments and evaluation the expression of genes encoding lipases (*lipA, lipB*) in KM02 was evaluated. Based on the Pffafl calculations, the ratio of the expression of the *lipA* gene encoding the major lipase synthase ranged from 0.1 to 0.9 regardless of the culture medium used (Fig. 8). The highest decrease in *lipA* gene transcription was observed in cells treated with BPEO and TEO, which confirmed the phenotypic observations. Because the *lipA* and *lipB* genes are linked in a single operon, a disruption of even one of them results in a lipase-negative phenotype[61]. In the previous work, the *LipB* gene was also downregulated to the highest extent by whole EOs. According to the work of Christensen et al.[62], the absence of the LipB protein in *Serratia proteamaculans* resulted in no spoilage of milk-based products. The aforementioned works indicate that changes in the expression of the *lipA* and *lipB* genes may result in a reduced rate of food biodeterioration[6].

Effect of subMICs of BPEO, TEO, and their major compounds on *P. psychrophila* KM02 T2SS. LipA and LipB are known type 2 substrates that degrade lipids[60]. Ogierman et al.[60] noticed that a lipase-deficient *lipA* mutant of *Vibrio cholerae* was not able to grow on olive oil, and complementing the T2SS mutant with a plasmid expressing LipAB did not reverse this defect suggesting that secretion of lipases is T2SS-dependent. T2SS apparatus proteins are considered antimicrobial targets; thus in this work changes in the

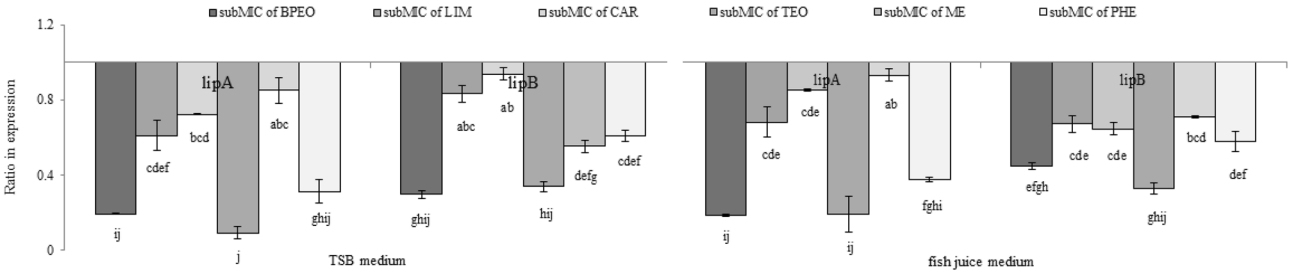

Figure 8. Ratio in expression of *lipA* and *lipB* genes in *P. psychrophila* KM02 grown on modified TSB and fish juice medium supplemented with subMICs of black pepper (BPEO) and tarragon essential oils (TEO), limonene (LIM), β-caryophyllene (CAR), methyl eugenol (ME), and β-phellandrene (PHE). Values are calculated from three independent replicates. Error bars represents standard deviation values. The same letter indicates not statistically differences in expression as provided by Tukey's test after ANOVA analysis ($F = 41.97$, $p < 0.05$).

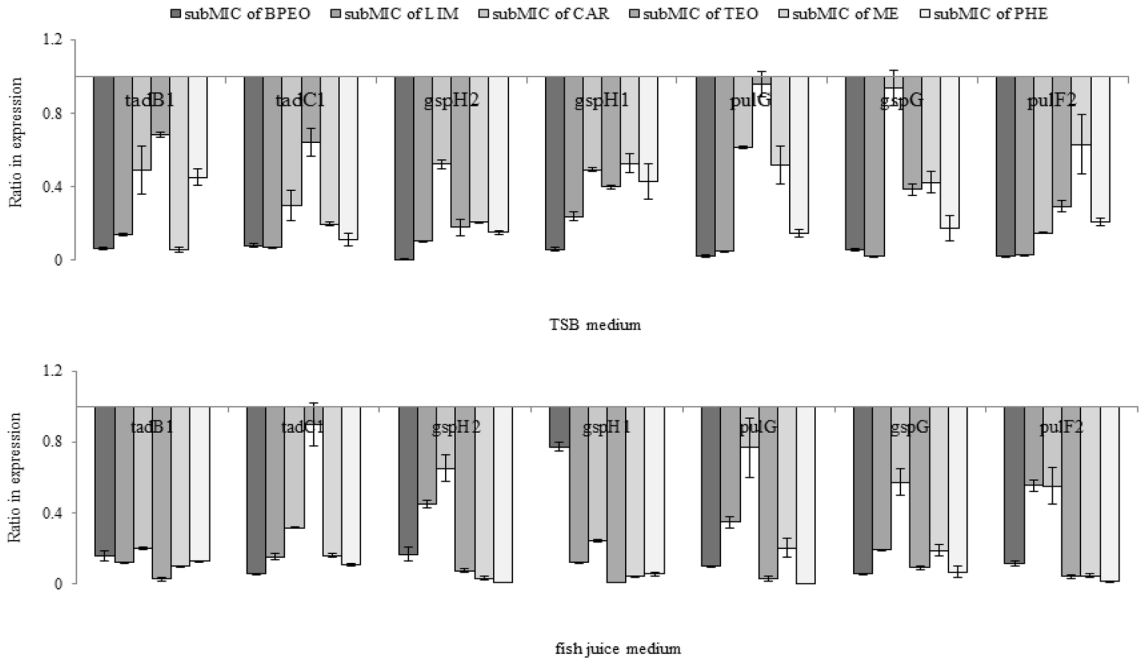

Figure 9. Ratio in expression of type II secretion system genes in *P. psychrophila* KM02 grown on modified TSB and fish juice medium supplemented with subMICs of black pepper (BPEO) and tarragon essential oils (TEO), limonene (LIM), β-caryophyllene (CAR), methyl eugenol (ME), and β-phellandrene (PHE). Values are calculated from three independent replicates. Error bars represents standard deviation values. The statistically differences in expression was provided by Tukey's test after ANOVA analysis ($F = 41.32$, $p < 0.05$).

mRNA levels of T2 secretome genes in KM02 cells were evaluated. For RT–qPCR experiments, KM02 cells were treated with subMICs of BPEO, TEO and major compounds of the oils both in vitro and in fish juice medium mimicking the seafood ecosystem.

Based on bioinformatic analysis of the KM02 genome, the following 7 potential genes responsible for T2SS function were identified: *pulG* and *gspG* genes encoding pseudopilins PulG and GspG respectively; *tadB1* and *tadC1* genes encoding integral proteins of the inner membrane involved in the general secretion pathway (GSP); *gspH2* and *gspH1* genes encoding proteins required for energy-related secretion from the periplasm; and *pulF* gene involved in lipase export (Supplementary Table S3). As presented in Fig. 9, regardless of the agents used, the expression levels of most T2SS genes were inhibited to relative levels of between 0.9 and 0.02 that of control. Under in vitro conditions the most efficient treatments for downregulation of the expression of T2SS genes were BPEO and LIM, with relative transcript levels ranging from 0.2 to 0.02 that of control. In fish juice medium the highest reductions in the mRNA levels of T2SS genes were recorded for TEO and its singular components (i.e., ME and PHE). The most considerable inhibition concerned *gspH1* (0.05) and *gspH2* (0.02). These results are in line with the work of Jain, Nale and Dabur[63], in which the response of pseudomonads to natural antimicrobials was evaluated at a proteomic level. Downregulation of proteins involved in secretion systems (e.g. xcp, PilS) in *P. aeruginosa* was caused by water extracts of the active fraction of catechins from *Saraca asoca* flowers[63]. Additionally, in the work of Singh et al.[64], the authors noted the role of thyme EO in targeting the virulence

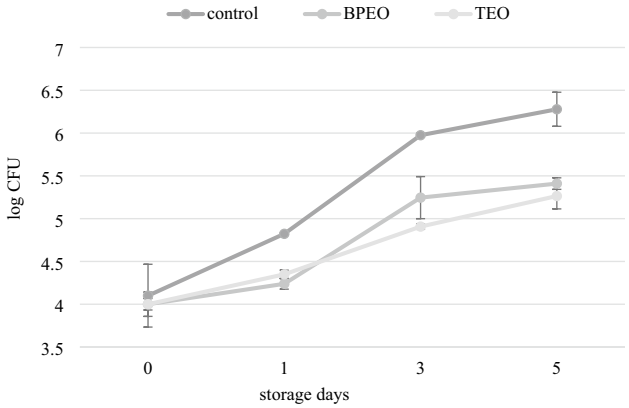

Figure 10. Combined effect of marinade and BPEO/TEO on *P. psychrophila* KM02 counts in salmon fillets stored at 4 °C in vacuum conditions. Data points represent the mean taken from two replicate experiments and error bars indicate the standard deviations (SD). The statistically differences was provided by Tukey's test after ANOVA analysis ($F = 50.34$, $p < 0.05$).

arsenal regulated by the T2SS of *Xanthomonas oryzae* pv. *oryzae* strains. The downregulation of virulence gene expression in *Xanthomonas* strains remained insignificant when the bacteria were treated with thymol alone[64].

Changes in *P. psychrophila* KM02 growth in salmon-model products with subMICs of BPEO/TEO. The observed effect of BPEO and TEO on the T2SS-dependent lipolytic activity of the KM02 strain, triggered the need to verify the biopreservative properties of the examined agents in salmon-model products. The application of EOs in food requires additional techniques to mask their strong odor and simultaneously ensure their effectiveness[65]. In this work, an oil-vinegar marinade supplemented with subMICs of BPEO and TEO was formulated to improve the quality of fresh salmon fillets. The model product inoculated with standard amount of KM02 was next packed under vacuum conditions to prevent the degradation of EO components by oxygen.

The KM02 count after 1, 3, and 5 days of storage were evaluated (Fig. 10). After 1 day from an initial value of 4 log CFU/g, the KM02 control culture reached 4.8 log CFU/g, while BPEO and TEO impeded cell proliferation to 4.2 and 4.3 log CFU/g, respectively. At 3 and 5 days of storage, both treatments resulted in a significant ($p < 0.05$) reduction in KM02 counts in relation to the control product, where only marinade and vacuum packaging were applied. KM02 cells in the control sample reached a critical spoilage value of 6 log CFU/g between 3 and 5 days of refrigerated storage. BPEO- and TEO-treated samples did not exceed the value of 5.5 log CFU, which indicates the antimicrobial effect of marinade supplemented with EOs. Interestingly, even as strictly aerobic bacteria, KM02, was still able to proliferate under vacuum conditions. A substantial number of pseudomonad cells, despite vacuum packaging, were also observed in refrigerated trout fillet[66]. This is probably due to an inadequate barrier material used for packaging or not completely evacuating the gas from samples and the ability of cells to thrive in microaerophilic conditions. However, in comparison with aerobic storage, reducing the amount of oxygen results in a considerable decrease in microbiological counts and is an effective method for fish preservation based on hurdle technology[67]. Inhibitory effects of marinades enriched with oregano, rosemary and juniper EOs on the growth kinetics of psychotropic bacteria- contaminated foods were also observed by Siroli et al.[68]. In that work, marination showed the highest inhibition against *Pseudomonas* spp. and total coliforms. The molecular studies of Wu et al.[69] revealed that selective compounds of EOs may competitively interact with the ATP binding site of the DNA gyrase B subunit of bacteria. Thus, natural antimicrobials combine with DNA to form a complex that eventually leads to DNA degradation, blocking cell transcription and replication[70]. Some bioactive agents may also cause the rearrangements of the nucleic acid double chain[21]. Interference with nucleic acids by bioactive compounds of EOs regulates bacterial metabolism and proliferation[21]. Moreover, aside from the ability to improve the safety and shelf-life of marinated fish, the utilization of EOs may also enhance consumers' willingness to buy, in light of the recent increasing consumption of clean-label products[71].

Conclusions

In this work, bioinformatic analysis of genome and pangenome of KM02 revealed the ability of the strain to spoil foods with high content of proteins and lipids. Inactivation of T2SS by subMICs of BPEO and TEO resulted in reduced synthesis and secretion of lipases in KM02. The expression levels of most T2SS genes as well as *lipA* and *lipB* genes encoding lipases of the KM02 strain were downregulated by EOs. These features were observed in in vitro conditions and fish juice medium which mimicked the seafoods ecosystem. The biopreservative properties of BPEO and TEO were confirmed in salmon-model products; the oil-vinegar marinade supplemented with subMICs of the examined EOs impeded KM02 proliferation in comparison to the growth of bacteria in the control product, where only marinade and vacuum packaging were applied. Marinade supplemented with

subMICs of BPEO and TEO can improve the quality of fresh salmon fillets in light of the recent increasing consumption of clean-label products.

Data availability

The data that support the findings of this study are available from the corresponding author upon reasonable request. All of the sequencing data were deposited in NCBI under Accession Number NZ_CP049044.1.

Received: 21 December 2021; Accepted: 21 March 2022
Published online: 31 March 2022

References

1. Jia, S. *et al.* Biochemical changes induced by dominant bacteria in chill-stored silver carp (Hypophthalmichthys molitrix) and GC-IMS identification of volatile organic compounds. *Food Microbiol.* **84**, 103248 (2019).
2. Comi, G. Spoilage of Meat and Fish. in *The Microbiological Quality of Food* 179–210 (Elsevier, 2017). https://doi.org/10.1016/B978-0-08-100502-6.00011-X.
3. Ghaly. Fish spoilage mechanisms and preservation techniques: Review. *Am. J. Appl. Sci.* **7**, 859–877 (2010).
4. Chaijan, M., Benjakul, S., Visessanguan, W. & Faustman, C. Changes of lipids in sardine (Sardinella gibbosa) muscle during iced storage. *Food Chem.* **1**, 83–91 (2006).
5. Andersson, R. E., Hedlund, C. B. & Jonsson, U. Thermal inactivation of a heat-resistant lipase produced by the psychrotrophic bacterium pseudomonas fluorescens. *J. Dairy Sci.* **62**, 361–367 (1979).
6. Narvhus, J. A., Nilsen Bækkelund, O., Tidemann, E. M., Østlie, H. M. & Abrahamsen, R. K. Isolates of Pseudomonas spp. from cold-stored raw milk show variation in proteolytic and lipolytic properties. *Int. Dairy J.* **123**, 105049 (2021).
7. Sterniša, M., Purgatorio, C., Paparella, A., Mraz, J. & Smole Možina, S. Combination of rosemary extract and buffered vinegar inhibits *Pseudomonas* and *Shewanella* growth in common carp (*Cyprinus carpio*). *J. Sci. Food Agric.* **100**, 2305–2312 (2020).
8. Sobieszczańska, N. *et al.* Tarragon essential oil as a source of bioactive compounds with anti-quorum sensing and anti-proteolytic activity against Pseudomonas spp. isolated from fish – in vitro, in silico and in situ approaches. *Int. J. Food Microbiol.* **331**, 108732 (2020).
9. Rosenau, F. Bacterial lipases from Pseudomonas: Regulation of gene expression and mechanisms of secretion. *Biochimie* **82**, 1023–1032 (2000).
10. Waack, U. *et al.* Targeting the type II secretion system: development, optimization, and validation of a high-throughput screen for the identification of small molecule inhibitors. *Front. Cell. Infect. Microbiol.* **7**, 380 (2017).
11. Rantsiou, K. *et al.* Next generation microbiological risk assessment: Opportunities of whole genome sequencing (WGS) for food-borne pathogen surveillance, source tracking and risk assessment. *Int. J. Food Microbiol.* (2017).
12. Kisand, V. & Lettieri, T. Genome sequencing of bacteria: sequencing, de novo assembly and rapid analysis using open source tools. *BMC Genomics* **14**, 211 (2013).
13. Sterniša, M., Klančnik, A. & Smole Možina, S. Spoilage *Pseudomonas* biofilm with *Escherichia coli* protection in fish meat at 5 °C. *J. Sci. Food Agric.* https://doi.org/10.1002/jsfa.9703 (2019).
14. Tomaś, N. *et al.* Effect of black pepper essential oil on quorum sensing and efflux pump systems in the fish-borne spoiler Pseudomonas psychrophila KM02 identified by RNA-seq, RT-qPCR and molecular docking analyses. *Food Control* **130**, 108284 (2021).
15. ISO 3061:2008. *ISO* https://www.iso.org/cms/render/live/en/sites/isoorg/contents/data/standard/04/16/41617.html.
16. ISO 10115:2013. *ISO* https://www.iso.org/cms/render/live/en/sites/isoorg/contents/data/standard/05/61/56159.html.
17. Moosavi-Nasab, M. *et al.* Biodegradable chitosan coating incorporated with black pepper essential oil for shelf life extension of common carp (Cyprinus carpio) during refrigerated storage. *J. Food Prot.* **79**, 986–993 (2016).
18. Farsanipour, A., Khodanazary, A. & Hosseini, S. M. Effect of chitosan-whey protein isolated coatings incorporated with tarragon Artemisia dracunculus essential oil on the quality of Scomberoides commersonnianus fillets at refrigerated condition. *Int. J. Biol. Macromol.* **155**, 766–771 (2020).
19. Socaciu, M.-I. *et al.* Effects of whey protein isolate-based film incorporated with tarragon essential oil on the quality and shelf-life of refrigerated brook trout. *Foods* **10**, 401 (2021).
20. Bakkali, F., Averbeck, S., Averbeck, D. & Idaomar, M. Biological effects of essential oils—A review. *Food Chem. Toxicol.* **46**, 446–475 (2008).
21. Pan, Y., Deng, Z. & Shahidi, F. Natural bioactive substances for the control of food-borne viruses and contaminants in food. *Food Prod. Process. Nutr.* **2**, 27 (2020).
22. Wikler, M. Methods for dilution antimicrobial susceptibility tests for bacteria that grow aerobically: Approved standard. *CLSI NCCLS* **26**, M7-A7 (2006).
23. Darling, A. C. E., Mau, B., Blattner, F. R. & Perna, N. T. Mauve: Multiple alignment of conserved genomic sequence with rearrangements. *Genome Res.* **14**, 1394–1403 (2004).
24. Petkau, A., Stuart-Edwards, M., Stothard, P. & Van Domselaar, G. Interactive microbial genome visualization with GView. *Bioinformatics* **26**, 3125–3126 (2010).
25. Chaudhari, N. M., Gupta, V. K. & Dutta, C. BPGA- an ultra-fast pan-genome analysis pipeline. *Sci. Rep.* **6**, 24373 (2016).
26. Kanehisa, M. & Goto, S. KEGG: kyoto encyclopedia of genes and genomes. *Nucleic Acids Res.* **28**, 27–30 (2000).
27. Kanehisa, M. Toward understanding the origin and evolution of cellular organisms. *Protein Sci. Publ. Protein Soc.* **28**, 1947–1951 (2019).
28. Kanehisa, M., Furumichi, M., Sato, Y., Ishiguro-Watanabe, M. & Tanabe, M. KEGG: integrating viruses and cellular organisms. *Nucleic Acids Res.* **49**, D545–D551(2021).
29. Wu, S., Zhu, Z., Fu, L., Niu, B. & Li, W. WebMGA: a customizable web server for fast metagenomic sequence analysis. *BMC Genomics* **12**, 444 (2011).
30. Stuer, W., Jaeger, K. E. & Winkler, U. K. Purification of extracellular lipase from Pseudomonas aeruginosa. *J. Bacteriol.* **168**, 1070–1074 (1986).
31. Ye, J. *et al.* Primer-BLAST: A tool to design target-specific primers for polymerase chain reaction. *BMC Bioinformatics* **13**, 134 (2012).
32. Ruijter, J. M. *et al.* Amplification efficiency: linking baseline and bias in the analysis of quantitative PCR data. *Nucleic Acids Res.* **37**, e45–e45 (2009).
33. Pfaffl, M. W. A new mathematical model for relative quantification in real-time RT-PCR. *Nucleic Acids Res.* **29**, 45e–445 (2001).
34. Xie, J., Zhang, Z., Yang, S.-P., Cheng, Y. & Qian, Y.-F. Study on the spoilage potential of Pseudomonas fluorescens on salmon stored at different temperatures. *J. Food Sci. Technol.* **55**, 217–225 (2018).
35. Aarestrup, F. M., Wegener, H. C. & Collignon, P. Resistance in bacteria of the food chain: Epidemiology and control strategies. *Expert Rev. Anti Infect. Ther.* **6**, 733–750 (2008).

36. Jiang, B. *et al.* Genome sequence of a cold-adaptable sulfamethoxazole-degrading bacterium, pseudomonas psychrophila HA-4. *J. Bacteriol.* https://doi.org/10.1128/JB.01377-12 (2012).
37. Abraham, W. P. & Thomas, S. Draft Genome Sequence of Pseudomonas psychrophila MTCC 12324, Isolated from the Arctic at 79°N. *Genome Announc.* https://doi.org/10.1128/genomeA.00578-15 (2015).
38. Land, M. *et al.* Insights from 20 years of bacterial genome sequencing. *Funct. Integr. Genomics* **15**, 141–161 (2015).
39. Wessels, L. *et al.* Draft genome sequences of pseudomonas sp. isolates recovered from ghanaian fish food samples in 2018. *Microbiol. Resour. Announc.* (2021). https://doi.org/10.1128/MRA.01332-20.
40. Stanborough, T. *et al.* Genomic and metabolic characterization of spoilage-associated Pseudomonas species. *Int. J. Food Microbiol.* **268**, 61–72 (2018).
41. Jin, L., Chen, Y., Yang, W., Qiao, Z. & Zhang, X. Complete genome sequence of fish-pathogenic Aeromonas hydrophila HX-3 and a comparative analysis: insights into virulence factors and quorum sensing. *Sci. Rep.* **10**, 15479 (2020).
42. Li, J. *et al.* Complete genome sequence provides insights into the quorum sensing-related spoilage potential of Shewanella baltica 128 isolated from spoiled shrimp. *Genomics* **112**, 736–748 (2020).
43. Ge, Y., Zhu, J., Ye, X. & Yang, Y. Spoilage potential characterization of Shewanella and Pseudomonas isolated from spoiled large yellow croaker (Pseudosciaena crocea). *Lett. Appl. Microbiol.* **64**, 86–93 (2017).
44. Sterniša, M., Bucar, F., Kunert, O. & Smole Možina, S. Targeting fish spoilers Pseudomonas and Shewanella with oregano and nettle extracts. *Int. J. Food Microbiol.* **328**, 108664 (2020).
45. Lo, R., Stanton-Cook, M. J., Beatson, S. A., Turner, M. S. & Bansal, N. Draft genome sequence of pseudomonas fluorescens SRM1, an isolate from spoiled raw milk. *Genome Announc.* https://doi.org/10.1128/genomeA.00138-15 (2015).
46. Yon Rhee, S., Wood, V., Dolinski, K. & Draghici, S. Use and misuse of the gene ontology annotations. *Nat. Rev. Genet.* **9**, 509–515 (2008).
47. Liu, X., Xu, J., Zhu, J., Du, P. & Sun, A. Combined transcriptome and proteome analysis of rpos regulon reveals its role in spoilage potential of pseudomonas fluorescens. *Front. Microbiol.* **10**, 94 (2019).
48. Liu, X. *et al.* Role of RpoS in stress resistance, quorum sensing and spoilage potential of Pseudomonas fluorescens. *Int. J. Food Microbiol.* **270**, 31–38 (2018).
49. El-Gebali, S. *et al.* The Pfam protein families database in 2019. *Nucleic Acids Res.* **47**, D427–D432 (2019).
50. Wu, J.-W. & Chen, X.-L. Extracellular metalloproteases from bacteria. *Appl. Microbiol. Biotechnol.* **92**, 253–262 (2011).
51. Zhuang, S., Hong, H., Zhang, L. & Luo, Y. Spoilage-related microbiota in fish and crustaceans during storage: Research progress and future trends. *Compr. Rev. Food Sci. Food Saf.* **20**, 252–288 (2021).
52 Hyldgaard, M., Mygind, T. & Meyer, R. L. Essential oils in food preservation: Mode of action, synergies, and interactions with food matrix components. *Front. Microbiol.* **3**, (2012).
53. Smith-Palmer, A., Stewart, J. & Fyfe, L. Influence of subinhibitory concentrations of plant essential oils on the production of enterotoxins A and B and alpha-toxin by Staphylococcus aureus. *J. Med. Microbiol.* **53**, 1023–1027 (2004).
54. Srinivasan, R., Devi, K. R., Kannappan, A., Pandian, S. K. & Ravi, A. V. Piper betle and its bioactive metabolite phytol mitigates quorum sensing mediated virulence factors and biofilm of nosocomial pathogen Serratia marcescens in vitro. *J. Ethnopharmacol.* **193**, 592–603 (2016).
55. Myszka, K. *et al.* In situ approaches show the limitation of the spoilage potential of Juniperus phoenicea L. essential oil against cold-tolerant Pseudomonas fluorescens KM24. *Appl. Microbiol. Biotechnol.* **105**, 4255–4268 (2021).
56. Bassolé, I. H. N. & Juliani, H. R. Essential oils in combination and their antimicrobial properties. *Molecules* **17**, 3989–4006 (2012).
57. van Vuuren, S. F. & Viljoen, A. M. Antimicrobial activity of limonene enantiomers and 1,8-cineole alone and in combination. *Flavour Fragr. J.* **22**, 540–544 (2007).
58. Perricone, M., Arace, E., Corbo, M. R., Sinigaglia, M. & Bevilacqua, A. Bioactivity of essential oils: a review on their interaction with food components. *Front. Microbiol.* **6**, (2015).
59. Rao, J., Chen, B. & McClements, D. J. Improving The Efficacy Of Essential Oils As Antimicrobials In Foods: Mechanisms Of Action. *Annu. Rev. Food Sci. Technol.* **10**, 365–387 (2019).
60. Ogierman, M. A. *et al.* Characterization of the Vibrio cholerae El Tor lipase operon lipAB and a protease gene downstream of the hly region. *J. Bacteriol.* **179**, 7072–7080 (1997).
61. Frenken, L. G. J., Groot, A., Tommassen, J. & Verrips, C. T. Role of the lipB gene product in the folding of the secreted lipase of Pseudomonas glumae. *Mol. Microbiol.* **9**, 591–599 (1993).
62. Christensen, A. B. *et al.* Quorum-sensing-directed protein expression in Serratia proteamaculans B5a. *Microbiology* **149**, 471–483 (2003).
63. Jain, P., Nale, A. & Dabur, R. Antimicrobial metabolites from Saraca asoca impairs the membrane transport system and quorum-sensing system in Pseudomonas aeruginosa. *Arch. Microbiol.* **200**, 237–253 (2018).
64. Singh, A., Gupta, R., Tandon, S. & Pandey, R. Thyme oil reduces biofilm formation and impairs virulence of xanthomonas oryzae. *Front. Microbiol.* **8**, 1074 (2017).
65. Hassoun, A. & Emir Çoban, Ö. Essential oils for antimicrobial and antioxidant applications in fish and other seafood products. *Trends Food Sci. Technol.* **68**, 26–36 (2017).
66. Frangos, L., Pyrgotou, N., Giatrakou, V., Ntzimani, A. & Savvaidis, I. N. Combined effects of salting, oregano oil and vacuum-packaging on the shelf-life of refrigerated trout fillets. *Food Microbiol.* **27**, 115–121 (2010).
67. Mexis, S. F., Chouliara, E. & Kontominas, M. G. Combined effect of an oxygen absorber and oregano essential oil on shelf life extension of rainbow trout fillets stored at 4 °C. *Food Microbiol.* **26**, 598–605 (2009).
68. Siroli, L. *et al.* Use of essential oils to increase the safety and the quality of marinated Pork Loin. *Foods* **9**, 987 (2020).
69. Wu, T., Zang, X., He, M., Pan, S. & Xu, X. Structure-activity relationship of flavonoids on their anti-Escherichia coli activity and inhibition of DNA gyrase. *J. Agric. Food Chem.* **61**, 8185–8190 (2013).
70. Fang, Y. *et al.* 3D-QSAR and docking studies of flavonoids as potent *Escherichia coli* inhibitors. *Sci. Rep.* **6**, 23634 (2016).
71. Asioli, D. *et al.* Making sense of the 'clean label' trends: A review of consumer food choice behavior and discussion of industry implications. *Food Res. Int. Ott. Ont* **99**, 58–71 (2017).

Acknowledgements

This study was funded by a grant from the National Science Centre, Poland (no. 2016/23/D/NZ9/00028).

Author contributions

N.T. and K.M. conceived and designed the study and performed experiments; N.T. wrote original draft of the manuscript; K.M. reviewed the manuscript; Ł.W. performed bioinformatics analysis. All the authors have read and agreed to the final version of the manuscript.

Funding

This article was funded by Narodowym Centrum Nauki (Grant no. 2016/23/D/NZ9/00028).

Competing interests
The authors declare no competing interests.

Additional information
Supplementary Information The online version contains supplementary material available at https://doi.org/10.1038/s41598-022-09311-9.

Correspondence and requests for materials should be addressed to N.T.

Reprints and permissions information is available at www.nature.com/reprints.

Publisher's note Springer Nature remains neutral with regard to jurisdictional claims in published maps and institutional affiliations.

Supplementary data

Black pepper and tarragon essential oils suppress the lipolytic potential and the type II secretion system of *P. psychrophila* KM02

Natalia Tomaś [a]*, Kamila Myszka [a], Łukasz Wolko [b]

[a] Department of Biotechnology and Food Microbiology, Poznan University of Life Sciences, Wojska Polskiego 48, 60-637 Poznań, Poland

[b] Department of Biochemistry and Biotechnology, Poznan University of Life Sciences, Dojazd 11, 60-632, Poznań, Poland

* corresponding author: natalia.tomas@up.poznan.pl

Supplementary Table 1. The list of primers used in RT-qPCR experiments.

Gene name	**Forward primer**	**Reverse primer**	**Tm °C**	**Product length**
lipA	GTGGGGCAATTGGTTTGA	TGATTGACCATGCGCTGA	57	148
lipB	CTACCTTTTTGTTACCCGTT	ATCACGTCGTAGCATTTC	53	118
tadB1	CCCAGTACCAAAGCCGTCAT	CAACGTTCAGATGGGGGTGA	60	231
tadC1	TGCTGAAGAATCACGCAGGT	AGAGACGGCAACAGGAAGTG	60	262
gspH2	TCCACCAGCACTTGCAGATT	CCTCGCAACGTGGTTTTACC	60	244
gspH1	CGCTTTTGATGTCTGCCACC	CGCTACTTCAACAGCCTGGA	60	244
pulG	CCACTGACTGGGAAAGTCCG	AAGACCTGTTGCAGGACGAG	60	179
gspG	TTGGTGGTACTGGTGGTCCT	CTGCAAGCCTTGTTCGGTTG	60	177
pulF	TCAGCCAGGAACTGACAACC	CACAAGTGCAACGTAGAGCG	60	200

Supplementary Table S2. Features of *Pseudomonas psychrophila* KM02 genome.

Attributes	**Values**
Genome size	5,313,922 bp
GC content	57.4 %
Plasmid	0
Total predicted genes	4,813
Total CDS	4,713
Pseudogenes	54
Total RNAs	100
rRNAs (5S, 16S, 23S)	25 (9, 8, 8)
tRNAs	71
ncRNAs	4

Supplementary Table S3. Characteristic of the selected CDSs involved in the type II secretion system of *P. psychrophila* KM02.

CDS	Gene name	Gene definition and probable role
WP_048352188.1	*tadB1*	Type II secretion system F family protein, highly hydrophobic integral protein of the inner membrane involved in a general secretion pathway (GSP) for the export of proteins
WP_046810475.1	*tadC1*	Type II secretion system F family protein, highly hydrophobic integral protein of the inner membrane, involved in a general secretion pathway (GSP) for the export of proteins
WP_019825587.1	*gspH2*	Type II secretion system GspH family protein, required for the energy-dependent secretion of extracellular from the periplasm
WP_019825589.1	*gspH1*	Type II secretion system GspH family protein, required for the energy-dependent secretion of extracellular from the periplasm
WP_019825591.1	*pulG*	Type II secretion system protein, pseudopilin PulG, one of the secretion pseudopilins is found to assemble into pilus-like bundles
WP_046809061.1	*gspG*	Type II secretion system major pseudopilin GspG, it delivers toxins and a range of hydrolytic enzymes to the cell surface or extracellular space
WP_019825560.1	*pulF*	Type II secretion system F family protein involved in the export of proteins (toxins and a range of hydrolytic enzymes including proteases, lipases and carbohydrate-active enzymes) to the cell surface or extracellular space

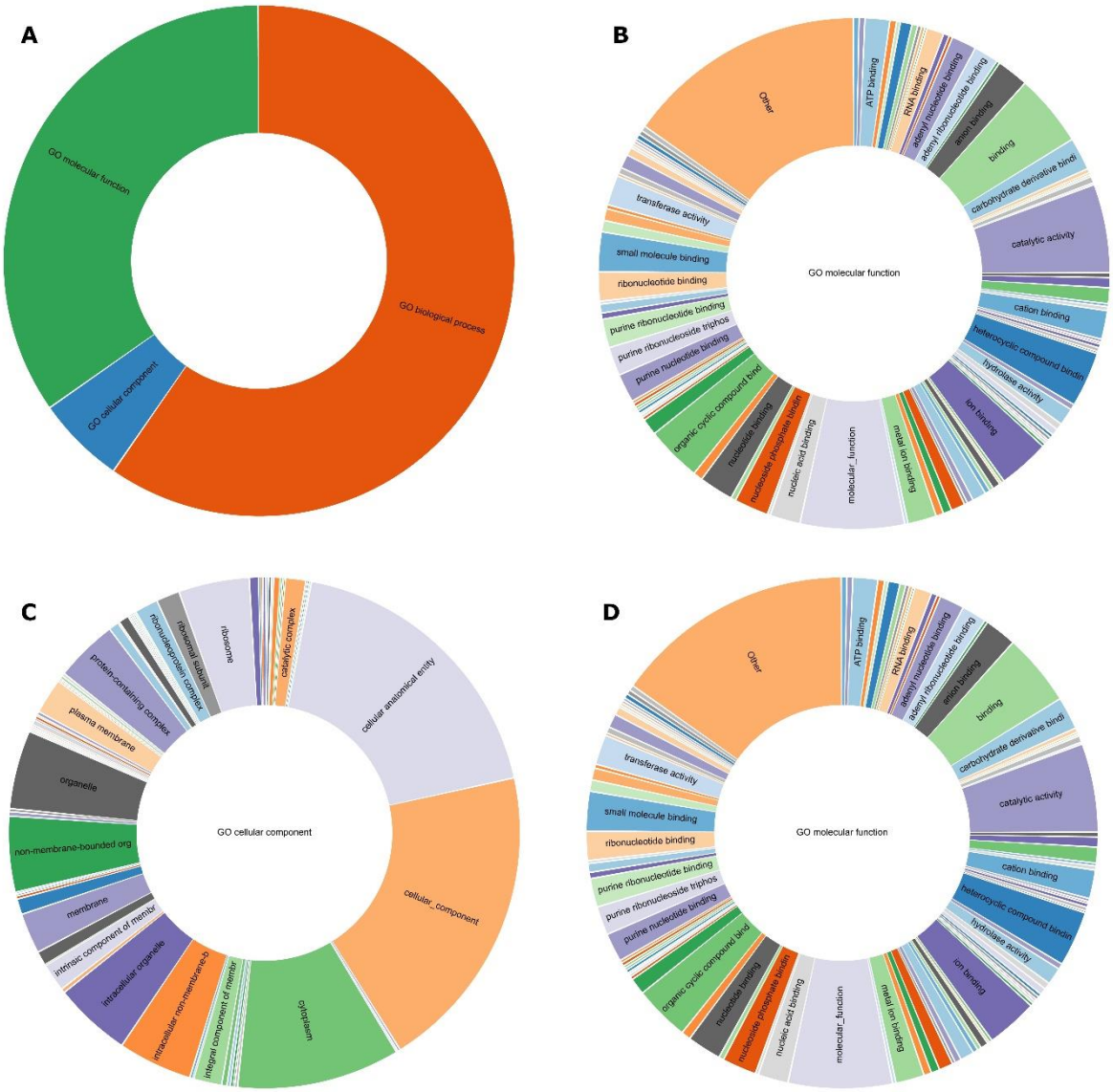

Supplementary Fig. S1 Distribution of GO annotations of *P. psychrophila* KM02 genome.

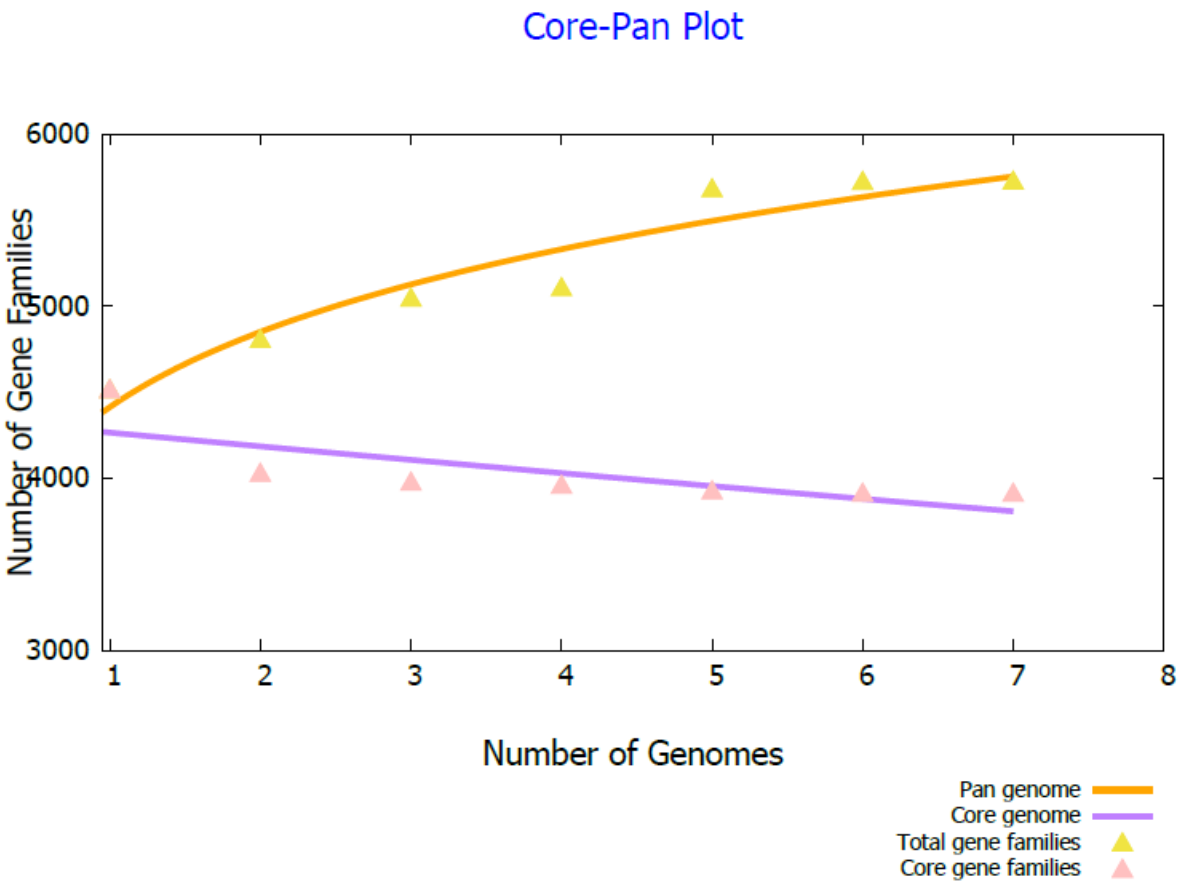

Supplementary Fig.S2. Core-pangenome plot of *P. psychrophila* species.